CFTRI-MYSORE
4217
Ultracentrifugat

duplicate

Ultracentrifugation in Biochemistry

Optical Patterns from the Ultracentrifuge

SEDIMENTATION VELOCITY

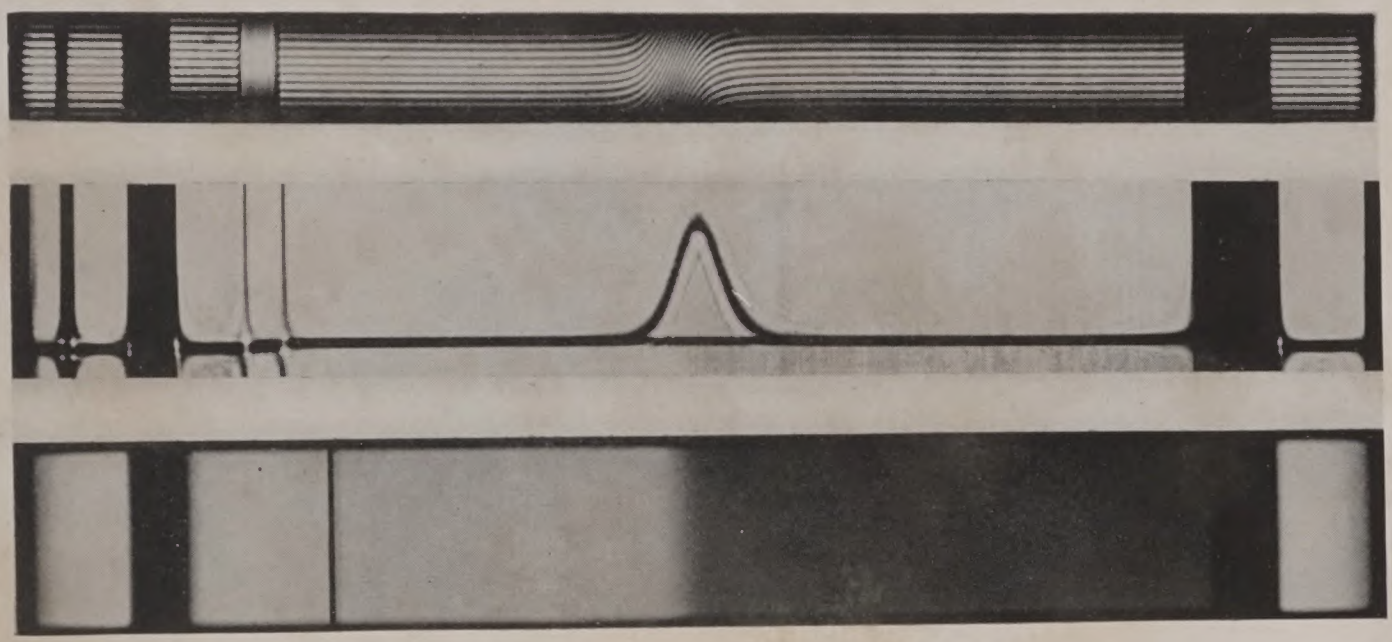

SEDIMENTATION EQUILIBRIUM

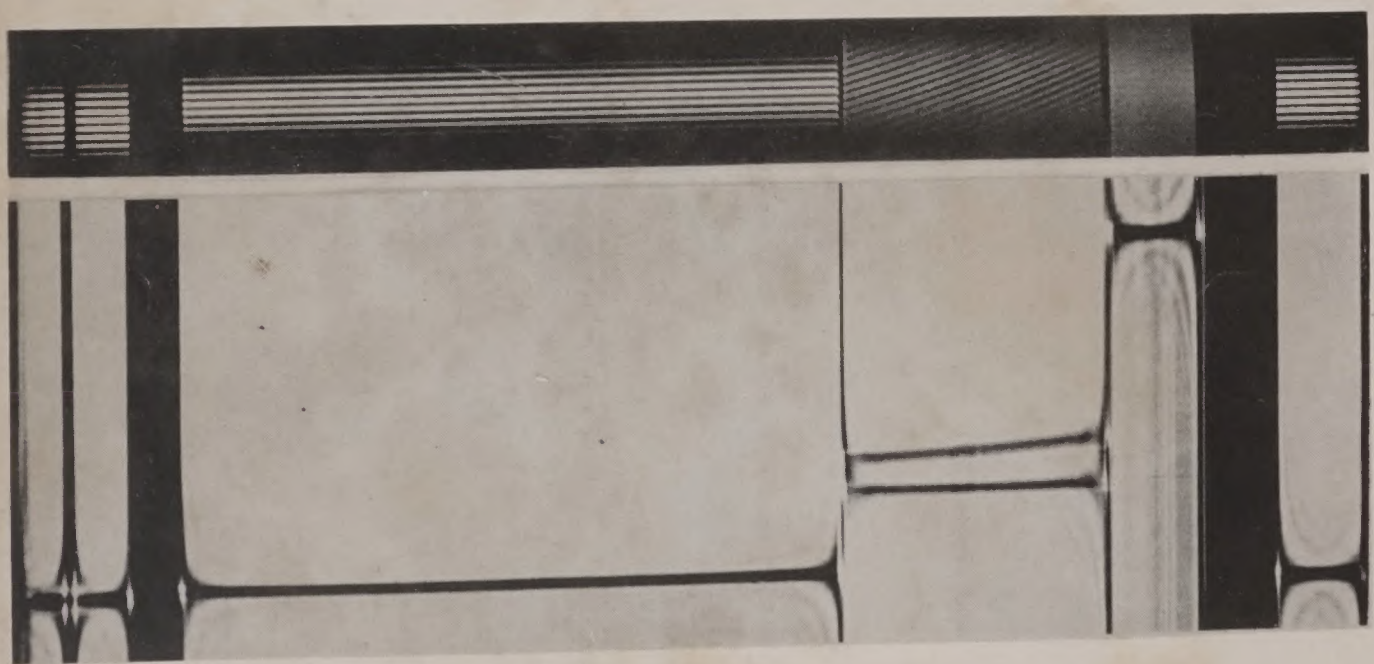

The upper two patterns (Rayleigh and schlieren) were obtained in an experiment on bushy stunt virus, the next one (ultraviolet absorption) was obtained with poliovirus at an extremely low concentration, and the lower two represent patterns for sucrose at a concentration of 1 g/100 ml at 50,000 r.p.m.

Ultracentrifugation in Biochemistry

HOWARD K. SCHACHMAN

Biochemistry and Virus Laboratory
University of California
Berkeley, California

CENTRAL FOOD TECHNOLOGICAL RESEARCH INSTITUTE
LIBRARY
MYSORE.

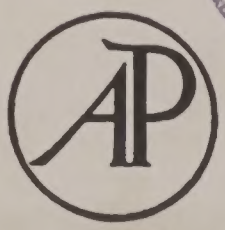

1959

ACADEMIC PRESS • NEW YORK AND LONDON

ACADEMIC PRESS INC.
111 Fifth Avenue
New York 3, N. Y.

United Kingdom Edition
Published by
ACADEMIC PRESS INC. (London) Ltd.
40 Pall Mall, London SW 1

Copyright ©, 1959, by Academic Press Inc.

ALL RIGHTS RESERVED

NO PART OF THIS BOOK MAY BE REPRODUCED IN ANY FORM,
BY PHOTOSTAT, MICROFILM, OR ANY OTHER MEANS,
WITHOUT WRITTEN PERMISSION FROM THE PUBLISHERS.

4217
GX3,111U
N59

Library of Congress Catalog Card Number 59-7688

CFTRI-MYSORE
4217
Ultracentrifugat.

PRINTED IN THE UNITED STATES OF AMERICA

Foreword

Over the past decade the use of the ultracentrifuge as a tool in biochemical research has developed in a dramatic fashion. Problems scarcely imagined ten years ago can now be investigated with brilliant success and with techniques only recently developed. Moreover the theoretical analysis of the processes occurring in sedimentation has been refined and deepened and placed upon a surer foundation. For a brief and clear perspective on these advances the reader may turn to the introductory chapter of this book. These developments have occurred with almost bewildering rapidity, and one who wishes to attain a comprehensive view of them has had to turn to many scattered papers and review articles. The classic monograph of Svedberg and Pedersen on the ultracentrifuge is still of vital interest for those who are concerned with research on sedimentation, and an important review of some of the theoretical aspects of sedimentation by Williams, van Holde, Baldwin, and Fujita, has recently appeared. There remains, however, need for an extended discussion of these more recent developments, combined with a statement of the basic and indispensable theory and a general description of the old and new experimental techniques.

I believe that these needs are admirably met by the present book. I cannot speak of it with complete detachment since, as one of the editors of *Advances in Protein Chemistry*, I had something to do with its origins. Dr. Schachman had, indeed, been invited by us to write a chapter for the *Advances*, dealing with the uses of the ultracentrifuge in protein chemistry. He responded with enthusiasm to the invitation, but soon found the scope of the discussion growing inevitably far beyond what he had originally contemplated; it evolved from a single chapter into an independent book, which is here presented.

This book is likely to become an indispensable companion to the laboratory worker who is planning and conducting an ultracentrifuge run for almost any purpose. It should also be of fundamental value to the thoughtful student or investigator who wants to know the present state of our knowledge in the field, both experimental and theoretical. No technique has done more than ultracentrifugation for the fundamental physical chemistry of macromolecules, and in recent years it has become increasingly applicable to small molecules as well. As a tool for the preparation and separation of proteins, viruses, and many other substances it is of great and growing importance. Moreover the processes occurring in a sedimentation experiment are complex and fascinating; it is important for the experimenter to under-

stand them, for many workers have gone astray through failure to interpret correctly the phenomena they observed. Dr. Schachman has, I believe, performed a major service by portraying the broad range of experimental techniques in sedimentation experiments and by providing a rigorous discussion of the underlying principles.

JOHN T. EDSALL

March, 1959

Preface

This monograph had its inception at the invitation tendered the author (by the Editors of the *Advances in Protein Chemistry*) to write a review dealing with recent advances in the application of the ultracentrifuge. To the author's chagrin it soon became apparent that the advances were occurring at a rate exceeding that achieved in the actual writing. Moreover, ultracentrifugal theory and practice had developed to such a degree that a description of them consumed space beyond the bounds of the typical review published in the *Advances in Protein Chemistry*. Consideration of this dilemma by the Editors and the Publisher led to the decision to publish this particular review as a separate monograph. This brief historical explanation has been presented here for two reasons. First, the author wishes to thank the Editors of the *Advances in Protein Chemistry* for providing the stimulus for this article, for their encouragement, and for the constructive criticisms they offered upon examination of the manuscript. Dr. J. T. Edsall, in particular, has been most generous with his time, and his suggestions have been of considerable value. Second, much has been added to the manuscript subsequent to the time it went to press as an article for the *Advances in Protein Chemistry*. Some of the inadequacies in organization can be attributed to the belated insertions and revisions. Though the author would like to be able to account for other deficiencies in a similar fashion, few valid justifications come to mind; he alone is responsible.

Despite the expansion of the manuscript while "in press," the goal initially set, i.e., to describe the principles of ultracentrifugation, remains unchanged. Many applications of interest and importance in biology are not discussed since they were considered to be outside the scope of this monograph. As a consequence the reader will not find in this volume detailed discussions, for example, of the behavior of serum albumin or the polydispersity of deoxyribonucleic acid or the properties of many other macromolecules of biological interest. When such materials are cited, only those aspects dealing with fundamentals of ultracentrifugation are stressed. Also missing from this volume are considerations of preparative centrifugation. Thus the reader will find no detailed treatment of the powerful methods of "zone centrifugation." Although one form of this technique—namely sedimentation equilibrium in a density gradient—is described, the emphasis is toward the theoretical side and the much more important practical aspects are scarcely mentioned. The results of several recent significant investigations were added while the monograph was "in press."

Further important contributions have since appeared, and the author regrets that it was not feasible to include a discussion of these later efforts. Already the monograph needs revision and extension. Perhaps others who have courage, energy, and patience may undertake such a task.

A considerable amount of hitherto unpublished work from the author's laboratory is described in this volume. Thus the reader will find more mention of the Rayleigh interferometer and examples of its application than could be justified by the existing literature. A similar situation exists with regard to the discussion of the application of the ultracentrifuge to the analysis of interacting systems composed of large and small molecules. In both instances the author was motivated not only by his own present research interests but also by the conviction that these areas are likely to become of paramount interest in the near future. Others no doubt would have emphasized different areas now under development.

Since the review was already set in print before the publication plans were altered, the original format containing sections, rather than chapters, was maintained. The first of these, *Introduction*, is a sketch of the field highlighting some of the principal developments. Following this is the section, *General Considerations*, in which ultracentrifugation is discussed in general terms and the division of the field into three major areas is described. This categorization is somewhat arbitrary, to be sure, but it has pedagogical value. The underlying theoretical considerations basic to all types of ultracentrifugal practice are presented in this section as well. The third section deals with developments of the experimental aspects of the field such as improvements in the instrument itself, cells, rotors, measurement and control of temperature, and the various optical systems. Included is a qualitative discussion of convection in ultracentrifuge cells. Despite the title, *Experimental Aspects*, no attempt was made to present here a guide for conducting experiments. For such material the reader will have to look elsewhere. The following three sections deal with the fundamental principles of the major divisions mentioned above: *Sedimentation Velocity*, *Transient States*, and *Sedimentation Equilibrium*. Much of the literature in the last mentioned area is concerned with nonbiological materials, and omission of pertinent discussions of some important developments is justified only by the decision to concentrate on ultracentrifugation in biochemistry. It is clear that these studies are rapidly becoming relevant to biochemists as they study nonideal solutions of materials like deoxyribonucleic acid. Future volumes will doubtless devote considerable space to consideration of the sedimentation equilibrium of charged macromolecules. Finally a section is included which deals with interpretation of sedimentation data in terms of hydrodynamic models, charge effects, and interactions in multicomponent systems.

Of the experimental work (cited in this monograph) which has been done

in the author's laboratory, much has been supported generously over a period of years by the Office of Naval Research under contract with the University of California. Substantial support has been received as well from the National Science Foundation. It is the hope of the author that the contributions of his former colleagues to the research activities of this laboratory have been adequately set forth. To each of them, P. Y. Cheng, Ann Ginsburg, W. F. Harrington, R. T. Hersh, S. Katz, E. G. Richards, V. N. Schumaker and J. Stenesh, and to Pearl Appel and Jean Miller for their able and enthusiastic technical assistance, he wishes to express his indebtedness and thanks. Also the author has had the benefit over many years of pleasant and stimulating discussions with R. L. Baldwin, G. Kegeles, E. G. Pickels, R. Trautman and D. F. Waugh on many diverse aspects of ultracentrifugation. Each of them has made available results of his own work prior to publication. Finally the indebtedness of the author to W. M. Stanley and M. A. Lauffer cannot be overemphasized: to the former for his continued support and encouragement over a long period of time and to the latter for the author's initial exposure to the field of ultracentrifugation and for the stimulation of his interest in the study of macromolecules of biological interest.

In the preparation of this monograph many valuable suggestions and criticisms have been made by R. L. Baldwin, S. Hanlon, W. F. Harrington, P. Johnson, E. G. Richards, and V. N. Schumaker and their help is gratefully acknowledged. Miss Jean Miller is largely responsible for the expert photographic work involved in transferring patterns from the ultracentrifuge plates to the printed page, without, I might add, the use of a paint brush. Considerable help has been given the author by Mary Abbott in the preparation of the manuscript. A major part of this review was written during the author's tenure at the Department of Microbiology, Washington University School of Medicine as a John Simon Guggenheim Memorial Fellow, 1957–58. The author would like to express his thanks to A. Kornberg and others in that department for their hospitality.

HOWARD K. SCHACHMAN

March, 1959

Contents

Foreword by J. T. Edsall v

Preface vii

I. Introduction 1

II. General Considerations 5

III. Experimental Aspects 13

1. The Electrically Driven Ultracentrifuge 13
2. The Magnetically Suspended Ultracentrifuge 15
3. Analytical Rotors 16
4. Temperature Measurement and the Stretching of Rotors 17
5. Analytical Cells 21
   a. Double Sector Cell 22
   b. Synthetic Boundary Cells 25
   c. Separation Cells 28
   d. Other Cells 31
6. Optical Methods 32
   a. Lamm Scale Method 34
   b. Schlieren Methods 34
   c. Interference Methods 38
   d. Light Absorption Methods 47
7. Convection-free Sedimentation 55

IV. Sedimentation Velocity 63

1. The Relationship between Boundary Movement and the Sedimentation Velocity of Individual Molecules 63
2. Radial Dilution 70
3. Measurement of Sedimentation Coefficients 75
   a. Moving Boundary Method 75
   b. The Transport Method 85
4. Dependence of Sedimentation Coefficient on Concentration 90
5. Differential Sedimentation Rates 103
6. Sedimentation of a Slow Component in the Presence of a Faster Species. 108
7. Analysis of Mixtures of Several Sedimenting Components 116
8. Analysis of Boundaries in Terms of Homogeneity or Polydispersity 128
   a. Spreading of Boundaries Due to Diffusion 129
   b. Spreading of Boundaries Due to Polydispersity 131
   c. Self-Sharpening of Boundaries Due to the Concentration Dependence of Sedimentation Coefficients 138
   d. Distortion of the Boundary Due to the Johnston-Ogston Effect 148

c. General Considerations in the Demonstration of Homogeneity..... 149
9. Analysis of Systems of Reversibly Interacting Components..... 151
a. Association-Dissociation Equilibria Involving a Single Component.. 152
b. Interactions among Different Molecular Species..... 157
10. A Differential Method for the Direct Measurement of Small Differences in Sedimentation Coefficients..... 170
11. The Effect of Pressure on Sedimentation..... 174
V. The Transient States during the Approach to Sedimentation Equilibrium.. 181
1. Molecular Weight Determinations by the Archibald Method..... 182
2. Distributions throughout the Entire Cell..... 194
VI. Sedimentation Equilibrium..... 201
1. General Considerations..... 201
2. Two Component Systems..... 203
3. Charged Macromolecules..... 208
4. Multicomponent Systems and Sedimentation in a Density Gradient... 210
VII. Interpretation of Sedimentation Data..... 215
1. The Svedberg Equation..... 215
2. The Effect of Solvation..... 219
3. Nonideal Solutions..... 222
4. Effect of Charge on Sedimentation..... 225
5. Multicomponent Systems..... 228
6. The Frictional Coefficient..... 236
References..... 249
Glossary of Terms..... 259
Author Index..... 263
Subject Index..... 269

I. Introduction

The past 10 years has been a period of revolutionary change in research with the ultracentrifuge—almost as dramatic as the era beginning in 1923 when Svedberg and his collaborators (Svedberg and Nichols, 1923) first began exploiting centrifugal fields for the study of macromolecules and colloidal particles. As recently as 1947, there were in operation throughout the world only about 8 oil turbine ultracentrifuges of the Svedberg design and about an equal number of air-driven ultracentrifuges of the Beams-Pickels type. Now in addition to those instruments, there are in widely separated laboratories over 300 electrically driven ultracentrifuges. Moreover preliminary results herald even more radical departures in instrument design and performance. As a consequence of this tremendous increase in research activity, a review of the field by a single author is a formidable task destined to fall short in some areas which workers consider of great significance and to be too detailed in other areas which to some are trivial. Fortunately there have been excellent reviews, in recent years, which add to the classic and definitive work of Svedberg and Pedersen (1940), so that the arbitrary concentration, in the present review, on certain aspects of the field should give not too distorted a picture of the growing discipline called ultracentrifugation. The reader is referred for other outlooks to Nichols and Bailey (1949), Kinell and Rånby (1950), and Williams (1954). A thorough treatment of the theoretical aspects of different types of ultracentrifugal problems has just appeared (Williams *et al.*, 1958).

Developments of note have included new types of ultracentrifuge cells which permit measurements hardly visualized by even the most farsighted research workers of the 1930's. Coupled with these radical modifications in ultracentrifuge cells has been the exploitation of multicell rotors so that many different samples can be examined simultaneously. The adaptation of optical systems hitherto unused in connection with the ultracentrifuge, tremendous improvements in older, familiar techniques, and the rebirth of discarded optical methods have all occurred in the past 10 years, and it is now safe to predict that at least three different optical systems will be in routine use on many ultracentrifuges in a short time. Factors hardly considered for many years, such as the precise measurement of temperature and the effect of pressure, are now either clarified or the subject of active and productive investigation. Older views emphasizing the instability of

ultracentrifuge boundaries in experiments at concentrations below 0.01 % have required modification, and now meaningful, quantitative ultracentrifuge analyses on certain types of systems are being performed routinely at concentrations of several thousandths of a per cent.

Advances of a theoretical nature have been just as rapid. Interpretation of data from ultracentrifugal studies in terms of the properties of the sedimenting substance is now on a more firm basis. Because of theoretical developments, molecular weights can now be determined with accuracy in a single experiment of very short duration. Analysis of mixtures is now feasible. The effects of concentration have been carefully considered and reliable theories presented. We now recognize that many of the claims of the 1930's and 1940's regarding the homogeneity of proteins were ill-founded and must be modified in keeping with recent theoretical treatments. Despite this we can return, with greater confidence, to the view that the ultracentrifuge is one of the most powerful tools available for the study of the distribution of molecular weights within a given preparation. Moreover, considerations of polydispersity are no longer restricted to sedimentation rates or molecular weights. Ultracentrifuge data in conjunction with other measurements can provide valuable information about the variations in shape among a collection of macromolecules in a given preparation. Even without additional data, polydispersity with respect to density, and therefore with regard to chemical composition, is amenable to direct analysis by ultracentrifugation. The changes over the past years have been so extensive that even the term "sedimentation constant" is disappearing from the literature to be replaced by the more appropriate "sedimentation coefficient." New areas of research have led to the introduction of terms like the "second moment of the gradient curve," "differential sedimentation rate," and the "Archibald method."

In response to newer demands of the protein chemist, we seem to be approaching an era already reached in diffusion measurements where results with an accuracy of 0.1 % can be expected. Thus the presence or absence of the contribution of a single amino acid to the molecular weight of a large protein molecule will be detected by ultracentrifugal methods already available or in process of development. Similarly, configurational changes in protein molecules in complicated solvent systems will be followed with the aid of the ultracentrifuge. Already techniques and theories have been developed for the determination of molecular weights of biologically active material, even in impure preparations and with 1-μg. quantities of material. All that is required is a sensitive and accurate biological assay specific for the entity under investigation and an ultracentrifuge cell capable of dividing the solution into two fractions at some desired time. It seems likely that enzymologists will employ these greatly

improved methods to an extent not hitherto contemplated. Most experiments can be performed rapidly and at low temperature, so that labile proteins can be examined with little risk of denaturation. For most substances, a complete study can be performed with as little as 10 to 20 mg., and in special circumstances microgram quantities will suffice. Newer ultracentrifugal methods are equally applicable to the examination of molecules considerably smaller than most proteins and can be used, therefore, in studies of coenzymes and substrates or the products of action of proteolytic enzymes or nucleases. As a consequence, it can be anticipated that the ultracentrifuge will find increasing application to studies of the mechanism of enzymatic action on large substrate molecules. In certain systems, the ultracentrifuge has already been extensively used in the study of protein-protein interaction, but surprisingly little use has been made of quantitative ultracentrifugal analysis in the examination of interactions between large and small molecules. Also little use of the ultracentrifuge has been reported in the study of the mode of synthesis of biologically important macromolecules or the path of labeled atoms of an infecting virus particle upon its invasion of a susceptible cell where more virus particles are produced at a later time. Many substances of interest to biochemists, such as the cytochromes, hemoglobins, nucleic acids, and nucleoproteins, have such high extinction coefficients either in a particular region of the visible spectrum or in the ultraviolet that the sedimentation of these materials is readily examined by absorption techniques even at concentrations of only 0.001%. Moreover, these substances have characteristic absorption spectra and can, therefore, be examined in the ultracentrifuge even in crude mixtures as long as light of the appropriate wavelength is available. Absorption methods are particularly valuable for the study of the interaction of dyes or coenzymes with specific proteins or enzymes. In structural studies of nucleoproteins, heme proteins, or cell particulates in which the macromolecules are being degraded by enzymes or chemical reagents, these absorption methods provide additional information because they can be used to determine the physical properties of a specific part of the macromolecule. The next few years are likely to produce more applications of the ultracentrifuge to these fascinating biological problems, while the application of the instrument to studies of purity and molecular size and shape are relegated to a more routine role.

Despite the phenomenal progress both experimentally and theoretically which has been outlined above, gaps in our knowledge still exist both with respect to understanding some effects already being studied and, even more, with regard to the potentialities of ultracentrifugation. This review deals principally with ultracentrifugation as it is currently being applied or, in the author's opinion, likely to be applied to biological systems. Of

necessity there will be speculation on the part of the author, and the treatment which follows will reflect his prejudices and interests. Some of the areas discussed are presently not investigated from an experimental point of view, and doubtless revision of some of the ideas will be required as data become available. This course was chosen rather than an alternative one involving a compilation, perforce less critical, of the manifold applications of the ultracentrifuge to this or that protein. These examples are more profitably examined along with other physical and chemical data on a specific protein. Admirable reviews bringing together pertinent information on individual systems are now available (Edsall, 1953; Waugh, 1954; and Anfinsen and Redfield, 1956).

Much of the ultracentrifugal data in the literature require revision either because of improvements in experimentation or because theoretical developments have shown that the results are calculated or interpreted incorrectly. For this reason, we will concentrate on fundamental aspects of ultracentrifugation. Illustrations when given are to demonstrate a particular problem in ultracentrifugation, and diagrams frequently will be those obtained in the author's laboratory only because original ultracentrifuge patterns could not be obtained readily.

II. General Considerations

Ultracentrifuges can be used either to measure the velocity of movement of macromolecules in a solution under the influence of a centrifugal field or to determine the distribution of the macromolecules in a centrifuge cell which is rotating at comparatively low speeds. In the latter after a fixed period of time, an equilibrium state is established in which the concentration of solute at each level in the cell no longer varies.

The former method is known as the *sedimentation velocity method* and to date has been the more widely used. In a sedimentation velocity experiment, the ultracentrifuge rotor is operated at speeds up to 60,000 r.p.m. so that the solute molecules which initially were uniformly distributed throughout the solution in the ultracentrifuge cell are caused to settle at appreciable rates toward the periphery of the cell. This migration of the solute molecules leaves a region containing only solvent molecules in addition to the region in the cell where the concentration is uniform. Between the supernatant and the solution of uniform concentration, known as the "plateau region," there is a transition zone in which the concentration varies with distance from the axis of rotation. This transition zone is called the boundary, and the sedimentation velocity method is generally based on observations, by optical methods, of the movement of such boundaries, which in turn are a measure of the movement of the solute molecules in the plateau region. Sedimentation velocity data can be obtained, however, even in the absence of a complete boundary and this will be discussed presently. Figure 1A shows schematic drawings of the concentration of solute as a function of distance in the cell at different times. Since the more commonly used optical systems do not record concentration, but rather the change in concentration (more properly, the change in refractive index) with distance, the corresponding curves are drawn in Fig. 1B. It is such diagrams as illustrated in Fig. 1B, which are generally used to study the purity of a given preparation and to determine the sedimentation coefficient of the sedimenting material. It should be noted that the sedimentation velocity method permits the direct measurement of sedimentation coefficients which are related to both the size and shape of the sedimenting molecules. Other independent data are needed for the evaluation of molecular weights. Under certain circumstances fairly reliable diffusion coefficients can also be obtained from sedimentation

velocity experiments, and, therefore, molecular weights can be obtained solely from sedimentation velocity studies. Figure 1 shows the changes which occur for solute molecules which are more dense than the solvent and therefore migrate in a centrifugal direction leaving the newly created solvent region near the meniscus. For solutes which are less dense than

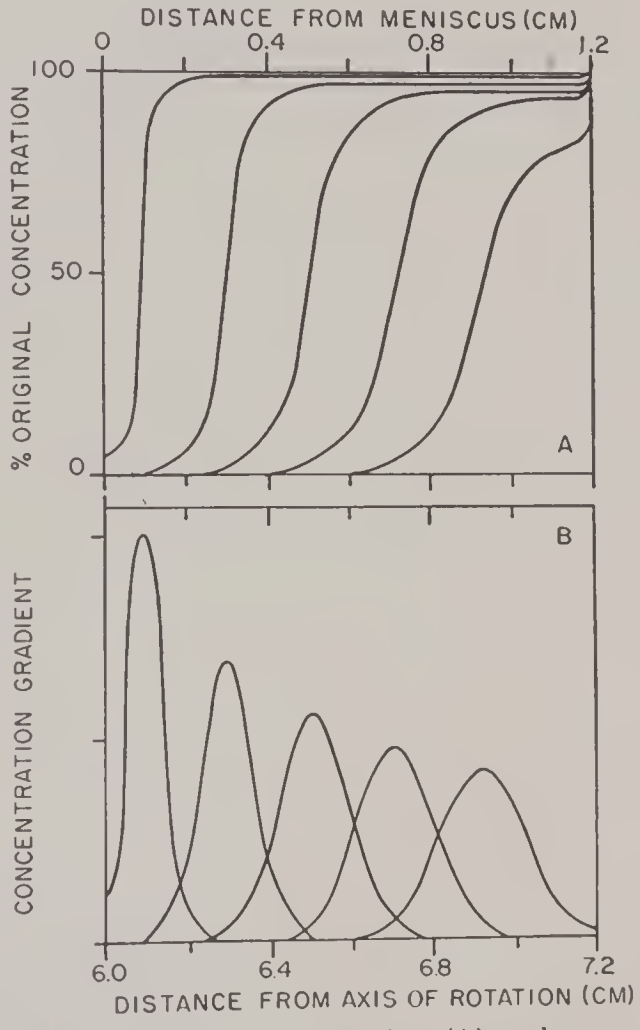

FIG. 1. Schematic diagram of the concentration (A) and concentration gradient. (B) as a function of distance in the centrifuge cell during a sedimentation velocity experiment.

the solvent, such as lipoproteins in concentrated salt solutions, the solute molecules tend to float (migrating in a centripetal direction) leading to a region of pure solvent at the bottom of the cell. Sedimentation coefficients in the latter system would be negative. The concentration gradients (and generally the refractive index gradients) across the boundaries developed in such systems are negative, and the observed ultracentrifuge patterns, as a consequence, are inverted.

In the second application of the ultracentrifuge, known as the *sedimentation equilibrium method*, the ultracentrifuge is operated at relatively

low speeds (about 8000 r.p.m. for a protein with a molecular weight of 60,000). Under these conditions the transport of solute in a centrifugal direction due to sedimentation is sufficiently slow as to be counterbalanced by transport in a centripetal direction by the diffusion resulting from the concentration gradient created by the partial sedimentation of the macromolecules. During the first stages of a sedimentation equilibrium experiment, the concentration decreases at the meniscus and increases at the bottom of the cell, owing to sedimentation. As a consequence of back diffusion, however, a region devoid of solute is not created as in the sedimentation velocity method. Instead, the concentration will remain finite at the meniscus as long as the centrifuge is not operated at too high a speed. Under conditions which are ideal for precise experimentation, the concentration at the meniscus will approach a value about one-half its initial value. Similarly, sedimentation plus back diffusion near the cell bottom leads to a region in which the concentration is about twice the original concentration. In the sedimentation velocity method, the role of diffusion at the bottom of the cell is less important, and this region of high concentration is restricted to a very thin layer on the cell bottom, where the sedimented material is packed as a gellike pellet. During the early stages of a sedimentation equilibrium experiment, the concentration near the center of the cell is independent of position and practically the same as the initial concentration. As the run proceeds, the plateau region disappears, and there is only one position in the cell with a concentration equal to the initial concentration. Finally, after a considerable period of time, an equilibrium state is reached and no further changes in concentration occur with time. These variations in concentration with distance as a function of time are visualized in Fig. 2A and the corresponding gradient curves are illustrated in Fig. 2B.

In contrast to the sedimentation velocity method, measurement of the concentration distribution at sedimentation equilibrium gives directly the molecular weight of the sedimenting macromolecules (both methods require knowledge of the partial specific volume of the macromolecules). Despite this obvious advantage and the additional factor that the theoretical foundations for the equilibrium method are more firm than those for the sedimentation velocity method, there are only few recorded examples of the application of the sedimentation equilibrium method to the study of proteins. This seemingly anomalous situation has arisen both because of the lack of apparatus capable of sustained, continuous use for the long periods (days, in the case of proteins) required before equilibrium is reached, and because many proteins are not sufficiently stable to withstand such experiments. Apparatus is now available which is capable of continuous operation even at low temperature, but of greater importance,

perhaps, are the considerable theoretical advances which permit determinations of molecular weight from experiments in which equilibrium is not attained.

Owing largely to the theoretical work of Archibald (1947b) and certain technical improvements, especially with regard to optical methods, it seems likely that measurements during the approach to sedimentation equilibrium

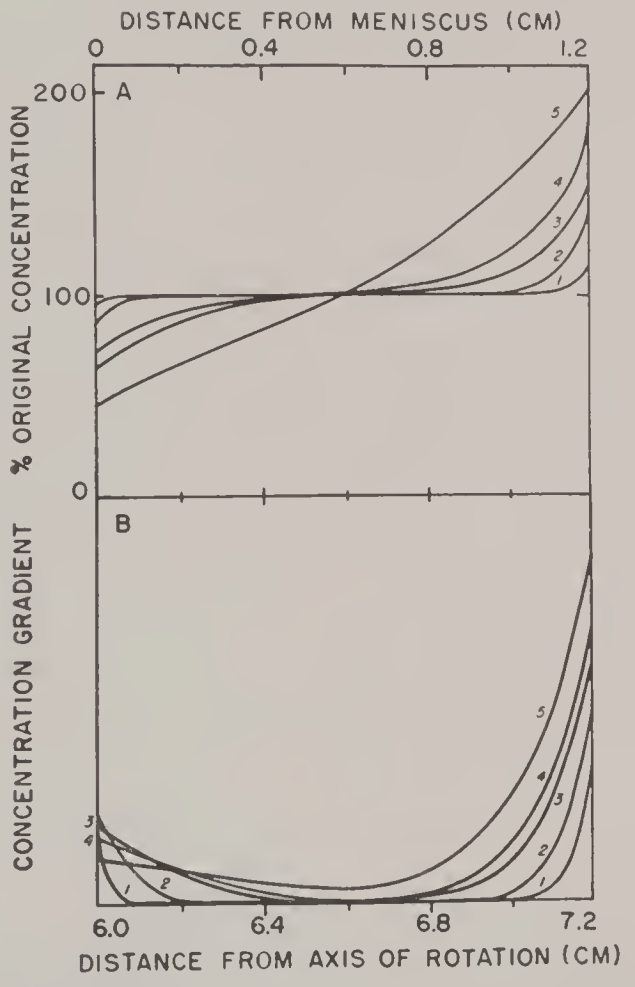

FIG. 2. Schematic diagram of the concentration and concentration gradient as a function of distance in the centrifuge cell during a sedimentation equilibrium experiment.

will become as routine as those by the currently more popular sedimentation velocity method. We are here using the term "approach to sedimentation equilibrium" loosely since this title leads to the implication that the experiments are conducted for times almost sufficient to obtain equilibrium throughout the cell. Actually, for the use of the equations of Archibald, there are no restrictions that the entire system be near equilibrium. There might be serious objection then to our inclusion of this method under the classification "approach to sedimentation equilibrium." To some extent our classification is arbitrary, although it can be justified

operationally. If the experiments are designed so as to measure most accurately the velocity of transport of material through the cell, as by the proper choice of the centrifugal field for the system under investigation, then the experiments can be classified as sedimentation velocity studies. There is no requirement in such an experiment that a complete boundary be formed as with relatively large proteins which sediment away from the meniscus to leave a region of pure solvent. In fact, for small, highly diffusible molecules the diffusion from the bulk of the solution toward the meniscus and from the sedimented material at the bottom of the cell precludes the formation of complete boundaries. Nonetheless, sedimentation coefficients can still be determined as long as the net transport of solute across a given plane is measurable. If, alternatively, the experimental conditions are selected so as to measure precisely the distribution of matter throughout the cell, then the experiments are of the sedimentation equilibrium type. Even if the data from these experiments are obtained long before equilibrium is established at each level in the cell, we can classify this method as the approach to sedimentation equilibrium or the transient state method. In principle, of course, if we wait sufficiently long an equilibrium state will be attained in the sedimentation velocity experiments, but there will be so little solute throughout most of the cell as to be undetectable, and the bulk of the material will be packed into a thin layer of extremely high concentration at the bottom of the cell. Although the theories of sedimentation equilibrium would be applicable to this situation, meaningful results could not be expected. Similarly, equilibrium conditions can be attained after long periods of operation at very low speeds, but the concentration change throughout the cell for small molecules would be immeasurably small, and molecular weight calculations could not be performed.

In summary, we can divide ultracentrifugation into three areas: sedimentation velocity, sedimentation equilibrium, and the approach to sedimentation equilibrium or the transient states. This classification is based in part on an operational point of view, and it is clear that the lines of distinction among the three are not sharp, despite very significant differences from a theoretical point of view. In fact, it is possible under carefully selected experimental conditions to obtain, from a single experiment, data which can be treated according to the theories for all three types of ultracentrifugation. Further unification of the different approaches has been achieved through the derivation of thermodynamic equations for the various types of analyses.

Basic to nearly all types of ultracentrifuge experiments is the differential equation, or the "continuity equation" as it is sometimes called, of the ultracentrifuge. This equation derived by Lamm (1929a) is developed

as follows. Consider a volume element in the rotating, sector-shaped ultracentrifuge cell (Fig. 3) bounded by the cylindrical surfaces at the distances x and $x + dx$, respectively, from the axis of rotation. The amount of solute transported per unit time across a given surface by sedimentation, dm_s/dt, is given by the product of the concentration of the solution, c, at the surface, the area of the surface, and the velocity of sedimentation of the macromolecules. Since the velocity of sedimentation at some particular position in the cell can be expressed as the velocity per

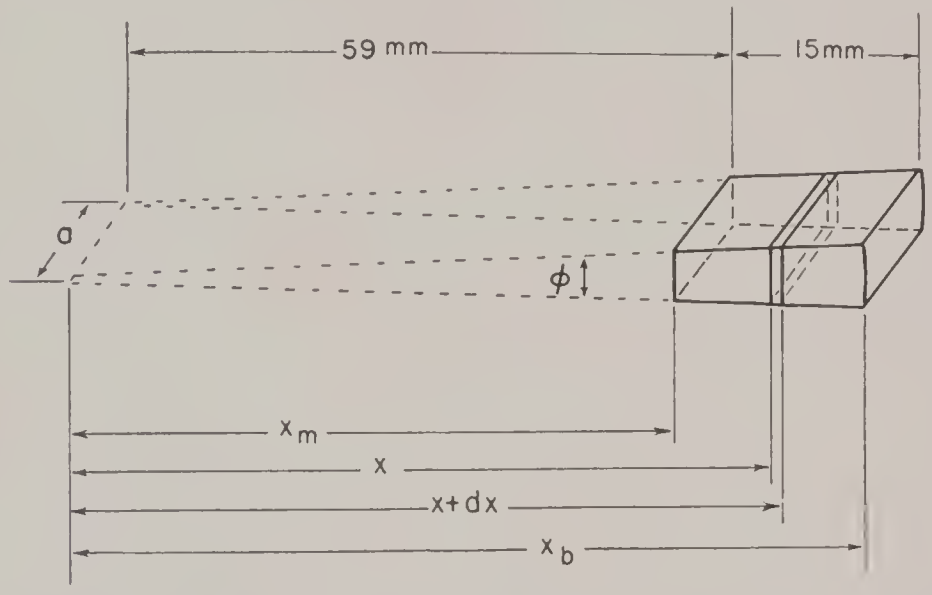

FIG. 3. Schematic diagram of a sector-shaped ultracentrifuge cell at a distance from the axis of rotation corresponding to its position in the rotor. The angle, ϕ, is generally 4°, but smaller angles are often used. The distance a represents the optical path in the cell, i.e., the thickness of the liquid column contained between the quartz windows.

unit field, known as the sedimentation coefficient, s, times the magnitude of the centrifugal field, $\omega^2 x$, we can write

$$\frac{dm_s}{dt} = c\phi x a s\omega^2 x \tag{1}$$

In Eq. (1), the area of the cylindrical surface in the cell is $(\phi x a)$ where ϕ is the angle of the sector in radians, and a is the thickness of the cell along the optical path, and ω is the angular velocity of the cell in radians/sec. Equation (1) provides a definition of the sedimentation coefficient as the proportionality constant relating the mass transported across a surface per unit time to the concentration at the surface, the area of the surface, and the magnitude of the centrifugal field. The sedimentation coefficient is written, therefore, as

$$s \equiv \frac{dx/dt}{\omega^2 x} \tag{2}$$

and has the units cm./sec./dyne/g. or sec. Sedimentation coefficients are now reported in svedbergs (S) where $1S = 10^{-13}$ sec. Since there is also transport of solute in the opposite direction because of diffusion, we can write, following Fick's first law (1855), for the mass transported centripetally per unit time, dm_D/dt,

$$\frac{dm_D}{dt} = -D\phi xa\frac{\partial c}{\partial x}. \tag{3}$$

In Eq. (3), D is the diffusion coefficient and $\partial c/\partial x$ is the concentration gradient at the surface, x cm. for the axis of rotation. The net transport per unit time, dm/dt, across this surface in a centrifugal direction is the sum of these terms.

$$\frac{dm}{dt} = \phi xa\left[cs\omega^2 x - D\frac{\partial c}{\partial x}\right]. \tag{4}$$

A similar equation can be written for the net transport across the surface at the distance $x + dx$ from the center of rotation. Subtraction of the second from the first gives the net accumulation of solute per unit time in the volume element, $\phi xadx$. This accumulation per unit time

$$-\frac{\partial}{\partial x}\left[x\left(cs\omega^2 x - D\frac{\partial c}{\partial x}\right)\right]\phi adx$$

can also be expressed as the change in concentration with time, $\partial c/\partial t$ in that volume element times the volume, $\phi xadx$, of the region considered. Thus we obtain

$$\frac{\partial c}{\partial t} = \frac{1}{x}\frac{\partial}{\partial x}\left[\left(D\frac{\partial c}{\partial x} - cs\omega^2 x\right)x\right]. \tag{5}$$

If it is assumed that s and D are independent of x and, therefore, of concentration, Eq. (5) takes the form

$$\frac{\partial c}{\partial t} = D\left[\frac{\partial^2 c}{\partial x^2} + \frac{1}{x}\frac{\partial c}{\partial x}\right] - s\omega^2\left[x\frac{\partial c}{\partial x} + 2c\right]. \tag{6}$$

It should be emphasized that Eq. (6) contains the restrictions that s and D are independent of concentration. As we shall see, these assumptions are unwarranted for many systems. Fujita (1956a) has recently discussed this problem in great detail for systems in which s varies linearly with concentration.

Equation (6) is derived here because it is fundamental to all types of ultracentrifugation. For sedimentation velocity experiments in which the concentration near the meniscus becomes essentially equal to zero, the solution of the differential equation describes the shape of the resulting

boundary (Faxén, 1929). In sedimentation equilibrium experiments when $(\partial c/\partial t)$ becomes zero, this equation yields the Svedberg equation (1925; Oka, 1936), showing the relationship of the sedimentation and diffusion coefficients to the molecular weight. Also for transient states during the approach to sedimentation equilibrium, solutions of this equation either by approximate methods (Yphantis and Waugh, 1956a) or by means of a differential analyzer (Waugh and Yphantis, 1953) give the distribution of the solute throughout the cell for different times. Finally, in sedimentation velocity experiments in which there is a plateau region, i.e., $\partial c/\partial x = 0$, the differential equation yields the so-called radial dilution rule (Svedberg and Rinde, 1924; Trautman and Schumaker, 1954), describing the decrease in concentration in the plateau region during an experiment.

III. Experimental Aspects

Just as the production of a compact commercial spectrophotometer is responsible in part for some of the great strides in modern biochemistry, so the development of ultracentrifugation to its present state can be attributed to the availability of a versatile and reliable commercial instrument. It is of interest that the apparatus currently being used extensively bears so little physical resemblance to either the oil turbine or air-driven ultracentrifuges which historically form the background for instrumental design in this field. This is not to indicate that experience of the 1920's and 1930's with the early designs did not have a profound influence on the shaping of newer instruments (Pickels, 1952). Rotor design and the basic features of cell design (Pickels, 1942b) have been altered in only relatively minor ways, and even the location of the cell at a distance of 65.0 mm. from the axis of rotation has not been varied. What follows is a brief discussion of newer developments in instrumentation. The reader is directed to other sources (e.g., Svedberg and Pedersen, 1940) for excellent accounts of the apparatus in use prior to 1947.

1. The Electrically Driven Ultracentrifuge[1]

The 9-pound rotor, oval shaped to increase its speed rating, is caused to rotate by a 1½-H.P. electric motor acting through a cylindrical gear housing which drives a high speed spindle at a rate 5⅓ times that of the motor (Pickels, 1950). Pinned to the high speed spindle, capable of speeds up to 70,000 r.p.m., is a flexible $\frac{1}{10}$ inch piano-wire shaft terminating in a screw-type coupling onto which the rotor is fastened. Flexibility of the shaft plus loose mounting of the driving mechanism on shock-absorbing neoprene permits sufficient freedom to the rotor for it to become self-balancing. Thus precision balancing of the cells placed in the rotor is not necessary, and, more important, inadvertent leakage of a cell during high speed operation causes no harm to the driving mechanism. This self-balancing feature of the drive mechanism actually allows for slight shifts in the axis of rotation at different speeds, a fact which must be reckoned with in considerations of the measurement of stretching of the rotor and the precise location of the analytical cell at high centrifugal

[1] Available from Spinco Division, Beckman Instruments, Inc., Palo Alto, California.

fields. Heating of the rotor is minimized by its operation in a vacuum chamber at pressures below 1 μ of mercury. The mechanical bearings which support the rotor, the gear train, and the motor itself are cooled by means of flowing water so that heat generated in the driving mechanism is not transferred to any extent to the rotor below. Most of the temperature changes in the rotor during a long experiment have their origin in heat transferred along the drive shaft. Maintenance of the vacuum about the shaft is achieved by close fitting bearings through which small amounts of oil flow into an oil gland surrounding the shaft. To reduce fogging of the lenses by the oil in the vacuum chamber a device has now been constructed to conduct most of this oil into a tube, which then directs the oil out of the chamber into a vessel on the outside of the chamber.

With special attachments, the rotor can be operated at numerous discrete speeds from about 1800 to 60,000 r.p.m., with an average deviation of only 0.1% and instantaneous deviations less than 0.5%. Speed control is achieved by means of a differential gear assembly which in effect applies or removes fixed amounts of resistance in the power supplied to the motor, and thereby causes it to accelerate or decelerate, as required, to maintain the preselected speed. Below the principal, nonmetallic gear in the drive assembly is a double reduction system of worm gears driven by the motor shaft. This system of gears drives an output shaft connected with the speed control unit. Opposing this rotary motion in the differential gear box is that from a shaft driven by a low speed synchronous motor. When the rotary motions from the drive and synchronous motor exactly match, the rotor can be considered as operating at the indicated setting within the limits of variation of the frequency of the power supplied to the instrument. Deviations between the speed of the shaft from the drive unit and that from the synchronous motor causes a displacement of a gear in the differential speed control unit, which then produces the necessary change in the drive voltage to adjust the speed to the desired value.

When the rotor is operated at its maximum speed in a chamber evacuated to a pressure below 1 μ Hg, by means of an oil diffusion pump backed by a mechanical vacuum pump, the temperature rise is only about 1°C. per hour. For runs of long duration, this rise can be virtually eliminated by the controlled operation of a refrigerating unit within the instrument, which pumps a coolant through coils surrounding the rotor in the vacuum chamber. Temperatures of the rotor in a given experiment have customarily been taken as the average of the initial and final temperatures as measured by means of a contact thermocouple in conjunction with a galvanometer. When the temperature rise during a run is several degrees or more, the temperature at any period of the run is determined by linear interpolation between the initial and final temperatures. This practice has been shown

to be invalid because the rotor during high speed operation assumes a temperature different from that at rest (cf., Section III,4).

The speed of the centrifuge rotor is indicated in three different manners. Most precise for average operation is that indicated by the differential gear selector. As long as the proper voltage is used for a given speed setting so that the braking mechanism is not forced into operation, the average and even instantaneous speed will be close to that selected. There is, in addition, an electric tachometer which gives an indication of instantaneous speed and is useful for measuring fluctuations rather than the absolute speed. Finally there is a revolution counter which makes 1 turn for every 6400 revolutions of the rotor. Measuring the number of revolutions of this counter over a long period of time gives an accurate indication of average speed. Some workers use this routinely as a measure of speed although it is clear that accuracy comparable to that obtained from the differential gear assembly can be obtained only if care is used in employing the revolution counter.

Three complete optical systems are contained in the ultracentrifuge in such a manner as to be isolated from vibrations caused by moving mechanical parts within the instrument and by other equipment in the building. The optical systems are made vibration-free by floating the optical bench within the outer frame of the ultracentrifuge. Facilities are available for automatic sequence photography at preselected time intervals and exposure times. Photographs can be taken simultaneously with two different optical systems.

Numerous safety features are incorporated in the apparatus and occasional failures of the rotor even at high speed have resulted in damage to only the ultracentrifuge with no injury to the operator or other equipment in the laboratory. Continuous operation of the ultracentrifuge for long periods of time is feasible, and the presence of an operator is not required.

2. The Magnetically Suspended Ultracentrifuge

In the electrically driven ultracentrifuge, the rather heavy rotor is supported by mechanical bearings. This represents one of the principal changes in this instrument as contrasted to its predecessor, the air-driven ultracentrifuge, in which the load was supported by an air lift (Henriot and Huguenard, 1925, 1927; Beams, 1930; Beams and Pickels, 1935). Similarly the air lift has been replaced in the new instrument designed by Beams and co-workers (1951, 1954, 1955). Here the rotor is supported by a magnetic field. This magnetic lift permits the rotor to be freely suspended while rotating in a vacuum. As a consequence there is very little frictional resistance, and the temperature of the rotor can be maintained constant by thermostating the walls of the vacuum chamber. Speed

control is also very precise since the only friction on the rotor originates from the residual gas in the vacuum chamber. Once the rotor attains its operating speed after being driven by an auxiliary system, which can be disconnected at will, it coasts in the vacuum chamber losing speed at the remarkably low rate of 0.3 r.p.s./day. Hunting of the rotor about some mean speed is thus avoided. The rotor is accelerated by means of an air turbine which is situated below the vacuum chamber. A thin, flexible steel shaft connects the turbine to the rotor by means of a slot in the rotor. The rotor is maintained coaxial with the support solenoid by means of an iron core placed in an oil damping device in the center of the coil. Vertical displacements of the rotor can be controlled by variations in the current flowing through the solenoid. Under ideal conditions, no vertical or horizontal displacement of the rotor can be detected even when viewed under magnification. Speed can be measured to 1 part in 10^6 by monitoring of the signal resulting from a light beam passing through a hole in the rotor and impinging on a photomultiplier tube. The light beam to the photomultiplier tube is interrupted by the rotor which acts as a chopper, and the signal is compared with that from some standard generator.

This instrument has been used thus far principally at low speeds for sedimentation equilibrium studies. Experiments are under way to replace the air turbine with an electric drive in which the rotor is essentially the armature of a synchronous motor. For this to function without undue heating of the rotor, the rotating magnetic field must have a frequency equal to and continuously increasing with the speed of the rotor. After the desired speed is obtained, control is maintained by another circuit. Beams and his co-workers hope to adapt this instrument to the high speeds which are customarily employed for sedimentation velocity studies.

As the demands for greater precision in sedimentation analysis increase, it is likely that greater interest will be focused on this type of instrument. This design may also find greater use for ultracentrifugal analyses which are conducted at very low concentrations of the sedimenting material. For such studies, temperature and speed fluctuations would be much more hazardous since the stabilizing effect of the density change at the boundary would be so small and the risk of convective disturbances correspondingly greater.

3. Analytical Rotors

Relatively little change has occurred in the design of ultracentrifuge rotors although new rotors of the same basic pattern are finding more and more use. The bursting strength of the rotors is still the limiting feature in terms of the maximum centrifugal field attainable in ultracentrifuges.

Different aluminum alloys have been used, and it is likely that further changes in this direction will continue. In the magnetically suspended ultracentrifuge, the rotors are made either of a central steel core surrounded by an aluminum alloy, or they are constructed solely of steel. The strength of a rotor is largely determined by the ratio of yield strength to density. As a consequence, duralumin rotors are almost as satisfactory as steel rotors despite the much higher yield strength of the latter. Conventional rotors with two holes for analytical cells are ellipsoidal in shape so that stresses are not localized near the cell holes. Although the impression is common that the scope of the ultracentrifuge would be greatly increased by rotors of higher strength which would facilitate higher speed operation, it seems likely that the gain resulting therefrom would be only slight, for cell distortion and window breakage would then probably constitute the limitations. With new theoretical and experimental developments, the need for higher speed rotors does not seem so pressing. It should be noted, however, that the availability of higher centrifugal fields would permit the analysis of polydisperse systems of materials having a high diffusion rate. Rotors of higher strength would be useful also for the handling of cells with longer sedimenting paths, for this would increase the resolving power of the ultracentrifuge without concomitant problems in cell design.

The new rotors include those which can accommodate 2, 4, or 6 cells. Some sacrifice in speed is necessary for the latter rotors. In the 2-cell rotor, a special small rectangular opening is made on the minor axis of the rotor so that light passing through it can be recorded on each photographic pattern to give reference distances from the axis of rotation. The other multicell rotors employ a reference cell for this purpose. Thus 3 or 5 samples can be studied simultaneously in these rotors. Another rotor coming into popular use is much larger in a vertical direction so that cells with longer optical paths, up to 30 mm., can be accommodated.

4. Temperature Measurement and the Stretching of Rotors

For experiments of long duration, Waugh and Yphantis (1952) have designed and incorporated into the ultracentrifuge a "radiation" thermocouple which provides a continuous indication of the temperature of the base of the rotor. In conjunction with a circuit controlling a special heating coil and the refrigerating unit supplied with the instrument, they were able to maintain temperatures constant to ± 0.05°C. for indefinite periods. Other workers, Ecker *et al.* (1949) and Bauer and Pickels (1937), had previously used mechanical devices on the rotor to provide electrical contacts so that the temperature of the rotor could be measured during operation. Following these earlier leads, the electrically driven ultra-

centrifuge now has, as a temperature-sensing device, a rod-shaped thermistor which is embedded in a brass plug mounted on the base of the rotor. One end of the thermistor is in thermal and electrical contact with the rotor while the other end contacts a tungsten needle which dips into a pool of mercury contained in an adjustable cup mounted on the base of the vacuum chamber. The thermistor in conjunction with the rotor and a modified drive unit forms one arm of a resistance bridge which can be balanced by an appropriate setting of a potentiometer. With suitable calibration, the resistance of the thermistor as indicated on the dial gives a direct measure of the temperature of the rotor accurate to $\pm 0.02°C$. This same unit, because of the high temperature coefficient of resistance of the thermistor, is a sensitive indicator of temperature variations and is used to control and activate an 18-watt heater mounted below the rotor. In conjunction with continuous operation of the refrigerating unit, suitably adjusted for the desired temperature, the heating coil can be controlled to function intermittently yielding over-all temperature control to $\pm 0.1°C$. for indefinite periods. It is important that the mercury pool which serves as the lower contact for the thermistor be covered by a thin film of silicone oil so as to prevent evaporation of the mercury and loss of the high vacuum.

Since the temperature can appreciably affect the rate at which solute molecules migrate in a solvent, it is imperative that calibration of the thermocouple or the thermistor be accurate. Svedberg and Pedersen (1940) described a direct method for calibrating the thermocouple in their centrifuge in terms of the cell temperature by optical observation of the interface between a solid and its molten liquid in the rotating cell. From knowledge of the melting point of the solid (usually diphenyl ether), accurate calibration is possible. A critical discussion of this method is presented by Cecil and Ogston (1948). Because of large discrepancies between experimental results obtained on the same materials examined in the oil turbine and electric-driven ultracentrifuge, Shulman (1953a) examined this matter further. His results showed conclusively that errors in measuring the temperature of the rotor were responsible for the discordant results. In a particularly thorough experimental study of rotor temperature, Biancheria and Kegeles (1954) described a modification of this method, which avoids some of the deficiencies of the melting point method as used by other workers. Ordinarily, the interface is observed at different temperatures so as to permit extrapolation to zero thickness of liquid above the liquid-solid interface. This would correspond to pressures of 1 atmosphere for comparison with standard freezing point measurements. However, any impurities present in the diphenyl ether would concentrate in the liquid layer, thereby causing a lowering of the melting point. From thermodynamic data, Biancheria and Kegeles (1954) were

able to obtain a relation describing the melting point in terms of pressure in the ultracentrifuge cell. Thus precise temperature measurements could be made at different speeds of the rotor without resort to the extrapolation to zero layer of molten liquid.

During their careful studies of temperature measurement of the rotor, Waugh and Yphantis (1952) observed a decrease in temperature of the rotor upon acceleration from rest to 60,000 r.p.m. This was attributed to stretching of the rotor at the higher speeds, and a simplified calculation of the temperature change upon acceleration of the rotor to 60,000 r.p.m. gave results in satisfactory agreement with the measured temperature change of $-1.0°C$. Though this adiabatic cooling effect was contested by Hiatt (1953), it has been completely confirmed by Biancheria and Kegeles (1954) in their melting point experiments and by direct measurement with a thermistor in the rotor (Pickels, 1953). Waugh and Yphantis showed that the negative temperature change is linear with the square of the speed of the rotor. It now is well established that the cooling of the rotor upon its acceleration to 60,000 r.p.m. is very close to 0.8°C. Much of the data in the literature must be modified because of neglect of this factor.

This stretching of the rotor leads to another source of difficulty, because it renders uncertain the position of the cell in terms of the distance from the axis of rotation. Although the errors resulting from neglect of this effect are small, the demands of greater precision in sedimentation measurements require that allowances for this be made. Stretching of the rotor is customarily determined from the movement of the reference holes upon changing the speed of the rotor. Such movement can be precisely measured from double exposures of low and high speed pictures (Kegeles and Gutter, 1951). However, the movement of the reference hole does not give an unambiguous measure of rotor stretch, for a shift of the axis of rotation could produce the same effect. An unequivocal answer to this question must come from measurements with two different optical systems which are situated 180° apart from one another. Thus a shift of the axis would cause one reference image to move further from the axis of rotation, while the image of the same reference viewed with the second optical system would appear to move closer to the axis of rotation. If the apparent stretching of the rotor were the same when detected by the two optical systems, then the values obtained would be real. Table I shows some data obtained in this way in this laboratory. It is clear that the axis of rotation must have moved about 0.005 cm., and the true rotor stretch is 0.04 cm. The reference hole in the side of the rotor does not move as far, and workers who use this rotor must take this into consideration. Various values ranging from 0.02 to 0.04 cm. have been reported for the stretching of the rotor, and it seems likely that deviations from 0.03 cm. resulted from

TABLE I

Stretching of Analytical Rotors[a]

Photographic sequence	Inner reference distance (cm.)						Outer reference distance (cm.)					
	Schlieren			UV			Schlieren			UV		
	Low	High	Stretch	Low	High	Stretch	Low	High	Stretch	Low	High	Stretch
LH[b]	5.702	5.742	0.040	5.702	5.735	0.033	7.298	7.339	0.041	7.298	7.331	0.033
HL[b]	5.702	5.746	0.044	5.702	5.734	0.032	7.298	7.343	0.045	7.298	7.330	0.032
LH[c]	5.702	5.745	0.043	5.702	5.731	0.029	7.298	7.341	0.043	7.298	7.328	0.030
HL[c]	5.702	5.749	0.047	5.702	5.736	0.034	7.298	7.345	0.047	7.298	7.330	0.032
LH[c]	5.702	5.745	0.043	5.702	5.735	0.033	7.298	7.341	0.043	7.298	7.330	0.032
HL[c]	5.702	5.750	0.048	5.702	5.741	0.039	7.298	7.346	0.048	7.298	7.338	0.040

Movement of Reference on Side of Rotor

Photographic sequence	Rotor reference distance (cm.)					
	Schlieren			UV		
	Low	High	Stretch	Low	High	Stretch
L[d]	7.333			7.333		
LH[e]	7.333	7.355	0.022	7.333	7.344	0.011
HL[e]	7.333	7.357	0.024	7.333	7.342	.009

[a] All measurements were made from double exposures.
Low speed—5000 r.p.m. (L); high speed—59,780 r.p.m. (H).

[b] A rotor.

[c] D rotor.

[d] In this experiment, one counterbalance cell was placed in the rotor with an analytical cell; plug in rotor hole was removed.

[e] Two analytical cells were used; plug in rotor hole was removed.

shifts in the axis of rotation rather than from variations in the rotors themselves.

5. Analytical Cells

Cell design during the past 10 years has occupied the interest of many workers motivated by problems substantially different from those confronting the workers using the ultracentrifuge shortly after its initial development. As a result, there are now a variety of special cells for the study of small molecules, a new type of separation cell for the examination of biologically active materials, a cell for the simultaneous recording of concentration and concentration gradient, a cell in which a base line is automatically recorded along with the pattern of the unknown sedimenting substance, and a cell with a prismatic window for shifting the photographic pattern, thereby permitting analysis of different samples in a single run. There are also cells for measuring the compressibility of liquids, cells with special features for interferometric optical methods, and cells constructed of different materials for solvents which may be injurious to one or another of the cell parts.

Among the conventional sector-shaped cells themselves, there is considerable variety. For example, the optical path can vary from 1.5 to 30 mm. in different cells, and the choice of cells depends upon factors such as availability of solution and the concentration of the material. An optical path of 30 mm. is very useful for materials which require studies at great dilution. The cells with very short optical path require even less than 0.2 ml. of solution; but, of course, optical registration of the pattern suffers unless high concentrations are used. For many years, the sector angle was 4°, but cells are now available with 3°- and 2°-sectors. The latter require longer exposure times and more care in alignment of the cell in the rotor, but they have the decided advantage of requiring smaller volumes of solution. As the sector angle is decreased, surface imperfections on the sectorial walls of the centerpiece become more serious, and convective disturbances are more likely to occur (Pickels, 1942b; Moore, 1943). The existence of spurious boundaries has been attributed to irregularities in the cell wall. When these irregularities are removed by careful polishing of the walls, these boundaries, resulting presumably from accumulation of sedimenting solute at crevices, also vanish. Great care is necessary in the handling of ultracentrifuge cells to prevent the etching and scratching of the walls which would lead to bizarre ultracentrifuge patterns. In this regard, it is important that plastic cells are now available for studies of alkaline or acidic solutions. With plastic cells, no gaskets are required between the centerpiece and the windows, so that assembly of the cell is facilitated and many organic solvents can be employed without inadvertent

leakage. Both Kel-F and aluminum-filled epoxy cells are in common use. The quality of the latter is so high that they may prove to be the cell of greatest practicability and economy.

Cells with the upper window prismatic rather than flat are coming into popular use when it is desired to analyze more than one sample at a time (de Lalla and Gofman, 1954). If two cells are used simultaneously, one of these would have a wedged upper window, and the second could be either flat or wedged in the opposite direction. This has the effect of creating two slit images at the focal plane of the upper collimating lens. If nothing is done to interfere with either of these slit images, the schlieren patterns of each cell which are recorded on the photographic plate will be slightly displaced from one another. Some overlap with consequent loss of contrast results but, for many studies, the gain resulting from analysis of two samples simultaneously more than compensates for the slight loss in optical registration. Even this disadvantage can be eliminated either through the use of an optical selector (Spinco, 1954) or by means of an appropriate mask placed at the schlieren diaphragm (Trautman, 1956). The optical selector, which is more complicated and involves some additional expense, consists of a rotatable compensating prism placed in a tube above the upper collimating lens. This prism which can be adjusted to either of two fixed positions separated by 180° corrects for the bending of the light due to the prismatic windows. Thus each cell can be viewed independently of the other as desired by the experimenter. Some laboratories have used cells with positive and negative wedges along with a third cell with flat windows, so that three samples can be analyzed in a sample run. It should be noted that the wedged windows in use in these experiments deviate the light in either a centrifugal or centripetal direction. Thus light deviated by refractive index gradients within a cell may overlap with the undeviated light from the second cell with the wedged window. For interference optics with the slit at the light source oriented along the direction of the centrifugal field, separation of patterns from different cells is achieved by wedges which are perpendicular to the direction of movement of the sedimenting material. At present these wedges are in effect liquid wedges created by having the faces of the centerpiece at a slight angle relative to one another (Spinco, 1956). This causes the interference patterns from each cell to be slightly displaced from one another on the photographic plate.

a. Double Sector Cell. The double sector cell first visualized by workers (Philpot and Cook, 1948; Beams and Dixon, 1953; Milch, 1953) interested in adapting interferometric optical principles to the ultracentrifuge is now coming into routine use for additional reasons. This cell, illustrated in Fig. 4, is filled with solution on one side and solvent on the other. Since the window distortion is essentially the same across the cell (at any given

hydrostatic level), the registration on the photographic plate of the refractive index gradients in the solvent provides a base line along with the pattern of the solution. This is of inestimable value in the detection of small amounts of polydisperse material either larger or smaller than the principal component. With such material present in the solution, there will be an absence of coincidence of the patterns on either side of the boundary. Such impurities are readily detected when both solution and solvent patterns are recorded simultaneously on the photographic plate, whereas they may be easily overlooked when the patterns from separate runs of solution and solvent are compared. This is illustrated by the

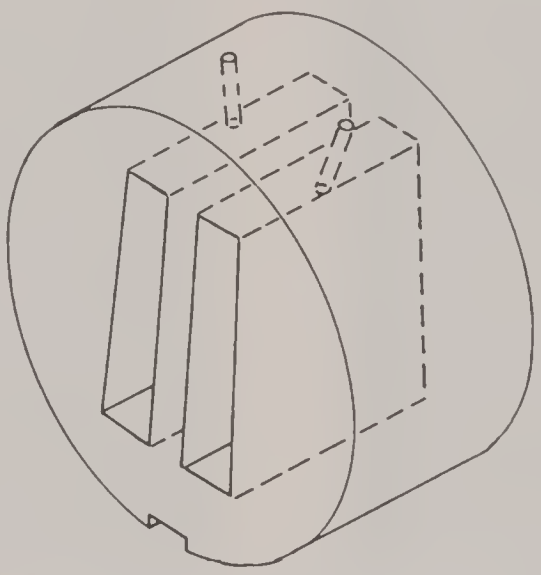

FIG. 4. Schematic drawing of a double sector cell. This type of cell is used with interferometric optical systems. Each sector has a 2.5°-angle. The solution is placed in one sectorial cavity and the solvent in the other. For schlieren optical systems, this arrangement gives simultaneous patterns of the base line (solvent) and the boundary (solution).

patterns presented in Fig. 5. Determination of the concentration of a sedimenting substance can be made with great accuracy through the use of the double sector cell since uncertainites in the base line construction are virtually eliminated. There is some loss of contrast on the photographic plate in the regions where the patterns do not superimpose; however, this disadvantage is negligible compared to the gain produced by the simultaneous registration of base lines.

The double sector cell is valuable for sedimentation analysis of multicomponent systems in which there is, in addition to the sedimentation of the protein, partial sedimentation of a low molecular weight component, such as urea, sucrose, or buffer ions. In these experiments, the refractive index gradients observed at the meniscus originate from changes in the concentration of all components. The gradients from the smaller molecular

weight component not only change with time, but they may, in fact, even exceed in magnitude those from the protein alone. This results in a pattern in which the protein boundary will be superimposed on a sloped base line. Considerable warping of the true protein pattern occurs, and appreciable errors would be made if corrections were neglected. It is essential that duplicate runs be made of the solution and solvent, and patterns from the latter subtracted from corresponding patterns of the former so as to obtain the correct pattern resulting from the sedimentation of only the macromolecules. These effects are illustrated in Fig. 6

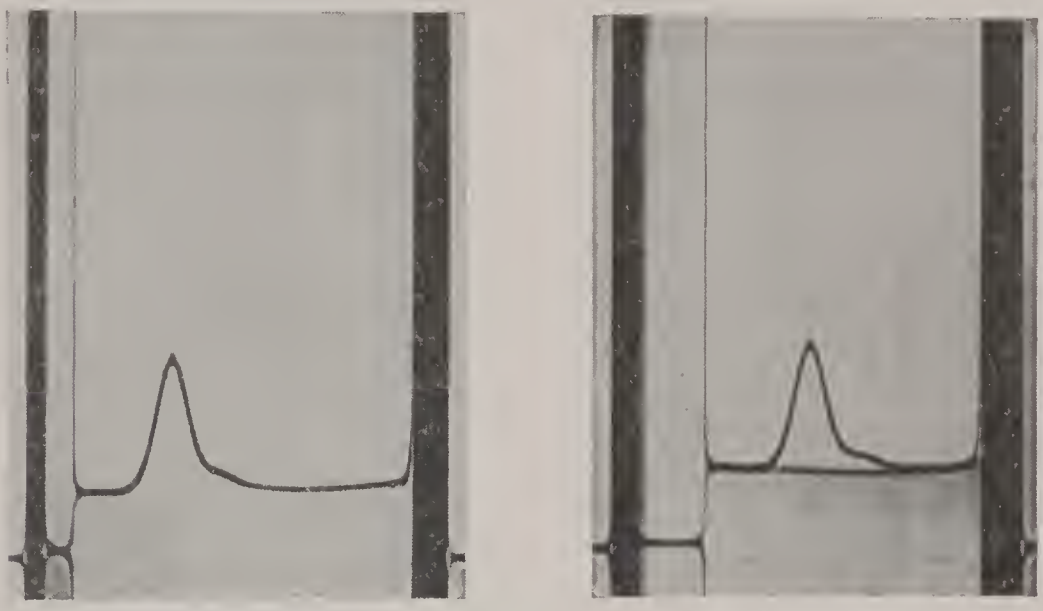

Conventional Cell Double Sector Cell

FIG. 5. Ultracentrifuge patterns obtained with a double sector cell and a conventional cell. The sedimenting material is bovine serum albumin at a concentration of 1.0 g./100 ml. in a 0.1 *M* sodium chloride solution. The presence of the base line in the experiment in the double sector cell improves the precision in the determination of the amount of the faster component.

by patterns of a protein in a concentrated salt solution. Not only is the shape of the protein pattern warped by the refractive index gradients from the salt, but even the maximum value is shifted so that an incorrect value of the sedimentation coefficient would result if corrections were not performed. Considerable saving in effort along with enhanced accuracy is effected by the use of the double sector cell which combines both runs in a single experiment. It is imperative in the use of this cell for such systems that the two compartments be filled to the same level.

For interference optical methods, the double sector cell is used with an appropriate mask containing two fine, parallel slits. The mask is actually incorporated in the holder for the lower quartz window. Thus the difference in refractive index between the solution and solvent can be

measured with great precision at any level in the cell. It should be noted, of course, that the situation in an ultracentrifuge is markedly different from that in a diffusion cell. In the latter, there is generally a gradient of refractive index in only one compartment of the cell, whereas the other is uniform with respect to refractive index. During centrifugation, there may be gradients in the direction of the centrifugal field in each of the sectors of the cell due to the redistribution of the buffer ions which are present in each compartment. In one compartment of the cell, there are also gradients caused by the sedimentation of the macromolecules.

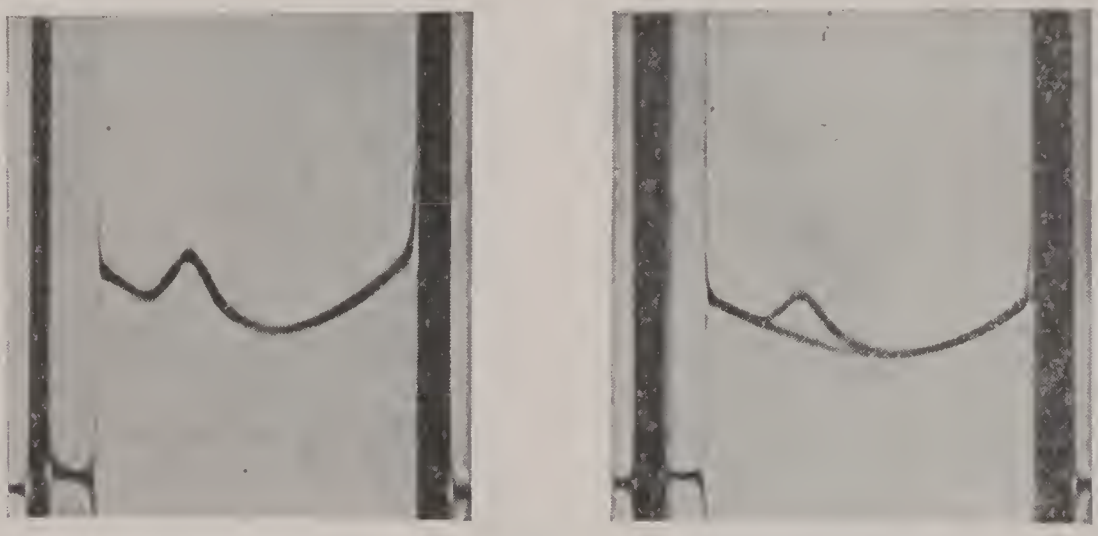

Conventional Cell Double Sector Cell

FIG. 6. Illustration of the advantage of the double sector cell in determining the correct base line. Much of the curvature of the pattern on the left is due to the redistribution of the sodium chloride, as is evident from the pattern on the right which shows the pattern from the solvent alone and from the solution containing the protein. The concentration of bovine serum albumin was 0.3 g./100 ml. and the solvent was 2.0 *M* sodium chloride.

b. Synthetic Boundary Cells. About 5 years ago, special ultracentrifuge problems involving boundaries which could not be examined by conventional techniques prompted several workers to investigate the design and construction of ultracentrifuge cells which permitted the layering of one fluid over a more dense liquid during the operation of the ultracentrifuge. As a result of these investigations, two satisfactory cells (Kegeles, 1952; Pickels *et al.*, 1952) were constructed, and many experiments of different types have been conducted with the original cells, modifications of them, or newly designed cells. A detailed comparison of the merits of the different cells has not been made, and there appear now to be four versions in active use. In three of these cells, the boundary is formed at the desired position by the slow layering of the less dense liquid onto the more dense fluid which is contained initially in the sectorial cavity of the

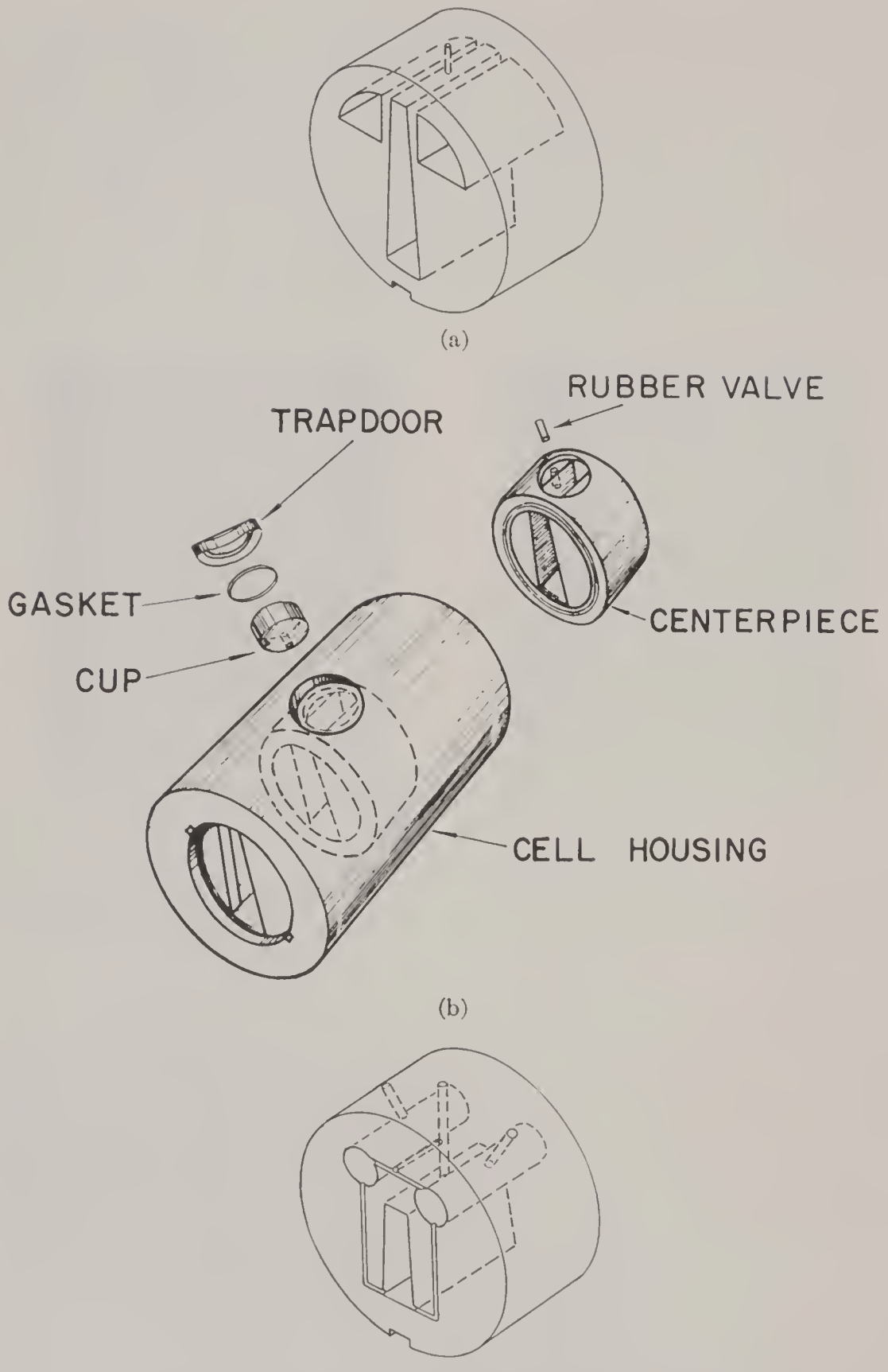

FIG. 7. Diagrams of different types of synthetic boundary cells:
(*a*) Modified cell designed by Kegeles (1952). This is a conventional metal center-

cell. The other cell (Meyerhoff, 1955), constructed of plastic so as to avoid contact of organic liquids with the gaskets which are required with metal cells, layers the more dense solution beneath the other solution, and the boundary formed at the base of the cell is then caused to move upward in the cell to a position determined by the amount of the more dense liquid which can flow into the sectorial opening from an independent reservoir. A very recent cell for use with interferometric optical methods employs the plastic, double sector cell modified by the accurate placement of fine grooves connecting the two channels. The lower of these grooves acts as a path through which the less dense liquid flows to layer onto the other solution. In order to prevent the development of air pressure in the compartment into which liquid is flowing, a second connecting groove is pressed into the surface of the center plastic rib near the very top of the cell. Diagrams of three of the synthetic boundary cells are shown in Fig. 7.

There is still not a completely satisfactory name for such cells although "synthetic boundary cell" is being used rather widely. It appears that the version of the cell now commercially available (Spinco, 1955) is the most flexible in design, although the cell constituted by Kegeles (1952) may be more satisfactory for volatile solvents. From the patterns that have been published to date with the different cells, it seems that the cell containing a cup and a rubber valve to control the layering process produces the sharpest and most nearly symmetrical boundaries. It is not at all unlikely, however, that new designs or further modifications of existing cells will lead to boundaries of higher quality and greater reproducibility. Among the various applications of these synthetic boundary cells are the determination of the sedimentation coefficient of a small molecule in the presence of a more rapidly migrating component, the measurement of the

---

piece into which two reservoir chambers (for solvent) are machined. The reservoirs are open on one face only. During acceleration of the rotor, the liquid flows between the surface of the centerpiece and the quartz window into the sector opening where it layers on the solution.

(*b*) New version of the cell designed by Pickels *et al.* (1952). This cell contains a rubber plug which acts as a valve, closing the exit hole in the cup containing the solvent. Upon acceleration of the rotor, the rubber valve is compressed, allowing the liquid to flow through the hole in the cup into the sectorial cavity where the boundary is formed.

(*c*) Cell proposed by Meyerhoff (1955). This is a plastic centerpiece onto one surface of which are engraved fine grooves. These grooves, after the quartz window is in place, act as capillaries to conduct the solution (the more dense of the two liquids) from the upper reservoir chambers to the bottom of the sectorial opening. In this way the solution is layered beneath the solvent, which is initially placed in the sectorial cavity. After the boundary is formed at the bottom of the opening, it is displaced upward by the continued flow of solution.

displacement of an indicator boundary due to the backward flow of liquid caused by the sedimentation of much larger components, the study of interacting components, the determination of differential sedimentation rates, the evaluation of sedimentation coefficients for molecules even as small as sucrose, and the measurement of diffusion coefficients even at great dilution. Most of these experiments could not have been done without such a cell, and the remainder would certainly not have been performed as conveniently nor perhaps as accurately.

Like the double sector cell, the synthetic boundary cell is of value in minimizing the problems of establishing the base line. Here we are referring to the difficulties of determining the contribution of the sedimentation of a small protein to the observed pattern when the partial sedimentation of buffer ions or another component such as urea causes a large gradient at the top or bottom of the cell. With the synthetic boundary cell, the protein boundary is created near the middle of the cell or, in any case, at some distance from the air-liquid meniscus. As shown in Fig. 2, the changes in concentration of slowly sedimenting material occur predominantly at the two ends of the cell. There is a region near the center of the cell in which the concentration hardly changes for many hours. Thus the refractive index gradient of a boundary formed near the center of the cell can be observed without being complicated by superimposed gradients resulting from redistribution of other components. Not only is this optical distortion avoided by the use of the synthetic boundary cell, but also the composition of the medium in the vicinity of the boundary is known. In experiments in conventional cells, the composition of the medium is changing continuously in the region where the boundary is observed.

c. Separation Cells. Techniques have been available for some time whereby an ultracentrifugal analysis of a biologically active material can be conducted even on impure preparations and with only microgram quantities. Despite the power of the method, it has been used infrequently. Experiments until recently were performed in the separation cell of Tiselius *et al.*, (1937). This cell contains a thin, perforated plate placed at right angles to the direction of sedimentation at a fixed position two-thirds of the distance from the top to the bottom of the cell. A piece of filter paper is overlaid on the plate, and this combination serves to divide the contents of the cell into two parts at the conclusion of the run. Implicit in the use of this cell is the assumption that the partition does not interfere with sedimentation during the experiment and that ideal, convection-free sedimentation occurs throughout. For some types of experiments, this assumption is of questionable validity since data do show that the partition is a barrier to sedimentation (Harrington and Schachman, 1953). As a consequence,

there is a pile-up of sedimented material on the filter paper. This coupled with independent sedimentation in the lower compartment produces a density inversion just below the partition, and convective flow of liquid ensues. Epstein and Lauffer (1952) circumvented the effect of the barrier by adding a small amount of sucrose to the solution below the barrier, thereby causing this solution, even if there is some removal of solute by sedimentation, to be heavier than the solution centripetal to the partition. In this manner, the disturbances in the upper liquid can be effectively eliminated.

Yphantis and Waugh (1956b) adopted the view that a satisfactory separation cell should fractionate the contents of a solution at the termination of the run and that the separating device should not be in the path of sedimentation during the actual ultracentrifuge experiment. Accordingly, they arrived at a design in which the separation plate was, in effect, spring-mounted. At high centrifugal fields the plate, made of plastic and not perforated, is forced to the bottom of the cell, collapsing the rubber strips which serve as a spring. The plate now acts as a cell bottom, and the cell simulates a conventional ultracentrifuge cell. On deceleration, at 2000 to 3000 r.p.m., the centrifugal force on the plate is no longer sufficient to counteract the lifting action of the rubber springs, and the plate rises very slowly until it comes to rest against specially constructed stops in the centerpiece. If the cell and the movable partition are made and assembled correctly so that there is a precise fit when the plate is in its rest position, the solutions in the two compartments are effectively isolated from one another. Static experiments with a dye present in the centrifugal compartment and absent in the centripetal part showed that there is little mixing of the liquids when the cell is handled in a fashion simulating a typical ultracentrifuge experiment. Thus a fractionation could be performed at the conclusion of the experiment with little risk of mixing of the two solutions. Similar tests of the functioning of the cell revealed that the slow movement of the partition from the bottom of the cell to its rest position causes little or no generalized stirring of the contents of the cell. In experiments in which the partition was caused to move back and forth through a boundary of 0.5% bovine plasma albumin by the alternate deceleration and acceleration of the rotor, there was only a little distortion of the boundary. Moreover, there was no discernible disturbance in the pattern centripetal to the rest position of the plate. Thus the small disturbances created by the movement of the partition through a boundary do not lead to transport of solute into the centripetal compartment. It is of interest that the liquid must flow around the partition when it moves through the cell, since the platform is not perforated.

The success of this technique depends, as in the case of the synthetic

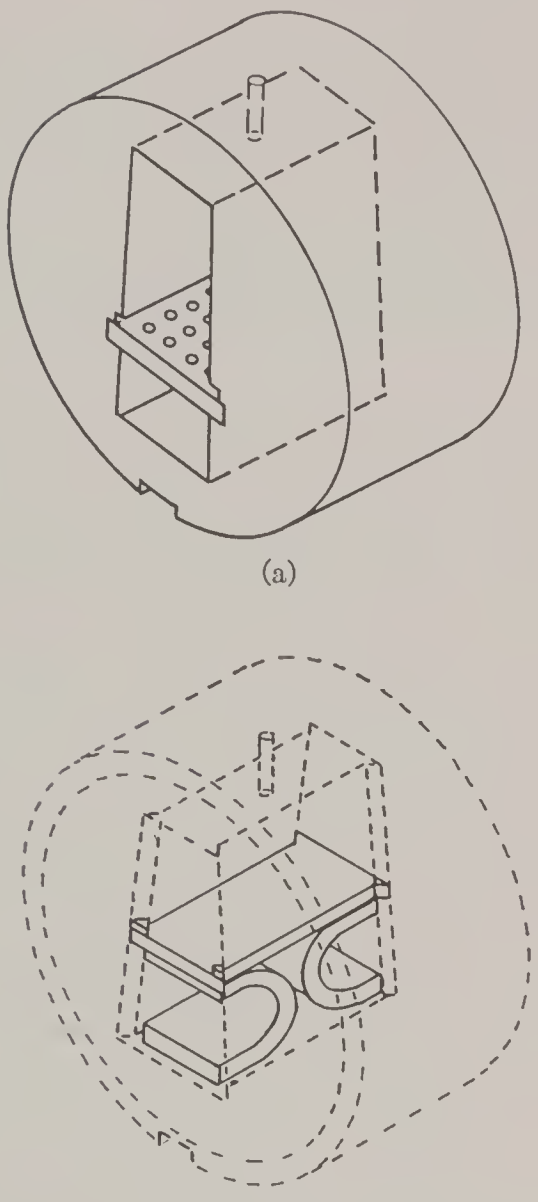

FIG. 8. Diagrams of separation cells:

(*a*) Fixed partition cell (Tiselius *et al.*, 1937). In this cell, a fixed, porous metal plate is built into the cell at a position about ⅔ of the distance from the centripetal surface. Filter paper is overlaid on the metal plate, and this unit acts as a barrier against mixing of the contents of the upper and lower compartments at the conclusion of the experiment. The sedimentation of the macromolecules occurs through the filter paper-plate combination.

(*b*) Movable partition cell (Yphantis and Waugh, 1956b). The partition in this cell is supported by two synthetic rubber strips which act as a spring. Under the influence of the centrifugal field developed during acceleration of the rotor, the plate, which is solid and plastic, settles to the bottom of the cell. Sedimentation then occurs undisturbed by the presence of the barrier at the bottom of the cell. At the conclusion of the run, during deceleration, the rubber springs cause the plate to rise slowly to its rest position, thereby effecting a separation of the contents of the cell into centripetal and centrifugal fractions which can be removed readily without intermixing.

boundary cell, on the stability resulting from magnification of small density gradients under the influence of a centrifugal field. Whereas stirring of stratified layers of solution differing in density by only 0.001 g./ml. will occur readily when the liquid is subject to the force of gravity only, such stirring will not take place in a centrifugal field in which the force on the liquids is many hundreds of times that of gravity.

There is not as yet sufficient experience with the movable partition cell for a detailed comparison with the older separation cells. Both cells are illustrated in Fig. 8. Though functioning in quite different ways, they achieve, to more or less the desired extent, the same purpose. It appears that the newer cell will function better for proteins and low molecular weight solutes for which unrestricted diffusion is essential. On the other hand, for larger materials, packing of the sedimented material onto the movable plate may lead to contamination at the end of the run, and the fixed partition cell may therefore be the cell of choice. Further experimentation by many workers will be necessary before definitive conclusions can be drawn.

d. Other Cells. Until very recently the optical systems employed in ultracentrifugation, with the exception of the light absorption system, produced curves of refractive index gradient versus distance from the axis of rotation. For sedimentation equilibrium experiments, however, it is useful to have the concentration distribution throughout the cell. Such information would then eliminate the need for precise knowledge of the total amount of solute in the cell as well as the necessity for a tedious integration of the gradient curves. To accomplish the purpose of providing concentration data even with the existing optical methods, Kegeles (1947) designed a double prismatic cell containing the solution in one prismatic chamber and the solvent in the other. Light traversing this cell enters normal to a window, as in most cells, and then passes through about 4.6 mm. of a protein solution before it strikes a glass window, inclined at an angle of 41°. The light striking this window is deviated in a direction perpendicular to the direction of sedimentation and then passes through an almost equivalent thickness of liquid containing pure solvent before leaving the cell through a window parallel to the entrance window. In addition to the deviation mentioned above, which is a function of the prism angle and the difference in refractive index between the two liquids at any level, there is also a deviation of light along the direction of sedimentation which is related to the refractive index gradient at each level. With this cell and the Lamm scale method (1937) modified by the addition of a scale line perpendicular to the ordinary numbered scale lines, Kegeles obtained simultaneously the concentration distribution and the variation of concentration gradient with distance through the cell. Since the descrip-

tion of this cell and its application to the study of the sedimentation equilibrium of ovalbumin, there have been no further examples of its use despite the promise it offers.

There have been occasional reports of other types of cells for specific purposes. Sharp (1949) has described a cell into which a collodion coated plate is inserted for collecting the sedimented material from a known volume of solution. The collecting screen can then be placed directly in the electron microscope. In this way, counting of the number of particles on the screen gives directly the number of particles per unit volume of solution. This number, along with a reasonable value for the density of the material, is then compared with the measured dry weight of the solute. The results of this comparison provide a valuable criterion of the purity of the countable particles.

In the author's laboratory, a special cell has been used for the measurement of the compressibility of some of the liquids employed in ultracentrifugation. Rather than using conventional, sector-shaped cells in which the movement of the meniscus is very slight due to compression of liquids, we have constructed a cell containing a large reservoir, made as flat as possible, connected to a thin vertical slit in which the liquid meniscus is observed. Thus small volume changes in the liquid when it is subjected to the pressure generated at high centrifugal fields are more readily measured because the movement of the meniscus (from low to high speed) is effectively magnified. The vertical column is as long and thin as possible compatible with simplicity of filling of the cell and the cell size. Movement of the meniscus in such a cell may be as large as several millimeters. Although some distortion of the cell windows still occurs, the contribution of the increase in volume of the cell (resulting from the bulging of the cell windows) to the movement of the meniscus is appreciably less in this modified cell than in the sector-shaped cell (Cheng and Schachman, 1955b). Further, this increase in volume of the cell resulting from distortion and bulging of the windows is reproducible, so that comparative or relative compressibilities of different liquids can be readily determined.

6. Optical Methods

The revolution which has occurred in the measurement of diffusion coefficients during the past 10 years has its origin in the adaptation of interferometric optical methods to diffusion experiments. Unfortunately, at this writing, comparable progress in ultracentrifugation has not been realized although there have been very substantial changes and improvements in the past 10 years, and interferometric methods are just coming into use.

Most early ultracentrifuge experiments were based on the differential

absorption or scattering of the sedimenting material as compared to the solvent. At first, visible light was used, but this was soon replaced by ultraviolet light since most biological substances absorb this light whereas the solvents are generally transparent. These light absorption methods were early superseded by techniques which were based on the observation and analysis of the deviations of light rays which pass through regions of a solution containing refractive index gradients. The first of these refraction methods was that developed by Lamm (1937), known as the scale method. In the late 1930's two different refraction methods, classified as schlieren methods, were adopted by many workers. This occurred because both the cylindrical lens (Philpot, 1938; Svensson, 1939, 1940) and scanning methods (Longsworth, 1939) provided, on the photographic plate, tracings of the refractive index gradient versus distance in the cell, whereas the construction of analogous curves with the scale method required many hours of tedious labor. In just the past few years, there has occurred the adaptation of interferometric methods to ultracentrifugal analysis in the form of a modified Jamin interferometer and the Rayleigh interferometer. Experience with the latter methods is at the moment very limited, and predictions of their applicability to ultracentrifugation are, of necessity, hazardous. To this reviewer, it appears likely that future applications of the ultracentrifuge will involve principally three optical systems: the absorption method, the cylindrical lens method, and the Rayleigh interferometric method.

It is important to bear in mind that the optical problems are compounded when the different methods are adapted to the analysis of refractive index changes in a cell which is revolving about some axis of rotation. Boundaries representing changes in index of refraction with distance are not planes, but rather they are surfaces of a cylinder. Further, the cells sweep by a fixed optical bench which is generally aligned with some stationary, ruled glass scale in place of the cell. Since the photographs are not taken by means of high speed photography synchronized with the speed of the rotor, the patterns represent time averages of the different patterns which would be obtained with the cell and boundary placed at various orientations relative to the axis of the optical system. Since boundaries in an ultracentrifuge cell are nonplanar, the cylinder lens cannot, of course, be oriented correctly in relation to the entire cylindrical cross section of the cell. As the cell sweeps by the light beam, the refractive index gradient along a given arc will have varying angles of inclination to the axis of the cylinder lens. Depending upon the limiting aperture that is used to restrict the time of observation of the cell during a single rotation, these angles can be more or less significant. Ideally, the limiting aperture placed in the chamber above the rotating cell should be extremely narrow, but the

amount of light reaching the photographic plate would then be so small as to require exposure times that are prohibitively large. As a consequence, a compromise is made. This aperture is sufficiently large in current instruments that the arc generated by a rotating cell containing a boundary, or the air-liquid meniscus, or even a small straight edge, is readily discernible if the cylinder lens is removed. Since the optical system records the refractive index gradients in a series of parallel planes (instead of cylindrical surfaces), the gradient recorded for each plane must represent some average of the true gradients at corresponding levels in the cell. At present these effects, which are no doubt small, are ignored. Schlieren methods are not sufficiently sensitive to detect these effects, but they are worthy of attention in considerations of the design of interferometric optical systems.

a. Lamm Scale Method. A precisely and uniformly ruled glass scale, which is illuminated by monochromatic light, is focused by an appropriate lens onto a photographic plate. Between the scale and the lens at a distance of a few centimeters from the scale is the rotating cell. When the cell is uniform in refractive index, the photographic image of the scale bears a simple relationship to the scale itself, with the lines on the image corresponding faithfully to those on the scale. If, however, there is a boundary in the cell, the light rays passing through the boundary will suffer deviations proportional to the refractive index gradient at each level, and the images of the scale lines corresponding to those positions will be shifted accordingly. From the measured positions of the image of individual scale lines relative to their positions in the absence of a boundary, a plot is constructed of the deviation (or refractive index gradient) versus distance in the cell. Details of this method and analysis of some of its problems are presented by Lamm (1937), Geddes (1949), Nichols and Bailey (1949), Bridgman and Williams (1942), and Adler and Blanchard (1949).

This method, now used only rarely, has been discarded not because other methods are more accurate but rather because of the very tedious work involved in reading the plate and converting the measured values into a plot of refractive index gradient versus distance.

b. Schlieren Methods. Almost simultaneously, the schlieren method which originated with Thovert (1914) was modified in two different manners, the first by Philpot (1938) and Svensson (1939, 1940), to give the cylindrical lens method, and the second by Longsworth (1939), resulting in the schlieren scanning optical system. With the gradual development of cylindrical lenses of high quality, the schlieren optical system using this lens has become the more popular. As a consequence, most ultracentrifuge workers today employ this method for viewing and analyzing refractive index gradients.

Light from an intense source passes through a horizontal slit which

is oriented perpendicularly to the direction of the centrifugal field, and is collimated by a lens at the base of the vacuum chamber. The resulting parallel light traverses the rotating cell and is focused by a condensing lens located at the top of the vacuum chamber to give an image of the light source. The collimating and condensing lenses are frequently termed "schlieren lenses" and are used in present instruments rather than the single schlieren lens which had been used earlier with much longer optical tracks. If the liquid in the rotating cell is homogeneous with respect to refractive index, a single image of the slit is produced. In the presence of a refractive index gradient, light rays passing through the cell in the region of the boundary will be deviated, in the direction of increasing refractive index, by an amount directly proportional to the magnitude of the gradient at that level. As a consequence, a series of images of the slit are produced at the focal plane of the upper schlieren lens. The principal or uppermost image arises from all the light rays passing through the regions in the cell which are homogeneous with respect to refractive index regardless of whether these regions contain solvent or solution. At the lower extreme of this group of images, which appears as a band of light, is the image corresponding to the maximum refractive index gradient. It is important to recall that the deviation is toward the higher refractive index and that upper and lower directions, as used here, imply a vertical cell with a boundary in a horizontal plane. In the ultracentrifuge, "upper" is the centripetal part of the cell and "lower" is in the centrifugal direction.

Beyond the plane containing the images of the light source is a camera lens which collects all these rays and images the ultracentrifuge cell on the photographic plate. Since the cell has appreciable thickness along the optical path, there are problems of focusing the camera lens. For some time, it has been the practice to focus the camera lens on a plane at the center of the cell, but recent discussion of this point indicates that perhaps the lens should be focused on a plane two-thirds the distance from the entrance plane (Svensson, 1954; Forsberg and Svensson, 1954). With no mechanical devices to interrupt the deviated light at the focal plane of the upper condensing lens, all the rays will reach the plate, and the cell will appear uniformly illuminated. Thus no boundary could be detected even if present. The schlieren methods function by interfering with the deviated light in some manner or other. In the scanning method, this interference is in the form of an opaque edge which can be moved in a vertical direction in the plane of the slit images to cut off first the most deviated light, then a little more light which contains some less deviated rays, and so on until all light is cut off. Coupled with the movement of this knife edge is the horizontal movement of the photographic plate behind a very thin slit. The resultant picture would then be a continuous

series of very thin vertical streaks of light imaging the vertical coordinates of the cell with some horizontal dark bands which depend upon the location, shape, and magnitude of the refractive index gradients. As indicated already, the scanning knife edge at its lowest position would not block any light, and upon its vertical movement gradually a band of light would be interrupted, with the band increasing in thickness until finally all light is cut off. The resultant pattern would be a plot of dn/dx versus x where dn/dx is the refractive index gradient (n being refractive index and x being the distance along the cell).

A similar plot is achieved without moving mechanical parts by the combination of a diagonal knife edge (in place of the horizontal one) and a cylinder lens with its axis vertical (or perpendicular to the plane of the boundary) and so placed as to focus the plane of the knife edge on the photographic plate. In a vertical direction this cylinder lens has no effect, and therefore vertical coordinates in the cell (distance from the axis of rotation) are still faithfully imaged by the camera lens. In order to describe this method, it may be easier to consider instead of a single knife edge a thin slit through which light rays can pass. With this slit at some fixed angle, all undeviated light passes through the slit at a given point (with a fixed horizontal coordinate). This light then passes through both the camera lens and the cylinder lens to form a thin vertical line whose vertical coordinates are images of the cell, and whose position in a horizontal direction depends on the cylinder lens. Light rays passing through the boundary are deviated vertically, and as a consequence of the diagonal slit, they pass through the slit at some horizontal displacement relative to the undeviated light. As before, the greater the refractive index gradient, the greater will be the vertical deviation and, therefore, the greater the horizontal displacement. Thus these deviated rays will strike the cylinder lens at different places and will be focused on the photographic plate at different horizontal positions. They will, however, not suffer any vertical displacement. In this way, the vertical coordinates measure distance in the cell, the horizontal coordinates indicate the refractive index increment, and the continuous tracing produced at the photographic plate gives a plot of dn/dx versus x. The visualization of this pattern directly on a screen comprises one of the principal merits of the cylindrical lens method.

The sensitivity of the schlieren optical systems is readily altered. In the scanning method, a change in gears so as to make the plate travel much faster than the vertical knife edge magnifies the height of the apparent "peak" on the plate. A similar effect is achieved in the cylinder lens method by orienting the diagonal slit so that the angle of inclination to the plane of the boundary is very small. Thus very small vertical deviations of light are caused to suffer large horizontal displacements in

terms of their passage through the slit. Consequently, they strike the cylinder lens at a great horizontal distance from the undeviated light rays and cause tall peaks in the resultant pattern.

Various types of schlieren diaphragms have been proposed and employed in both the scanning and cylindrical lens systems. Most workers have now adopted either a bar (Pickels, 1942a), a wire, sometimes, or a narrow slit (Moore and White, 1948). With the former, the photographic plate shows a light tracing of the pattern on a dark background, whereas the latter produces the converse distribution of light and dark. Since the opaque edge which interrupts the deviated light to produce a shadow is not in focus at the photographic plate, the transition from light to dark on the plate is not sharp, and along with this diffuse transition is a series of diffraction fringes in the illuminated area at the edge of the pattern (Longsworth, 1943). It is difficult, therefore, to locate on the photographic plate the positions corresponding to the true geometric edge of the bar or wire. As a consequence, there is uncertainty in determining the correct value of the refractive index gradient at different parts of the boundary. Variations in exposure time markedly affect the apparent location of the geometric edge, and very large errors often result from analysis of patterns obtained with a single edge as the schlieren diaphragm. With a bar, however, two patterns are produced, and similar treatment of these patterns eliminates errors of this type. Kegeles and Gutter (1951) pointed out that over-exposed schlieren patterns with a bar as the diagonal diaphragm exhibit a symmetrical system of fringes within the geometrical shadow. These fringes, which are analogous to the Fresnel diffraction pattern from a wire, can be used for accurate measurements of boundary position and for area determinations when concentrations of the sedimenting substances are desired.

Since the patterns with bars are very thick and therefore necessitate the construction of two independent tracings, several workers (Baldwin, 1953b) have employed a thin wire (0.020 in.) as the schlieren diaphragm. This functions satisfactorily for the base line and for boundaries which are not too steep, but optical registration for sharp boundaries is very poor. Consequently many workers view with considerable enthusiasm the introduction very recently of a new type of schlieren diaphragm which seems ideal in nearly all respects. Wolter (1950) suggested the incorporation of the principle of the phase contrast microscope into schlieren optical systems. This takes the form of the insertion of a completely transparent phase plate as the schlieren diaphragm. A phase plate is an optical glass disc half of which is coated, on one surface only, with a thin transparent film of thickness such that rays passing through the coated portion are one-half a wavelength out of phase with adjacent rays passing through the

uncoated portion. The optical edge between the uncoated and coated portions thus replaces the opaque edge of mechanical diaphragms by causing destructive interference among rays suffering essentially the same deviations due to the refractive index gradients within a boundary. The shadows thus produced are very sharp and well defined, thereby permitting precise determination of the refractive index gradient at different places in the boundary. Unfortunately, with ideal optical adjustment, the base line and the maximum refractive index gradient are not registered with a phase plate presumably because of the absence of pairs of light rays which can destructively interfere to produce a null in light intensity. Trautman and Burns (1954), in a thorough study of the theory and experimental test of a phase plate in the cylindrical lens system, suggested the incorporation of an extremely thin wire (0.003 in.) superimposed on the phase border for the optical registration of base lines and maxima in the gradient curves. This combination works extremely well, and the present, commercially available phase plates now possess a fine opaque line of evaporated metal along the edge of the coating. This line functions as an opaque edge for recording the base line, while the phase plate creates the shadow for regions of the cell containing the boundary. There is already sufficient experience with the phase plate, since Trautman and Burns experimentally demonstrated its great potential for different types of ultracentrifuge boundaries, to draw the conclusion that very large increases in precision will be obtained through its uses. Figs. 5 and 6 show some typical patterns with the phase plate as the schlieren diaphragm. These can be compared with the patterns shown in Fig. 19, which were taken with a bar as the schlieren diaphragm.

c. Interference Methods. With the development of the phase plate as the schlieren diaphragm and the production of cylindrical lenses of high optical quality, the schlieren methods in practice now appear to be limited no longer by experimental errors but rather by the theoretical limitations in the theory for the bending of light in refractive index gradients. As in the study of diffusion, further progress in analyzing boundaries in the ultracentrifuge would seem to depend on the adaptation of reliable interference optical systems. At this writing, two such systems are just coming into use and a discussion of them follows.

Jamin or Mach-Zender interferometer. Beams and co-workers (1954) have employed a modified Jamin interferometer in combination with a light chopper for measuring the differences in refractive index between a solution and a solvent at different levels in the ultracentrifuge cell. The system is mechanically and optically very complicated containing 6 mirrors and numerous slits and lenses in addition to the interferometer plates, and it is questionable whether alignment and use of this system could become

a routine operation in many laboratories. Figure 9 is a schematic diagram of the system. Monochromatic light is focused by a lens in conjunction

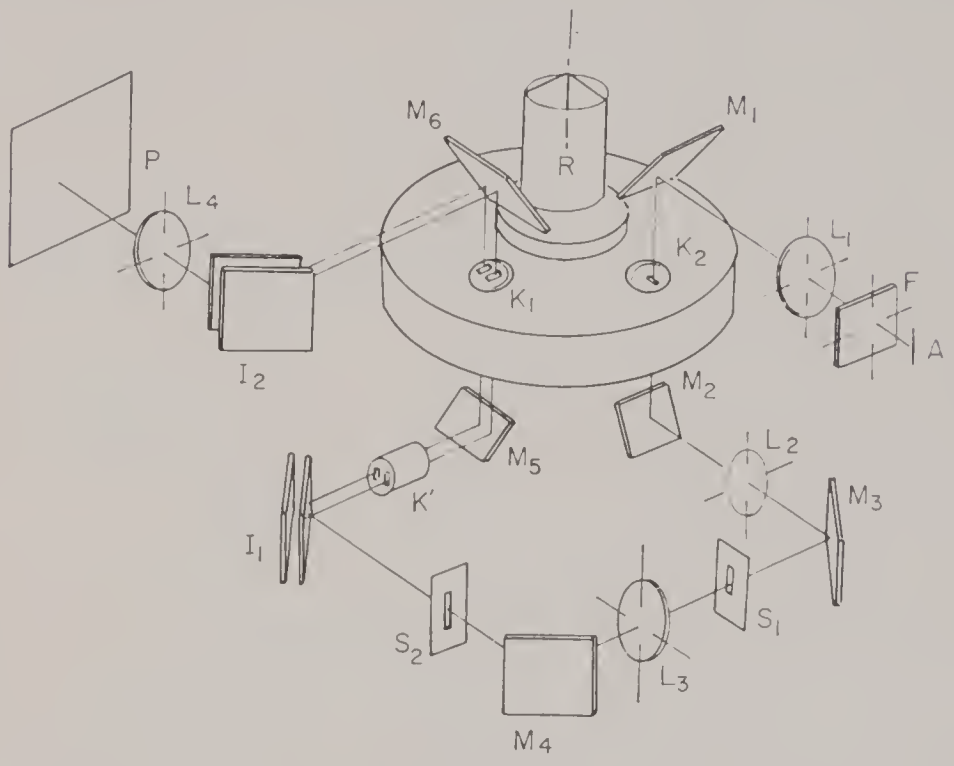

FIG. 9. Schematic diagram of the modified Jamin interferometer used by Beams *et al.* (1954). Light from a mercury arc, A, is filtered by an interference filter, F, and then focused by the lens, L_1, on a narrow radial slit at K_2 after being reflected by the mirror, M_1. The slit is placed 90° ahead of the double sector cell and acts as a light chopper. Only when the narrow slit is over the beam from L_1 does light pass through the cell which is at K_1. After the light passes through K_2, it is reflected by the mirror, M_2, and focused by the lens, L_2, after reflecting from the mirror, M_3, onto the narrow slit, S_1. The lens, L_3, renders the light parallel, and it is again reflected by a mirror, M_4. The single parallel beam is narrowed by the slit diaphragm, S_2 and is split into two parallel beams by the interferometer plates, I_1. The two parallel beams pass through a cell, K', which is a duplicate of the ultracentrifuge cell, and are reflected by the mirror, M_5, so as to pass through the rotating cell, K_1, onto another mirror, M_6. Then the beams are recombined by the second pair of interferometer plates, I_2. The lens, L_4, focuses the cell onto the photographic plate where the interference fringes are recorded. The cell, K', is a compensating cell in which the solution and solvent are reversed relative to the rotating cell. This pair of cells in conjunction with white light (filter, F, removed) serves to locate the position in the cell at which the concentration is equal to the initial concentration. For sedimentation velocity experiments, this compensating cell is not used, since the plateau region is readily observed.

with a mirror onto a narrow radial slit mounted in the centrifuge rotor in a position 90° removed from that of the double sector cell. The light traversing this lit, only for a brief period every revolution, then strikes several mirrors and lenses where it is made parallel and passes through a slit diaphragm of about the same width as the sector-shaped cells. Before

passing through the cell, the parallel light is separated into two beams by the beam splitting interferometer plate combination. This interferometer mirror is composed of two accurately parallel plates, the first of which is only partially reflecting so that some of the light is transmitted, only to be totally reflected by the second plate. By this combination, two parallel beams of light are created from the single entrance beam. These beams strike a mirror which directs them vertically through the double sector cell onto another mirror which directs the resultant light beams onto another interferometer plate which reflects the single recombined light beam onto the photographic plate. In addition to the lens in the optical system which focuses the fringes on the plate, there is an independent lens which focuses on the cell. This camera lens focuses the cell in both the radial direction and in a direction perpendicular to the radius. Thus gradients across the cell as well as along the cell can be measured precisely.

If the refractive index difference between the solution and solvent were constant throughout the radial length of the cell, as it is before centrifugation begins, a series of parallel fringes would appear on the photographic plate. These result from the constructive and destructive interference among rays originating at the same source and following different paths (through the two cells) to the photographic plate. Such fringes are observed only with monochromatic light. With white light as the source, an intense central fringe will be observed only if the optical path lengths from source through the cells to the plate were the same, i.e., if the refractive index of both liquids were equal. To compensate for the different path lengths through the cell, this apparatus has facilities for incorporation of a duplicate ultracentrifuge cell on the outside of the vacuum chamber. This cell is filled in a manner opposite to the revolving cell so that the two light beams from the interferometer plate pass through solution and then solvent, on the one hand, and through solvent and solution on the other. With the use of this compensating cell, a single central straight fringe is observed before redistribution of the solute begins. After some changes in concentration occur in the revolving cell, there will be only a very small region in the cell possessing a concentration equal to the initial concentration, and the white light reference fringe will be observed for only that region in the ultracentrifuge cell. Insertion of the appropriate interference filter to isolate the desired monochromatic light produces a series of curved fringes throughout the entire cell. Each of these is a section of a curve plotting refractive index versus distance. Instead of attempting to follow the contour of a single fringe throughout the cell, which in principle would give the concentration at every level, the number and position of the fringes is recorded in a radial direction. Each fringe corresponds to a given refractive index difference between solution and solvent, and therefore the

fringes are a measure of concentration. With the use of the white light and the compensating cell, the central fringe is located. Thus the fringe on either side of this position can be numbered. From the known optical constants of the instrument and the concentration and the refractive index increment of the solution, each fringe can be related to a specific concentration. In this way, the concentration of solute throughout the cell is precisely determined.

A basic feature of this optical system developed by Beams and co-workers (1954) is the light chopper which permits light to pass through the cell during only a very small rotation about the axis. In this way, the patterns simulate those which would be obtained if the rotor were stationary during the sweep by the optical bench. Rather than attempting to synchronize a light source with the speed of the rotor, these workers employ the rotor itself as a chopper allowing light to pass through a slit in the rotor 90° ahead of the cell. Only when this slit is over the light beam can light pass through the optical system. Viewing occurs while the cell turns through an angle of only 0.003 radian. Incorporation of this light chopper complicates the mechanical and optical problems, but the results with this method are certainly very promising (Beams *et al.*, 1955).

Rayleigh interferometer. The second interference optical system presently adapted to ultracentrifugal studies is the Rayleigh method. For the incorporation of this system (Philpot and Cook, 1948; Svensson, 1949, 1950) to ultracentrifuges already in use with schlieren optics, relatively minor changes were required in the existing instrument, and an important feature of its design is its complete compatibility with the cylindrical lens system. As a result, patterns can be observed with either system while the ultracentrifuge is in operation by making changes only in the orientation and length and width of the slit at the light source.

In a Rayleigh interferometer as used by Longsworth (1951), monochromatic light from a point source passes through a lens which focuses an image of the source onto a plate. Between the lens and the plate is the double cell, containing solution in one limb and solvent in the other. At the entrance window to the cell is a special Rayleigh mask containing two vertical slits of definite width and separation. Light rays from the source pass through the two halves of the cell and then recombine to produce the Rayleigh fringes which are caused by the vertical slits. In order to focus the vertical coordinates of the cell on the photographic plate, a cylinder lens with a horizontal axis is inserted at the appropriate place on the optical bench. This lens does not affect the horizontal spacing of the fringes. If the optical system were to be used in that form, which places great demands on the quality of the cylinder lens, it would preclude simultaneous use as a schlieren system. Therefore, we will turn to other forms of the Rayleigh

interferometer which have been adopted for diffusion experiments, but first we will examine briefly the simple interferometer.

Because of diffraction of light by the edges of a single slit, the light pattern from a single slit will consist of a fairly broad central band with bands of much less light intensity on either side. The bandwidth is proportional to the wavelength of the light and inversely proportional to the width of the slit in the mask. With two slits instead of one, there is a finer structure within the bands of light. This results because light rays passing through the two slits to the photographic plate will traverse paths of different lengths. As a consequence, there will be constructive and destructive interference at different horizontal positions in the central band of light, and this band instead of being continuous, as with a single slit, will be made up of alternate dark and light regions known as interference fringes. For our purposes, it is important to note that the fringe spacing in this band is proportional to the wavelength of light, and the number of fringes depends on the separation of the slits in the mask.

If the liquid in the two halves of the cell is the same, e.g., solvent, the fringes will be straight, and the central fringe corresponding to the center of the slit image originates from rays having equal path lengths. The first fringe on either side of this central or zeroth fringe corresponds to path lengths from the two cells differing by 1 wavelength of light. The second fringe on either side of the central fringe corresponds to path lengths differing by 2 wavelengths, and so on for successive fringes. Replacing the solvent in one cell by solution will cause a shifting of the fringes, but they will still remain straight, and a cursory examination of the pattern will not reveal any changes. This shift in the position of a given fringe to a new position results because the optical path in one cell is altered due to the change in refractive index. For there to be constructive interference, there must be a corresponding change in the geometric path in air so that the total optical path remains unchanged. Thus the central and all other fringes will be shifted by a distance related to the refractive index change. If instead of each of the solutions being uniform in a vertical direction, one contains a boundary separating uniform regions of solvent and solution, the fringe pattern would contain straight portions, corresponding to the top and bottom regions of the cell, separated by a region of curved fringes at the level of the boundary. In fact, each fringe describes a curve of refractive index versus distance. Because of the limited width of the central diffraction band, only about 7 fringes can be observed, and therefore a single fringe cannot be traced throughout the whole pattern unless the refractive index change across the boundary is very small. The displacement of a fringe, shown hypothetically in Fig. 10, can be reported directly in fringe numbers, rather than in terms of distance, and this can be meas-

ured precisely even in the absence of a complete pattern by counting the fringes crossed in traversing the boundary. Even though the fringe shift is perpendicular to the length of the fringes, this lateral displacement in terms of number of fringes is readily determined by counting the fringes crossed in following a given fringe from one side of the boundary to the other. From the number of fringes, J, the thickness of the cell along the optical path, a, and the wavelength, λ, of the monochromatic light, the change in refractive index, Δn across the boundary can be determined from Eq. (7).

$$\Delta n = \frac{J\lambda}{a} \tag{7}$$

In many experiments, there will be about 20 fringes across the boundary. Since the number can be estimated to about 0.04 fringe, the accuracy in the determination of concentrations is considerably greater than is possible with schlieren optical systems.

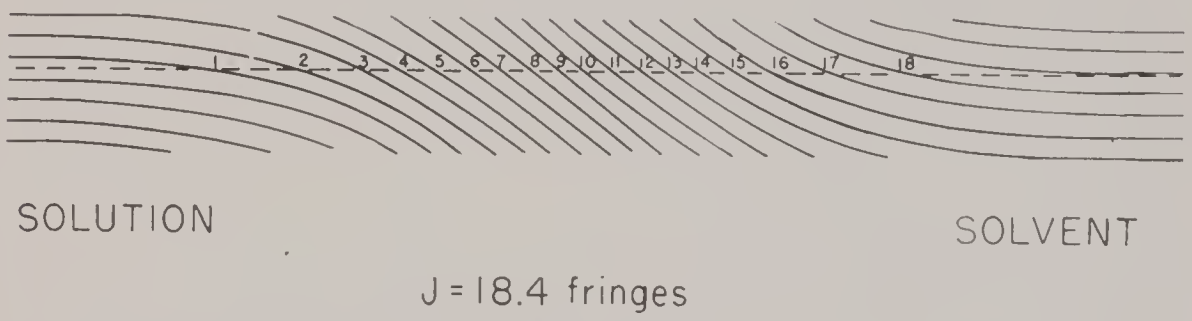

FIG. 10. Hypothetical Rayleigh fringe pattern of a boundary in a cell. The concentration is readily determined by counting the number of fringes from one side of the boundary to the other, as shown by the numbers on the dashed line. Similarly, the concentration at any position in the boundary is measured by counting the number of fringes from a known reference, such as the meniscus, to the point in question.

The apparatus described above is a simple form of the Rayleigh interferometer, but its use in the ultracentrifuge in that form would prevent the utilization of the cylindrical lens schlieren method unless substantial changes are made each time one or the other optical system is used. It has been shown by Svensson (1950) that the cylindrical lens optical system can be used as a Rayleigh interferometer by the simple expedient of changing the slit at the light source from horizontal to vertical, by insuring that monochromatic light is employed, and by having a double cell with its appropriate mask. Also precautions must be taken that the schlieren diaphragm does not intercept any of the light when the instrument is used as an interferometer. With a phase plate as the schlieren diaphragm, this complication does not exist, since it is transparent and its position is readily adjusted so that the image of the vertical slit is on the uncoated region.

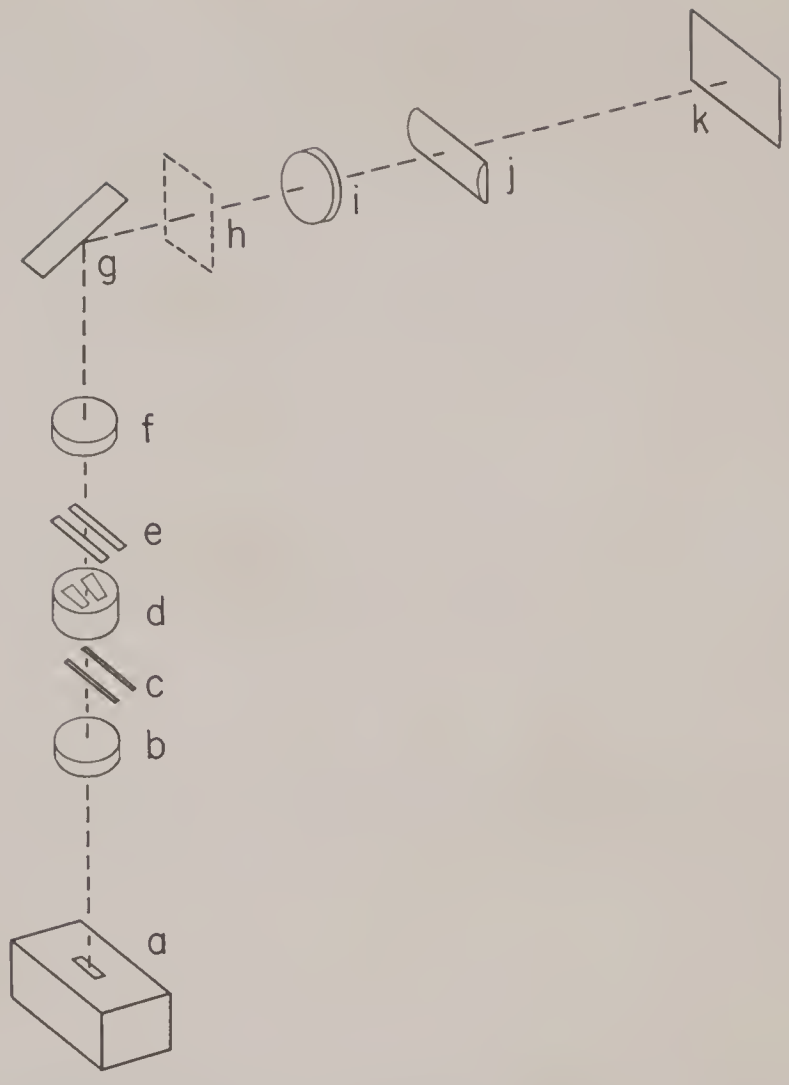

FIG. 11. Schematic drawing of the Rayleigh interference optical system used in the Spinco ultracentrifuge. This optical system can be used alternately with the schlieren optical system, a few minor changes being required. Light from the mercury arc (*a*), which is oriented so that the slit is at 90° relative to its normal position for schlieren optics, is filtered by an interference filter (not shown) and then rendered parallel by the lower schlieren or collimating lens (*b*) situated at the base of the vacuum chamber. The parallel light then passes through a pair of fine slits (*c*) which divide the single beam into two beams, which then traverse the double sector cell (*d*). The slits at (*c*) are incorporated into the holder for the lower quartz window, and the whole unit is a special assembly for the interference optical system. The two slits are parallel even though the paths of sedimentation are not. After the light passes through the rotating cell, it enters a pair of wider slits (*e*) which acts as a diaphragm to limit the angle through which the rotor can turn while conditions for interference are still observed. The light is then focused by the lens (*f*), which is the upper schlieren or condensing lens, after being reflected by the mirror (*g*). The plane (*h*) is the focal plane of the upper schlieren lens, and it is there that the schlieren diaphragm (phase plate or bar, for example) is located. This schlieren diaphragm can be adjusted so as to avoid the path of light for the interference optical system. The lens (*i*) is the camera lens which forms an image of the cell on the photographic plate (*k*), and (*j*) is the cylinder lens in its normal position and orientation for the schlieren optical system.

Moreoever, the use of the cylindrical lens schlieren system as a Rayleigh interferometer places less stringent demands (Svensson, 1951) on the quality of the cylinder lens than does the simpler form of the interferometer in which the cylinder lens is used to image the cell. The optical system as it is used in the ultracentrifuge is shown schematically in Fig. 11. With this system, the interference pattern which in the simple interferometer described above is imaged by the schlieren lenses at the plane of the schlieren diaphragm is, in effect, magnified by the cylinder lens with vertical axis (i.e., parallel to the fringes) to produce an enlarged image at the photographic plate. As in the schlieren system, vertical coordinates in the cell are imaged by the camera lens, and horizontal distances at the focal plane of the schlieren lens system are imaged by the cylinder lens. When this optical system is used as a Rayleigh interferometer, the orientation of the cylinder lens is much more critical than is its alignment in the schlieren system.

In order to produce fringes with this optical system, a special mask is incorporated into the metal cup (disc holder) which holds the lower quartz window of the ultracentrifuge cell. This mask contains two parallel slits (0.020 in. wide) which allow light to pass through only a small segment of each sector of the double cell. It should be noted that neither of these slits are along radii from the axis of rotation. Above the rotating cell, in the vacuum chamber, is mounted a special mask which acts as an aperture, allowing light to pass through the cell during only a small angle of its rotation. This aperture, like the mask in the cell, is composed of two parallel slots, of greater width than those in cell mask. One of these slots is centered in the optical system along a radius from the axis of rotation, and the other is displaced laterally. The light rays can traverse the double sector cell to form interference fringes only when the cell is located in such a way that light can pass through both sectors simultaneously. Thus the double aperture is designed so that the interference conditions obtain when only the solution cell is directly beneath that slot which is aligned radially. This calls for an unalterable procedure in filling the cell so that the solution and solvent are placed in the appropriate sectors. Of course the comparison, or solvent, cell will be at some angle to the opening in the aperture above it, and the interferometer, with cylinder lens oriented along the radial opening, will compare levels in the two cells that are not at equal distances from the axis of rotation. Since the refractive index gradients in the comparison cell will generally be small compared to those in the solution and the levels compared are not very different, this lack of comparison of exactly equivalent levels in the cells produces only insignificant errors. If the cell were filled incorrectly so that the solvent part is aligned with the optic axis, then the boundary being examined would no

longer be at an angle of 90° relative to the axis of the cylinder lens, and the angle would vary as the cells sweep by the fixed optical system. Blurring of the fringes and distortion of the pattern would result as a consequence of lack of correct orientation of the cylinder lens relative to the boundary. Another important factor dictating this offset arrangement of the limiting aperture is the fact that light deviated because of refractive index gradients in the solution will not be cut off by the upper aperture nor will it suffer any displacement by the cylinder lens if both of these are aligned parallel to the refractive index gradient. Some light reaches the photographic plate during the rotation of the rotor even while both cells are not in proper alignment for the conditions of interference. This light creates a background on the photographic plate and the fringe pattern is superimposed on this "fogged plate." With photographic emulsions of high contrast, this does not cause much difficulty, although the quality of the fringe pattern is not as good as those obtained with stationary cells.

For some purposes (see Section IV, 10) this offset arrangement of the slots in the upper aperture is not satisfactory. Therefore, in the author's laboratory, experiments have been conducted in which this limiting aperture contains two parallel slits arranged symmetrically on either side of a radius from the axis of rotation. To be sure, interference conditions are satisfied when each cell is at an incorrect angle of inclination to the axis of the cylinder lens. This seems to introduce only negligible errors, however, and the advantages of this arrangement seem to offset its drawbacks. Neither system is ideal and some compromise is required; only with more detailed studies can we conclude which arrangement is preferable.

The Rayleigh interferometer as now used gives the refractive index as a function of distance in only a narrow segment of each compartment of the cell. This procedure was adopted because it appears that the present limitations of interferometer optical methods reside mainly in the cell distortion rather than in difficulties inherent in the optical systems. It is tacitly assumed in these interferometers that the window distortions in both halves of the double sector cell are the same. Actually, the bulging of the window is such that at high speed the light beams traversing the two halves of the cell do not reunite completely to form a simple image of the slit so that the interference fringes are indistinct. At speeds below about 40,000 r.p.m., however, window distortion, though still present and causing warped fringes even with water in both cells, does not interfere with the attainment of great precision in measuring the refractive index changes within a cell. Recent experience with sapphire windows in place of the quartz windows customarily used indicates that good fringe patterns can be obtained even at 60,000 r.p.m. No facilities have yet been provided with the Rayleigh interferometer for introducing a compensating cell like that employed by

Beams and co-workers (1954) with the Jamin interferometer although this is feasible. To determine the relationship between fringe number and concentration, a system is provided for almost continuous scanning of the pattern at a place in the cell where the concentration hardly changes throughout an entire equilibrium run. In this way, the fringes can be related unambiguously to concentration. Also a special double sector, synthetic boundary cell is available for use as a refractometer. Thus the number of fringes resulting from a known concentration change can be directly measured to an accuracy better than 1 part in 500.

Only three papers in the literature at this writing contain data obtained with an interferometer incorporated into the ultracentrifuge. From the results of these studies and preliminary investigations in the author's laboratory, it is clear that most sedimentation equilibrium experiments in the future will be conducted with interferometric optics. Furthermore, with improvements in cell construction, it is likely that these interference optical methods will find wide applicability to many types of sedimentation velocity studies. Figures 12 and 13 present Rayleigh patterns obtained in sedimentation equilibrium and sedimentation velocity studies, respectively.

d. Light Absorption Methods. Evaluation and interpretation of the ultracentrifuge patterns exhibited by many macromolecules is often difficult because of the high degree of particle interaction present in solution at the concentrations customarily employed in the ultracentrifuge. This difficulty applies to the determination of the sedimentation coefficient at infinite dilution and more particularly to the analysis of the shape of the ultracentrifuge boundary in terms of the homogeneity of the sedimenting material. For elongated macromolecules or particles, such as deoxyribonucleic acid (Peacocke and Schachman, 1954) and tobacco mosaic virus (Schachman, 1951a), particle interaction even at concentrations of only 0.2% is marked, resulting in a large dependence of sedimentation coefficient on concentration and in boundaries which are hypersharp, often causing the misleading impression that the sedimenting material is homogeneous with regard to size and shape. These effects can be avoided by performing the experiments at very great dilution. However, conventional optical methods based upon the gradient of refractive index are usually restricted to solute concentrations greater than 0.1%, thereby precluding studies at sufficiently low concentrations. Interferometric methods would appear to have slightly greater sensitivity than the schlieren methods, but even these are not applicable at concentrations much below 0.05%. To circumvent the difficulties imposed by the limitations of present optical methods, some workers (Schumaker and Schachman, 1957) are returning to the use of absorption optical methods similar to those first employed by Svedberg and collaborators (Svedberg and Pedersen, 1940) during the de-

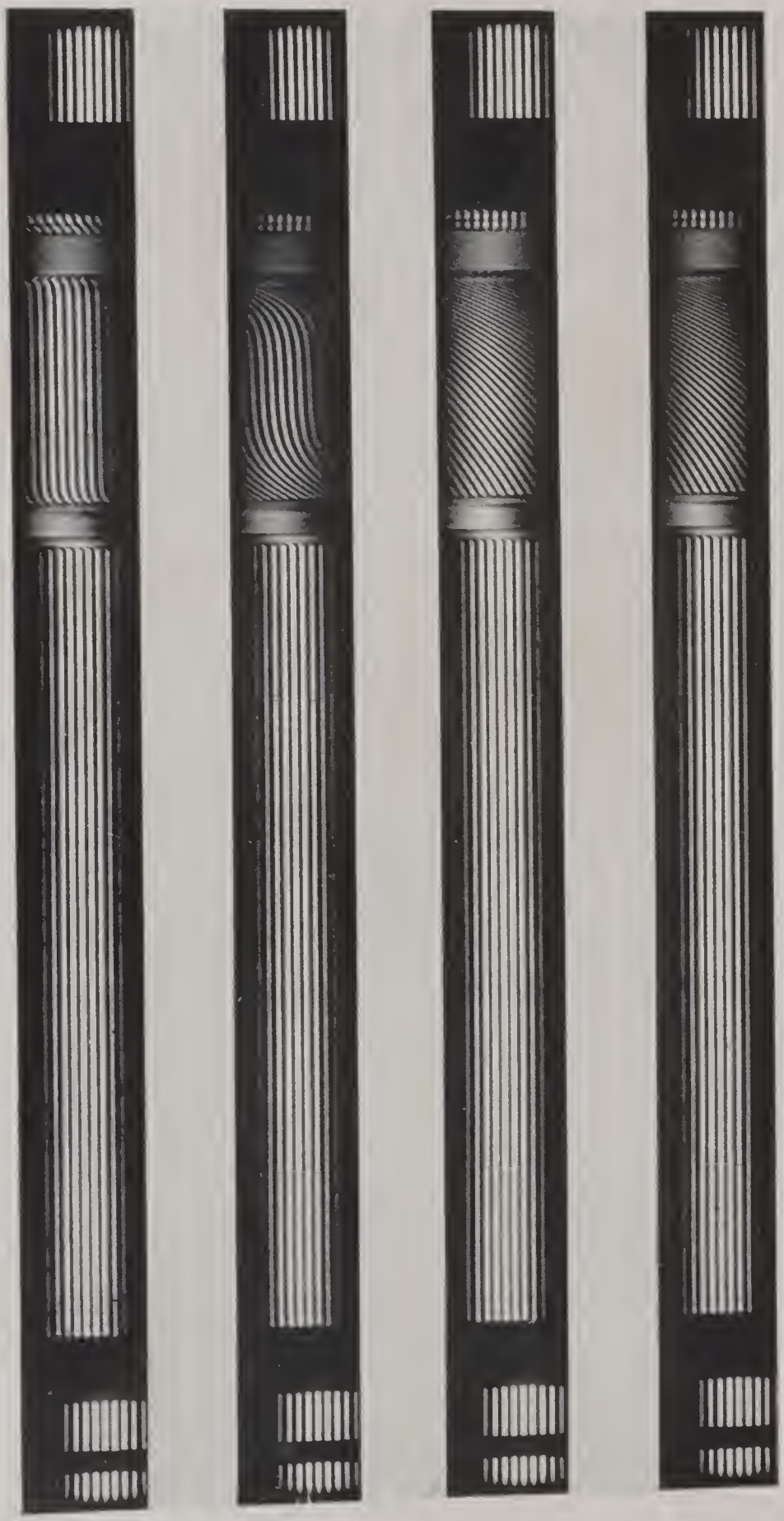

FIG. 12. Rayleigh interference patterns of a sedimentation equilibrium experiment with ribonuclease (from Richards and Schachman, unpublished). The horizontal fringes at the extreme left and right of each pattern correspond to the reference holes in the counterbalance cell, and the fringes throughout the remainder of the patterns represent rays which pass through the cell. Since the cell is incompletely filled (about one-third full), there is an extended region (on the left) in which the rays pass through the air above the solution and solvent columns. The fringes there remain straight throughout the experiment. The meniscus is not clearly defined because more solvent was placed in one sector than solution in the other. The region where the fringes are curved shows the redistribution of the solute (ribonuclease). When there is no region in the cell for which the fringes are straight, an integration procedure is necessary for the determination of the absolute concentration at any position. Alternative methods are available but not illustrated here. To the right of the solution is the region of the cell containing silicone oil, which is added to give a transparent and sector-shaped bottom in the cell. The concentration was 0.5 g. 100 ml. The pictures reading from top to bottom correspond to 20,410 r.p.m., 0 min.; 29,500 r.p.m., 15 min.; 20,410 r.p.m., 84 min.; and 20,410 r.p.m., 496 min. The first picture was taken in order to establish a base line and then the rotor was overspeeded for about 60 min. followed by deceleration to a speed below the selected speed. Finally it was maintained at 20,410 r.p.m. until equilibrium was attained. This process of over- and underspeeding was employed in order to attain the equilibrium distribution in a shorter period of time than is ordinarily required.

CENTRAL FOOD TECHNOLOGICAL RESEARCH INSTITUTE * MYSORE * LIBRARY

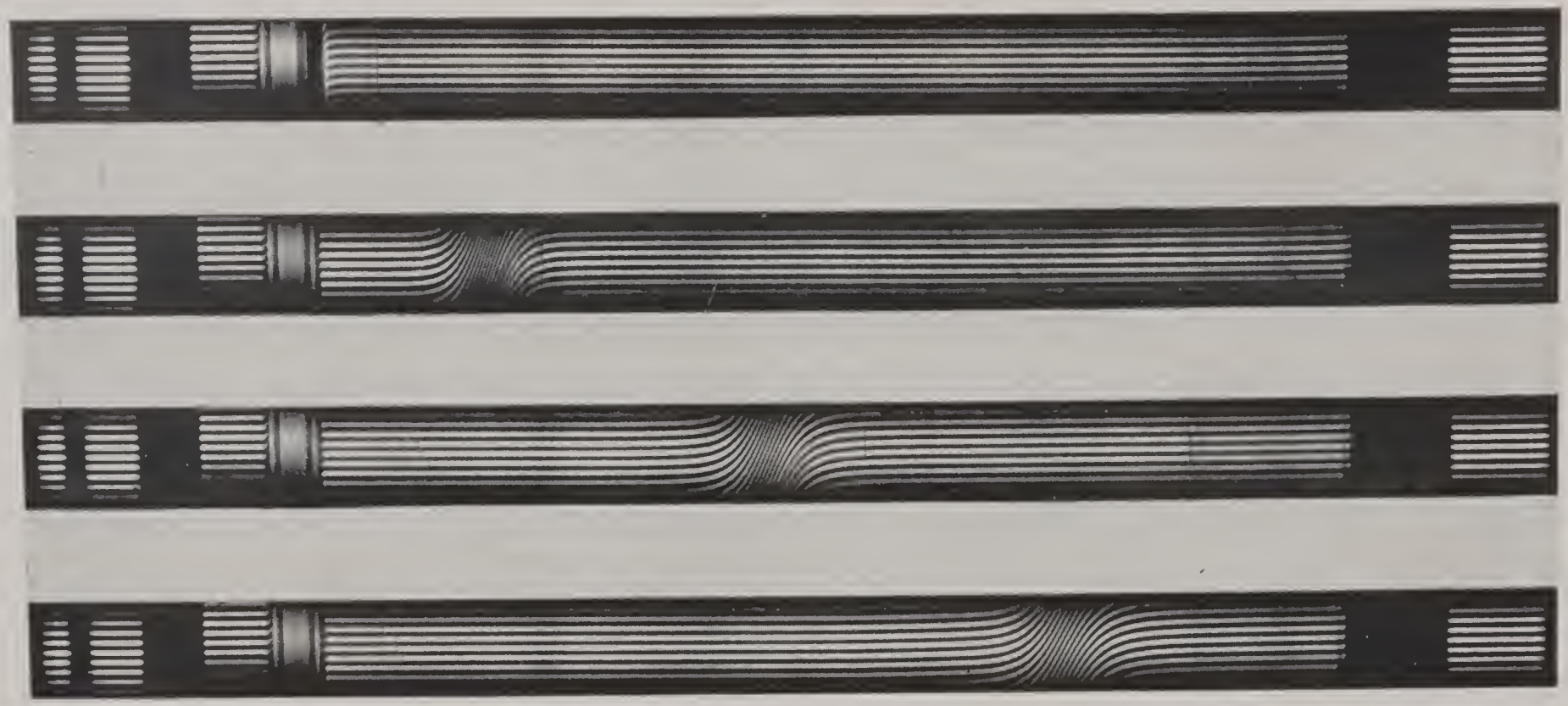

FIG. 13. Rayleigh interference patterns of a sedimentation velocity experiment with bushy stunt virus (from Richards and Schachman, unpublished). In these patterns, the regions where the fringes are straight on either side of the curved fringes correspond, respectively, to the supernatant and plateau. The moving boundary is readily discernible from the location of the curved fringes, and the position corresponding to the second moment of the gradient curves can be evaluated accurately from these patterns. Since each fringe represents a known concentration change the shape of the boundary in terms of concentration versus distance can be determined accurately. The experiment was conducted with bushy stunt virus at a concentration of 0.5 g./100 ml. and the rotor was operated at 14,290 r.p.m. The pictures from top to bottom correspond to 0 min., 64 min., 96 min. and 128 min. After the boundary had moved from the meniscus the rotor was decelerated to 5,563 r.p.m. at which speed it was maintained for 50 min. This was done in order to permit sufficient diffusion so that the fringes were completely resolved. Then the rotor was maintained at the operating speed, 14,290 r.p.m., for the duration of the experiment.

velopment of the ultracentrifuge. The results of the recent, limited studies (Shooter and Butler, 1956; Schumaker and Schachman, 1957) employing light absorption techniques have been so promising that it seems likely that concerted activity will be devoted to the improvement of these methods and to their application to a large variety of biochemical problems.

Earlier it was pointed out that redistribution of low molecular weight buffer ions produces refractive index gradients at the meniscus and bottom of the cell, and that these gradients superimpose on the gradient due to the sedimentation of the macromolecules of interest. Such redistribution of buffer ions does not produce complications in the absorption method since most buffers used in biochemical studies are transparent to visible light and even to ultraviolet light. This represents one of the special virtues of absorption methods which can be contrasted with schlieren or interferometer methods. The latter are not at all selective. Nearly all substances produce approximately equal specific increments in refractive index when added to a solvent. With regard to absorption characteristics, of course, there are large differences. Of all of the optical methods which have been used in conjunction with the ultracentrifuge, the absorption systems are the simplest in design. In practice, however, numerous technical problems remain only partially resolved. As a result, data obtained by this method are not as precise as those produced by other optical techniques. The optical system consists of a light source which, in conjunction with appropriate filters, emits light of a specified wavelength and of constant intensity, a pair of lenses which renders this light parallel during its passage through the rotating ultracentrifuge cell and then focuses it at some position along the optical track, and finally a camera lens which projects onto the photographic plate an image of the illuminated cell. If the cell is filled with a solution which absorbs about 90% of the light passing through it, the amount of light reaching the plate will be so small that the image of the cell will be very faint. As the molecules sediment toward the bottom of the cell, a transparent solvent region is created, and the image of that portion of the cell will be much darker. Across the boundary will be varying degrees of absorption due to the change in concentration at the boundary. This will be apparent on the photograph by the change in the degree of blackening of the plate at a position corresponding to the boundary (Fig. 14). From separate measurements, the degree of blackening of the photographic plate can be related to the concentration of the sedimenting substance. Thus the concentration of the sedimenting material is determined as a function of position in the cell at the time of the photograph. Like the interference optical methods already discussed, the absorption optical system yields curves of concentration versus distance rather than the

concentration gradient versus distance curves revealed by schlieren methods.

For studies in the ultraviolet, the light source is generally a low pressure mercury arc used in conjunction with a quartz filter containing gaseous chlorine and bromine. This combination isolates the 248, 254, and 265 mμ lines of the mercury spectrum along with some light of wavelength above 550 mμ. When used with nonsensitized photographic emulsions, the optical system is effectively measuring absorption at about 260 mμ and is, therefore, ideal for experiments with nucleic acids and nucleoproteins. Comparable filters for the isolation of light with wavelengths about 280 mμ have not yet become readily available. This has no doubt impeded research on proteins with ultraviolet absorption optics. Recently, special interference filters which pass the 280-mμ region of the spectrum and absorb

FIG. 14. Ultracentrifuge experiments with absorption optics in the ultraviolet for recording boundary positions. Sedimenting material is β-lactoglobulin at a concentration of 0.06 g./100 ml. The black regions correspond to optically dense zones and, therefore, to the solution; the white regions refer to the solvent.

in others have been developed, but their use in the ultracentrifuge has not yet been reported. In the author's laboratory, the schlieren optical system with suitable modifications has been employed as an absorption system for light in the visible region of the spectrum. Principal among the alterations is the incorporation of interference filters to isolate light of the desired wavelength. More recent work has shown that the conventional ultraviolet absorption optical system now commercially available, with only minor alterations, serves better as an absorption system even for visible light. By enclosing the chlorine-bromine filter in a plastic holder which can be removed from below the vacuum chamber, it is possible to substitute the desired interference filters and thereby change wavelengths readily, even during an ultracentrifuge experiment.

Most of the difficulties experienced in the use of absorption techniques reside in the inherent limitations of the photographic plate (Svedberg and Pedersen, 1940; Nichols and Bailey, 1949). Exposure of a given plate to light of varying intensity for uniform periods of time produces different

degrees of blackening. If the density of blackening is plotted against the logarithm of the light intensity an S-shaped curve is produced. Insufficient light hardly affects the plate, whereas overexposure of the plate with increasing amounts of light yields degrees of blackening of the plate independent of exposure. There is a region of light intensities between those of underexposure and overexposure in which the amount of blackening is proportional to the logarithm of the light intensity striking the plate. It is important that appropriate experimental conditions be maintained so that this region of the blackening curve is employed for all measurements. In order to relate the blackening of the plate to concentration of the sedimenting material, it is necessary to perform experiments with different concentrations of the sedimenting material. Accordingly, photographs are taken successively, and on the same plate, with the centrifuge cell filled with solutions at different concentrations. These photographs are taken at low speed so that sedimentation of the macromolecules is negligible. If monochromatic light is employed, substances other than the sedimenting material can be substituted for the purposes of obtaining the calibration of the plate in terms of the concentration of the absorbing substance. Blackening of the plate is measured quantitatively by some type of recording microphotodensitometer. In this laboratory, plates are measured with a Model R Analytrol, manufactured by the Spinco Division, Beckman Instruments, Inc., equipped with a microanalyzer attachment. This consists of an adapter for holding and moving the photographic plate at a very slow rate across a thin slit (0.004 in.) through which a light beam passes to a photovoltaic cell. The light intensity passing through the film or plate and striking the photocell is automatically balanced against that impinging on a matched cell. Balancing is achieved by means of a motor operated, logarithmic cam which turns in front of the control cell, thereby varying the size of the aperture of the cell. Coupled with the rotation of the cam is the linear movement of a pen which traces a curve on a chart which moves at a rate 5 times that of the film. Since the optical system produces a 2-fold magnification of the cell, the final tracing corresponds to a 10-fold magnification along the direction of sedimentation. The height of the tracing at each point is proportional to the blackening of the film and, therefore, is a direct measure of the concentration of the sedimenting component. Typical tracings of the patterns exhibited during a sedimentation velocity experiment on β-lactoglobulin are presented in Fig. 15. Patterns similar to those shown in Fig. 15 have been produced directly by a self-plotting absorption optical system (Philpot, 1939). An optical density wedge (on film) is placed directly in front of the photographic plate with the gradient of density on the wedge oriented at an angle of 90° to the gradient produced by the sedimenting material. This combination of op-

tical density gradients produces an S-shaped pattern (black on one side and decreasing to white on the other). Any line of constant blackening on the plate is a measure of concentration versus distance. This system has been used only rarely; as a result its limitations and potentialities are difficult to assess. No doubt a considerable saving of labor can be effected through its use.

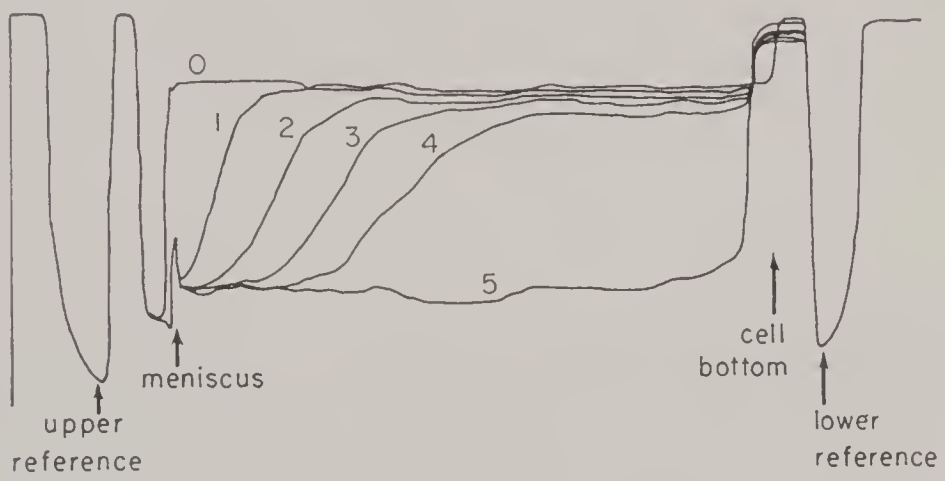

FIG. 15. Densitometer tracings of absorption patterns shown in Fig. 14. The tracings have been inverted to present optical density (or concentration) in the cell as a function of distance.

Uniformity of illumination of the cell is, of course, desirable, and adjustment of the position of the light source is made until the plates show uniform blackening across the image of the cell. Special efforts should be made to secure uniform procedures for processing the film or plates with regard to development, fixing, washing, drying. Some internal standardization is achieved by the existence on each pattern of reference bands resulting from light passing through holes in the counterbalance cell. Their principal function is to provide some fixed reference for measurement of distances from the axis of rotation, but they also serve to monitor the intensity of the light source. If uniform illumination across the cell is not attained, then the photometer curve for the solvents is used as a base line to correct the curves produced by the solution. It should be noted that the reference holes in the counterbalance cell have the same dimensions. As a result, the blackening on the plate corresponding to the inner reference is greater than that for the outer reference. Recently Robkin *et al.* (1959) have designed a reference containing a logarithmically shaped opening. This produces a linear blackening of the plate at a level corresponding to the reference and provides, thereby, a convenient calibration of the photographic plate.

With the recent development of photomultiplier tubes of high sensitivity and small cross section, it seems likely that the photographic procedure in

absorption optical methods will be eliminated and replaced by direct recording through such sensitive detectors. This will, no doubt, add considerably to the reproducibility and precision of absorption optics. Further, it seems likely that multicell rotors will find use in this method too, so that many samples or controls of different concentrations can be photographed simultaneously. Then variations in light intensity would no longer constitute a hazard. In this laboratory, wedged cells are now being used along with a movable diaphragm which can interrupt either of the two light beams. In this way, two samples can be examined in a single run, although the pictures from each cell are not being taken simultaneously. If prisms can be incorporated into the optical system so as to direct the light beams from different cells to different places on the photographic plate, then pictures could be taken at the same time. With photocells it seems likely that the rotor itself can be used as a chopper so that the intensity of light passing through various cells can be compared, and only the small difference then amplified. Further, we may even hope that the development of photocells of high sensitivity and small cross section may permit the construction of a compact unit containing two paired cells mounted behind two fixed slits which are separated by a very small distance. Suitable electronic circuits could then provide a measure of the difference in intensity of light transmitted through regions in the cell which are only a short distance apart. In this way, not only would the effect of fluctuations in light intensity be minimized, but the incorporation of appropriate scanning arrangements would yield the derivative pattern which is so useful in the Archibald method. Finally, the flexibility of absorption optics may be exploited further by the development of new light sources and interference filters (or perhaps even a monochromator) so that measurements could be made in the shorter wavelength region of the ultraviolet. Although the specificity exhibited by different proteins would no longer be manifest at 2300 A., the larger extinction coefficients of proteins at such wavelengths would permit measurements on proteins at concentrations now used routinely for nucleic acids (ca. 0.001 g./100 ml.). To be sure, there would be more difficulty with solvent absorption in that region of the spectrum, but the employment of differential spectrophotometry with the rotor as a chopper could obviate these limitations.

7. Convection-free Sedimentation

Implicit in all of the considerations presented in subsequent sections is the hypothesis that transport of solute occurs only by sedimentation of individual molecules through a viscous medium. Transport by convective flow of solution must be avoided through the use of appropriate experimental technique; otherwise many of the measurements and the interpretations of them would be misleading.

The introduction of the sector-shaped ultracentrifuge cell by Svedberg and his collaborators (Svedberg and Pedersen, 1940) was the key to all of the progress in eliminating, or at least minimizing, convective flow during sedimentation experiments. This design was prompted by the realization that the particles during their radial migration must move unobstructed by the cell walls. Only at the bottom of the cell should the particles collide with a surface of the cell. Of course, there are collisions with the side walls and the windows because of the random Brownian motion of the solute molecules. Such collisions are not serious, however, since they do not lead to accumulation of solute at a specific location, whereas those collisions resulting from the directed motion of the particles due to the centrifugal field do lead to an enhanced concentration at the site of the collision. This zone of higher concentration has, of course, a density greater than that of the original solution. If such a zone is created in which the density is greater than that of adjacent regions at the same radial distance from the axis of rotation, convective flow must ensue, with the more dense liquid flowing quickly toward the cell bottom and the less dense fluid rising toward the meniscus. The depletion of solute from a given region, without the simultaneous removal of solute from zones at the same hydrostatic level, also causes convection. Therefore cells with walls which diverge more rapidly than radii from the axis of rotation are as unsatisfactory as cells which are, say, rectangular.

Despite the important contribution of Svedberg and his colleagues in their design and construction of the sector shaped cell, it seems likely that convective transport does occur in many ultracentrifuge experiments. This may be due to scratches in the surfaces of the radial walls creating crevices or protuberances which cause both the accumulation and depletion of solute molecules in the vicinity of the imperfection. Until recently, most ultracentrifuge cells were constructed with the cell bottom having the curvature of an arc drawn from the center of the cell rather than an arc with a center at the axis of rotation of the rotor. As a result, molecules sedimenting along radii from the center of rotation strike the cell bottom at the sides of the cell sooner than they strike the bottom at some distance from the radial walls of the centerpiece. This produces across the cell (at a constant distance from the axis of rotation) a concentration gradient which is, of course, gravitationally unstable. Convective stirring must occur, although it is difficult to assess how localized this stirring would be. For systems in which the macromolecules migrate in a centripetal direction, the shape of the cell bottom is likely to be more serious, at least during the early stages of the experiment. Other cells are constructed with a bottom which is flat and approximates more closely a sector drawn from the axis of rotation. Disturbances in this cell, though apparently reduced, still oc-

cur. These could be avoided by the creation of a liquid bottom in the cell by adding to the cell, first, some dense immiscible liquid like carbon tetrachloride or silicone oil, and then adding the solution under investigation. The interface between the two liquids assumes the shape of an arc from the center of rotation when the rotor is accelerated (Ginsburg *et al.*, 1956). In the most recently constructed cells, special efforts were made to produce a centerpiece of the correct theoretical shape. It must be recognized, however, that a cell which would be classified as perfect when the instrument maker completes his work may become distorted at the high centrifugal fields. Walls which were originally radial may bow in near the cell bottom and thereby cause convection.

The orientation of the cell in the rotor is also critical, if convection is to be avoided (Pickels, 1942a, b). Some years ago the rotors had a key-way cut into the cell hole and the cells possessed a pin which fit the key-way. With this mechanical arrangement, the alignment of the cell was extremely reproducible, but this practice was abandoned when it was found that the key-way appeared to be the site of local stresses which were responsible for the failure of the rotor. Now fine lines are engraved both on the rotor and the cells so that the latter are oriented to produce a matching of the inscribed lines. It is clear that this is not an infallible procedure with regard to both the engraving of the lines and the judging as to which orientation is best. Some misalignment is bound to occur, and when it does a fraction of the sedimenting molecules will strike the cell wall before they reach the cell bottom. On the opposite side of the cell, there will be a depletion of solute. Both of these effects cause convection, as can be seen readily when the cell is deliberately oriented incorrectly. Quantitative measures of the amount of convection are lacking and it is difficult to state at present how serious is a given misalignment. Hersh and Schachman (1958) found that alignment of the cell was most critical when there is (behind a moving boundary) some sedimenting material which moves faster than the boundary. Misalignment of the cell causes material to strike the side wall where a more dense layer is formed. This can either flow into and merge with the boundary or, if the accumulation is great enough, the liquid near the wall becomes so dense that it flows directly to the cell bottom thereby causing a large negative displacement of the boundary. As the sector angle becomes smaller, the alignment of the cell becomes more critical as a larger fraction of the total number of particles strike the side wall for a given misalignment. It is likely, as a result, that convection in cells with 2° sector angles is more common than in the older 4° sector cells.

There are at least two types of disturbances which may lead to convective flow in an ultracentrifuge cell. The first may be classified as mechanical and is likely attributable to vibrations introduced through the drive shaft

by a malfunctioning drive unit. A second type of disturbance results from temperature gradients across the cell and the consequent density change in the liquid (Pickels, 1942a). As the rotor is accelerated, the liquid near the cell bottom is subjected to a pressure of several hundred atmospheres. This leads to an elevation in the temperature of the liquid at the cell bottom relative to the temperature near the meniscus. Moreover, the stretching of the rotor produces the greater stress near the rotor center, and the consequent cooling of the rotor would lead to a temperature gradient within it, the periphery being warmer than the center. How much of this gradient is transferred to the liquid within the cell is difficult to determine. Differences can be noted between cells with plastic centerpieces as compared to those constructed of metal. This may be attributed to variations in the heat conductivity of the centerpieces, but detailed evidence for this is lacking. In any case, both the temperature gradient within the liquid due to pressure and that in the rotor due to its stretching tend to reinforce with the result that liquid at the cell bottom would become less dense than that at the top of the cell. This is seen most readily in experiments with the synthetic boundary cell. Rapid acceleration of the rotor after the boundary is formed at low speed causes considerable distortion of the boundary by convective disturbances. However, the boundary is not noticeably disturbed if the rotor is accelerated at a slower rate. If there is no boundary in the cell, the convection would not be observed since the flow would occur throughout the entire cell and there would be no way of detecting this movement of the liquid. After the operating speed is attained the temperature gradients would be dissipated rapidly through convective flow of the liquid and because of the high heat conductivity of the rotor. Then temperature gradients could be introduced in only two ways. One of these would be due to peripheral heating of the rotor as a result of friction from the residual air in the vacuum chamber. Also some temperature gradient may be introduced by the transfer of heat from the drive assembly down the shaft into the rotor. With ultracentrifuges in common use now, the temperature gradients produced in these ways are likely to be small.

There are two factors which tend to stabilize the system against the disturbing influence of convection. The first is due to the concentration (or density) gradient from the sedimenting macromolecules themselves, and the second arises from the density gradient owing to the redistribution of the low molecular weight buffer ions. In the absence of density variations resulting from concentration gradients, any disturbance, mechanical or temperature, would cause convective flow throughout the entire cell. No net work is required to interchange two regions of liquid if they are both either solvent or solutions of identical composition. Even the density gradient due to compression of the liquid is not a stabilizing factor. This

can be seen by considering the exchange of two volume elements of liquid, one at the top of the cell and the second at the bottom. The latter liquid is more dense, to be sure, because of the pressure. If this volume element is removed and placed at the top of the cell where the pressure is less, a larger volume element of liquid must be removed there to create the space for the liquid that is being raised. The liquid removed from the top would then be transferred to the cell bottom where it is compressed to just the volume of the hole produced by the initial removal of liquid. After this interchange the entire liquid column would be identical to the situation before the exchange. Thus the density gradient resulting from the pressure gradient is not a stabilizing factor against convective disturbances (see Pickels, 1942a for useful remarks on this subject). If solution were exchanged for solvent, however, the resulting arrangement would be unstable. Therefore convective flow involving the interchange of solvent and solution is not as likely to occur. Any convective flow would tend to be localized within the regions where there is no concentration or density gradient. The flow, in effect, would be turned back by the boundary because of the density change there. Disturbances in the boundary region would be manifest principally at the ends of the boundary (both on the solvent and solution sides) where the density gradients are the smallest.

Various workers (Sharp *et al.*, 1946a; Kerby *et al.*, 1949; Sharp and Beard, 1950; Singer and Siegel, 1950) have raised serious doubts as to the stability of boundaries when there is a concentration change of only a few thousandths of a percent across the boundary. They have cited evidence from their experiments with bacteriophage and polystyrene latex particles to the effect that convective flow prevailed, thereby leading to either an abrupt decrease in the sedimentation coefficient or deterioration of the boundaries as the more dilute solutions were examined. More recent, detailed studies (Schumaker and Schachman, 1957) have shown, however, that convective flow, if present at all, did not preclude obtaining meaningful data from solutions at a concentration of only a few thousandths of a percent. The latter workers showed that a cytochrome boundary behaved ideally at 0.005 g./100 ml., and the apparent diffusion coefficient measured from the spreading of the boundary was independent of the centrifugal field at which the measurements were made. Also the sedimentation coefficient of carboxyhemoglobin at 0.005 g./100 ml. was in accord with the data obtained at substantially higher concentrations. Finally tests were made with deoxyribonucleic acid, and it was found that the distribution curve of the sedimentation coefficients was independent of both the time during experiment and the magnitude of the centrifugal field. Yphantis and Waugh (1956b) also have demonstrated that ultracentrifugal analyses can be performed successfully with materials at very low concentration. In attempt-

ing to reconcile these apparently divergent results, a variety of factors must be considered. First of all, the ultracentrifuge itself has been improved considerably since the older experiments were conducted, and the convection observed in the earlier studies may be attributable to mechanical vibrations. Also due allowances must be made for the fact that it is the density change across the boundary, not the concentration change, which is responsible for the stabilization. Hence, boundaries due to nucleic acids or proteins would be more stable intrinsically than those resulting from a comparable concentration gradient of polystyrene latex particles. Moreover, the sharpness of the boundary is important since the density gradient involves both the change in density across the boundary as well as the width of the boundary. Finally, considerations of convection in the ultracentrifuge must include evaluation of the role of the centrifugal field itself. A boundary may not be stable against mechanical vibrations if the experiment is performed at low speed or in only a gravitational field, but the same mechanical disturbances would have no deleterious effect if the centrifugal force is many thousand times the force of gravity. Thus increasing the centrifugal field, through its effective magnification of small density differences arising from concentration gradients, tends to offset the effect of mechanical vibrations; but it should be noted that no stabilization against the disruptive influence of temperature gradients can be achieved in this way. In some of the experiments of Schumaker and Schachman (1957) and Yphantis and Waugh (1956b) stability may be attributable to the redistribution of buffer ions which creates a density gradient much larger than that resulting from the sedimentation of the solute of interest.

Convective disturbances may also be attributable to the material itself. Schachman and Harrington (1954) have shown that convection resulted when some associating-dissociating systems were studied in the synthetic boundary cell. When the interconversion among the polymers was extremely rapid no convection was detected. However, convection was observed with insulin and it was suggested that the disturbances resulted from density inversions due to the slow interconversion of monomers into polymers and vice versa. Many of the ultracentrifuge patterns in the literature show evidence of convective disturbances in the experiment, although there is rarely any comment to this effect. An extreme example of this is given for illustrative purposes in Fig. 15A. Similar patterns can be seen in experiments on hemocyanin (Pickels, 1942b) and lipoproteins (Trautman and Burns, 1954). The saw tooth spikes are indicative of convective disturbances which lead to extremely sharp concentration gradients.

Convective flow can take two forms. In one, the flow of liquid occurs throughout large regions of the cell as in the plateau region or in the super-

FIG. 15A. An ultracentrifuge pattern illustrating convection during a sedimentation velocity experiment. The sedimenting material is serum albumin in which most of the disulfide bonds have been reduced and the resulting sulfhydryl groups have reacted with iodoacetic acid. The reacted protein aggregates considerably (from Karush and Schachman, unpublished).

natant. Such flow may be difficult to detect. The flow, on the other hand, may be localized into narrow zones. This flow may be from window to window or from one radial wall to the other. If this flow is in opposite directions from zone to zone, the resulting shear would be very large and the hyper-sharp gradients shown in Fig. 15A may be expected. It is difficult to determine why the flow patterns vary, giving localized convective disturbances in some experiments and generalized flow in others. Very slight temperature gradients across the cell (from the walls to the center of the liquid at a fixed distance from the axis of rotation) may cause the flow to break up into eddies. A detailed study of the patterns like that shown in Fig. 15A is lacking. It seems as if the patterns extend below the base line as well as above it. But it is not clear whether the patterns are biphasic. If further work shows that to be the case, we can conclude that there are regions in the cell in which the concentration is higher than that in adjacent regions. Also there may be regions in which there is a depletion of concentration relative to zones on either side. Such distributions of concentration are, of course, intrinsically unstable; and there must be density gradients to compensate for these. The appearance of the spikes below the base line may be deceiving, in which case the interpretation proposed above would be erroneous. If the concentration gradients are sufficiently sharp, the deviation of the light rays would be so great that some of the deviated rays would be intercepted by an opaque element in the optical system, such as a lens holder. In that case there would be a fine line (like the image of the meniscus) extending both above and below the base line. The spikes would then be interpreted in terms of steplike variations in concentration with the concentration increasing progressively throughout the cell. This problem merits attention, and only after more illustrations become available can an understanding of the patterns be achieved. At present there seems to be a correlation between the existence of these convective spikes and the tendency of the sedimenting material to exhibit association-dissociation equilibria. Another type of convection has been described by Harrington and Schachman (1953). They pointed out that convection occurs during the sedimentation of mixtures as a consequence of the change in the Johnston-Ogston effect during an experiment (see Section IV, 7).

IV. Sedimentation Velocity

1. The Relationship Between Boundary Movement and the Sedimentation Velocity of Individual Molecules

Most determinations of sedimentation coefficients involve the measurement of the rate of displacement of boundaries such as those illustrated in Fig. 1. Seldom is it recognized, however, that it is the movement not of the maximum ordinate (sometimes termed the peak) but rather of another position in such boundaries which theoretically provides a precise measure of the sedimentation rate of individual molecules. Further, it is often overlooked that the movement of the boundary, in which the concentration changes from zero to some fixed value, provides a sedimentation coefficient not at some average concentration within the boundary region, but rather at a concentration corresponding to the plateau region in the cell ahead of the boundary. Finally, it is not realized that for *some* systems the movement of boundaries is not a measure of the sedimentation rate of individual molecules. Certain boundaries can provide information not about the sedimentation rate of macromolecules but instead about the concentration dependence of the sedimentation rate. Since most sedimentation velocity experiments are dependent on the analysis of both the shape and displacement of moving boundaries, it is important to consider the relationship of these boundaries to the contents of the cell.

A centrifuge cell which is completely full of solution initially will have a concentration distribution at some later time, t, as illustrated by Fig. 16. In the plateau region, the concentration, c_t, is less than c_0 because of the dilution of the contents owing to the sector shape of the cell and the inhomogeneity of the centrifugal field. This relationship between c_t and c_0 follows directly from Eq. (6). Examination of the continuity equation for regions in the cell in which there is no concentration gradient, i.e., $\partial c/\partial x = 0$ and $\partial^2 c/\partial x^2 = 0$, gives

$$\frac{\partial c}{\partial t} = -2\omega^2 sc \tag{8}$$

or

$$c_t = c_0 e^{-2\omega^2 st} \tag{8a}$$

In the integration of Eq. (8) to give (8a) it was assumed that s and ω were constant throughout the experiment. Often s changes during an experi-

ment (see Section IV, 2 and Table II); for such cases Eq. (8a) should be written in the form

$$c_t = c_0 e^{-2\omega^2 \int_0^t s\, dt} \tag{8b}$$

Were diffusion negligible and the particles uniform in size, shape, and density, the transition zone between the supernatant liquid and the solution would be infinitely sharp. The boundary representing the trailing particles would then move at a velocity characteristic of the individual particles. For such a collection of particles, there would, of course, be no problem in

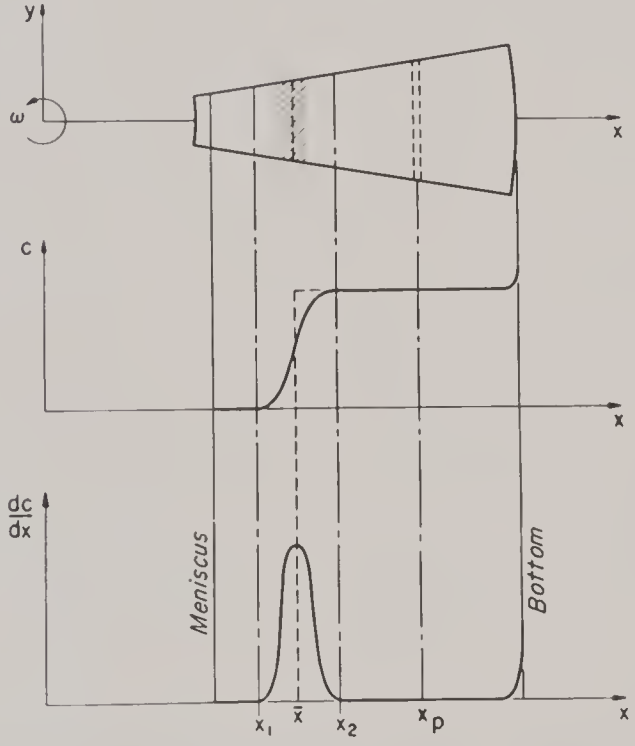

FIG. 16. Distribution of mass during sedimentation in a sector cell (from Trautman and Schumaker, 1954).

locating the position within the boundary region which moves at the same velocity as the molecules ahead. In most sedimentation velocity studies, however, the boundaries are somewhat diffuse or blurred, even with homogeneous particles. Further, this spreading of the boundary increases during the experiment due to diffusion, and for slowly sedimenting substances the trailing region of the boundary can move backward despite the fact that on the average the sedimenting material is being transported in a positive direction. It is important, therefore, to locate the one point in the boundary region which suffers a displacement per unit time equal to that of the sedimenting molecules ahead. This point corresponds to the position of the square root of the second moment of the concentration gradient curve, as was shown by Goldberg (1953) in the following manner.

The total mass of solute transported across a surface at x_p in the plateau region is the product of the area of the surface, the concentration and velocity of movement of the particles at the surface, and the time. During this time period, the boundary moves from the meniscus at x_m to some position in the cell as shown in Fig. 16. The total amount of solute behind x_p at the end of this period can be written

$$q \int_{x_m}^{x_p} cx\,dx$$

where q is a constant accounting for the sector angle and the thickness of the cell along the optical path, and the concentration, c, is a function of x, the distance from the axis of rotation. This mass is, of course, independent of the shape of the boundary, and we might imagine replacing the real boundary by a hypothetical infinitely sharp boundary whose velocity is identical to that of the particles crossing the surface at x_p. In the time period considered, this hypothetical boundary would have moved from the meniscus to a position $\bar{x}$. The mass of solute behind x_p can be written as

$$q \int_{\bar{x}}^{x_p} c_p x\,dx = \frac{q}{2} c_p(x_p^2 - \bar{x}^2).$$

As already indicated, the amount of solute behind x_p is independent of the shape of the boundary, so we can equate the above terms to give

$$\int_{x_m}^{x_p} cx\,dx = \frac{1}{2} c_p(x_p^2 - \bar{x}^2). \tag{9}$$

The left-hand side of Eq. (9) can be integrated by parts, and the resulting equation rearranged to give

$$\bar{x}^2 = \frac{\displaystyle\int_{x_m}^{x_p} x^2 \frac{\partial c}{\partial x}\,dx}{\displaystyle\int_{x_m}^{x_p} \frac{\partial c}{\partial x}\,dx}. \tag{10}$$

To obtain Eq. (10), it is assumed that sedimentation is sufficiently rapid and diffusion correspondingly slow that no solute remains at the meniscus, i.e., $c_m = 0$. The denominator of Eq. (10) is, of course, c_p, and it varies with time according to Eq. (8*a*).

For optical systems which produce curves of concentration versus distance, Eq. (9) can be rearranged directly to give

$$\bar{x}^2 = x_p^2 - \frac{2}{c_p} \int_{x_m}^{x_p} cx\,dx. \tag{11}$$

Data obtained with absorption optical systems or the Rayleigh interferom-

eter can be evaluated according to Eq. (11) rather than through the use of the point at which the concentration in the boundary is one-half the plateau concentration. The latter corresponds to the use of the maximum ordinate in the gradient curve for symmetrical boundaries. Since equal increments of concentration are readily measurable from the patterns provided by either the absorption or interferometric optical systems, it is preferable to rearrange Eq. (11), as before, through integration by parts to give an equation analogous to Eq. (10),

$$\bar{x}^2 = \frac{\int_{x_m}^{x_p} x^2 dc}{\int_{x_m}^{x_p} dc}. \tag{10a}$$

Despite its fundamental importance, Eq. (10) or its equivalent, Eq. (10a), is only rarely employed in the location of boundary positions for the determination of sedimentation coefficients. Nearly all sedimentation velocity experiments have employed the maximum ordinate of the gradient curve as the position of the boundary rather than the square root of the second moment. Justification for the use of the maximum ordinate, x_H, in the determination of s from gradient curves is provided by the calculations of Lamm (1929b) based on Faxén's (1929) approximate solution of the continuity equation. With the assumptions that s and D are constant and that the sedimentation process is sufficiently rapid that the boundary migrates from the meniscus very early in the experiment (so that restricted diffusion at the meniscus is negligible), Faxén showed that the gradient curve was, with only very slight corrections, Gaussian in shape. Lamm's calculations indicated that a term, $D/\omega^2 x^2$, should be added onto the sedimentation coefficient determined from the positions of the maximum ordinate. This is expressed in an alternative way (Baldwin, 1957b),

$$\ln \frac{\bar{x}}{x_m} = \ln \frac{x_H}{x_m} + \frac{Dt}{\bar{x}^2} + \cdots \tag{12}$$

For symmetrical boundaries and especially for the relatively sharp, symmetrical boundaries frequently observed with proteins, the error in using the maximum ordinate is very small, rarely exceeding a few tenths of 1%. Errors greater than 1% would be indicated for molecules of the order of molecular weight of 1000, but the assumptions employed by Faxén would no longer be admissable for such systems. Consequently, the determination of s for such molecules is generally approached in a different way.

In an experiment with pepsin at a concentration of 0.84%, the calculated position of the boundary after 52 minutes of operation at 59,780 r.p.m. was, according to Trautman (1956), about 0.05 mm. farther from the axis of

rotation when determined from the second moment than when evaluated from the position of the maximum ordinate. Judging from the patterns, this difference would correspond to almost a 1% error. It is clear, however, from the diagrams presented by Trautman, that the ultracentrifuge pattern of pepsin is not quite symmetrical, and the differences between the two calculated positions are, in part, a reflection of the presence of some material in the sample which sediments slightly more rapidly than the bulk of the material. For such skew boundaries, the difference between the maximum ordinate and the square root of the second moment is accentuated, and the laborious calculation of the theoretically correct boundary position is not only profitable but frequently essential (Trautman *et al.*, 1954).

In the derivation of Eq. (10), we employed a surface in the plateau region and considered the amount of solute left behind this surface after a given time of sedimentation. Since the amount of solute initially contained between surfaces at the meniscus and the arbitrary position in the plateau region is known, the amount left behind is a direct measure of the transport across the chosen surface. Thus the displacement of the position of the square root of the second moment is shown to be a measure of the flux across a surface in the cell corresponding to a region free of concentration gradients, and the sedimentation coefficient refers to the concentration in the plateau region at the time of the measurement. This has been stressed by Baldwin (1953b), who emphasized the differences involved in the measurement of sedimentation and diffusion coefficients. When diffusion coefficients are calculated from the shape of a boundary, the resulting values refer to some mean concentration within the boundary. As will be shown later, the sedimentation coefficient can be calculated even in the absence of a complete boundary, and the values so calculated, like those above, refer to the concentration in the plateau region.

Since the sedimentation coefficient is a direct measure of the transport of solute across a given surface (where there is no concentration gradient, and transport by diffusion can accordingly be neglected) and the transport is also proportional to the concentration of the sedimenting species, we can write that the total transport of solute in a mixture of sedimenting materials is proportional to

$$c_1 s_1 + c_2 s_2 + \cdots c_i s_i + \cdots c_n s_n$$

where c_i and s_i are the concentrations and sedimentation coefficients of the different molecular species. This expression can clearly be written as

$$\bar{s} \sum_{i=1}^{n} c_i$$

where $\bar{s}$ must be the weight-average sedimentation coefficient of the mixture.[2] Thus it is important in analyses of unsymmetrical boundaries that the sedimentation coefficient be evaluated from the second moment of the gradient curve to give a truly representative average value of the sedimentation rates of all the different constituents within the preparation. This procedure can be used for a compound boundary which clearly is made up of several different boundaries or for a broad boundary whose resolution into separate boundaries cannot be expected. Furthermore, weight-average sedimentation coefficients can be obtained for a mixture of components for which the ultracentrifuge pattern shows complete resolution into separate boundaries. It is, of course, mandatory for the latter situ-

[2] This can be shown rigorously by examination of the continuity equations for each of the individual components. Assuming that the components are independent of one another, we can write for any specific component

$$\frac{\partial c_i}{\partial t} = \frac{1}{x}\frac{\partial}{\partial x}\left[xD_i\frac{\partial c_i}{\partial x} - \omega^2 x^2 s_i c_i\right].$$

The various equations can be summed for all of the components to give

$$\frac{\partial}{\partial t}\sum_i c_i = \frac{1}{x}\frac{\partial}{\partial x}\left[x\sum_i D_i\frac{\partial c_i}{\partial x} - \omega^2 x^2\sum_i s_i c_i\right].$$

This equation accounting for all of the components has the same form as Eq. (5) and can be written in the form

$$\frac{\partial \bar{c}}{\partial t} = \frac{1}{x}\frac{\partial}{\partial x}\left[x\bar{D}\frac{\partial \bar{c}}{\partial x} - \omega^2 x^2 \bar{s}c\right]$$

with $\bar{D}$, $\bar{s}$, and c replacing the diffusion coefficients, sedimentation coefficients, and concentrations of each of the various species. The above equation serves as a definition of $\bar{D}$ and $\bar{s}$ and shows that the measurement of the transport of solute across a surface in the plateau region, where $(\partial c/\partial x) = 0$, gives the weight average sedimentation coefficient, $\bar{s}$, which is expressed by

$$\bar{s} = \sum_i c_i s_i / c$$

where

$$\bar{c} = \sum_i c_i .$$

When ultracentrifuge data are used in the determination of weight average sedimentation coefficients, it is assumed of course that each component involved in the summation makes an equal contribution (by weight) to the optical pattern. If the components do not possess equal specific refractive increments or equal specific extinction coefficients (optical density per unit weight), then corrections are necessary to account for variations in the optical constants among the molecular species. The ultracentrifuge patterns give, in effect, a "weight optical average sedimentation coefficient."

ation that the integration in Eq. (10) be continued until a plateau region is reached in which all components are present. When interacting components are present, the second moment produces a constituent sedimentation coefficient representing the different molecular species in which the sedimenting molecules appear (Baldwin, 1953b; Svedberg and Pedersen, 1940, p. 28; see Section IV,9*b*).

In the study of electrophoresis, much attention has been directed toward the formulation of the so-called moving boundary theory, which is an expression of the conservation of mass within a volume defined by two planes encompassing the moving boundary. The singular success of this approach to the examination of concentration distributions in solutions subjected to an electric field commends it to workers analyzing the boundaries formed in a homogeneous solution subjected to a centrifugal field. As Trautman (1952), who first discussed the problems of developing a moving boundary theory for the ultracentrifuge, pointed out, such a theory is complicated greatly by the sector shape of the cell, the dependence of the centrifugal field on the distance from the axis of rotation, and finally the dependence of sedimentation coefficients on concentration. Nonetheless, it is pertinent to examine ultracentrifuge boundaries in these terms, because the movement of a boundary does not always provide a measure of the migration of the solute molecules ahead.

The net amount of solute accumulating between two fixed surfaces in a centrifuge cell can be expressed in terms of the sedimentation rates and concentrations of the solute entering and leaving the two surfaces. If, between these two surfaces, there is an infinitely sharp boundary separating homogeneous solutions containing solute at two different concentrations, the rate of movement of this boundary is governed by the net amount of material entering or leaving the volume element under consideration. A detailed discussion of this type of problem is presented in Section IV,5, and it is sufficient here to illustrate the problem of a moving boundary theory with several examples. If the concentration of the solution at the upper plane were zero, our problem would reduce to that already considered in Fig. 16. There would be considerable depletion of solute in the region contained between the two surfaces, and the hypothetical boundary would then migrate at the same rate as the particles crossing the lower surface. Alternatively, we might have a situation in which the concentration at the upper surface is not equal to zero but is less than, say, one-half that at the lower one. Suppose, also, that the sedimentation rate of the molecules in the dilute solution is much greater than (say, about twice as great as) that of the molecules in the lower solution. For this system, the total amount of material crossing the upper surface (concentration times sedimentation velocity) will be equal to that leaving the lower surface. Inspection of the

boundary would not reveal any movement, and a casual examination of the ultracentrifuge pattern would provoke the conclusion that no sedimentation was occurring. If the concentrations and sedimentation coefficients could be so adjusted that the flux of material at the upper surface was larger than that crossing the lower one, there would be an accumulation of solute within the selected volume element, and the boundary would therefore migrate in a negative (centripetal) direction. This would occur despite the fact that the molecules themselves are moving centrifugally. Thus it is seen that a boundary does not always provide a measure of the migration velocity of molecules on either side of it. However, the motion of a boundary can be predicted quantitatively from equations expressing the conservation of mass, and the examination of a conventional ultracentrifuge boundary might well be considered as a special case in which the concentration above the boundary is zero.

2. Radial Dilution

It has already been shown with the aid of the differential equation of the ultracentrifuge that the contents of the plateau region of the cell undergo a progressive dilution during an experiment. This was first discussed by Svedberg and Rinde (1923, 1924) ,who derived in a simple manner the so-called radial dilution equation, which relates the concentration of the solution at some time, t, to the initial concentration, c_0, in terms of the boundary positions at the respective times. Their derivation considered only materials for which the sedimentation coefficient is independent of concentration, although the approach they used to develop the desired relationship is sufficiently general to encompass other systems as well. Despite a report by Kinell (1947b) that the radial dilution equation, in the form developed earlier by Svedberg and Rinde, does not hold for materials exhibiting concentration-dependent sedimentation coefficients, its validity for such materials has been demonstrated theoretically by Trautman and Schumaker (1954). However, it should be noted here (also see Section IV, 11) that the radial dilution equation does not apply if pressure effects are not negligible (Fujita, 1956b). Actually, in that case the concentration varies slightly with distance in the region which would ordinarily be called the plateau region. Similar effects must occur as well when, in the region of the boundary, there is a redistribution of salt or a third component like urea. These complications are not considered here.

Earlier it was shown that the displacement of the square root of the second moment of the gradient curve provides a precise measure of the sedimentation coefficient of the individual molecules. Therefore we can write, according to the definition of the sedimentation coefficient (Eq. 2)

$$\frac{d\bar{x}/dt}{\omega^2\bar{x}} = s. \tag{2}$$

Combination of this with Eq. (8) and integration from c_0 and x_m at $t = 0$ to c_t and $\bar{x}_t$ at time, t, gives

$$\frac{c_t}{c_0} = \left(\frac{x_m}{\bar{x}_t}\right)^2. \tag{13}$$

As Trautman and Schumaker stressed, Eq. (13) is valid even if the sedimentation coefficient changes markedly during the experiment because of sectorial dilution. Also they extended the treatment to analysis of multicomponent systems of noninteracting components and derived the following equation for a polydisperse system for which only a single boundary was observed:

$$c_0 = \int_{x_m}^{x_p} \left(\frac{x}{x_m}\right)^2 \frac{\partial c}{\partial x}\, dx. \tag{14}$$

This of course follows directly from Eqs. (10) and (13). For multicomponent systems which reveal a series of boundaries in the ultracentrifuge, Trautman and Schumaker showed that:

$$c_0 = \left(\frac{\bar{x}_t}{x_m}\right)_1^2 c_{1,t} + \left(\frac{\bar{x}_t}{x_m}\right)_2^2 c_{2,t} + \cdots + \left(\frac{\bar{x}_t}{x_m}\right)_n^2 c_{n,t} \tag{15}$$

where $c_{1,\,t}$, $c_{2,\,t}$, $\ldots$ $c_{n,\,t}$ are the observed concentrations of the different components, 1, 2, $\ldots$ n, at the time, t.

In an effort to reduce the labor in obtaining correct values for the initial concentrations of materials examined in the ultracentrifuge, Trautman and Schumaker have introduced a technique using warped coordinates for integrating the observed refractive index gradient patterns. Their procedure involves only an adding machine and eliminates the laborious multiplication of each value of dc/dx by x^2 followed by a summation of the products. Instead, they substitute a radius-cubed scale for the graphical integration in place of the normal scale along the radius of rotation. Although this method would not effect a saving in time or effort when such calculations are performed infrequently, it can be systematized for routine work and thus prove useful.

As a consequence of the dilution of the contents of the ultracentrifuge cell during an experiment, the observed values of the sedimentation coefficients of many substances actually change by measurable amounts during a run. This was shown clearly by Lauffer (1944b) in an experiment with tobacco mosaic virus. These particles exhibit a pronounced dependence of sedimentation coefficient on concentration, and Table II shows the variation in sedimentation coefficient during an experiment with a solution at a concentration of 1.34 g./100 ml. Similar results were obtained with mixtures of tobacco mosaic virus and bushy stunt virus (Harrington and Schachman, 1953), and the change in sedimentation coefficient of the former

TABLE II

Variation in Sedimentation Coefficient of Tobacco Mosaic Virus as a Result of Sectorial Dilution during an Experiment[a]

(c_o = 1.34 g./100 ml.)

Distance from axis of rotation (cm.)	Sedimentation coefficient (S)
5.8311	145
5.8654	144
5.8995	153
5.9360	147
5.9715	145
6.0068	146
6.0424	149
6.0788	146
6.1147	148
6.1514	148
6.1882	149
6.2256	153
6.2643	150
6.3024	150
6.3406	151
6.3795	154
6.4193	154
6.4593	159
6.5010	159
6.5428	155
6.5839	151
6.6244	154
6.6657	154
6.7073	157
6.7500	156
6.7927	156
6.8355	159
6.8796	160
6.9243	157
6.9685	163
7.0145	155
7.0586	166
7.1060	

[a] From Lauffer, 1944b.

during an experiment causes convective disturbances which will be elaborated upon in Section IV,7.

With the development of the phase plate as the schlieren diaphragm and the introduction of interferometric methods, concentration determinations should have an accuracy better than a few tenths of 1 %, and a direct con-

firmation of Eqs. (13) or (14) should be feasible within such limits. The older methods have an accuracy of only 2 to 5%, and concentration determinations with the aid of the ultracentrifuge are in satisfactory agreement with values obtained in other ways. Cecil and Ogston (1948) with lactoglobulin were able to account for essentially all of the solute in the solution by means of measurements of the integral of the refractive index gradient curves. Furthermore, the calculated concentration was inde-

TABLE III

Measurement of Concentration from Areas of Schlieren Patterns[a]

Time after reaching speed (min.)	Estimated refractive increment ($\times 10^5$)	Refractive increment % of total
Lactoglobulin, 1 g./100 ml.; total refractive increment 182 $\times$ 10^{-5}		
68	184	101
78	173	96
88	184	102
98	181	100
108	182	101
110	173	96
118	176	98
	Mean 179 $\pm$ 4.9	98.4 $\pm$ 2.7
Lactoglobulin, 0.526 g./100 ml.; total refractive increment 94.7 $\times$ 10^{-5}		
82	92	97
102	96	101
112	92	97
122	95	100
132	97	102
	Mean 94.4 $\pm$ 2.3	100 $\pm$ 2

[a] From Cecil and Ogston, 1948.

pendent of time throughout the experiment, thus showing the validity of Eq. (14). Their data is reproduced in Table III not only because it shows the precision obtainable with the older schlieren diaphragms such as a knife edge, but also because it represents one of the very few examples of accurate measurement of the areas of the schlieren diagrams. Kegeles and Gutter (1951) similarly found good agreement between the concentration of protein calculated from the ultracentrifuge pattern and the known weight concentrations. In a study of mixtures of two sedimenting components, Harrington and Schachman (1953) found deviations from the radial dilution equation, but these deviations are to be expected in terms of the more detailed theory presented in Section IV,7. For their control solution of only

one component, the concentration throughout the experiment decreased in accordance with Eq. (13).

If the concentration dependence of the sedimentation coefficient is very large, the decrease in concentration with time will not be exponential as shown in Eq. (8*a*), but rather the concentration tends to approach a linear function of time (Alberty, 1954). Nonetheless, the concentration at any time can be correlated with the initial value in terms of the positions of the boundaries at the respective times, according to Eq. (13).

If claims of homogeneity of a protein are to be made, a basic requisite to further detailed analysis of the patterns (as presented in Section IV,8*e*) is the demonstration that the amount of protein present in solution as determined by Kjeldahl analysis, for example, is fully revealed by the area of the schlieren patterns. More often than not, the areas indicate less protein than is measured by conventional chemical methods, and the difference between the two provides evidence of the presence in the solution of either aggregated material, or contaminants of low molecular weight, or partially degraded material. In their careful study, Cecil and Ogston (1948) discuss at length the problem of construction of reference base lines for measurement of areas. The hazards in selecting the proper base line are virtually eliminated now by the use of the double sector cell, one section of which contains the solvent or dialyzate. A singular advantage of the absorption system resides in its ability to provide, in effect, measurements of areas (more properly, the total extinction, and thus the concentration) even while the rotor is accelerating and before the boundary migrates from the meniscus. From the change in the degree of blackening of the plate upon accelerating the rotor from low speed (a few thousand r.p.m.) to the desired operating speed, a direct measure is available of the amount of aggregated material in the preparation. Such information can be derived from schlieren optical methods but only with the expenditure of considerable labor. It should be emphasized that the equations presented above must be translated into areas with the appropriate optical constants, such as the thickness of the cell, the optical lever arm, the angle of the schlieren diaphragm relative to the orientation of the image of the slit at the light source, the specific refractive increment of the solute, and the concentration of the sedimenting material. If the area calculated from these parameters is greater than that measured after the boundary has just migrated from the meniscus, then material other than the principal component is present. Whether that extraneous substance is larger or smaller than the component of interest requires further analysis of the base line, particularly in the region of the meniscus. None of these parameters, including the concentration of the sedimenting material, is required for the absorption system, and the differentiation between large and small impuri-

ties is readily made by casual inspection of the ultracentrifuge patterns. The interference optical system also gives valuable information regarding the sedimentation of aggregated material even before the principal component migrates from the meniscus. With the use of the synthetic boundary cell some of the advantages of the absorption method can, in fact, be achieved with the schlieren system. Here the area can be measured at low speed. If this area decreases more rapidly than expected according to the radial dilution equation, the material is not homogeneous.

3. Measurement of Sedimentation Coefficients

a. Moving Boundary Method. Generally, sedimentation coefficients are evaluated from the slope of the line relating the logarithm of the boundary position to the time. This is based, of course, on Eq. (2), which can be written in the alternative form

$$s = \frac{1}{\omega^2} \frac{d \ln \bar{x}}{dt} \tag{16}$$

The procedure employing Eq. (16) has replaced that used commonly some years ago in which individual sedimentation coefficients were calculated from successive patterns with the equation,

$$s = \frac{2(\bar{x}_{t_2} - \bar{x}_{t_1})}{(\bar{x}_{t_2} + \bar{x}_{t_1})\omega^2(t_2 - t_1)} \tag{17}$$

Equation (17) is a satisfactory expression for Eq. (2) if $\bar{x}_{t_2}$ is not much larger than $\bar{x}_{t_1}$, and calculations with Eq. (17) produce reliable sedimentation coefficients for the time period concerned. However, the subsequent averaging of all the tabulated, individual values of s, in effect, cancels those obtained at intermediate times during the experiment, and as Oncley (1941) pointed out, the final sedimentation coefficient calculated in that manner employs only the first and last patterns, which are apt to be the most unreliable.

If the temperature increases appreciably during the experiment, the resulting decrease in the viscosity of the solvent causes a marked increase in the sedimentation coefficient with time. As a consequence, plotting of the data according to Eq. (16) is unacceptable. To allow for such variations, Oncley (1941) has proposed the use of a corrected time in handling the data. Even though the pictures are taken at equal intervals of time, the increase in temperature during an experiment makes the time intervals during the latter part of an experiment effectively longer than those early in the run. Therefore, the time intervals are corrected by a factor allowing for the variation in the viscosity of water with temperature, and these

corrected times are employed in a plot of ln $\bar{x}$ versus t_{cor}.[3] Cecil and Ogston (1948) have used a somewhat similar procedure and reported precise values of the sedimentation coefficient of different materials. They plotted the total distance moved by the boundary versus the total corrected time for each observed pattern. In this plot, the corrected time contains not only a factor accounting for temperature effects on the viscosity of the solvent but also a factor including the square of the speed and the average distance of the boundary from the axis of rotation. Kegeles and Gutter (1951) have used a modified procedure to make the most use of the available data. They calculated individual values of the sedimentation coefficient from successive pairs of photographs obtained over equal time intervals. Each of these sedimentation coefficients, calculated according to Eq. (17), was then corrected for temperature variations by an equation presented later, and an average value for the four intervals was calculated from

$$s_{av} = \frac{1}{10}(2s_1 + 3s_2 + 3s_3 + 2s_4). \tag{18}$$

They stated that this procedure is equivalent to a determination of the slope of the least squares line of temperature corrected ln $\bar{x}$ versus time. Further attention was directed toward this problem by Schwert (1954), who recommended that an average temperature correction be applied to the value of the sedimentation coefficient determined from the plot of all of the data of the experiment as ln $\bar{x}$ versus time. It would appear, despite the considerations of Schwert, that the individual data should be corrected if large temperature changes occur throughout the experiment. With present equipment, these procedures are all equivalent, since the temperature changes throughout a run can be so small as to have an undetectable effect in changing the sedimentation coefficient.

Whereas the effect of temperature variations can now be controlled experimentally, the change in sedimentation coefficient during a run as a result of dilution of the contents with time cannot be eliminated experimentally. It is well to recognize that the contents of the ultracentrifuge cells now in normal use may be diluted to about 70% of their initial value. Therefore, for accurate work the data must be treated in a manner to account for this dilution effect. Most ultracentrifuge data in the literature on the dependence of sedimentation coefficient on concentration are ob-

[3] It should be noted that, in many of the studies cited in this and subsequent sections, the investigators measured the position of the maximum ordinate, x_H, of the gradient curve rather than the position, $\bar{x}$, corresponding to the square root of the second moment of the gradient curve. Although there is generally little difference between x_H and $\bar{x}$, we will designate, in our discussion, the position of the boundary as $\bar{x}$ (Goldberg, 1953).

tained from an average sedimentation coefficient from individual experiments, which are then usually plotted against the initial concentration of the particular solutions examined. Clearly the concentrations used in establishing the relationship between s and c should be the average concentration between the first and last pictures within each experiment. This procedure was used by Jullander (1945) and Kegeles and Gutter (1951), and it, or one of the following, should be employed routinely. As an alternative to this averaging procedure and one that potentially provides additional information of value, the data from each experiment can be treated in a manner to produce a sedimentation coefficient which corresponds to the very beginning of the experiment when the concentration is that of the solution placed in the cell. Extension of the treatment provides values of the sedimentation coefficient throughout the experiment so that, within limits, the dependence of s upon c can be measured in a single ultracentrifuge run.

Different methods have been proposed for evaluating both the sedimentation coefficient at zero time and its variation during an experiment. Trautman *et al.* (1954) used a method, illustrated in Fig. 17, which is frequently employed for gently curving lines when accurate values of the slope at different locations are required. The slight curvature is barely detectible in the plot of ln $\bar{x}$ versus t shown in Fig. 17*a*. In order to measure accurately the curvature, or in turn to evaluate the initial slope (sedimentation coefficient), the equation for the straight line constructed between the first and last points is determined, and the difference between ln $\bar{x}$ on the straight line (calculated from the equation of the line) and the observed ln $\bar{x}$ at corresponding times is calculated. This difference is then plotted as a function of t, as shown in the lower curve of Fig. 17. This is an expanded plot on which tangents can be drawn representing the difference in slope between the real curve of ln $\bar{x}$ vs. t and the arbitrary straight line. Subtraction of the initial slope on this expanded plot from the slope of the chosen straight line gives directly an accurate value of the initial sedimentation coefficient. This value of s corresponds, of course, to c_0 and to the temperature of the rotor directly after attaining the desired speed. If the temperature change during an experiment is assumed to be linear with time, this factor can also be incorporated into the plot. The slope of the expanded plot at any time, t, subtracted from the slope of the straight line, gives directly the sedimentation coefficient at the concentration $c_t = c_0(x_m/\bar{x}_t)^2$ and at the corresponding temperature. Alberty (1954) has suggested another method based on the assumption that the sedimentation coefficient, s_t, at time, t, can be expressed as a power series in time

$$s_t = s_{t=0}(1 + a_1 t + a_2 t^2 + \cdots) \tag{19}$$

where $s_{t=0}$ is the initial value of the sedimentation coefficient and a_1 and a_2 are constants. Combination of Eq. (19) and the definition of the sedimentation coefficient followed by integration gives

$$\frac{1}{\omega^2 t} \ln (\bar{x}/x_m) = s_{t=0} + (a_1/2)t + (a_2/3)t^2 + \cdots \tag{20}$$

Thus individual sedimentation coefficients are calculated with the initial

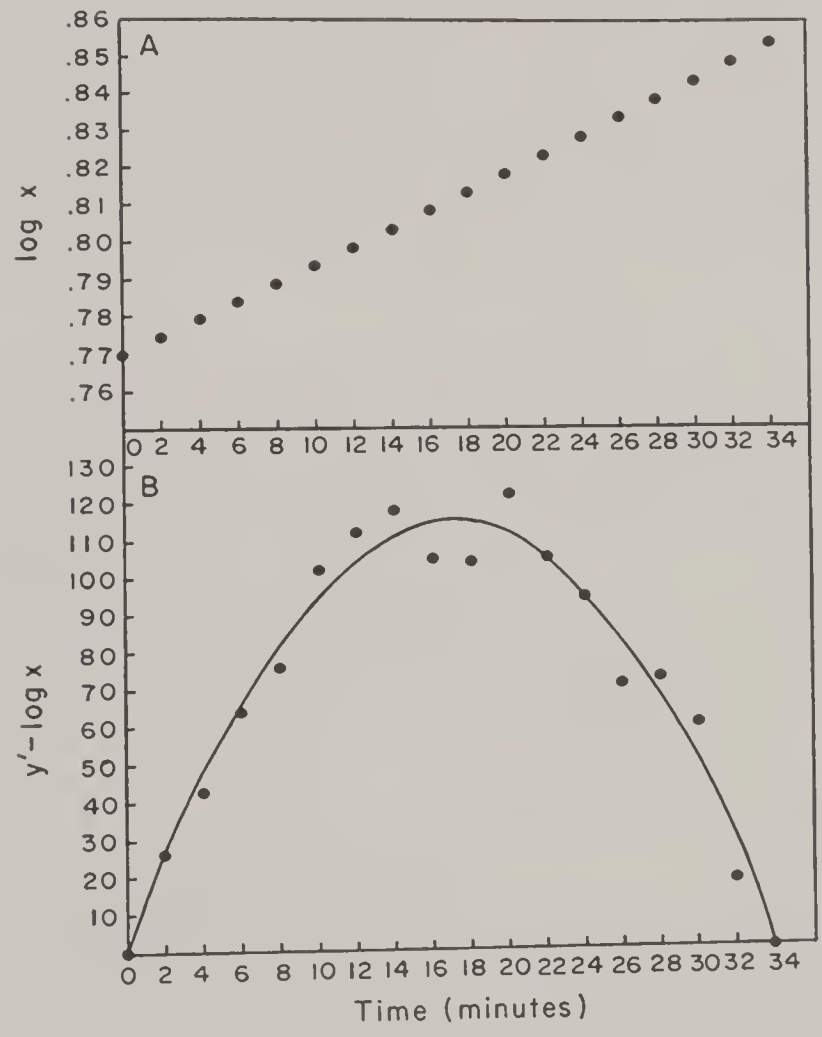

FIG. 17. Determination of sedimentation coefficient at zero time. A plot of log x vs. t (upper) and an expansion of plot of log x vs. t (lower) for a solution of tobacco mosaic virus at a concentration of 1 g./100 ml. (from Trautman, *et al.*, 1954).

boundary position being paired with some other $\bar{x}$ value for each calculation. For most substances the term in t^2 is negligible, and the data calcuated according to Eq. (20) fit a straight line. The intercept gives the sedimentation coefficient at zero time. Just as was described earlier, the time scale for these calculations can be adjusted to account for temperature variations. Both this method and that illustrated in Fig. 17

when used with the same data produce almost identical values for the initial and final sedimentation coefficients. It should be noted that the values of $\ln(\bar{x}/x_m)$ in Eq. (20) show the greatest scatter at low values of t since the difference between $\bar{x}$ and x_m is very small early in the experiment, and errors in the location of the boundary are, in effect, magnified. Therefore, just the region of the curve that is necessary for the highest precision in the determination of the intercept suffers most from the limitations in the measurements of the position of the boundary. The method illustrated by Fig. 17 is not so severely restricted, since the tangent is drawn from the smooth curve on the expanded plot. Another method for the evaluation of sedimentation coefficients at zero time has been introduced recently by Baldwin (1957b). From a combination of Eq. (19), an expression relating s as a quadratic function of c, and the continuity equation for the plateau region, the sedimentation coefficient, s_t, can be written as a function of time, t, the initial concentration, c_0, and $s_{t=0}$. By comparing terms in this equation with those in Eq. (19) and employing the radial dilution rule, Baldwin obtained the equation

$$\ln \frac{\bar{x}}{x_m} - s_{t=0}s_0\omega^4t^2(k_1c_0 + 2k_2c_0^2) + \cdots = s_{t=0}\omega^2t \tag{21}$$

where k_1 and k_2 are the coefficients in the power series in c relating s to the value of the sedimentation coefficient, s_0, at infinite dilution. An apparent sedimentation coefficient, s_{app}, is then defined as

$$s_{app} = [\ln(\bar{x}/x_m)_t - \ln(\bar{x}/x_m)_{t_0}]/\omega^2(t - t_0) \tag{22}$$

where $(t - t_0)$ is the time from the first photograph, usually taken after the boundary has migrated away from the meniscus and the whole pattern of the boundary has been resolved. In this way, there is no need to determine the time when sedimentation begins. For most ultracentrifuge experiments, the zero time correction (the effective time of sedimentation before the desired speed is attained) is one-third of the time required for acceleration of the rotor. This assumes a constant rate of acceleration. With data from the ultracentrifuge patterns obtained at various times, values of s_{app} can be calculated from Eq. (22). Combination of Eqs. (21) and (22) gives an expression relating s_{app} to $s_{t=0}$ as shown in the following,

$$s_{app} = s_{t=0}[1 + s_0\omega^2(t + t_0)(k_1c_0 + 2k_2c_0^2) + \cdots] \tag{23}$$

Rather than plot s_{app} as a function of $(t + t_0)$ so as to extrapolate the data to zero time to obtain $s_{t=0}$, Baldwin devised another method which avoids the introduction of errors due to the overemphasis of data from the early stages of the experiments. From a series of ultracentrifuge runs at different concentrations, the values of s_{app} at fixed values of $s_0\omega^2(t + t_0)$

are selected. These values of s_{app} at different concentrations can be used directly to give s_0 as seen by examination of Eq. (24), which results from the substitution of the quadratic equation relating s to c into Eq. (23).

$$s_{app} = s_0\{1 - k_1c_0[1 - s_0\omega^2(t + t_0)] - c_0^2[k_2 - 2k_2s_0\omega^2(t + t_0) + k_1^2s_0\omega^2(t + t_0)] - \cdots\} \quad (24)$$

For fixed values of $s_0\omega^2(t + t_0)$, the data from a series of experiments can

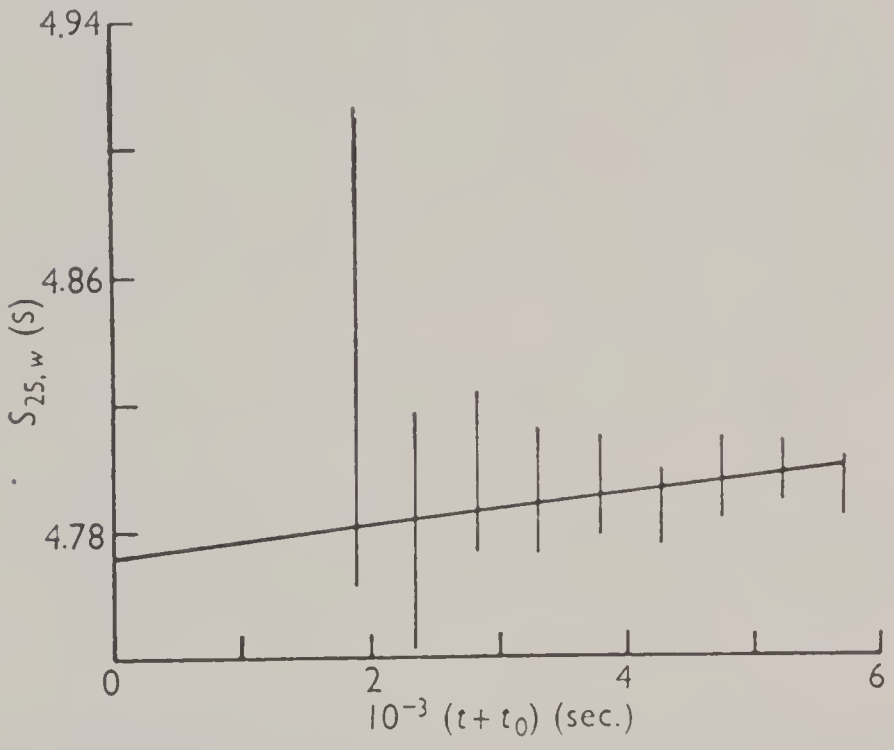

FIG. 18. Determination of sedimentation coefficient at zero time. A plot of s_{app} (expressed as $s_{25,w}$) versus $(t + t_0)$ according to Eq. (23). The data are from an experiment with bovine albumin at a concentration of 0.87 g./100 ml. The line through the points is determined from a series of experiments at different concentrations as described by Eq. (24) (from Baldwin, 1957b).

be extrapolated to $c_0 = 0$ to give s_0; then from the slope and intercept of a plot of $(s_0 - s_{app})/s_0c_0$ against c_0, the values of k_1 and k_2 can be evaluated. With these values, the slope of the curve of s_{app} versus time (as shown by Eq. 23) is known. An example of such a calculation is presented in Fig. 18. The length of the vertical lines shows the uncertainty in s_{app} caused by an error of 0.001 cm. in locating the position of the boundary. It is clear that this uncertainty in the value of s_{app} from the early photographs is so great that the slope of the line through the data could not be measured with accuracy. However, the method of handling the data described above (Baldwin, 1957b) permits the construction of the line drawn on the

graph as long as data from experiments at different concentrations are available.

As will be shown later, the change in s during an experiment can be interpreted in terms of parameters characterizing the sedimenting material. When the data are treated in the manner indicated by any of the above methods, the precision in the determination of s at the beginning and end of the experiment is insufficient to provide a value of the constant relating s to c, except for those materials which show a pronounced concentration dependence. For the maximum accuracy, experiments should be done at different concentrations and the values of $s_{t=0}$ can then be plotted in the appropriate form against c_0. Golder (1953) derived a relationship between boundary position and time in terms of s_0 and the constant describing the concentration dependence of the sedimentation coefficient.

Not only do these procedures avoid the difficulties arising from the dilution of the contents of the cell during an experiment, but they also provide, at the same time, sedimentation coefficients corresponding essentially to atmospheric pressure. (The slight pressure in excess of 1 atmosphere due to the effect of the centrifugal field on the air above the liquid column is negligible.) This extrapolation to zero time thereby obviates the complications originating from the changes with pressure in the density and viscosity of the solvent and the partial specific volume of the sedimenting material. Since these changes for certain rare systems (see, e.g., Cheng and Schachman, 1955b) may cause the sedimentation coefficient to vary in a weird fashion during an experiment, a procedure such as the expanded plot illustrated in Fig. 17 must be employed.

It is of interest to note that the fractional change in sedimentation coefficient, $\Delta s/s_{t=0}$, during an experiment is, for dilute solutions, proportional to the initial concentration (Cheng and Schachman, 1955a) and can be expressed as

$$\frac{\Delta s}{s_{t=0}} = \frac{\bar{x}_t^2 - x_m^2}{\bar{x}_t^2} \frac{kc_0}{1 + kc_0 x_m^2/\bar{x}_t^2} \tag{25}$$

In Eq. (25), k is a constant which relates the sedimentation coefficient to concentration (see Eq. (32) below). When $kc_0 \ll 1$, the fractional increase in sedimentation coefficient (k is usually positive, although there are special types of systems for which $k < 0$), or alternatively the curvature of the plot of ln $\bar{x}$ versus t, is directly proportional to the initial concentration.

To facilitate comparison of experimental values of the sedimentation coefficient measured with different solvents (such as the type and concentration of electrolytes) or at various temperatures, the results are usually converted to a standard basis corresponding to a reference solvent having the viscosity and density of water at 20°C. This is accomplished by the

method introduced by Svedberg and his colleagues (Svedberg and Pedersen, 1940) with the use of Eq. (26), where $s_{20,w}$ is the sedimentation coefficient under standard conditions (assuming no alteration of the protein).

$$s_{20,w} = s \frac{\eta}{\eta_{20,w}} \frac{(1 - \bar{V}\rho)_{20,w}}{(1 - \bar{V}\rho)} \tag{26}$$

The term $(\eta/\eta_{20,w})$, in which η is the viscosity of the solvent at the temperature of the experiment and $\eta_{20,w}$ is the viscosity of water at 20°C., can generally be written as the product of two factors, the first giving the viscosity of the solvent relative to that of water at a convenient temperature (this assumes that the temperature coefficients for the viscosities of the solvent and water are the same) and the second involving the correction of the viscosity at the temperature of the ultracentrifuge experiment to the value for water at 20°C. The other correction term in Eq. (26) is generally smaller, but for materials like lipoproteins it can be very important. This correction involves $\bar{V}$, the partial specific volume of the solute, and ρ the density of the solution and accounts for the difference between the buoyancy term, $(1 - \bar{V}\rho)$, in the experiment and its value had the experiment been performed in water at 20°C. and at a pressure of 1 atmosphere. These corrections are discussed in detail by Svedberg and Pedersen (1940). In Section VII,5 the basis for Eq. (26) is presented, and it is clear that the equation in that form is valid only for two-component systems, e.g., a solution of a protein in water. When this equation is used for experiments in salt solutions, it is assumed that the solvent, containing water and electrolytes of low molecular weight, can be treated as a single component. As will be shown later, Eq. (26) may not be valid for correction of sedimentation coefficients measured in 6 *M* urea, for example. Because of this theoretical limitation and because only very recently have experimental results of high precision become available, it is fair to state that the validity of Eq. (26) has not yet been adequately demonstrated. Occasional reports (Koenig and Perrings, 1952a,b) purporting to show the inadequacy of Eq. (26) have appeared, but it is likely that these results are more a reflection of experimental errors than a demonstration of the limitation of the above equation. This is not to imply that future measurements will be strictly in accord with Eq. (26). On the contrary, some deviations are to be expected, at least with small molecules, on the basis of the precise diffusion measurements of Longsworth (1954) which showed the inadequacy of a diffusion equation analogous to Eq. (26). This demonstration by Longsworth was concerned largely with small molecules diffusing in a solvent composed of molecules of comparable size. Hence, an assumption that the solute molecules migrate in a medium which may be considered as a continuum is inadmissible. Even for bovine

plasma albumin, however, the diffusion behavior at 1°C. and 25°C. could not be accounted for by the diffusion equation similar to Eq. (26). Though it may be tempting to attribute this to inherent limitations in the diffusion equation it is likely that the experimental observations are an indication of changes in the protein molecules themselves. A critical evaluation of Eq. (26) is needed; but such a study, to be of value, must involve a system for which Eq. (26) was derived, i.e. a two component system. Thus there is no justification to claim, as Parrish and Mommaerts (1954) have done, that Eq. (26) is invalid for myosin. These workers [see also Mommaerts and Aldrich (1958) where this conclusion was reiterated] employed solvents of high ionic strength in their experiments, and no evidence has yet been presented that a 0.4 *M* KCl solution containing phosphate ions can be considered as a one component solvent. A test of Eq. (26) must include a careful evaluation of many factors. First of all the data must be extrapolated to correspond to infinite dilution of the sedimenting material because the concentration dependence of s is likely to be temperature dependent (see Section IV, 4 for a discussion of this problem). It is interesting to note that all claims of a pronounced temperature effect on $s_{20,w}$ are based on experiments with materials which exhibit a large dependence of sedimentation coefficient on concentration (see e.g. Goring and Chepeswick, 1956). In effect, these studies introduce the viscosity dependence on temperature twice. Second, the partial specific volume must be measured at different temperatures so as to permit the precise evaluation of $(1 - \bar{V}\rho)$ for the different experimental conditions. Third, pressure corrections are necessary. Fourth, the data should involve the second moment of the gradient curve. Finally, if a two component solvent is employed, allowances for redistribution of the salt must be made.

For small, highly diffusible molecules, the diffusion from the solution toward the meniscus and from the sedimented molecules at the bottom of the cell makes it difficult to produce complete boundaries. Even if sedimentation of the molecules could be sufficiently prolonged to yield a clear supernatant, the plateau region would be obliterated by diffusion from the bottom of the cell. When special layering cells are employed, however, a clear supernatant is present immediately after the formation of the boundary (Fig. 19), and a considerable period of time is available for measurements before diffusion renders the supernatant no longer free of solute or causes the plateau region to disappear. Displacement of the boundary can then be followed within the time period available, and sedimentation coefficients determined as indicated above. Even for molecules as small as sucrose, the movement of the boundary is measurable (Fig. 20), although the displacement is so small that experimental errors are presently about 5% in the determination of sedimentation coefficients

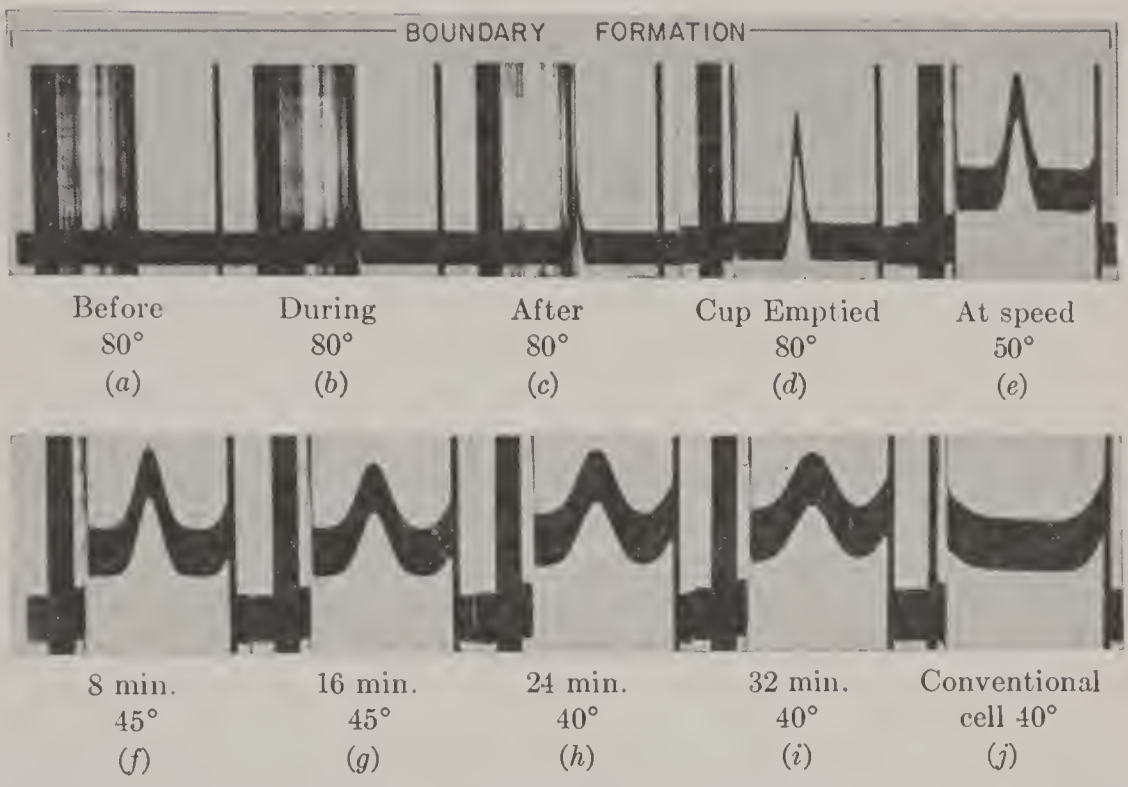

FIG. 19. Determination of the sedimentation coefficient of sucrose in a synthetic boundary cell. Ultracentrifuge patterns showing the formation of the boundary and its changes during the experiment. Upper solution: H_2O; lower solution: 1% sucrose in H_2O. (*a*) Prior to formation of boundary; (*b*) during formation of boundary; (*c*) immediately after formation of the boundary; (*d*) cup emptied; (*e–i*) 0, 8, 16, 24, and 32 min. after reaching speed, respectively; (*j*) 1% sucrose in conventional analytical cell after 32 min.; angles of the schlieren diaphragm are given beneath the pictures (from Pickels, *et al.*, 1952).

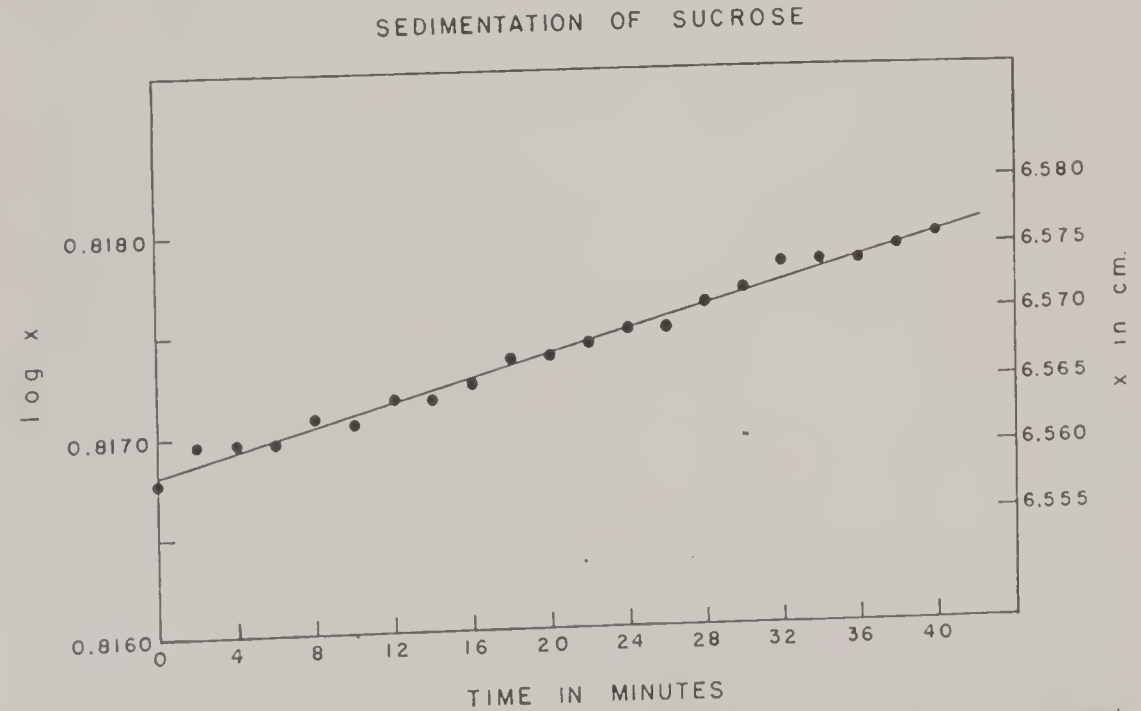

FIG. 20. Determination of sedimentation coefficient of sucrose from movement of boundary formed in a synthetic boundary cell. Plot of log x and x (where x is in cm. from the axis of rotation) vs. t (in min.) (from Pickels *et al.*, 1952).

for such low molecular weight solutes (Schachman and Harrington, 1954). A critical examination of the measurement of sedimentation coefficients of small molecules by this method has not yet been reported, but it appears that values of 0.5 S can be determined with an accuracy about 4%. Prior to the development of such techniques, the lower limit in the determination of sedimentation coefficients from the movement of boundaries was about 1 S, corresponding to the molecular weights in the neighborhood of 10,000.

b. The Transport Method. As early as 1937, Tiselius *et al.* (1937) suggested a technique for determining sedimentation coefficients by measuring the total amount of solute transported across an arbitrary surface in the ultracentrifuge cell. They also designed a special separation cell for facilitating such measurements. This procedure was discussed further by Svedberg and Pedersen (1940) in connection with the optical determination of the total transport. It was not, however, until Gutfreund and Ogston (1949) exploited this approach for the study of small molecules that the necessary equations were adequately developed. Though these workers and others who subsequently employed this technique (Baldwin, 1953b; Webber, 1956) have concentrated on molecules too small for conventional sedimentation velocity analysis, there is nothing in the method which restricts it to molecules of a certain size. There are different ways to derive the necessary equations which arise from a statement of the conservation of mass and the development presented here is in the form suggested by Baldwin (1953b).

Consider a cylindrical surface at a distance, x_p, such that dc/dx in the vicinity of this surface is at all times of the experiment equal to zero. Initially, the mass of solute contained in the volume defined by the meniscus, the surface at x_p, and the walls of the cell can be written $\frac{1}{2} qc_0(x_p^2 - x_m^2)$ where q is an apparatus constant depending on the thickness of the cell along the optical path and the angle of the sectoral cavity, and c_0 is the initial concentration. After a given time of sedimentation, t, there is remaining in this volume element an amount given by

$$\int_{x_m}^{x_p} qcx\, dx$$

The difference between these two quantities is, of course, the total amount of solute which crossed the surface at x_p during the time, t. As before, the rate at which solute crosses this surface can be written as the product of the area of the surface, the concentration at the surface, and the velocity of the molecules crossing x_p. Expressing the total transport in terms of the sedimentation coefficient and the cell parameters and writing the

above statement of the conservation of mass in the form of an equation gives

$$\frac{1}{2} qc_0(x_p^2 - x_m^2) - \int_{x_m}^{x_p} qcx\, dx = \int_0^t qx_p c_t \omega^2 x_p s\, dt \tag{27}$$

The concentration c_t can be written in terms of c_0 and s by means of Eq. (8*a*). Assuming s to be constant, integration of the right-hand side of Eq. (27) after the appropriate substitution gives

$$c_0(x_p^2 - x_m^2) - 2\int_{x_m}^{x_p} cx\, dx = x_p^2 c_0(1 - e^{-2\omega^2 s t}). \tag{28}$$

Equation 28 can be used directly for the determination of s, if concentration data are available at different positions in the cell. Thus Eq. (28) should find wide applicability with absorption optical systems or the Rayleigh interference method. The necessary integration in Eq. (28) can be readily performed by a process of summation. It should be noted that the only restriction imposed on the use of Eq. (28) is the existence of a plateau region somewhere in the cell and the location of x_p in that region.[4] Whether or not the solute molecules have sedimented away from the meniscus to form a complete boundary is unimportant. It is essentially this equation, in a slightly modified form, which is employed in sedimentation velocity determinations with the use of the separation cell (Tiselius *et al.*, 1937; Yphantis and Waugh, 1956b). In such experiments

$$\int_{x_m}^{x_p} qcx\, dx$$

is measured analytically, either by a chemical or biological assay, and reported as Q_t, the total amount of solute remaining above the surface of the separating partition at the time, t. For this situation, Eq. (28) can be written in the form given by Svedberg and Pedersen (1940),

$$s = -\frac{1}{2\omega^2 t} \ln\left[\frac{2Q_t}{qx_p^2 c_0} + \frac{x_m^2}{x_p^2}\right] \tag{28a}$$

or

$$s = -\frac{1}{2\omega^2 t} \ln\left[\frac{x_m^2}{x_p^2} + \frac{c_u}{c_0}\left(1 - \frac{x_m^2}{x_p^2}\right)\right] \tag{28b}$$

where c_u is the average concentration of the thoroughly mixed solution withdrawn from the upper compartment. A more general expression for

[4] It must be emphasized that s was assumed to be constant. When s cannot be considered constant, Eqs. 28, 28*a*, 28*b*, and 28*c* should be modified just as Eq. (8a) was altered to give Eq. (8b).

the use with optical systems stems from rearrangement of Eq. (28) to give

$$s = -\frac{1}{2\omega^2 t} \ln \left[\frac{2 \int_{x_m}^{x_p} cx\, dx}{x_p^2 c_0} + \frac{x_m^2}{x_p^2} \right]. \qquad (28c)^5$$

This equation has apparently not been used to any extent with the exception of experiments in the separation cell and for small molecules which do not form complete boundaries. For optimum use of this approach, the surface at x_p should be selected for each pattern at the innermost (or centripetal) part of the plateau region. In this way, the difference between the first and second terms in Eq. (28) is maximized, thereby granting the optimum sensitivity in the evaluation of s. A corollary of this for the separation cell would, of course, involve sedimenting the material sufficiently so as to cause the boundary to approach the partition as closely as possible without loss of the plateau region at x_p. When a separation cell is employed, the time, t, must represent the total time of sedimentation and includes, therefore, the effective time during acceleration and deceleration of the rotor.

In its present form, Eq. (28) is not too useful for experimental data produced by schlieren optical systems. Rather than integrating the gradient curves to obtain concentration curves which then must be integrated again (Gutfreund and Ogston, 1949), Baldwin (1953b) suggested that the integral in Eq. (28c) be evaluated through integration by parts. This produces terms involving the concentration gradient which can be measured directly from the schlieren patterns, as follows:

$$\int_{x_m}^{x_p} cx\, dx = \frac{1}{2} [c_p x_p^2 - c_m x_m^2] - \frac{1}{2} \int_{x_m}^{x_p} x^2 \frac{dc}{dx}\, dx. \qquad (29)$$

But c_p can be written as $c_0 e^{-2\omega^2 s t}$, and c_m can be expressed in terms of c_p and the concentration gradient pattern by

$$c_m = c_p - \int_{x_m}^{x_p} \frac{dc}{dx}\, dx. \qquad (30)$$

Incorporation of these into Eq. (28c) gives the equation developed and

[5] Equation (28c) should be employed in studies of polydisperse materials like deoxyribonucleic acid. When the extinction coefficient is independent of molecular weight, as is frequently the case, this method of handling the data (with absorption optics) gives a weight average sedimentation coefficient. It is assumed, of course, that the components are independent of one another, i.e. there are no reactions among them such as those involved in association-dissociation equilibria (see footnote on page 68). For this situation, Eq. (27) can be written for each component and the summation of all of the equations can then be rearranged to give an expression for the weight average sedimentation coefficient.

used by Baldwin (1953b) for the determination of sedimentation coefficients of small molecules.

$$s = -\frac{1}{2\omega^2 t} \ln \left[1 + \frac{x_m^2 \int_{x_m}^{x_p} \frac{dc}{dx}\, dx - \int_{x_m}^{x_p} x^2 \frac{dc}{dx}\, dx}{x_m^2 c_0} \right]. \tag{31}$$

Recently Webber (1956) has derived this identical equation in a slightly different manner, although the basis of this derivation, like that presented

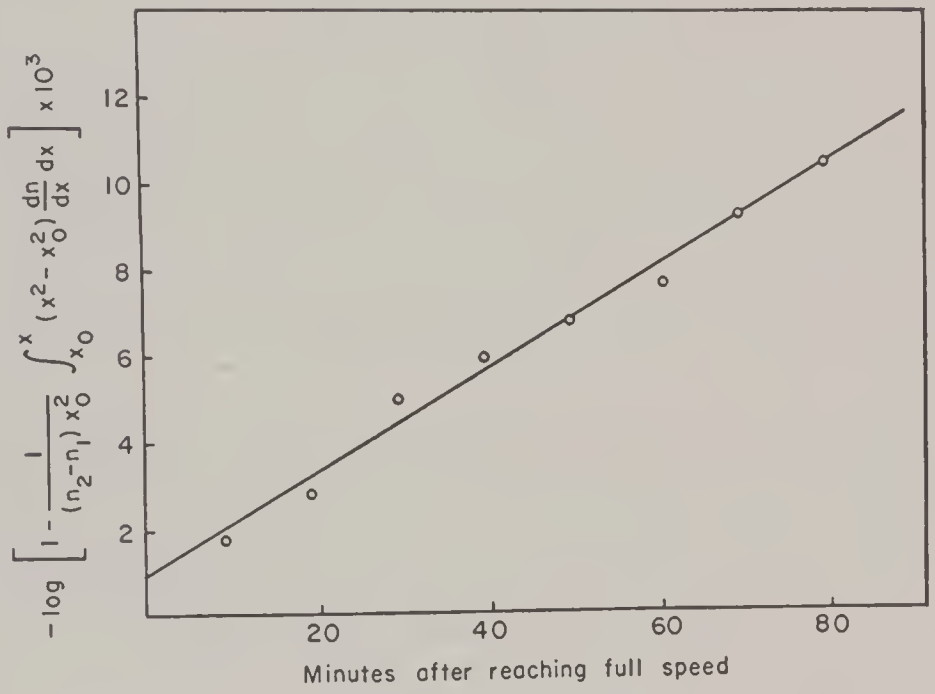

FIG. 21. Determination of sedimentation coefficient of amyloheptaose by the transport method. The experimental data are plotted according to Eq. (31) with dn/dx replacing dc/dx and $(n_2 - n_1)$ instead of c, where n corresponds to the refractive index, and the subscripts 1 and 2 refer to the solvent and solution, respectively (from Webber, 1956).

above, is a statement of the conservation of mass. Attention should be directed to the use of Eq. (30) in this derivation. If c_m becomes zero, Eq. (31) reduces directly to the Eqs. (10) or (13), derived earlier.

To illustrate the application of these transport equations for the determination of sedimentation coefficients of small molecules, the data from an experiment of Webber (1956) are presented in Fig. 21, plotted in a form essentially that indicated by Eq. (31). The material examined in this experiment is amyloheptaose, which has a molecular weight of only 1152. It is gratifying to note that the results of Webber, insofar as they can be compared, are in excellent agreement with earlier experiments (Schachman and Harrington, 1954) with the synthetic boundary cell. Even for a molecule as small as sucrose, Webber obtained an average value

confirming the preliminary value reported by these workers. Both techniques are limited with regard to the length of the experiment. The free diffusion from the boundary formed in a synthetic boundary cell will, with time, cause the obliteration of the base line and distortion of the boundary. In the transport method also, diffusion causes the plateau region to disappear in about the same time, and the method becomes no longer applicable. There has not as yet been a detailed comparison of the two different approaches, and final conclusions as to which is more reliable, more easily employed, and more revealing as to the total contents of the solution will have to await such a study. The author's experiences have been restricted largely to the moving boundary method with the synthetic boundary cell, and his prejudice toward the use of that cell for small molecules is no doubt recognized. The flurry of application of these two methods for the measurement of sedimentation coefficients of small molecules, which in conjunction with diffusion coefficients yield molecular weights, has largely been dissipated. Such studies, when molecular weights are the principal object, are now performed by other ultracentrifugal techniques. Despite this recent trend, sedimentation coefficients of small molecules are still of interest, and methods described above are likely to be employed in a more critical way in the future. Considerable increases in accuracy over the measurements published in only the last few years can already be expected because of the new system for the measurement and control of temperature and the improvement in the patterns resulting from the employment of the phase plate as the schlieren diaphragm. Further gains are likely as a result of improvements in the ultracentrifuge cells. Probably the greatest source of error now is in the construction of the true base line so that the observed values of the refractive index gradient can be corrected adequately. With the double sector cells, the deviations in the base lines from the two sectors are apparently less than the variation in base line produced in a conventional cell when it is dismantled and reassembled for an experiment with a reference solvent. Thus the use of the double sector cell should lead to increased accuracy in the measurement of sedimentation coefficients.

Figure 22 represents an application of Eq. (28*a*) to the determination of the sedimentation coefficient of β-lactoglobulin at a concentration of 0.06 g./100 ml. Absorption optics with ultraviolet light were employed, and the patterns along with some typical microphotodensitometer tracings are shown in Figs. 14 and 15. Integrations for each pattern were restricted to regions from the meniscus to a position just beyond the boundary (in the plateau region). The value of c_0 in arbitrary units was obtained from the photometer tracing of a pattern obtained at very low speed. Although there is much room for improvement in absorption techniques, it is clear

that satisfactory data can be obtained by this method. The sedimentation coefficient calculated from Fig. 22 is 2.81 S (corrected to standard conditions). When the sedimentation coefficient is calculated from the 50%-point for each pattern, the value was 2.81 S. These are in excellent agreement with the value 2.83 S reported by Cecil and Ogston (1948) through the use of schlieren techniques. The amount of labor involved in calculations with Eq. (28a) is, of course, much greater than that required with the 50%-point. However, in the study of special problems, such as the examination of mixtures of proteins with small interacting molecules,

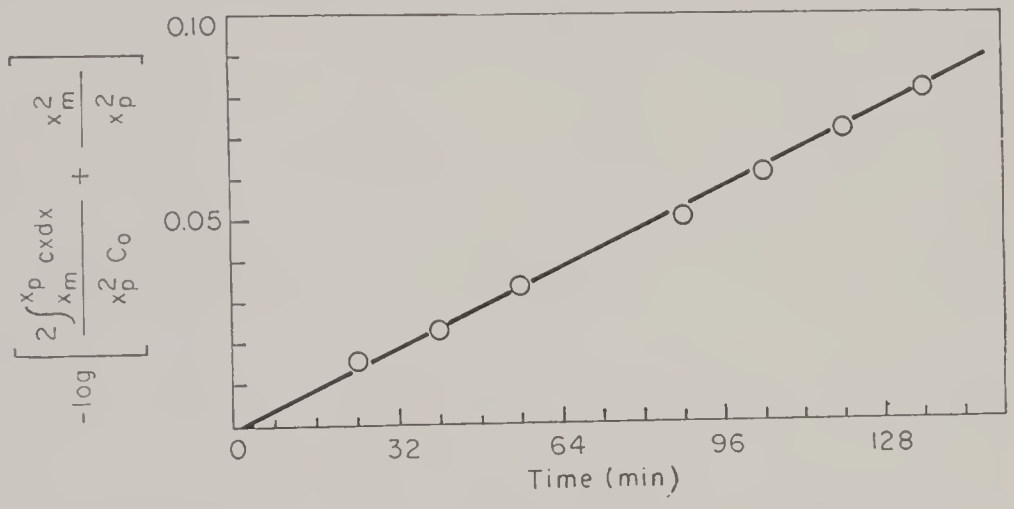

FIG. 22. Determination of sedimentation coefficient of β-lactoglobulin by the transport method. Patterns were obtained with the ultraviolet absorption optical system and are shown in Fig. 14. The densitometer tracings which, in effect, give a plot of c vs. x are shown in Fig. 15. In the above plot, the data are handled according to Eq. (28a).

use of the boundary movement may be precluded, whereas Eq. (28) has wide applicability.

Different methods have been employed by various authors (Baldwin, 1953b; Webber, 1956) to reduce the labor involved in calculations of sedimentation coefficients by the transport method. The paper by Trautman (1956) is especially valuable for workers in this field because it discusses various ways of handling the data so as to facilitate the tedious calculations and reduce the possibilities of inadvertent errors during the computations. This paper discusses many types of calculations and the experimental aspects concerned with different ultracentrifugal methods.

4. Dependence of Sedimentation Coefficient on Concentration

Sedimentation coefficients for nearly all substances thus far examined have been found to depend on the concentration of the sedimenting material. The degree of dependence, however, varies markedly from one

substance to another and is related to the physical properties of the macromolecules. Research on this general problem has been directed along different lines, and progress in some aspects has been striking, whereas in other lines the best theories are still inadequate. The most important strides are concerned with the quantitative understanding of the effect of this concentration dependence on the shape of boundaries at finite concentrations and the development of extrapolation procedures which yield reliable data at infinite dilution where concentration effects are no longer present. Still deficient is our understanding, in quantitative terms, of the reasons for the concentration dependence of sedimentation coefficients and the relation of this dependence to parameters of the macromolecules. Section IV,8c deals primarily with analysis of the shape of ultracentrifuge boundaries; here we shall discuss the various researches on the relationship of sedimentation coefficients to concentration.

Present theories for the interpretation of sedimentation velocity experiments require the value of the sedimentation coefficient at infinite dilution. This is generally inferred from data at finite concentrations which are extrapolated by either of the following equations:

$$s = \frac{s_0}{1 + kc} \tag{32}$$

or

$$s = s_0 (1 - kc) \tag{33}$$

In these equations, s_0 is the infinite dilution value of the sedimentation coefficient, k is a constant, and s is the sedimentation coefficient at the concentration, c. It should be stressed, at the outset, that neither of these equations applies over a wide concentration range, although Eq. (32) is generally more satisfactory in this regard. An additional term containing the square of the concentration has occasionally been included in Eq. (33). It is important to note here that charge effects influence not only the sedimentation rate of macromolecules (see Section VII,4) but also the dependence of sedimentation coefficient on concentration. All of the theories discussed here consider neutral molecules only; and for the application of the equations, neutral salts must be present in the solutions in order to damp out any charge effects arising from the migration of macromolecules possessing a net charge.

Kermack *et al.* (1929) and, independently, Burgers (1941, 1942) have performed detailed theoretical investigations of the hydrodynamic problem of the sedimentation of particles in a closed cell. It seems, as a result of these investigations and other considerations, that the sedimentation coefficient will depend on concentration for at least three reasons. The

effective viscosity of the medium surrounding each sedimenting particle will be some function of both the concentration of particles and their individual contributions to the macroscopic viscosity of the solution. Lauffer (1944b) has concluded that this is the dominant, and perhaps the only, factor. Secondly, the density of the solution through which the molecules sediment is certainly a function of concentration, and it is to be expected that sedimentation rates would be affected in some way by the density of the solution. A clear experimental demonstration of the role of the density contribution of protein molecules may be found in the work of Gofman *et al.* (1949). They showed that lipoprotein molecules, which sediment in one region of a centrifuge cell which is free of other proteins, actually float in the same run in another part of the cell which contains a high concentration of smaller protein molecules. This reversal of direction of migration of the large lipoprotein molecules on either side of the albumin boundary can only be interpreted as a reflection of the difference in sign of the effective buoyancy term owing to the contribution of other serum proteins to the density of the solution. It is true that the proteins which here affect the over-all density are smaller then the sedimenting lipoprotein molecules, but both materials are of the same order of molecular size. Finally, most workers recognize the contribution of backward flow of liquid as a partial explanation for the concentration dependence of the sedimentation coefficient. As molecules sediment in a closed vessel, there must be a flow of solvent in the opposite direction to make room for the migrating molecules and to fill the space formerly occupied by the molecules in the region above the moving boundary. This backward flow causes a decrease in the rate of sedimentation, which is measured relative to the cell walls, by an amount which might be expected to increase with an increase in concentration. Enoksson (1948) emphasized the role of backward flow of liquid and attributed the dependence of sedimentation coefficients on concentration solely to this effect. This view has been severely criticized (Cecil *et al.* 1949).

Though the calculations of Burgers (1941, 1942) were only preliminary and though they do not satisfactorily account for the sedimentation behavior of rigid, spherical particles at different concentrations, his theoretical papers do shed considerable light on the problems outlined above. Despite the temptation to attribute the concentration dependence to the viscosity of the solution, Burgers claims that the macroscopic viscosity cannot be operative in retarding the particles. Immediately adjacent to each macromolecule, according to Burgers, is a layer of liquid which has a lower viscosity than that of the bulk of the solution. This layer arises for purely geometrical reasons: the centers of two spherical macromolecules cannot come closer to one another than the sum of the two molecular radii,

so that no other molecular centers are ever found within one radius of the surface of a given particle. This region is therefore more dilute than the bulk of the solution. For elongated macromolecules there is even more steric exclusion because of the rotation of the long axes of the different particles. Burgers therefore concluded that the viscosity effective in retarding the motion of individual particles is less than the bulk viscosity. Kermack *et al.* (1929), who considered particles of different shapes, obtained a slightly different estimate for the effective viscosity relative to the bulk viscosity. Both theoretical treatments assume that the sedimenting particles transport some liquid plus their own volume to the bottom of the ultracentrifuge cell. This follows from the derivation of Stokes' law in which it is assumed that the fluid at the surface of a migrating particle does not slip relative to the particle and therefore moves with the same velocity as the particle. This layer in turn, through viscous forces in the liquid, drags along an adjoining layer of solvent at a slightly lower velocity, and so on out into the liquid until the velocity becomes zero. According to these workers, the backward flow of liquid must involve this additional fluid which is estimated by Burgers to be about 4 times the volume of the particles themselves. The remaining factor, the change in the buoyancy term with concentration, is generally much smaller than the other terms and is calculable. Questions have been raised as to whether the bulk density is operative in sedimentation velocity experiments as it is in sedimentation equilibrium experiments. Following Burgers' reasoning with regard to the effective viscosity, we might be tempted to conclude that an intermediate density is correct. This problem is discussed by Baldwin and Ogston (1954), who employ the solution density.

The concentration dependence of the sedimentation velocity of macromolecules has been ascribed completely by some workers to the change in the viscosity of the solution with concentration (Powell and Eyring, 1942; Lauffer, 1944b). Lauffer, in particular, has stressed this point of view and has amassed considerable data showing that for tobacco mosaic virus and a number of macromolecules, both natural and synthetic, the product of the sedimentation coefficient and the viscosity is nearly independent of the concentration of the macromolecules. In an exhaustive study on nitrocellulose, Jullander (1948) found that the product of the sedimentation coefficient and the relative viscosity of the solution actually increases with concentration. For bovine plasma albumin and ovalbumin, Kegeles and Gutter (1951) have shown the inapplicability of a viscosity correction in explaining the concentration dependence of the sedimentation coefficient. In consideration of this problem with special emphasis on another theory, Fessler and Ogston (1951) presented further criticism of explanations based on the viscosity of the solution. As they commented,

it would seem appropriate that the viscosity employed in this calculation be the viscosity of the solution at very low shear gradient rather than that measured at high shear gradient. However, the data they presented on hyaluronic acid and nucleic acid showed the opposite: namely, that the product of the sedimentation coefficient and the low shear gradient viscosity increased markedly with concentration. More recent data with different preparations of tobacco mosaic virus (Schachman and Kauzmann, 1949) do indeed show that the product of relative viscosity and sedimentation coefficient is independent of concentration, but the interpretation given these results by Schachman and Kauzmann is at variance with that proposed earlier. These workers concluded that there is no theoretical basis for the proposal that the product of sedimentation coefficient and relative viscosity should be concentration-independent, and further, they considered the results with tobacco mosaic virus as the product of a fortuitous cancellation of two opposing effects for particles of that particular shape. If the sedimentation coefficient in a concentrated solution is to be compared with that at very great dilution, the measured s at high concentration should first be corrected by the effective viscosity of the solution. This is, according to the ideas presented above, less than the bulk viscosity, but it is difficult to know how much less. Also the measured s at high concentration should be increased by a term accounting for the backward flow of liquid. Apparently for the virus particles the correction for backward flow is the same as the steric exclusion term so that neglect of both and use of the macroscopic viscosity of the solution gives a corrected value of s which is concentration-independent. For very elongated macromolecules, they concluded that the dependence of sedimentation coefficient on concentration is likely to be less than the dependence of viscosity on concentration; whereas for compact, globular macromolecules, correction of the sedimentation coefficient by the macroscopic viscosity of the solution will lead to an undercompensation. It is of interest to examine in Fig. 23 more recent data for tobacco mosaic virus along with those obtained on a preparation of a degradation product of the virus. The particles in the latter preparation have a length about two-thirds that of the native virus particles, and it is clear that the dependence of sedimentation coefficient on concentration is greater than would be expected if viscosity alone were responsible for this effect.

In view of the formal resemblance of Eq. (32) to the equation relating the sedimentation coefficient to molecular weight and the frictional coefficient, f, some workers state simply that the dependence of s upon c is no more than an expression of the dependence of the frictional coefficient on concentration (Newman and Eirich, 1950). The latter can, of course, be written as a power series in concentration. The constant k can thus

be related to parameters of flexible macromolecules, such as the molecular weight and configuration. In fact, Wales and Van Holde (1954) give explicit expressions for the relationship between k and the intrinsic viscosity. Though these equations are formally satisfactory, especially for flexible molecules, they do not, however, provide any physical insight into the magnitude of the relative factors considered by Burgers (1941, 1942). Furthermore, they employ the terms evaluated theoretically by Burgers, but it should be noted that this theory has been shown in experiments with polystyrene latex particles to be incapable of accounting for the data (Cheng and Schachman, 1955a). It should be noted that these particles

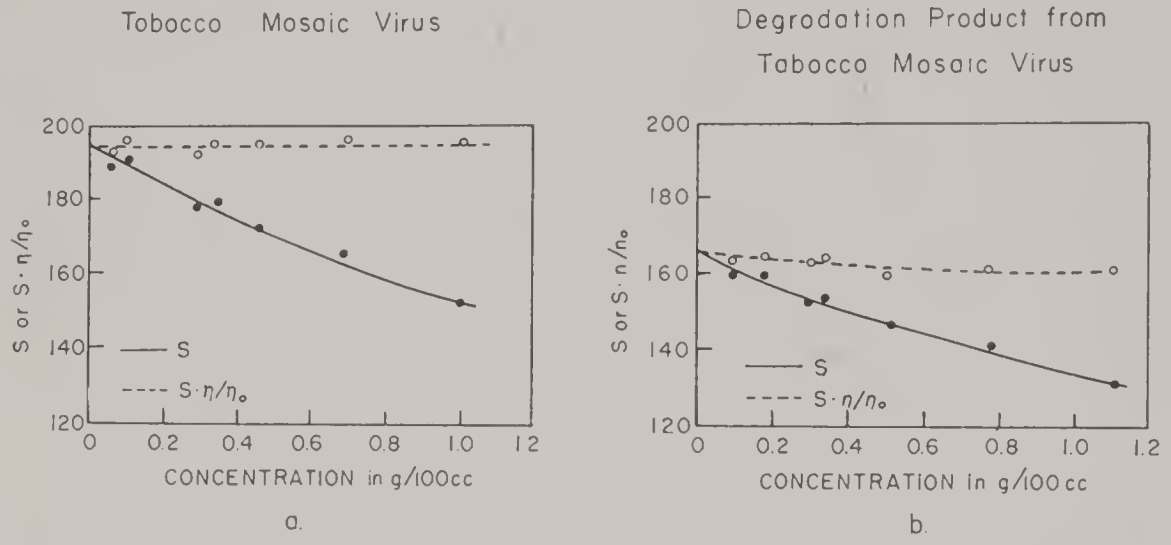

FIG. 23. Dependence of sedimentation coefficient on concentration (Schachman, unpublished).

(*a*) Data for tobacco mosaic virus. (*b*) Data for a degradation product of TMV produced by limited action of sodium dodecylsulfate. These particles are about ⅔ the length of the intact particles. Data are plotted as s or $s(\eta/\eta_0)$ vs. c where η/η_0 is the relative viscosity of the solutions.

constitute an excellent model, satisfying the requirements of the theory for rigid, solid, and impermeable spheres. These experiments provide more evidence demonstrating the inadequacy of a correction involving the solution viscosity, because the dependence of s upon c for the latex particles is greater than that which would be expected if only the macroscopic viscosity of the solution were operating in causing s to decrease at high concentrations. A term including a factor for backward flow is imperative. Further, it is of interest to note the inadequacies of the existing theories in another regard. For the latex particles, the coefficient of the square term which must be added to Eq. (32) is positive, whereas that coefficient for deoxyribonucleic acid is negative (Peacocke and Schachman, 1954).

Since many ultracentrifugal analyses are conducted on mixtures of sedimenting components, expressions are needed for the effect of one

component on the sedimentation coefficient of another. In fact, it would appear that with mixtures of the correct type, some experimental data could be provided which would be of value in estimating the relative contributions of backward flow and effective viscosity. In the analysis of mixtures, discussed in Section IV,7, it is necessary to know the sedimentation rate of one component, the slower of the two considered, in the presence of the other. Since the respective k values [Eq. (32) or (33)] for the two components are likely to be different, we might ask the following. Does the faster component affect the sedimentation rate of the slow relatively as much as (or more than) it affects its own sedimentation rate as its concentration is increased? Also does the k value for the slow component alone apply as well to the sedimentation rate of the fast component? Finally, does the presence of an additional sedimenting component affect the dependence of the sedimentation coefficient of the other on its own concentration? These questions, unfortunately, can only be partially answered at present, and the tentative answers may need drastic revision with time because of the inadequacy of the data on which the conclusions are drawn. We can rewrite Eq. (32) for two components when studied separately

$$s^{(1)} = \frac{s_0^{(1)}}{1 + k_1 c_1} \qquad \text{and} \qquad s^{(2)} = \frac{s_0^{(2)}}{1 + k_2 c_2} \tag{32}$$

where the superscripts, (1) and (2) and the subscripts, 1 and 2 refer to component 1 and 2, respectively. If we add a fixed amount of 2 to different solutions of 1, we can write

$$s^{(1)} = \frac{s_0^{(1)}}{1 + k_1 c_1 + k_{21} c_2} \tag{34}$$

where k_{21} represents the effect of component 2 on the sedimentation rate of component 1. Whether or not k_{21} is equal to k_2 will probably depend on the particular system. In the author's opinion, they are likely to be equal for mixtures of components with approximately equal sedimentation coeffcients. When $s_0^{(2)} \gg s_0^{(1)}$ it seems that k_{21} will also be greater than k_2. This can be shown qualitatively in an oversimplified treatment of the different effects considered by Burgers. Backward flow of solvent would be proportional to both the sedimentation rate of the migrating substance and its volume fraction, and we might write for the observed sedimentation rate in terms of only this effect

$$s = s_0(1 - k_{BF} c) \tag{35}$$

where k_{BF} is a constant referring to only the backward flow contribution to the dependence of s upon c. The term related to the effective viscosity

or the dependence of frictional resistance on concentration is likely to reduce the infinite dilution value, s_0, to some fraction of its value and can be expressed as

$$s = \frac{s_0}{1 + k_f c} \tag{36}$$

where k_f corresponds to the frictional contribution. Combination of these two effects for dilute solutions gives Eq. (32). It should be stressed that the molecular parameters responsible for the value of k_f would also control the magnitude of k_{BF} for a single component, and further, though these effects are written independently above, they are, indeed, for a single component inseparable (mathematically the term, $(1 - kc)$ is equivalent to $1/(1 + kc)$, if $kc \ll 1$). Justification for their separation arises in consideration of the questions posed above. Suppose a low molecular weight material (component 1) with $s = 1$ *S* is sedimenting in a mixture with a very large material (component 2) which possesses a large k, such as tobacco mosaic virus. If k_{21} is equal to k_2 and Eqs. (32), (34), or (36) apply, we could calculate how much less $s^{(1)}$ would be relative to $s_0^{(1)}$. These equations could not, however, predict a *negative* value for $s^{(1)}$; whereas, the separation of the terms as in Eq. (35) could indeed account for negative s values in such a mixture. Such negative sedimentation coefficients have been observed in certain mixtures (Lauffer and Taylor, 1952; Schachman and Harrington, 1954), although these experiments are not totally free from criticism as has been pointed out by the latter authors. In more recent experiments (Hersh and Schachman, 1958) which are free of convective disturbances (see Section IV,6), it is shown that the sedimentation coefficient of the slower component is relatively much more markedly affected by varying concentrations of the fast component than is the sedimentation rate of the fast influenced by its own concentration. It would seem that this can be best interpreted according to a factor resulting from backward flow as expressed by Eq. (35). Thus in mixtures of bushy stunt virus and deoxyribonucleic acid, it is as if the fast component, the virus particles, impart a certain absolute backward velocity to the liquid, say 3 *S*, which hardly affects the sedimentation rate of the fast component since its s is greater than 100 *S*. The slow component, which by itself has an s of only 7 *S* (at this concentration) suffers a 50% reduction in sedimentation velocity when the virus is added. At higher concentrations of virus, the backward velocity of the liquid is so great that the nucleic acid molecules have a negative sedimentation rate. On the other hand, studies of mixtures of two components of approximately equal sedimentation coefficient (Harrington and Schachman, 1953) indicate that varying the concentration of the fast has the same relative effect on the sedimenta-

tion rate of the slow as on the fast. An answer to the third question posed above is provided by the results of other experiments (Johnston, 1955; Hersh and Schachman, 1958). In studies of mixtures of hyaluronic acid and bovine plasma albumin, Johnston obtained data from which he concluded that the slow component (hyaluronic acid) did not affect the infinite dilution value of the sedimentation coefficient of the faster component, but rather it influenced the dependence of the sedimentation coefficient of the latter on its own concentration. With other systems composed of bushy stunt virus and either bovine plasma albumin or deoxyribonucleic acid, the results of Hersh and Schachman (1958) show

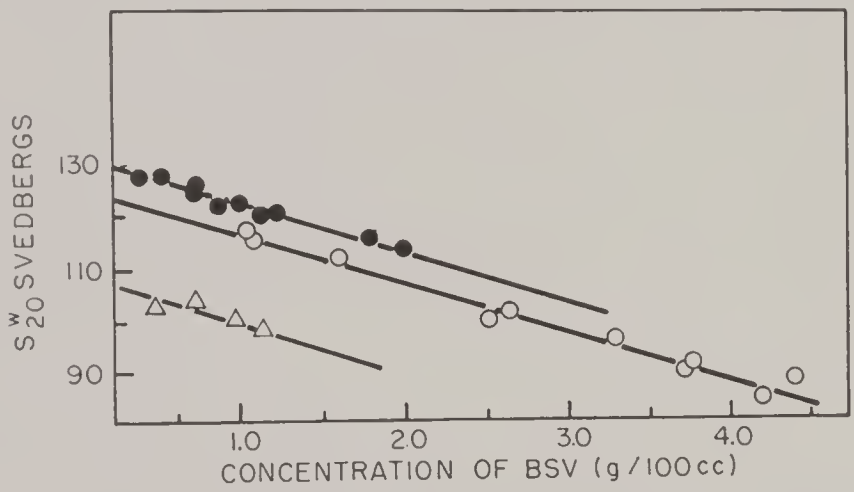

FIG. 24. The effect of a slow component on the concentration dependence of the sedimentation coefficient of a fast component. Upper curve: (●), is sedimentation coefficient of bushy stunt virus as a function of its concentration. Lower curves: (○), all solutions contain bovine plasma albumin at a concentration of 0.9 g./100 ml.; (△), all solutions contain deoxyribonucleic acid at a concentration of 0.1 g./100 ml. (from Hersh and Schachman, 1958).

clearly that the dependence of the sedimentation coefficient of the fast on its own concentration is not markedly affected by the presence of either of the two slower components. The absolute values of the sedimentation coefficient at different concentrations are, however, markedly influenced by the added component as seen in Fig. 24. Examination of the data given by Johnston reveals that they are not incompatible with those presented in Fig. 24. However, it should be emphasized that the mixtures are quite different in the two studies, particularly with reference to the relative sedimentation coefficients of the components. Though it appears that the conclusions of Johnston are not warranted, more data with mixtures such as he employed must be examined before the results presented in Fig. 24 can be considered as truly representative of all systems.

A demonstration of the risks of generalizing from limited data is shown in Fig. 25 which presents data (Schachman and Harrington, 1952 and

unpublished) on the sedimentation rate of different large particles in solutions containing varying amounts of deoxyribonucleic acid. In the same figure are given the relative viscosities of the nucleic acid solutions

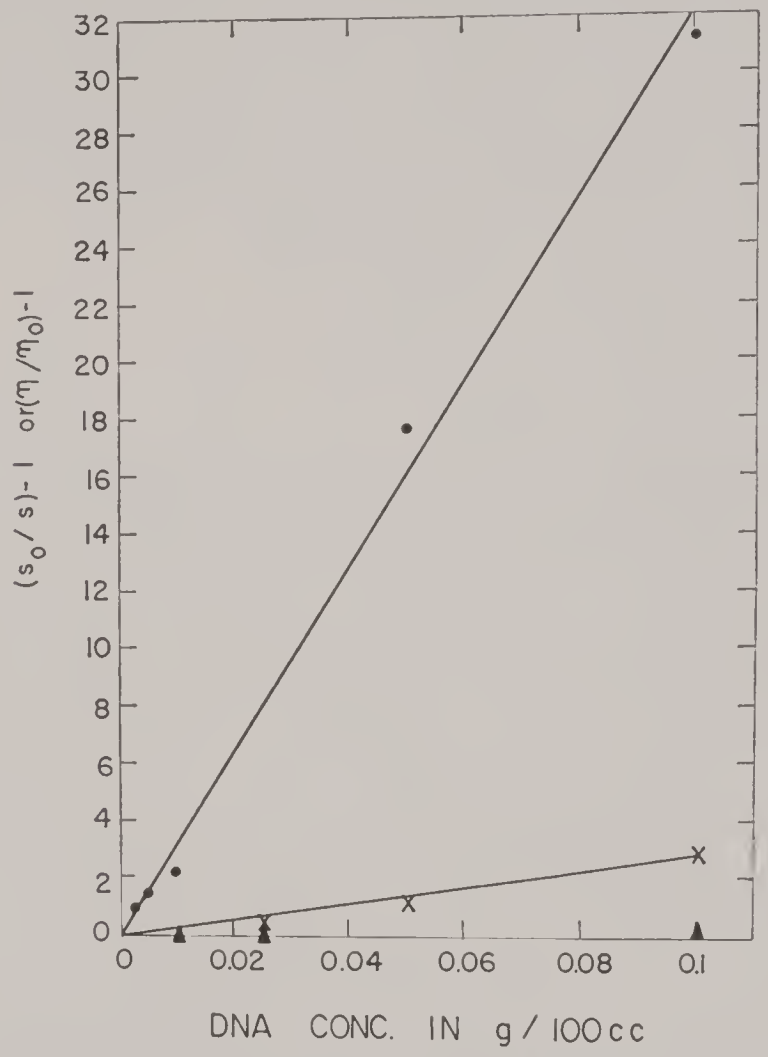

FIG. 25. The effect of different concentrations of a slow component on the rate of migration of various faster components. Sedimentation rates are expressed as $[(s_0/s) - 1]$ where s_0 is the sedimentation coefficient of the fast component alone, and s is the value in solutions containing various concentrations of the slow component, deoxyribonucleic acid (DNA). ● refers to data with polystyrene latex particles (PSL), and ▲ refers to data with bushy stunt virus (BSV). For comparison, the relative viscosity of the DNA solutions as measured in a capillary viscometer (×) is also shown (from Schachman and Harrington, unpublished).

measured in a capillary viscometer of low shear gradient. Although the sedimentation rate of the polystyrene latex particles through the nucleic acid solutions can be interpreted in the terms presented above (principally the viscosity contribution of the nucleic acid and its known variation with shear gradient), the difference in the behavior of bushy stunt virus in the same solutions requires an additional hypothesis. Presumably, the thread-like nucleic acid molecules form a loose entanglement which permits the

relatively small virus particles (300 A.) to pass through readily but allows the larger polystyrene latex particles (2600 A.) to proceed only at a greatly reduced velocity. The differences exhibited by these particles appear, from the limited data available, to be attributable to size alone, since the results are not altered by changes in the ionic strength or pH. For the latex particles, k_{12} is much larger than k_1 (where component 1 is deoxyribonucleic acid), whereas for bushy stunt virus, k_{12} is considerably less

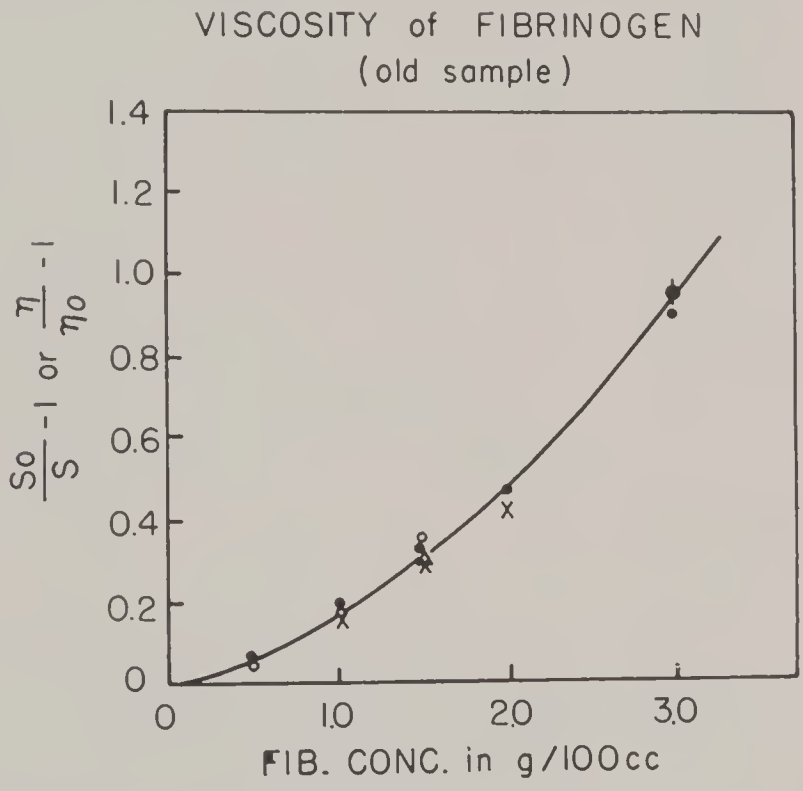

FIG. 26. Data similar to those of Fig. 25, showing the effect of varying concentrations of fibrinogen (FIB) on the sedimentation rates of T-3 bacteriophage, ●; bushy stunt virus, △; and tobacco mosaic virus (TMV), ○. The relative viscosity of the fibrinogen solution is also shown as × and ✹ (from Schachman and Harrington, unpublished).

than k_1. That these unusual results are a special characteristic of deoxyribonucleic acid and are not some ultracentrifugal anomaly is shown in Fig. 26 which presents analogous data (Schachman and Harrington, unpublished) with fibrinogen, as the so-called viscous component, and different larger materials sedimenting through solutions of it. Here the relative decrease of the sedimentation coefficient of the faster material is the same for all the substances examined. Since differences were observed with various fibrinogen samples, these data cannot be compared with the published data on the dependence of s of fibrinogen on its own concentration.

Ogston and co-workers (Fessler and Ogston, 1951; Ogston, 1953) consider sedimentation in a closed vessel to be analogous to the passage of a fluid through a stationary porous plug. Accordingly, they have adopted a treatment given by Sullivan and Hertel (1942) for the latter process with the suitable modifications necessary to obtain an equation of the correct form (Eq. 32). As Fessler and Ogston pointed out, the plug model which predicts infinite sedimentation coefficients at zero concentration must break down at great dilution. Therefore, they added a term to give the sedimentation coefficient at infinite dilution, and their equation takes the form

$$\frac{1}{s} = \frac{1}{s_0} + \eta A'^2 \frac{u'}{\zeta} \frac{100}{c(1 - \bar{V}\rho)} \left\{ \frac{cV'/100}{1 - (cV'/100)} \right\}^2 \tag{37}$$

In Eq. (37), s is the sedimentation coefficient at the concentration, c in g./100 ml., s_0 is the sedimentation coefficient at infinite dilution, η is the solvent viscosity, $\bar{V}$ is the partial specific volume, is the A' surface area of the hydrodynamic particle per unit hydrated volume, ρ is the density of the solution, V' is the effective hydrodynamic volume per gram of unsolvated mass, ζ is a constant which is a function of the shape of the particles, expressing the tortuosity of flow between them, and u' is another constant. Though Ogston and his co-workers have employed this equation for interpreting most of their results of the concentration dependence of sedimentation coefficients, it has not received much attention from other workers. Formally, the equation does provide a function of the correct form for the concentration dependence at low concentrations, but it does not account for the curvature of the $1/s$ versus c plots. Also the equation as it is presently employed contains assumptions and parameters which seem arbitrary to some workers. There is doubt as to the value of this equation in predicting the interrelationships for different components sedimenting in a mixture. In concentrated solutions of elongated, flexible macromolecules there is likely to be a network or gel formed among the molecules; in this case the porous plug model would be more meaningful than one based on an extension of the hydrodynamic theories presented above, since these were derived for dilute solutions. For proteins, even in concentrated solution, there is still freedom of motion of the macromolecules, and the treatments like those of Burgers (1941, 1942) are likely to be more fruitful. With concentrated solutions of polyelectrolytes like sodium carrageenate and sodium alginate, however, networks do form. These systems have been treated by Goring and Chepeswick (1955) in terms of a network model similar to that used by Signer and Egli (1950) and by Fessler and Ogston (1951).

All concentration effects considered thus far lead to a decrease in sedimentation coefficient at increasing concentrations. For flexible, highly charged macromolecules, it is possible that increasing the concentration may produce configurational changes which cause the frictional coefficient to decrease more than the effects mentioned above tend to increase the frictional resistance. If this occurred, the sedimentation coefficient would increase with concentration just as the reduced viscosity sometimes decreases with increasing concentration for polyelectrolytes. Such behavior has not yet been reported, and it is possible that the configurational changes are not sufficient to offset the other hydrodynamic effects which normally cause s to decrease with increasing concentration.

There are, however, some proteins which exhibit an increase in s as the concentration is raised despite the hydrodynamic factors enumerated above which tend to produce the opposite effect. In all cases examined thus far, this behavior is interpreted in terms of interacting systems involving association-dissociation equilibria with very rapid forward and backward reactions. These systems are considered in detail in Section IV, 9*a*.

If extrapolation to infinite dilution is desired, a plot of $1/s$ versus c generally gives good results. Many proteins show so little dependence of s upon c that a direct plot of those parameters will suffice for accurate extrapolation. It should be noted that for some systems which have been carefully examined, such as lactoglobulin (Cecil and Ogston, 1949), polystyrene latex particles (Cheng and Schachman, 1955a), and bovine plasma albumin (Baldwin, 1957b), the curvature actually decreases as the concentration approaches zero. A linear extrapolation of the data at high concentrations leads to infinite dilution values for such materials which are too high. For elongated macromolecules like deoxyribonucleic acid, the sedimentation coefficient becomes almost independent of concentration at higher concentrations, and preparations of very different molecular weights possess the same sedimentation coefficient. It is only when such materials are examined at very high dilution that differences in s are observed. Results with many different materials show that the preparations with higher s_0 also possess a larger k (Peacocke and Schachman, 1954). Signer and Egli (1950) discuss the analysis of sedimentation coefficients of concentrated solutions of flexible chain molecules. For such systems which show a pronounced dependence of s upon c, it is frequently advantageous to plot s and $s(\eta/\eta_0)$ versus c on the same graph. This gives two curves which must intersect at the same value as c approaches zero as in Fig. 23 (Lauffer and Stanley, 1944; Schachman, 1951b; Jullander, 1945).

For systems which exhibit a marked dependence of s upon c the position of the boundary as a function of time can be expressed by equations which

result from a combination of Eqs. (32) and (33) with Equations 13 and 16 followed by integration. This gives

$$\ln \frac{\bar{x}}{x_m} - \frac{kc_0}{2}\left[(x_m/\bar{x})^2 - 1\right] = \omega^2 s_0 t \tag{38}$$

for materials showing a dependence expressed by Eq. (32) (Golder, 1953; Trautman *et al.*, 1954; Fujita, 1956a). If the dependence is like that described by Eq. (33), the final equation (Trautman *et al.*, 1954; Hersh and Schachman, 1955) has the form

$$\bar{x}^2 = kc_0 x_m^2 + x_m^2 (1 - kc_0) e^{2\omega^2 s_0 t} \tag{39}$$

5. *Differential Sedimentation Rates*

Since the determination of the parameter, k, expressing the dependence of sedimentation coefficient on concentration, necessarily involves the small difference between two much larger numbers, small experimental errors in the measurement of s lead to a large uncertainty in the resulting value of k. Most values of k, now in the literature, doubtless require drastic revision. With the development of ultracentrifuge cells capable of forming sharp boundaries between any pair of solutions, an independent method is available for the determination of k in a single experiment. This method is new and has found only infrequent application, although it has features which commend it for such studies. Moreover, it provides the experimental background for the application of the moving boundary theory outlined earlier, and it furnishes a basis for the analysis of more complicated boundary systems by means of which, for example, the sedimentation coefficient of a slow component can be measured while it is sedimenting in the presence of more rapidly migrating material.

A solution of a sedimenting substance at concentration, c_1, can be layered over a second solution of the same material at a concentration, c_2, to produce a boundary which has been termed (Hersh and Schachman, 1955) a concentration or differential boundary by analogy with the nomenclature used in transference studies (Longsworth, 1943). The movement of such boundaries produces differential sedimentation rates. It should be noted here that differential methods which measure directly the small difference between the sedimentation coefficients of two different materials are also being developed. We are reserving the term "differential sedimentation rate" for the movement of boundaries between two solutions of the *same* substance, the *only* difference between the solutions residing in the concentration of the solute. This is emphasized because such measurements should be distinguished from differential techniques, such as that described in Section IV, 10, for measuring accurately very small differences

in sedimentation coefficients produced by some chemical or physical treatment or caused by the addition of another component. These latter measurements involve the comparison of solutions exhibiting differences in more than concentration alone.

Figure 27 is a simplified, schematic diagram of the process involved in measuring differential sedimentation rates. The cell is here considered rectangular in shape, and the field is assumed to be independent of position. Arbitrary planes are selected in the homogeneous solutions at some distance from the boundaries and the planes are considered to move at the velocities, s_1 and s_2, corresponding to the actual rates of migration of the molecules in the two solutions. Thus the amount of solute con-

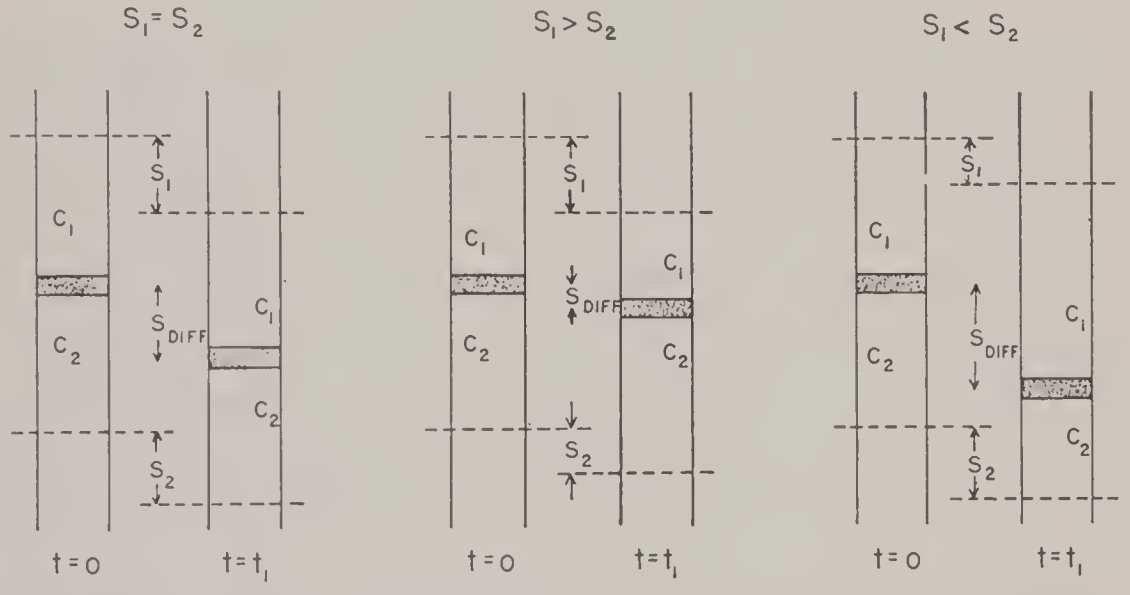

FIG. 27. Schematic diagram illustrating experiments for the measurement of differential sedimentation rates.

tained between the dotted lines (in each pair of drawings) is independent of time. If $s_1 = s_2$, as in the first case considered in Fig. 27, the volume containing all the solute molecules remains constant, and, therefore, the relative volumes of the regions with c_1 and c_2 must not vary with time. The differential boundary would, as a consequence, move at the same rate as the two imaginary planes. In the usual case in which $s_1 > s_2$, the total volume containing the solute molecules must decrease with time, since the leading plane moves a smaller distance than the trailing plane. This can be accounted for by the enlargement of the region with concentration, c_2, at the expense of some of the more dilute region. It is as if some material from the upper solution is concentrated to a level, c_2, and this solution is added onto the lower region. The differential boundary will therefore show less movement than either of the two planes. Just the

opposite situation obtains for systems which exhibit higher sedimentation coefficients with increasing concentration (as in associating-dissociating equilibria), and the differential boundary moves faster than either of the hypothetical planes as shown in Fig. 27.

These processes can occur continuously in a centrifuge cell without the creation of gravitational instability resulting from density inversions. Usually $s_1 > s_2$ (positive k), and the molecules in the upper, dilute solution which are moving more rapidly than those in the lower solution crowd together in the region of the differential boundary. This accumulation continues until a concentration equal to that in the lower phase is achieved. Once the concentration of the lower solution is attained, these molecules from the upper solution experience a new sedimentation velocity characteristic of those molecules present in the lower solution. In this way, as the particles in the lower solution just ahead of the initial differential boundary move through the cell, material at the same concentration is constantly being added behind them, and, for this reason, the differential boundary moves at a lower rate than do the molecules in the concentrated solution. It is to be expected that this process would continue without any convective disturbances if $s_1 > s_2$, and, indeed, the experiments described thus far appear to satisfy all of the requirements of convection-free sedimentation and the equations derived from considerations of the conservation of mass. Following this line of reasoning, we might expect that instability and, consequently, convection would result if the molecules in the lower solution move more rapidly than those in the upper solution. In such an experiment, beginning after the formation of the differential boundary, the molecules below will move more rapidly than those above can fill up the region at the differential boundary. As a consequence, a region is created in which the density is less than that of the solution above it. This, of course, is gravitationally unstable, and convective disturbances must occur. Experiments (Schachman and Harrington, 1954) with different proteins chosen with the appropriate sedimentation coefficients did produce convection whenever $s_2 > s_1$ except for some associating-dissociating systems.

With chymotrypsin under conditions in which the lower solution possessed a higher average sedimentation coefficient than the upper solution, no convection was observed. Since the aggregates here are presumed to be in very rapid equilibrium with the monomer, stability is achieved in this experiment by the dissociation of some of the aggregates at the trailing end of the lower solution to establish a mixture comparable to the upper solution. Whereas with chymotrypsin this apparently occurs without signs of gravitational instability and convection, comparable experiments with insulin (Schachman and Harrington, 1954) lead to convective dis-

turbances. This has been attributed to a slow rate of dissociation of the aggregates of insulin.

The moving boundary equation describing these experiments can be derived in the following manner (Hersh and Schachman, 1955). The total mass contained between two surfaces at x_2 and x_1 can be written

$$m' = q/2[c_2(x_2^2 - x_D^2) + c_1(x_D^2 - x_1^2)] \tag{40}$$

where x_D is the distance of the differential boundary from the axis of rotation and q is a constant expressing the thickness of the cell and the sector angle. As in Fig. 27 the surfaces at x_1 and x_2 in homogeneous solutions of concentrations, c_1 and c_2, respectively, are assumed to move with the sedimentation coefficients of the particles in those regions. Since no material is entering or leaving the volume element defined by these surfaces, m' must be independent of time and the derivative of Eq. (40) with respect to time must be zero. Thus we can write

$$\frac{dc_2}{dt}(x_2^2 - x_D^2) + 2c_2\left(x_2\frac{dx_2}{dt} - x_D\frac{dx_D}{dt}\right) + \frac{dc_1}{dt}(x_D^2 - x_1^2) + 2c_1\left(x_D\frac{dx_D}{dt} - x_1\frac{dx_1}{dt}\right) = 0 \tag{41}$$

In combination with the radial dilution equation presented earlier (Eq. 8) and the definition of the sedimentation coefficient (Eq. 2), this equation becomes

$$\frac{1}{\omega^2 x_D}\frac{dx_D}{dt} = s_D = \frac{c_2 s_2 - c_1 s_1}{c_2 - c_1} \tag{42}$$

Since c_2 can be written as $c_1 + \Delta c$ and $s_2 = s_1 + \Delta s$, Eq. (42) becomes, in the limit when Δc approaches zero,

$$s_D = s + c\frac{ds}{dc} \tag{43}$$

Thus the differential sedimentation rate provides a direct measure of the change in sedimentation coefficient with concentration. As already indicated (ds/dc) is usually negative and Eq. (43) shows that $s_D < s$. For associating systems, $(ds/dc) > 0$ and $s_D > s$.

These relations furnish the theoretical basis for the physical picture illustrated in Fig. 27. Consideration of Eq. (41) at different times shows directly that the change in concentration across the differential boundary must follow the radial dilution rule just as do conventional boundaries. Experiments with bushy stunt virus and chymotrypsin (Hersh and Schachman, 1955) produced results in direct accord with the theoretical consid-

erations presented above. For materials which exhibit a pronounced dependence of sedimentation coefficient on concentration, the above treatment must be modified to account for variations in sedimentation coefficient during an experiment. Although the equations are cumbersome and the position of the differential boundary as a function of time cannot be written in explicit form for a substance which obeys Eq. (32), the equations can be solved numerically. Deoxyribonucleic acid has such a large dependence of sedimentation coefficient upon concentration that the boundary created at the meniscus overtakes the differential boundary and merges with it, thereby forming a third boundary. Representative ultracentrifuge patterns from such an experiment are shown in Fig. 28. Thus three sedimentation coefficients can be evaluated in this single experiment. From the data provided by this experiment, the parameters, s_0 and k, can

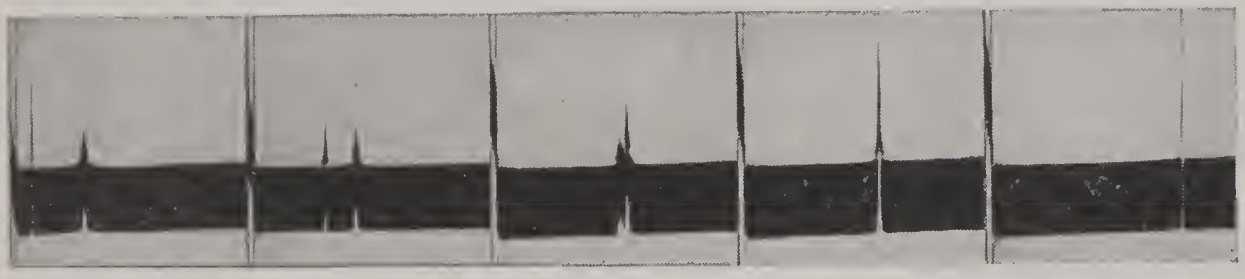

FIG. 28. Ultracentrifuge patterns illustrating the measurement of the differential sedimentation rate for deoxyribonucleic acid. The concentration of the upper and lower solutions were 0.05 and 0.10 g./100 ml., respectively; pictures correspond to 4, 24, 40, 44, and 64 min. after attaining speed, (from Hersh and Schachman, 1955).

be evaluated in different ways, and the theoretical curves relating boundary position to time can then be constructed. There is excellent agreement between the experimental data and the theoretically constructed curves using s_0 and k obtained in different ways.

A single differential sedimentation rate along with the conventional s value obtained in the same experiment are sufficient for precise calculations of s_0 and k whereas two experiments, in general, are ordinarily required for evaluation of those quantities. Moreover, errors in the individual experiments are in part obviated by the method described here since factors such as speed and temperature of the rotor are the same for both of the experimentally required measurements. As shown by Hersh and Schachman (1955) the differential boundary, for systems following Eq. (33), has a sedimentation coefficient equal to that which would be observed for a conventional boundary at a concentration equal to the sum of the concentrations of the upper and lower solutions. Thus a larger concentration range is studied, in effect, when s_0 is measured, and a saving of material is thereby effected.

In the next section we will discuss a much more complicated boundary system from the point of view of the moving boundary equation described by Eq. (42). This is a direct expression of the conservation of mass which is sometimes presented in the alternative form: the net transport of the sedimenting material *relative* to the movement of the differential boundary must be zero. Therefore, we can write

$$c_1(s_1 - s_D) - c_2(s_2 - s_D) = 0 \qquad (42a)$$

which is, of course, identical with Eq. (42). Such a formulation was first employed by Johnston and Ogston (1946) in theoretical considerations of the analyses of mixtures.

6. Sedimentation of a Slow Component in the Presence of a Faster Species

A critical appraisal of any quantitative theory for the analysis of mixtures of two or more sedimenting components is dependent on knowledge of the effect of the faster components on the sedimentation rate of the more slowly migrating material. For systems of interacting components such knowledge is required for the determination of the amount of the slower component in the uncombined form in an equilibrium mixture. Finally, precise data of the sedimentation coefficient of a slow component in the presence of faster species would be invaluable in discriminating among the different hydrodynamic factors discussed in Section IV,4.

If the sedimentation coefficient of the slow component alone is nearly zero (as with small molecules), then its sedimentation rate in the presence of a fast component is, in effect, a measure of the backward flow caused by the sedimentation of the fast component. No attempts at direct measurements of the backward flow contribution were made until Lauffer and Taylor (1952) devised an experiment for this purpose. There is presently some discussion (Lauffer and Bendet, 1954) not only as to how such measurements should be made but also as to whether these measurements can be performed in experiments which are free of convective disturbances. It is of interest to note that the experiment conceived by Lauffer and Taylor was first visualized (in a different way) by Lewis (1910) for the determination of the hydration of ions. Longsworth (1947) has since performed the Lewis experiment in an electrophoresis apparatus, and there are striking similarities between his results and those obtained with the ultracentrifuge.

If a solution of fast component is carefully layered over another solution containing both fast component (at the same concentration) and slow component, a boundary due to the slow component (in the presence of the fast) is created in the middle of the cell. Measurement of the rate of movement of this boundary, before the fast component overtakes it,

permits a determination of the sedimentation coefficient of the slow in the presence of the fast. This is essentially the experiment of Lauffer and Taylor except that their interest was solely in the determination of the hydrodynamic volume of the fast component. Accordingly, they selected as the slow, or indicator component, a material with nearly zero sedimentation coefficient such as sucrose. Moreover, they measured only the total negative (or centripetal) displacement of the indicator boundary as the molecules of the fast component were transported across the surface containing the indicator boundary. They then calculated with Eq. (44) the fraction, L, of the total cell volume which was originally above the indicator boundary and then migrated across it.

$$L = \frac{x_2^{\,2} - x_3^{\,2}}{x_2^{\,2} - x_1^{\,2}} \tag{44}$$

In Eq. (44), x_2 and x_3 are the initial and final positions of the indicator boundary and x_1 is the position of the boundary of the fast component initially (frequently, the meniscus). Corrections were made for the slight centrifugal migration suffered by the indicator in a control experiment. With the calculated value of L, the known dry weight concentration, and the partial specific volume of the fast component, Lauffer and Taylor inferred the amount of hydration of that material. Similar experiments were performed with the use of the synthetic boundary cell (Schachman and Harrington, 1954) with a variety of indicators such as proteins, sucrose, and sodium chloride. In these experiments, boundary positions were measured at different times, and sedimentation coefficients determined. If the indicators were of low molecular weight compared to the fast component, negative sedimentation coefficients were observed, in agreement with the boundary movement observed by Lauffer and Taylor. For indicators with comparable but still smaller sedimentation rates than exhibited by the fast component, the measured sedimentation coefficient was reported as the value for the slow component in the presence of the faster species (Harrington and Schachman, 1953). These papers called attention to the existence of complications in all of these experiments because the fast component in the upper part of the cell, where no indicator is present, is no doubt migrating at a faster rate than is the same component in the lower part of the cell owing to the viscosity and density contributions of the indicator. Such a difference in sedimentation rate of the fast component across the indicator boundary must lead to some accumulation of the fast component within the indicator boundary. As a consequence, density inversions and convection may result which would invalidate any calculations of hydration. Moreover, different results were obtained by Schachman and Harrington (1954), depending upon the nature

of the indicator. It seems, to this reviewer at least, that any calculations of hydration of the fast component from experiments of this type must be considered premature. Further, meaningful data on the amount of backward flow cannot be derived in these experiments if convection ensues.

In a further investigation of this problem with either deoxyribonucleic acid (DNA) or bovine plasma albumin (BPA) as the indicators and bushy stunt virus (BSV) as the fast component, Hersh and Schachman (1958) derived further information about the processes involved in the experiments outlined above. Further they designed an experiment which is apparently free of the objections leveled at the earlier experiments. Several conclusions can be drawn from the first part of their study: The backward velocity of the indicator boundary depends in a linear fashion on the concentration of the fast component above the indicator boundary. This is in direct accord with the basic formulation of the problem by Lauffer and Taylor. Further, the movement of the indicator boundary is independent of the concentration of the indicator. This, too, is a basic requirement if calculations of hydrodynamic volumes from such experiments are to have any validity. There is a substantial accumulation of the fast component within the indicator boundary. Area measurements of the fast boundary as it migrated from the meniscus to the indicator (DNA) boundary were in direct accord with the radial dilution rule. However, the area of the boundary of the fast component which emerged after passing the indicator boundary was increased by 10% over the initial value, and, moreover, this area then decreased in a normal manner as the boundary continued moving down through the cell. Attempts to calculate this accumulation were successful, but the computations were performed in a nonrigorous manner, and they involved the assumption of convective stirring in the lower part of the cell. Although there was agreement between the calculated and experimental values, we cannot consider this as proof of the hypotheses employed in the estimations. Finally, very large differences in the rate of backward movement were detected with different indicators, e.g., with DNA the rate was more than 10 times that observed with BPA as the indicator. If the backward motion of the indicator were a function only of the hydrodynamic volume of the fast component, then the motion of both indicators should be the same. That this is not the experimental result casts doubt on the value of an interpretation of these experiments in terms of the properties of the fast component.

From the experiments discussed above, it is clear that an accumulation occurs at the indicator boundary and that the concentration of the fast component in the lower part of the cell increases with time until the fast

component crosses the indicator boundary. Accordingly, experiments were performed in which initially a gradient of concentration of the fast component was superimposed on the gradient due to the indicator component. A schematic drawing of the concentration distribution in such an experiment after a time, t, is presented in Fig. 29. Since $s_F^{\beta} > s_F^{\gamma}$ accumulation would occur unless the concentrations of the fast component on each side of the $\beta\gamma$-(indicator) boundary were properly adjusted initially so as to prevent accumulation. Rather than attempt to find, either by trial and error or by some approximate calculation, the necessary concentrations, we can imagine an excess of fast component placed in the lower solution. The molecules of this fast component sediment away from

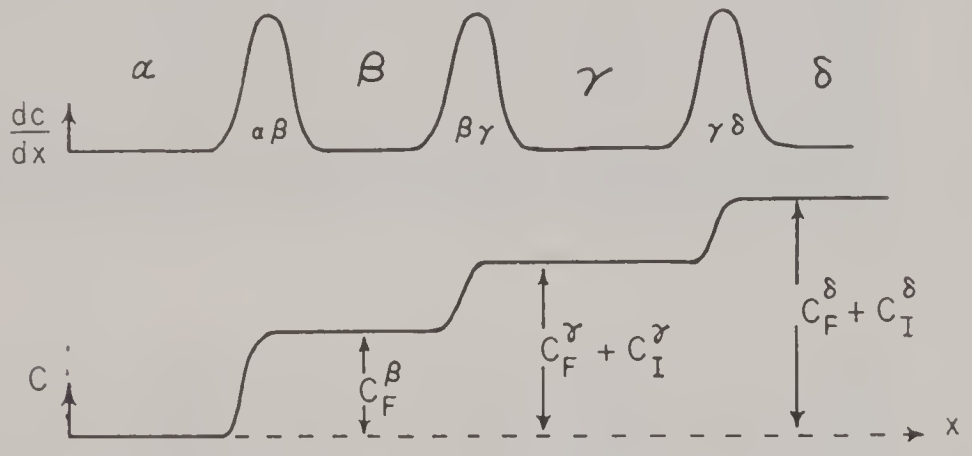

FIG. 29. Schematic diagram illustrating the concentration and concentration gradient as a function of distance in an experiment for the measurement of the sedimentation coefficient of a slow component migrating in the presence of a faster species (from Hersh and Schachman, 1958).

the $\beta\gamma$-boundary. Meanwhile other fast component molecules cross the $\beta\gamma$-boundary to replace the molecules of fast component originally in that region, but the concentration is now less. Thus a differential boundary, the $\gamma\delta$-boundary, of the fast component is formed. Actually the $\gamma\delta$-boundary is also a compound boundary (see Section IV, 7), but this can be ignored for our present purposes. Since the fast component sediments more slowly in the γ-region than in the β-region, a concentration gradient of the fast component is also formed at the indicator or $\beta\gamma$-boundary. Thus the $\beta\gamma$-boundary becomes a compound boundary across which the concentration change can be written.

$$\Delta c^{\beta\gamma} = c_F^{\gamma} - c_F^{\beta} + c_I^{\gamma} \tag{45}$$

where F and I refer to the fast and indicator components, and the superscripts correspond to the phases illustrated by Fig. 29. Equation 45 can be differentiated with respect to time and combined with the appropriate

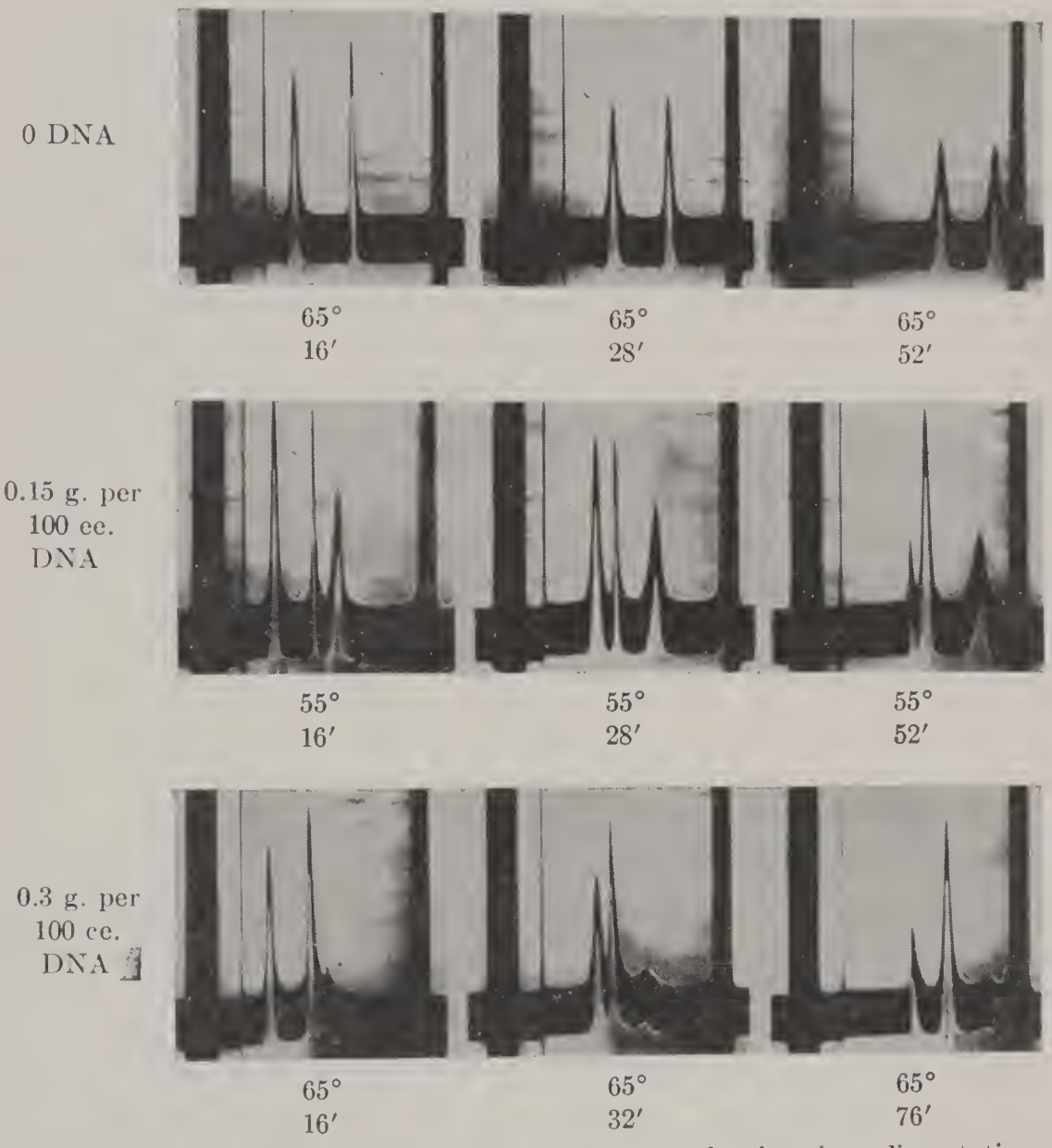

FIG. 30. Ultracentrifuge patterns from experiments showing the sedimentation of deoxyribonucleic acid (DNA) in the presence of bushy stunt virus (BSV). In all experiments the initial concentration of BSV in the upper part of the cell is 0.45 g./100 ml., and in the lower part the concentration of BSV is 0.89 g./100 ml. The upper experiment contains no DNA, the middle has 0.15 g./100 ml., and the lower, 0.3 g./100 ml. The pictures on the left are taken before the BSV boundary originating at the meniscus reached the indicator boundary. The next photographs were obtained just before the merging of the boundaries, and the final patterns are after the BSV boundary passes the indicator boundary. For the first experiment, the patterns illustrated correspond to 16, 28, and 52 min. after reaching speed, and the angle of the schlieren diaphragm was 65°, 65°, and 65°. In the second experiment these values were 16, 28, and 52 min., and the angles were 55°, 55°, and 55°. The times for the lower patterns were 16, 32, and 76 min. and the angles of the schlieren diaphragm were 65°, 65°, and 65° (from Hersh and Schachman, 1958).

independent expressions for the radial dilution equation and its general statement (Eq. 15) to give

$$\frac{d\Delta c^{\beta\gamma}}{dt} = -2\Delta c^{\beta\gamma}\omega^2 s^{\beta\gamma} \tag{46}$$

This shows that the compound boundary also follows the radial dilution rule, as long as there is no convection throughout the cell, and radial dilution occurs in other regions of the cell. Data from experiments of this type are completely consistent with the assumptions involved in deriving Eq. (46). Combination of Eq. (46) with that expressing the time derivative of Eq. (45) and the radial dilution expressions for each phase gives directly the moving boundary equation

$$s^{\beta\gamma} = \frac{c_F{}^{\gamma}s_F{}^{\gamma} - c_F{}^{\beta}s_F{}^{\beta} + c_I{}^{\gamma}s_I{}^{\gamma}}{c_F{}^{\gamma} - c_F{}^{\beta} + c_I{}^{\gamma}} \tag{47}$$

This is the direct analog of Eq. (42) presented earlier for differential sedimentation rates. Unfortunately, the equation in its present form cannot be verified readily by experiment since it contains both $s^{\beta\gamma}$ and $s_I{}^{\gamma}$, and the interrelationship of these sedimentation coefficients has not yet been described. This will be done presently.

Representative ultracentrifuge patterns from three separate experiments are presented in Fig. 30. The upper photographs can essentially be considered a control involving a differential boundary of BSV. Beneath these patterns are analogous photographs from experiments in which two different concentrations of the indicator (DNA) were added to the lower solution, the other concentrations being maintained constant. Had there been no hold-up of BSV at the indicator boundary in these latter experiments the area of the $\gamma\delta$-boundary would have been the same in all three experiments. The patterns show, however, that the distribution of BSV in the lower solution is markedly affected by the presence of DNA. In fact, so much of the BSV is held back at the indicator boundary in the experiment at 0.3 g./100 ml. of DNA that the $\gamma\delta$-boundary is almost completely annihilated. This hold-up is further reflected by the enormous enhancement of the area of the $\alpha\beta$-boundary after it crosses over the $\beta\gamma$-boundary. Quantitative measurement of the hold-up of the fast component, i.e., $(c_F{}^{\gamma} - c_F{}^{\beta})$, can be made either from the decrease in the area of the $\gamma\delta$-boundary (relative to the control experiment) or from the change in the $\alpha\beta$-boundary upon its crossing over the indicator boundary.

From considerations of moving boundaries presented earlier, we can conclude that the formation of the $\gamma\delta$-boundary which migrates away from the $\beta\gamma$-boundary must be attributable to the fact that initially more fast component is leaving the indicator boundary than is entering from above.

This is just the opposite of the experiments described earlier in which there was a uniform concentration of fast component throughout the cell. A direct measure of the net amount of fast component leaving the $\beta\gamma$-boundary is provided by the behavior of the $\gamma\delta$-boundary. Since the initial concentrations are known, this reveals the amount of fast component held up at the indicator boundary to form there a differential boundary. But this differential boundary, it must be emphasized, is formed at, and migrates with, the indicator boundary. Therefore, the net transport of fast component *relative* to the movement of the indicator boundary must be zero, and we can write

$$c_F{}^{\gamma}(s_F{}^{\gamma} - s^{\beta\gamma}) = c_F{}^{\beta}(s_F{}^{\beta} - s^{\beta\gamma}) \tag{48}$$

or

$$c_F{}^{\gamma} - c_F{}^{\beta} = \frac{c_F{}^{\gamma}s_F{}^{\gamma} - c_F{}^{\beta}s_F{}^{\beta}}{s^{\beta\gamma}} \tag{48a}$$

With this condition imposed on Eq. (47), we find, of course, that the indicator species must move with the sedimentation coefficient of the compound, $\beta\gamma$-boundary, i.e., $s_I{}^{\gamma} = s^{\beta\gamma}$.

Various lines of evidence are presented by Hersh and Schachman (1958) to demonstrate the validity of the above treatment and to show that the boundaries do obey the laws of convection-free sedimentation. Area measurements on both the $\alpha\beta$- and $\gamma\delta$-boundaries are in accord with the dilution rules, despite the fact that the area of the $\alpha\beta$-boundary increased over 30% upon passage across the indicator boundary. Equation (48*a*) shows that only one concentration of $c_F{}^{\gamma}$ can satisfy the equation if other quantitites are maintained constant. Experiments performed at fixed initial concentrations of $c_F{}^{\beta}$ and $c_I{}^{\gamma}$ with variable amounts of fast component (bushy stunt virus) placed in the bottom solution revealed always that a fixed amount of fast component was held up at the indicator (deoxyribonucleic acid) boundary; i.e., $c_F{}^{\gamma}$ was constant. This was demonstrated either by comparison of the area of the $\gamma\delta$-boundary from one experiment to another or by the change in the area of the $\alpha\beta$-boundary upon crossing the indicator boundary. Moreover the value of $c_F{}^{\gamma}$ evaluated by either of these methods is in good agreement with that computed from Eq. (48*a*). Finally Eq. (48*a*) was subjected to experimental test by conducting experiments at different indicator concentrations, $c_{I,0}^{\gamma}$, and measuring $s^{\beta\gamma}$ for fixed initial concentrations of $c_{F,0}^{\beta}$ and $c_{F,0}^{\gamma}$. Table IV summarizes the data from these experiments. Column 5 contains values of $\Delta c_F^{\beta\gamma}$ measured by the change in area of the $\alpha\beta$-boundary during the run, as indicated above, and column 6 presents the values calculated from Eq. (48*a*). The agreement between calculated and experimental values is excellent and can

be taken as strong evidence in support of the considerations presented above.

It is of interest to note that $s^{\beta\gamma}$ in the above mentioned experiments varies from 4 S to -1 S. For indicator concentrations of 0.10 g./100 ml., $s^{\beta\gamma}$ is 3 S in experiments of this type when $c^{\beta}_{F,0}$ is 0.58 g./100 ml. When $c^{\beta}_{F,0} = c^{\gamma}_{F,0}$ as in the experiment of Lauffer and Taylor (1952) $s^{\beta\gamma} = -50$ S. Thus, the presence of additional fast component in the lower solution (all other conditions being the same) changes by a huge amount the apparent negative sedimentation coefficient of the indicator. It is difficult to visualize how this could occur without invoking the view that convective transport of liquid must be responsible for the large apparent backward

TABLE IV

Amount of Bushy Stunt Virus Held up at the Indicator Boundary[a]

($c^{\beta}_{F,0}$ = 0.45 g./100 ml., $c^{\gamma}_{F,0}$ = 0.89 g./100 ml.)

$c^{\gamma}_{I,0}$ (g./100 ml.)	$s_F{}^{\beta}$ (S)	$s_F{}^{\gamma}$ (S)	$s^{\beta\gamma}$ (S)	$\Delta c_F^{\beta\gamma}$ Measured[b] (g./100 ml.)	$\Delta c_F^{\beta\gamma}$ Calculated[c] (g. 100 ml.)
0.10	126	107	+4	0.11 ± 0.02	0.08
0.15	119	100	+3	0.11 ± 0.02	0.09
0.20	124	93	+3	0.17 ± 0.02	0.15
0.30	126	75	−1	0.29 ± 0.01	0.30

[a] From Hersh and Schachman, 1958. The indicator used was deoxyribonucleic acid.

[b] Determined from $\gamma\delta$-boundary and the change in area of the $\alpha\beta$-boundary upon passing the $\beta\gamma$-boundary.

[c] Calculated from Eq. (48a).

flow in the one type of experiment. When such convection is eliminated as by the self-regulating and gravitationally stable experiments described here, the backward flow is greatly reduced, though still measurable. The variations in $s^{\beta\gamma}$ exhibited in Table IV are, of course, a reflection in part of the concentration dependence of the sedimentation coefficient of DNA, since each of these values should be compared with sedimentation coefficient of DNA when examined alone at the corresponding concentrations. In terms of the discussion in Section IV, 4, the tremendous change in s_I as a result of the addition of BSV should be compared with the almost negligible dependence of s_F on the concentration of BSV. This can only be explained, it seems, in terms of backward flow caused by the fast moving particles.

Some of the data in the literature certainly will need revision because of the existence of serious convection in the particular experiments, but it is

difficult to estimate the magnitude of the revision or even whether it is necessary in all experiments. As seen above, the system tends to be self-stabilizing. Since $s_F{}^\gamma$ is less than $s_F{}^\beta$, a differential boundary of fast component is formed during an experiment. If the concentration change established in this way is sufficiently large, accumulation can be prevented and convection-free sedimentation ensues. It seems advisable, however, that experiments designed to measure the sedimentation coefficient of a slow component in the presence of a faster species be performed with an excess of fast component in the lower solution so as to permit the proper concentration adjustments. In the analysis of interacting systems similar considerations must apply. Thus experiments on such systems (Brown *et al.*, 1955; Bensusan *et al.*, 1957) must be re-evaluated in terms of the discussion presented in this section.

7. Analysis of Mixtures of Several Sedimenting Components

With the improvement in experimental techniques during the 1930's, the ultracentrifuge found widespread application as an analytical tool for the study of mixtures of proteins in biological systems like sera. Soon a puzzling observation was made by McFarlane (1935) and confirmed by Pedersen (1936a, 1938) and others. These workers found that the ratio of the amount of slow component to fast component, as measured from the areas of the ultracentrifuge patterns, depended upon the total concentration of the sedimenting material examined in the ultracentrifuge. Dilution of a given mixture caused a decrease in the fraction attributable to the slow component with a concomitant increase in the relative area corresponding to the fast component. The effect was found to be negligible at low concentrations, but the anomaly became more and more prominent as the concentration was increased. At that time, the results were ascribed to little understood properties of the proteins themselves, and it was not until 10 years later that this view was abandoned as the result of a paper by Johnston and Ogston (1946), who proposed that the experimental observations were, in fact, a manifestation of an ultracentrifugal anomaly and not a characteristic of the material. These workers brought forth a host of valid objections to all of the hypotheses advocated prior to that time to account for the observations, and they presented a theory which was shown to account qualitatively for the experimental results. Since that time, expansion and revision of certain aspects of the Johnston-Ogston theory have led to equations which can account quantitatively for the data obtained with model systems of known mixtures.

Although only two boundaries are observed in the analysis of a mixture of two sedimenting components and, at first glance, there appear to be only two sedimentation coefficients of interest in such experiments, Johnston

and Ogston called attention to the obvious but neglected fact that some molecules of the slow component actually sediment in the presence of the fast component. These molecules of the slow component would have a different s from the other slow component molecules which sediment by themselves behind the boundary of the fast component. Therefore, there are three sedimentation coefficients pertinent to such experiments; and it can be shown that the relative magnitudes of these values affect the results which are obtained in the ultracentrifugation of mixtures.

In terms of the nomenclature adopted in previous sections, we can consider the ultracentrifuge cell at time, t, to be divided into three phases: (*1*) an α-phase, composed of pure solvent; (*2*) a β-phase, containing the slow component at a concentration $c_S{}^\beta$; and (*3*) a γ-phase, containing both the slow and fast components at the concentrations $c_S{}^\gamma$ and $c_F{}^\gamma$, respectively. Separating these phases are two infinitely sharp hypothetical boundaries, the slower being termed the $\alpha\beta$-boundary whose position is indicated by $\bar{x}_S$ and is a measure of $s_S{}^\beta$ and the faster, the $\beta\gamma$-boundary, the position of which is indicated by $\bar{x}_F$ and is a measure of $s_F{}^\gamma$. These phases and boundaries are illustrated in Fig. 31 which also presents a schematic diagram of the concentration and concentration gradient as a function of position in the cell. Because of the higher total concentration in the γ-phase and the usual dependence of s upon c, $s_S{}^\gamma$ will be less than $s_S{}^\beta$. Therefore, the slow component will accumulate within the moving volume element defined by the surfaces at x_1 and x_2 *unless* there is a readjustment of the concentrations of the slow component on either side of the $\beta\gamma$-boundary to compensate for the differences in sedimentation coefficients. The movement of the slow molecules relative to the faster component can be written as $s^{\beta\gamma} - s_S$, and the net accumulation would be zero if

$$c_S{}^\beta(s^{\beta\gamma} - s_S{}^\beta) = c_S{}^\gamma(s^{\beta\gamma} - s_S{}^\gamma) \tag{49}$$

This equation is analogous to Eq. (48) which deals with a similar problem, the accumulation of the fast component across a boundary of the slow component. Equation (49) written in an alternative form

$$c_S{}^\beta = c_S{}^\gamma \frac{(s^{\beta\gamma} - s_S{}^\gamma)}{(s^{\beta\gamma} - s_S{}^\beta)} \tag{49a}$$

shows that the observed concentration of the slow component, $c_S{}^\beta = c_S^{\text{obs}}$, as measured by the area of the $\alpha\beta$-boundary, is greater than the true concentration of the slow component ($c_S{}^\gamma$ corrected for sectorial dilution) in the bottom of the cell by an amount which depends on the three sedimentation coefficients. If $s_S{}^\gamma = s_S{}^\beta$, as in dilute solutions of the fast component, the observed concentration will be correct. On the other hand, in solutions containing high concentrations of the fast component

and especially for those fast components having a large k, $s_S^\gamma \ll s_S^\beta$ and $c_S^\beta > c_S^\gamma$. Equation (49a) shows, moreover, that the magnitude of the anomaly increases as the sedimentation coefficients of the two components

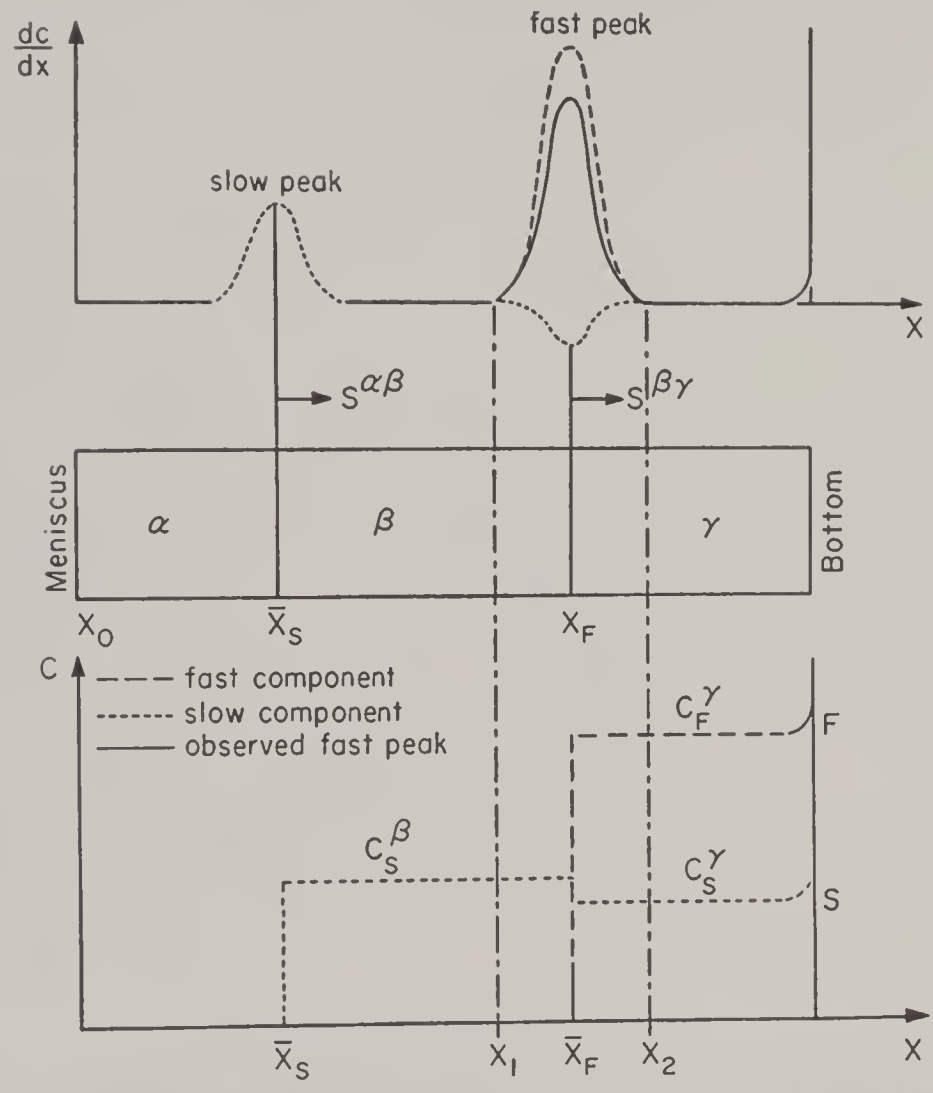

FIG. 31. Schematic diagram illustrating the distribution of material in a centrifuge cell during the analysis of a mixture of two sedimenting components. The dotted lines correspond to the concentration and concentration gradient of the slow component, and the dashed lines illustrate the concentration and concentration gradient for the fast component. The solid line in the upper diagram is the sum of the contributions of the fast and slow components to the refractive index gradients at that region of the cell (from Trautman, *et al.*, 1954).

approach one another. Confirmation of these qualitative conclusions is provided by data of Harrington and Schachman (1953) with mixtures of components which, with respect to their sedimentation coefficients, differ either considerably or by only a small amount. These results are presented in Table V. With the mixtures of tobacco mosaic virus and bushy stunt virus, or fibrinogen and bovine plasma albumin, the enhancement of the

concentration of the slower component was greater than 150% because the sedimentation coefficients of the slow and fast components in the mixture are similar. However, pairing these fast components even at the same concentration with other slow components possessing sedimentation coefficients which are considerably less leads to much smaller anomalies.

Equation (49*a*), which is in the form derived by Johnston and Ogston, deals only with the apparent enhancement in the concentration of the slow component. Since $c_S{}^{\gamma}$, except for sectorial dilution, is equal to the concentration of slow component placed in the cell, there is a decrease in concentration of the slow component across the fast or $\beta\gamma$-boundary. The negative concentration gradient due to the slow component cannot

TABLE V

Effect of Fast Component on Different Slow Components[a]

Fast component			Slow component			
Material	Concentration (g./100 ml.)	s_F (*S*)	Material	Concentration (g./100 ml.)	s_S (*S*)	$\frac{c_s^{obs}}{c^0_s}$
Tobacco mosaic virus	1.0	137	Bushy stunt virus	0.5	126	2.7
Tobacco mosaic virus	1.0	117	Fibrinogen	0.5	8.1	1.0
Fibrinogen	2.0	5.4	Bovine serum albumin	0.5	4.1	2.5
Fibrinogen	2.0	5.3	Lactoglobulin	0.5	2.7	1.5

[a] From Harrington and Schachman, 1953.

be detected directly (except in special cases by absorption optical methods) because the negative refractive index gradient arising from the slow component is located at the precise position of the $\beta\gamma$-boundary; only the sum of the positive gradient of the fast component and the negative gradient of the slower one is recorded by the schlieren optical system. Thus, as shown in Fig. 31 and Eq. (50),

$$c_F^{obs} = c_F{}^{\gamma} + c_S{}^{\gamma} - c_S{}^{\beta} \tag{50}$$

the amount of fast component as measured from the area of the $\beta\gamma$-boundary is too low by exactly the same amount as the enhancement in area of the $\alpha\beta$-boundary. The total area under the two boundaries is correct, however.

In the form presented above, the treatment does not allow for sectorial dilution nor the inhomogeneity of the centrifugal field. A formally dif-

ferent, but basically similar, approach was employed by Harrington and Schachman (1953) who considered these effects but with the restriction that the sedimentation coefficient did not vary during the experiment. Other discussions were presented by Trautman *et al.* (1954) and Claesson (1956). All of these involve statements of the conservation of mass and bear a close relationship to considerations invoked to explain analogous anomalies in electrophoresis (Svensson, 1946) and chromatography (Claesson, 1946a, b). The treatment given by Harrington and Schachman (1953) is outlined here because it provides a physical picture of the process of sedimentation in mixtures, and it represents another application of the transport equations derived earlier.

After a time, t, the amount of slow component, ${Q_S}^t$, behind the surface at $\bar{x}_F$ is readily expressed as the difference between the total amount of slow component above that surface initially and the amount which has crossed the surface during the time interval. According to Eqs. (27) and (28), this can be written

$$ {Q_S}^t = \frac{q{c_S}^0}{2} [{\bar{x}_F}^2 e^{-2\omega^2 {s_S}^\gamma t} - {x_m}^2] \tag{51} $$

where ${c_S}^0$ is the initial concentration of the slow component. It should be noted that the sedimentation coefficient involved in this equation is that for the slow component sedimenting in the presence of the faster species. Since this value is less than the sedimentation coefficient for that same material when migrating alone, there will be more of the slow component above any arbitrarily selected surface in mixtures than with pure materials; hence the Johnston-Ogston effect is observed. All of the slow component above the $\beta\gamma$-boundary is now confined to the region defined by the cell walls and the two boundaries. This volume is equal to $(q/2) \cdot (\bar{x}_F^2 - \bar{x}_S^2)$ and the concentration, ${c_S}^\beta$, in that region can be expressed as

$$ {c_S}^\beta = {c_S}^0 \left[\frac{{\bar{x}_F}^2 e^{-2\omega^2 {s_S}^\gamma t} - {x_m}^2}{\bar{x}_F^2 - \bar{x}_S^2} \right] \tag{52} $$

With the use of the integrated form of Eq. (16) and appropriate rearrangements and expansion of the exponentials, Eq. (52) leads to

$$ \frac{(\bar{x}_S/x_m)^2 {c_S}^{\text{obs}}}{{c_S}^0} = e^{2\omega^2 ({s_S}^\beta - {s_S}^\gamma) t} \left[\frac{{s_F}^\gamma - {s_S}^\gamma}{{s_F}^\gamma - {s_S}^\beta} \right] \tag{53} $$

This is analogous to the equation derived by Johnston and Ogston (Eq. 49*a*). It is assumed that $s^{\beta\gamma} = {s_F}^\gamma$. At zero time the exponential becomes unity, and the equation then has the form derived above for a cell of rectangular shape in a homogeneous field. The numerator of the term on the

left-hand side of Eq. (53) is the observed concentration corrected for radial dilution according to the rate of movement of the slow boundary. It should be noted that this corrected concentration (area) should increase during the run in accordance with the term, $e^{2\omega^2(s_S{}^\beta - s_S{}^\gamma)t}$, which is, of course, very small. In actual practice, however, the concentration corrected in the conventional way does not increase during the run, but rather it decreases markedly because of another factor which is the change of the Johnston-Ogston term as sedimentation proceeds.

Both of the derivations presented above for the analysis of mixtures of two sedimenting components implicitly assume that the sedimentation coefficients of the different species do not vary during the run. As shown in Section IV, 4, however, it is clear that an increase in sedimentation coefficient is to be expected because of the dilution of the contents of the cell. This was invoked by Harrington and Schachman (1953) to account for their observation with known mixtures of tobacco mosaic virus and bushy stunt virus. From qualitative reasoning, they concluded that the numerator in the Johnston-Ogston term would be relatively constant during an experiment since $s_F{}^\gamma$ and $s_S{}^\gamma$ would increase by about the same amount. The denominator, however, would increase considerably (and the enhancement in concentration of the slow component would decrease consequently) since $s_S{}^\beta$ is practically constant, whereas $s_F{}^\gamma$ increases. This reasoning was formulated in quantitative terms by Trautman *et al.* (1954) in a further examination of the data for mixtures of tobacco mosaic virus and bushy stunt virus. Starting with the generalized sectorial dilution equation (Eq 15), they were able to derive expressions for the corrected concentration for the slow and fast boundaries. These expressions were limited in their applicability, however, because they involved the terms, $c_S{}^\gamma$ and $c_S{}^0$, both of which may be unknown for the mixture being examined. Clearly $c_S{}^\gamma$ is related by $c_S{}^0$ by a term which expresses the rate at which the slow component sediments in the presence of the faster component. To evaluate this rate, $s_S{}^\gamma$, Harrington and Schachman (1953) proposed that $s_S{}^\gamma$ be determined by measurements of the movement of the boundary formed by layering a solution of the fast component over a mixture of the fast and slow components (see Section IV, 6). Alternative methods for evaluating this sedimentation rate were suggested on the basis of equations like Eq. (34). Trautman *et al.* (1954) related $c_S{}^\gamma$ to $c_S{}^0$ by an expression involving the sedimentation rates of the two components and the observed position of the fast boundary, $\bar{x}_F^{\text{obs}}$, as follows

$$\frac{c_S{}^\gamma}{c_S{}^0} = \left(\frac{x_m}{\bar{x}_F^{\text{obs}}}\right)^{2\psi} \tag{54}$$

This equation which serves as a definition of ψ can be combined with the

continuity equation and the definition of the sedimentation coefficient to give:

$$\psi = \frac{\ln (c_S^{\gamma}/c_S^{0})}{2 \ln (x_m/\bar{x}_F^{\text{obs}})} = \frac{\int_0^t s_S^{\gamma}\, dt}{\int_0^t s_F^{\gamma}\, dt} \tag{54a}$$

With the suggestion of Harrington and Schachman (1953) that the k of the fast component acting on itself is the same for the fast component acting on the slower molecules, ψ then becomes equal to the ratio of the infinite dilution values of the sedimentation coefficients of the slow and fast components. As already pointed out in Section IV, 6, this is reasonable because the two components have similar s values. Had this assumption been inadmissable because $s_S \ll s_F$, the functions relating s_S^{γ} to s_S^{0} and s_F^{γ} to s_F^{0} would be required. In such systems, of course, the enhancement of concentration would be much less and the treatment presented earlier (Eq. 52) would suffice. Trautman *et al.* (1954) then combined their equations for the observed concentration of the slow component with Eq. (54) and the value of ψ, (s_S^{0}/s_F^{0}), to give

$$\frac{(\bar{x}_S^{\text{obs}}/x_m)^2 c_S^{\text{obs}}}{c_S^{0}} = \frac{(\bar{x}_F^{\text{obs}}/x_m)^{2(1-\psi)} - 1}{(\bar{x}_F^{\text{obs}}/\bar{x}_S^{\text{obs}})^2 - 1} \tag{55}$$

The left-hand side of Eq. (55), which represents the enhancement of concentration of the slow component, has been termed r'.

Trautman *et al.* (1954) tested Eq. (55) in different ways. Knowing c_S^{0} and measuring c_S^{obs}, $\bar{x}_F^{\text{obs}}$, $\bar{x}_S^{\text{obs}}$, and x_m they were able to calculate ψ. Alternatively, they determined s_S^{0} and s_F^{0} from independent experiments with each of the two components and with the knowledge of ψ obtained in this way and with the other terms measured from the ultracentrifuge patterns of the various mixtures, they calculated c_S^{0}. The results of these extensive calculations are presented in Table VI. As shown in the table, the calculated values of c_S^{0} from different patterns for a given mixture and also for different mixtures are in close agreement with the known value of 50 ± 1. Similarly, the values of ψ calculated from the independent patterns with the known value of c_S^{0} are in satisfactory agreement with the value 0.70 for s_S^{0}/s_F^{0}. These results thus demonstrate the validity of this treatment of the Johnston-Ogston effect and provide justification for those analyses of unknown mixtures which include the factors discussed above.

During an ultracentrifuge run, there are marked decreases in the corrected concentration of the slow component, as shown in Table VI. This is due to the effect of the radial dilution of the fast component upon the sedimentation coefficient of the slow species in the γ-phase. Since the

TABLE VI

Analysis of Mixtures of Two Components[a]

(Slow Component—BSV at 0.3 g./100 ml.; Fast Component—TMV at Varying Concentration 0.2 to 1.0 g./100 ml.)

Frame	$(\bar{x}_s/x_m)^2\, c_S^{obs}$	$(r' - 1)100$ (%)	c_S^0	ψ
		0.3–0.2 Mixture		
5	62.0	24	47.6	0.713
6	60.6	21	46.5	0.721
7	61.5	23	48.3	0.710
8	60.1	20	46.4	0.721
9	58.9	18	45.4	0.724
10	58.9	18	45.5	0.726
		0.3–0.4 Mixture		
4	87.9	76	49.0	0.706
5	87.1	74	49.2	0.705
6	84.7	69	47.5	0.715
7	82.1	64	50.2	0.699
		0.3–0.6 Mixture		
5	114.8	130	53.1	0.682
6	108.6	117	50.9	0.695
7	107.8	116	52.7	0.684
8	102.1	104	49.7	0.702
9	98.9	98	48.8	0.704
10	94.2	89	46.4	0.721
		0.3–0.8 Mixture		
6	157.4	215	48.6	0.708
7	145.4	191	54.1	0.680
8	147.9	196	50.1	0.700
9	137.6	175	48.7	0.704
10	131.4	163	48.5	0.709
11	126.0	152	47.6	0.714
		0.3–1.0 Mixture		
8	201.0	302	51.3	0.692
9	199.8	300	54.4	0.676
10	191.9	284	51.4	0.692
11	174.5	249	49.5	0.703
12	174.4	249	51.1	0.694
13	182.4	266	50.2	0.698

[a] From Trautman *et al.*, 1954.

enhancement of concentration of the slow component decreases throughout the experiment, there is not sufficient slow component being uncovered by the movement of the fast boundary to maintain a plateau in the β-region. Consequently there is a tendency toward a density inversion in the region between the two boundaries. Such a negative density gradient would be

unstable, and we would expect convection to occur throughout the zone between the two boundaries. Careful examination of some of the patterns obtained by Harrington and Schachman (1953) revealed that the slow boundary was unsymmetrical, whereas this material when examined alone produced symmetrical boundaries. Trautman *et al.* (1954) emphasized that the departure of the behavior of the slow boundary from that expected on the basis of the radial dilution rule was further evidence for convective flow in these experiments. It should be emphasized that this system of tobacco mosaic virus and bushy stunt virus represents an extreme since the sedimentation coefficients of the two components are not too different and because the s versus c dependence for the fast component is large.

Several procedures can be employed for the analysis of unknown mixtures in terms of the relative amounts of the slow and fast components. The first of these involves progressive dilution of the mixture in concert with ultracentrifugal analysis at each concentration. The values for the relative composition can be extrapolated to infinite dilution, thereby eliminating the anomaly due to the Johnston-Ogston effect. In this way, a faithful analysis can be produced. Although this method is, in principle, satisfactory, it possesses several inherent disadvantages. Dilution of the mixture may be precluded because of special properties of the system such as a reversible interaction between the two components which may be disturbed if the total concentration is altered. Also, there is a loss in experimental precision in measurement of the areas as the solutions become more and more dilute. A second method, which is devoid of these limitations, involves the determination of ψ followed by calculation of c_S^0 in the manner described above. To determine ψ, the mixture is examined at a series of concentrations in order to provide sedimentation coefficients for extrapolation to infinite dilution. For the slow component, the s values are plotted against the apparent concentration, and the s of the fast component can be plotted as a function of the total concentration or the apparent concentration of the fast component. These plots give the sedimentation coefficients required for the calculation of ψ. In this case, a change in the relative concentrations of the two components by a shift in an equilibrium upon dilution of the mixture would not affect the results since only the sedimentation coefficients at the various dilutions are necessary. Data from these same dilutions can be used in still another way. The dependence of s upon c for the fast component provides a value of k for the fast component acting on itself. Care must be exercised in the determination of k because the slow component is also being diluted and the change in s_F might be attributable to the dilution of the slow component. This is readily detected, however, because s_S would then change by about the same relative amount. By careful implementation of Eq. (34) with

the appropriate data, the k value for the fast component can be determined. Following this, $s_S{}^{\gamma}$ can be related to the measured value of $s_S{}^{\beta}$ in the original mixture according to Eq. (32). Finally, $c_S{}^{\gamma}$ and $c_S{}^{0}$ can be calculated from Eq. (49*a*). Another method was suggested by Claesson (1956), who discussed the Johnston-Ogston effect for mixtures containing more than two components. She showed that the change in the pattern caused by the addition of a known amount of the slower component to a mixture of two components could be used for the evaluation of $c_S{}^{0}$ in the original solution. Other workers (de Lalla and Gofman, 1954; Baldwin, 1954a) also have discussed corrections for the Johnston-Ogston effect in mixtures containing many sedimenting components, but these considerations are postponed to the following section dealing with polydisperse systems.

For certain systems, the Johnston-Ogston effect can be exploited to provide information otherwise derived only with great difficulty. This is illustrated with investigations on the homogeneity of tobacco mosaic virus. Electron micrographs of virus preparations have shown consistently small numbers of particles of varying length with an average considerably less than that of the particles which were present in predominant amounts (Williams and Steere, 1951; Williams *et al.*, 1951). Despite this, the ultracentrifuge patterns for many similar preparations revealed sharp boundaries with no obvious evidence for the presence of shorter particles in the amounts indicated by the electron microscope. When small amounts of degraded virus, with lengths varying from one-half to two-thirds those of the intact particles, were added to concentrated solutions of undegraded virus, a second boundary or slow moving shoulder on the principal boundary was readily detected. However solutions of the degraded material alone at the same concentration as that added to the control showed no perceptible boundary because of the limitations of resolution of the schlieren optical system. That these added particles were readily observed in the mixture was a manifestation of a tremendous enhancement (over 10-fold) of their concentration due to the Johnston-Ogston effect. It was therefore concluded (Schachman, 1950, 1951a) that the presence of short particles in the amount of 1 to 2% of the total weight would be revealed by ultracentrifugal analysis. That these particles were not evident in many preparations of tobacco mosaic virus provided independent support for the conclusions of Williams *et al.* (1951) that their presence in the electron micrographs was the result of rupture of intact virus particles during the drying procedure employed for the microscopy. Similar experiments were conducted with deoxyribonucleic acid (Peacocke and Schachman, 1954) in order to provide an upper limit for the amount of low molecular weight material present in the preparations. Both of these systems are somewhat unusual in that the principal component exhibits a large dependence of s upon c and therefore

causes s_S^γ to be considerably less than s_S^β. Just as the Johnston-Ogston effect can be applied to advantage in the detection of small amounts of material with sedimentation rates lower than the principal component, so the search for faster sedimenting impurities is hindered by the same anomaly.

An unusual type of Johnston-Ogston effect was discovered by Gofman *et al.* (1949) in the course of an ultracentrifugal analysis of human serum. Bizarre patterns had been observed by McFarlane (1935) and Pedersen (1936a, 1938, 1945) when undiluted serum was examined directly in the ultracentrifuge. Accordingly, procedures were suggested by Pedersen to cir-

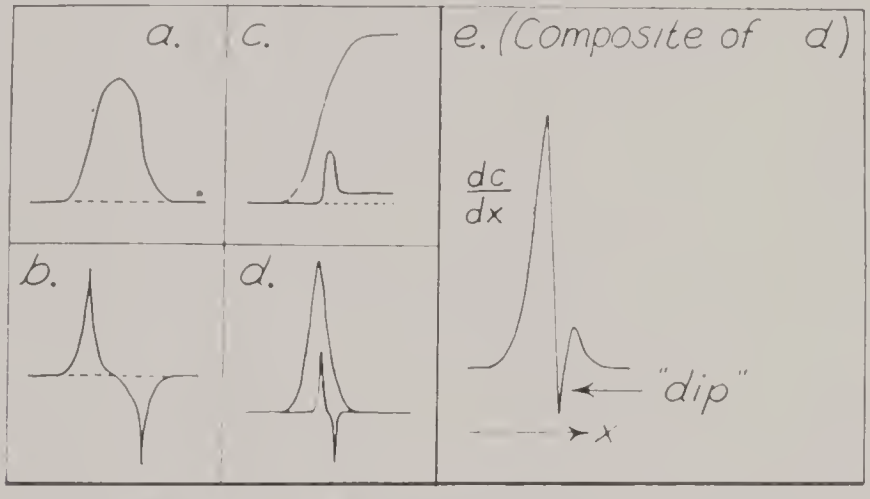

FIG. 32. Interpretation of patterns observed during ultracentrifugal analysis of undiluted serum. (*a*) Pile-up of lipoprotein as shown by plot of concentration versus distance; (*b*) Plot of concentration gradient versus distance for material distributed as in (*a*); Plot of concentration versus distance for albumin and pile-up of lipoprotein is shown in (*c*). The gradient curves for the albumin and lipoprotein are shown in (*d*). (*e*) presents the composite curve which would be seen in the schlieren optical system for the distribution of concentrations shown in (*c*) (from Gofman *et al.*, 1949).

cumvent the difficulties of interpreting the patterns. Not only did the pattern change in a weird fashion during the experiment, but also there was associated with the asymmetric boundary corresponding to serum albumin an inverted peak (or "dip") below the base line. Gofman and his co-workers (1949) pointed out that such an inverted boundary would result from a pile-up of lipoprotein within the concentration gradient of the albumin boundary. Such a pile-up of a component, with a lower concentration on both sides of the zone of accumulated material, must lead to a biphasic curve for the concentration gradient (or refractive index gradient) as a function of distance. If the pile-up occurs within a concentration gradient of another substance, the optical system will record the sum of the gradients only and patterns like the composite pattern shown schematically in Fig. 32*e* would obtain. A shift in the position of the accumulated lipoprotein relative to

the large albumin boundary would lead to patterns which changed with time in a fashion that had previously defied interpretation. This is shown in Fig. 33 for several variations in the position of the pile-up relative to the albumin boundary. The counterpart of each of the composite patterns was observed and photographed by Gofman *et al.* As they pointed out, the effective buoyant force on the lipoprotein molecules was not the same in the albumin solution as in the supernatant solution above the albumin boundary. Consequently, the sedimentation coefficient of the liproprotein might not only be different on the two sides of the albumin boundary, but

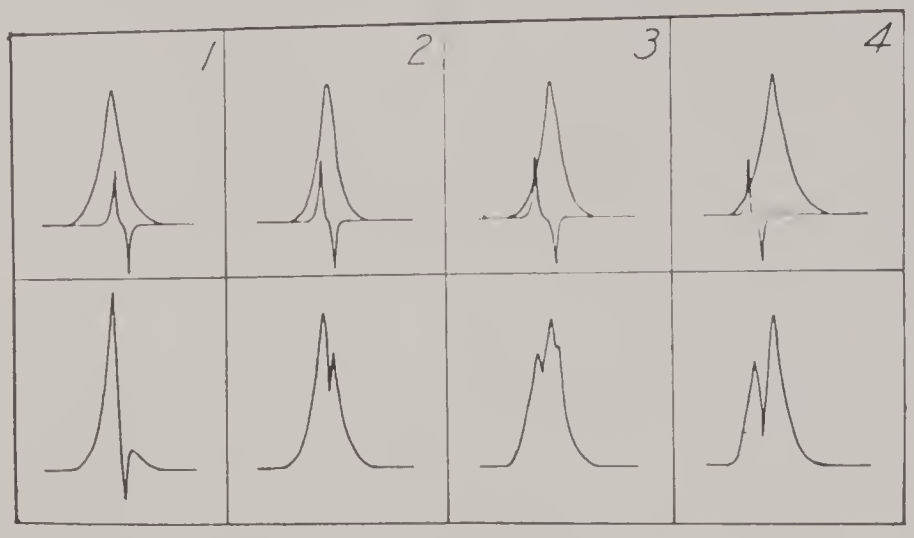

FIG. 33. Schematic ultracentrifuge patterns resulting from a pile-up of lipoprotein on the albumin boundary. The upper diagrams contain the separate refractive index gradient curves for the lipoprotein and albumin, and the lower curves correspond to the composite patterns as they would be recorded by the schlieren optical system. The analog of each of the lower curves has been observed during ultracentrifuge experiments on concentrated sera, and the bizarre patterns are attributed to slight shifts in the position of the pile-up of lipoprotein within the albumin boundary (from Gofman *et al.*, 1949).

even the sign of the sedimentation coefficient, i.e., the direction of migration, may be different. This occurs if the density of the lipoprotein ($\bar{V}$ is about 0.97 ml./g.) falls between the densities of the albumin solution and the supernatant salt solution. As long as the s of lipoprotein in the salt solution is greater than the s of albumin, an appreciable pile-up would be expected. The type of pattern can be varied by slight changes in the salt concentration which by virtue of their contribution to the density of the solution have a marked influence on the rates of migration of the lipoprotein. Gofman *et al.* (1949) indicated that the pile-up can occur in two different ways. The first, which they consider to be the dominant situation in undiluted serum, is that indicated above wherein there are both centrifugal and centripetal migrations of the lipoprotein. In more dilute serum, since the density is lower, there is only centrifugal migration of the

lipoprotein. However, the migration is more rapid at the trailing end of the albumin boundary than in the solution ahead of the boundary. Both the lower viscosity and the lower density in the supernatant region are responsible for this differential rate of migration of the lipoproteins.

As Gofman *et al.* demonstrated, the density of the solution can be raised by the addition of salts or sucrose thereby causing the lipoprotein to migrate in a centripetal direction throughout the entire cell, even while the albumin and other more dense proteins are sedimenting toward the bottom of the cell. Boundaries formed in this way are not complicated by the superposition of the gradients from other proteins, and reliable estimates of the concentration of the lipoproteins can be made. It is important to note here that such boundaries are inverted on the photographic plates since the refractive index gradients are negative. The addition of salts and the consequent flotation of the lipoproteins formed the basis for the centrifugal fractionation classes of lipoproteins differing in density and size (Lindgren *et al.*, 1951; Oncley *et al.*, 1957).

8. Analysis of Boundaries in Terms of Homogeneity or Polydispersity

It is in the analysis of systems containing macromolecules of many sizes and shapes (and even densities) that the ultracentrifuge exhibits its singular power among the modern tools now employed in the study of large molecules. Often it is desirable to determine not only an average molecular weight for a given preparation but also a distribution curve for all of the molecules in the preparation. Although the sedimentation velocity method gives a distribution curve in terms of sedimentation coefficients only, the latter can be translated into molecular weights with the aid of auxiliary data. Some information regarding molecular weight distributions can be obtained directly from sedimentation equilibrium measurements, but the resolving power of the velocity method far exceeds that of the equilibrium method, and this discussion will be limited to analysis of the patterns from sedimentation velocity experiments.

In general, the shape of a boundary in a sedimentation velocity experiment is controlled by four factors. First of these is, of course, the blurring of the boundary due to the diffusion which results from the concentration gradient formed by the migration of the solute molecules. Secondly, broadening of the boundary occurs during the sedimentation of polydisperse material as the faster moving molecules tend to become separated from the slower components. In principle, the observed boundary can be considered as a composite boundary resulting from the sum of the gradients from the individual components in the solution. Opposing these two effects, is, thirdly, the so-called sharpening effect, which is a consequence of the dependence of sedimentation coefficients on concentration. At the

trailing or solvent side of the boundary, the concentration is much lower than on the solution side. As a consequence, those molecules falling behind as a result of diffusion find themselves in an environment of lower concentration, and their sedimentation rate increases until they overtake the boundary. Self-sharpening of the boundary occurs continuously if the rate of movement of the boundary (which is a measure of the sedimentation coefficient at the concentration in the plateau region ahead of the boundary) is less than the migration rates of the molecules at much lower concentrations. Finally, the boundary is distorted by the existence of a series of Johnston-Ogston effects among the various macromolecular species present in the solution. This leads to an enhancement in concentration of the slower moving species with a corresponding reduction in the apparent amount of the more rapidly sedimenting components.

Despite the substantial progress with regard to our understanding of each of these effects, there is as yet no general and rigorous treatment which expresses all of the factors affecting the shape of a sedimenting boundary. Nonetheless, largely as a result of the investigations of Baldwin (1957a, 1957b), for some systems a synthesis of the various factors is now possible, so that the shape of certain types of boundaries can now be analyzed in terms of the homogeneity or polydispersity of the sedimenting material. These different factors will be discussed separately followed by some general remarks dealing with the demonstration of homogeneity for a given material.

a. Spreading of Boundaries Due to Diffusion. This subject has been considered at length by Svedberg and Pedersen (1940), who utilized the equation of a Gaussian curve for the analysis of boundaries. In that way they were able to calculate apparent diffusion coefficients from the ultracentrifuge patterns, and these calculated values were then compared with the diffusion coefficients measured by classic methods. Agreement between these two values was presented as strong presumptive evidence that the sedimenting material was homogeneous with regard to size, shape, and density. For certain conditions, this is a valid procedure, but as will be shown later, this method has been abused in its application to many systems. Justification for the use of the Gaussian equation in the analysis of the shape of boundaries is provided by Faxén's (1929) approximate solution of the differential equation of the ultracentrifuge (Eq. 6). He obtained

$$\frac{c}{c_0} = \frac{1}{2} e^{-2\omega^2 s t}\left[1 - \frac{2}{\sqrt{\pi}}\int_0^y e^{-y^2}\, dy\right] + \frac{e^{-y^2}}{x}\left[\frac{De^{-2\omega^2 s t}(1 - e^{-2\omega^2 s t})}{8\pi\omega^2 s}\right]^{1/2} + \cdots \tag{56}$$

where

$$y = (x_m e^{\omega^2 st} - x)\left[\frac{\omega^2 s}{2D(e^{2\omega^2 st} - 1)}\right]^{1/2} \tag{57}$$

The higher terms in the series described by Faxén have been evaluated by Gosting (1952). Also Baldwin (1954b) has confirmed the Faxén solution of the differential equation by evaluating different moments of the gradient curve and combining them with the continuity equation. A more general solution of Eq. (5) with s a function of c has been provided by Fujita (1956a), and he demonstrated that the result of Faxén was a special case of the more general equation.

It is important to note that this approximate solution applies only to those systems for which s and D can be considered constant throughout the entire boundary. Thus the equation is restricted to experiments at such dilutions that, across the boundary, the changes in D and, more particularly, in s are negligible. Also this solution applies to those experiments in which s is sufficiently large and D correspondingly small so that there is no restricted diffusion at the meniscus. Faxén's equation is limited in application also to those experiments in which there is still a plateau region between the boundary and the bottom of the cell. The first in the series of terms in Eq. (56) is the dominant term, and it is similar to the equation for diffusion between a solution and a solvent. The term $e^{-2\omega^2 st}$ corrects for the dilution of the solution due to the shape of the cell and the variation of the centrifugal field with distance. The term in brackets is the well-known probability integral. If $\omega^2 st \ll 1$, the quantity in the brackets in Eq. (57) reduces to $(1/4Dt)^{1/2}$ as in the Gaussian equation, and the first term in Eq. (56) describes a Gaussian curve about $x_m e^{\omega^2 st}$ as an origin. Note that this is the position of the boundary at that time and corresponds to the position of the square root of the second moment of the gradient curve and not to the maximum ordinate of the gradient curve. The equation of the concentration gradient follows directly from Eq. (56) and can be written (Gosting, 1952)

$$\frac{\partial c}{\partial x} = c_0 e^{-2\omega^2 st}\left[\frac{\omega^2 s}{2\pi D(e^{2\omega^2 st} - 1)}\right]^{1/2} e^{-y^2}\left[1 + \frac{x_m e^{\omega^2 st} - x}{2x}\right] - \cdots \tag{58}$$

Since the higher terms in Eqs. (56) and (58) are often small, Lamm (1929b) pointed out that the errors would also be small if the observed ultracentrifuge patterns were considered as Gaussian curves. Both the diffusion coefficients and the sedimentation coefficients calculated on that basis require some correction however. The diffusion coefficient evaluated from the ultracentrifuge diagrams would be too large because the term in brackets in Eq. (57) is not exactly equal to $(1/4Dt)^{1/2}$. By expressing the exponential

as a series and simplifying the resulting expression, Lamm showed that the true diffusion coefficient, D, can be obtained from the value, D_{sed}, calculated from the sedimentation velocity patterns

$$D = D_{sed}(1 - \omega^2 st) \tag{59}$$

Since $\omega^2 st$ is of the order of 0.1 in many ultracentrifuge experiments, the correction shown in Eq. (59) is necessary. As mentioned earlier, the error in using the maximum ordinate for the calculation of s is very small (see Eq. 12). This was found (Lamm, 1929b) by an examination of the magnitude of the higher terms in Eqs. (56) and (58).

Later, it will be shown that the method described here is not satisfactory even for globular proteins at the concentrations customarily employed. Thus evaluation of diffusion coefficients from ultracentrifuge diagrams must be made according to Fujita's (1956a) solution of Eq. (6) rather than with the method suggested by Lamm on the basis of Faxén's equation.

b. Spreading of Boundaries Due to Polydispersity. Polydispersity is recognized in many cases by the rapid and progressive blurring of the boundary as it traverses the ultracentrifuge cell. Frequently, however, casual inspection of boundaries is insufficient to detect inhomogeneity of the sedimenting substance, and quantitative measures of the extent of polydispersity are necessary. Moreover, it is often important to estimate the effect of diffusion in causing a broadening of the boundary so that the inherent polydispersity can be measured. As indicated above, the detection of polydispersity in a qualitative way is most readily performed by comparing the apparent diffusion coefficient obtained from the ultracentrifuge patterns with the measured diffusion coefficient. If the former is larger than the latter, heterogeneity is indicated, e.g., Krishnamurti and Svedberg (1930), Lauffer (1944a), and Record (1948). Until recently the discrepancy between these two diffusion coefficients was not expressed in quantitative terms as a measure of polydispersity.

Some workers (Gralén, 1944; Jullander, 1945) have measured certain parameters of the gradient curves and used these values to calculate heterogeneity coefficients for assumed distributions of sedimentation coefficients. Others (Baldwin and Williams, 1950; Williams *et al.*, 1952) have evaluated, in a much more detailed way, the complete distribution curve of the sedimentation coefficients. This, of course, is preferable to methods which assume a given form for the distribution curve. When, however, the number of components in the mixture is relatively small, though still continuous, and the diffusion rates rather high, the evaluation of a distribution curve may not be feasible. Polydispersity for this situation is best expressed in terms of a standard deviation of the sedimentation coefficients (Baldwin, 1957a). Regardless of the method selected, the effects of diffu-

sion and the concentration dependence of the sedimentation coefficient on the shape of the boundary produce complications which render a complete analysis difficult and time-consuming.

Gralén (1944) proposed that the width of the sedimenting boundary was an index of polydispersity. To define the width, B, he used the ratio of the area, A, to the maximum height, H. Since he was dealing with filamentous materials of large molecular weight, like derivatives of cellulose, spreading of the boundary due to diffusion was negligible. Experimentally, he found that B increased in a linear fashion with x, the distance moved by the boundary, and the slope of the plot of B versus x gave (dB/dx), which was then related to polydispersity. Although diffusion was negligible for the systems examined by Gralén (1944), the values of (dB/dx) were markedly concentration dependent. Therefore, he employed a plot of (dB/dx) versus c for the purpose of extrapolating the data to infinite dilution. The value of $(dB/dx)_{c=0}$ was then used in the calculation of the distribution or nonuniformity coefficient in the assumed logarithmic distribution,

$$dc = K_s e^{-y^2}\, ds \tag{60}$$

where

$$y = \frac{1}{\gamma_s} \ln\,(s/s_m) \tag{61}$$

In the above equation, s_m is the sedimentation coefficient at the maximum of the distribution curve, and K_s is a constant expressing the maximum weight of the distribution curve. This distribution was modeled after that employed much earlier by Lansing and Kraemer (1935) in their analysis of polydispersity from sedimentation equilibrium measurements. From the relationship of x to s and the above equations, Gralén found

$$(dB/dx)_{c=0} = \sqrt{\pi}\, \gamma_s\, e^{-\gamma_s{}^2/4} \tag{62}$$

Thus the value of γ_s, which is a direct measure of heterogeneity ($\gamma_s = 0$ for homogeneous materials), could be determined from analysis of the width of the boundaries at different times during a single experiment and from experiments at varying concentrations. The assumed distribution (Eqs. 60 and 61) shows a single maximum with a positive skewness. This type of distribution is particularly useful since it is of the form expected for polymeric substances produced from small units by condensation or chain reactions. Jullander (1945) pointed out, however, that this distribution does not permit independent variations of the skewness and the dispersion, and he therefore introduced a slightly different function containing three parameters instead of only two. From measurements of the skewness of the experimental curves (in effect, the fractional difference in area under

the curve with values greater than s_m as compared with the area for values below s_m), he evaluated γ_s and then K_s and the third parameter. Kinell (1947a) has considered the method of Gralén (1944) in detail and examined some of the factors not included in the treatment as used by Gralén and Jullander. This has led to certain changes in the method of handling the data. As used by Jullander, the experimental data at each concentration are used to calculate the three parameters defining the distribution. These parameters are independently extrapolated to provide values corresponding to infinite dilution, and the final distribution is then constructed. Difficulties are encountered in the formulation of the best plots for extrapolation purposes, and these are discussed by Jullander (1945) and Nichols and Bailey (1949). Since most, but not all, substances of interest in biochemistry show appreciable boundary spreading due to diffusion, this method is of limited value. It has, however, found wide application in the study of synthetic high polymers (Nichols and Bailey, 1949; Kinell and Rånby, 1950; Oth and Desreux, 1955). The Gralén method has been used extensively by Eriksson (1953) in an analysis of the molecular weight distribution of polymethylmethacrylate. Moreover, Eriksson has extended the treatment so as to include, in the evaluation of the sedimentation patterns, the contribution of diffusion to the boundary spreading. For many materials of biological interest the effect of diffusion cannot be neglected, and the procedure suggested by Eriksson should be employed.

As an alternative to the method of Gralén (1944), which utilizes only the width of the gradient curve and an assumed distribution, the entire experimental curve can be transformed directly into a distribution curve of sedimentation coefficients in the manner first proposed by Signer and Gross (1934). The values of (dc/dx) are first corrected for radial dilution through multiplication by $(x/x_m)^2$ and then converted to values of (dc/ds) through the use of (dx/ds) which can be written as $x\omega^2 t$. This follows from the definition of the sedimentation coefficient written in the form,

$$x = x_0 e^{\omega^2 s t}.$$

Combining these factors and dividing by c_0 (the initial concentration) gives the equation,

$$g(s) = \frac{1}{c_0}\frac{dc_0}{ds} = \frac{(dc/dx)}{c_0}\left(\frac{x}{x_m}\right)^2 (x\omega^2 t). \tag{63}$$

Thus the experimental refractive index gradient curves can be transformed directly by Eq. (63), and the weight-fraction of material with sedimentation coefficients between s and $s + ds$ is evaluated directly from these curves as $g(s)ds$. This treatment, like that employed by Gralén (1944) and Jullander (1945), requires that the spreading of the boundary is due

exclusively to polydispersity. Only few materials of biological interest exhibit behavior in accord with that restriction. Glycogen, for example, seems to exhibit no significant boundary spreading as a result of diffusion, and Bridgman (1942) calculated a distribution curve for it by means of Eq. (63). Recent experiments with deoxyribonucleic acid (DNA) (Shooter and Butler, 1956; Schumaker and Schachman, 1957) show clearly the negligible effect of diffusion on the shape of the boundary since the distribution curves calculated from the ultracentrifuge patterns were independent of

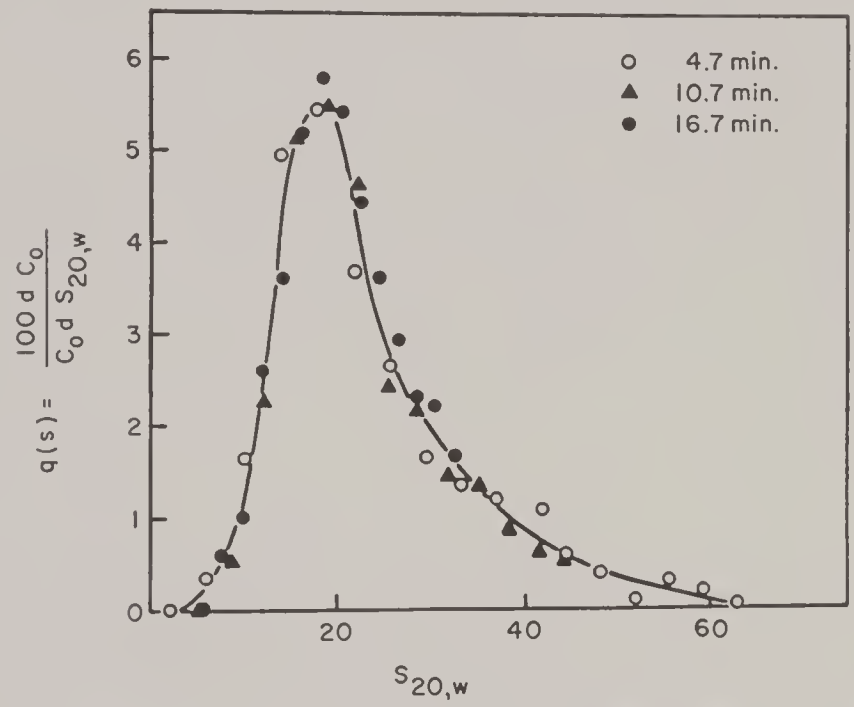

FIG. 34. Distribution of sedimentation coefficients in a preparation of calf thymus deoxyribonucleic acid at a concentration of 0.004 g./100 ml. The points are calculated values of $g(s)$ and $s_{20,w}$ from three different exposures in a single ultracentrifuge experiment. The times are noted. All measurements were made on microphotodensitometer tracings from patterns obtained with ultraviolet absorption optics (from Schumaker and Schachman, 1957).

time during the experiment. This is shown in Fig. 34 which gives the distribution curves for DNA over a time period during which the boundary width increased from 0.2 cm. to almost 1.0 cm. Signer and Gross (1934) gave a method for transforming coordinates so that the patterns at different times can be compared in order to determine whether the boundaries are significantly affected by diffusion. In the experiments with DNA, the concentrations were sufficiently low that the calculated distribution curves were essentially independent of concentration for solutions below 0.002 g./100 ml. Only at such low concentrations is there quantitative evidence of the polydispersity of DNA with respect to sedimentation coefficient, whereas, experiments at concentrations of 0.1 g./100 ml., utilizing schlieren

optics instead of ultraviolet absorption optics, yield extremely sharp boundaries. Since the ultraviolet absorption optical system produces plots of concentration versus distance, Shooter and Butler (1956) made only the square rule correction and a shift of the x coordinate to a scale of sedimentation coefficients. Schumaker and Schachman (1957), on the other hand, differentiated the concentration plots and made the necessary transformations to give $g(s)$ versus s. Visual inspection of curves of the latter are more informative than the integral curves, thereby providing compensation for the labor involved in converting the experimental curves into plots of $g(s)$ versus s.

For smaller molecules, such as most proteins, the boundary spreading might be attributable not only to polydispersity but to diffusion as well, and it would be erroneous to conclude that a distribution curve calculated according to Eq. (63) is a faithful index of polydispersity. Baldwin and Williams (1950) suggested that such calculated curves be considered as apparent distribution curves, $g^*(s)$, and they investigated the problem of correcting these curves for the effect of diffusion. Since the spreading of a boundary due to diffusion is proportional to $t^{1/2}$, whereas the separation of macromolecules of differing sedimentation coefficients is proportional to t, the contribution of the diffusion spreading becomes vanishingly small compared with the effect of polydispersity if the data are extrapolated to infinite time. Thus extrapolation of the apparent distribution curves to infinite time should give the true distribution. Williams *et al.* (1952) considered plots of $g^*(s)$ against $(1/t)$, $(1/xt)$, and $(1/x^2t)$ for the extrapolation to infinite time. In a theoretical investigation of this problem, Gosting (1952) derived important relationships about the limitations of the extrapolation procedure with regard to both the variable used and the period of time which should be the basis for the extrapolation. He first discussed the differential equation for the observed concentration gradient in terms of the distribution function of the sedimentation coefficients. With Faxén's (1929) solution of the continuity equation and the appropriate modification to include a series of components described by $g(s)$, he obtained a solution of the boundary spreading equation. Many of the terms in the series were negligible, and he showed that $g^*(s)$ plotted against $(1/x^2t)$ and extrapolated to $(1/x^2t) = 0$ yields $g(s)$. The limiting equation is applicable only when $\omega^2st < 1$, as other terms become significant at higher values of ω^2st. Moreover, t must be relatively large if some of the terms are to be sufficiently small that a linear extrapolation may be expected. Since the maximum value of ω^2st is limited experimentally by the length of the ultracentrifuge cell, it is not certain that sufficiently large values of t are attained to justify the neglect of the terms in Gosting's limiting equation which cause a departure from linearity. In order to provide more information on the ap-

plicability of the extrapolation procedure, Baldwin (1954b) investigated the boundary spreading for a system exhibiting a Gaussian distribution of sedimentation coefficients. He employed the boundary spreading equation of Gosting and Faxén's solution along with the assumed Gaussian distribution. In this way, an equation for $g^*(s)$ was derived as a function of t and the standard deviation of the sedimentation coefficient distribution. With this equation, Baldwin showed the limitations in the accuracy of determining $g(s)$ by extrapolation of $g^*(s)$ as a function of $(1/t)$. As these calculations indicated, the extrapolation leads to errors if the polydispersity is relatively small, and the diffusion coefficients are high. These results are illustrated in Fig. 35 for a system having a mean sedimentation coefficient of 4 S, a standard deviation of 1 S, and an average diffusion coefficient of 5×10^{-7}. As seen in Fig. 35*a*, the effect of diffusion in determining the spreading of the boundary is considerable during the early stages of the experiment, and even at the conclusion of the experiment, the boundary shape is due in part to diffusion. However, the distribution curve, $g(s)$, calculated by extrapolation to $(1/t) = 0$, as shown in Fig. 35*b*, is reasonably close to the known distribution. These calculations apply to a system which at the end of the experiment exhibits a boundary spreading due to heterogeneity which is 2.8 times the spreading from diffusion. For systems exhibiting less heterogeneity and comparable average sedimentation and diffusion coefficients, the extrapolated curve of $g(s)$ versus s would be much less precise. In such cases, as Baldwin (1954b) showed, the calculation of the standard deviation, p, of the sedimentation coefficient distribution is more meaningful.

Williams *et al.* (1952) employed an extrapolation against $(1/x^2t)$ to obtain the distribution curve of the sedimentation coefficients in a study of the action of pepsin on γ-globulins. They showed the importance of a detailed investigation of the boundary spreading as contrasted to a cursory examination of the ultracentrifuge patterns. An extrapolation against $(1/xt)$ was used by Cann (1953) in a study of the γ-globulins isolated by electrophoresis convection. This same extrapolation was used in a study of gelatin (Williams *et al.*, 1952) and in comparable investigations of dextran (Williams and Saunders, 1954; Ogston and Woods, 1954). Larner *et al.* (1956) also used such plots to eliminate possible contributions from diffusion in the examination of the polydispersity of glycogen and of the products resulting from the action of crystalline muscle phosphorylase.

The third method for describing the heterogeneity of a system involves the measurement of the standard deviation of the sedimentation coefficient distribution. Baldwin and Williams (1950) expressed the boundary spreading, measured by the second moment, σ^2, of the gradient curve about the mean, as the sum of the second moment due to diffusion and the corre-

sponding moment of the distribution curve describing the heterogeneity. To express the latter, they assumed that the standard deviation, p, of the

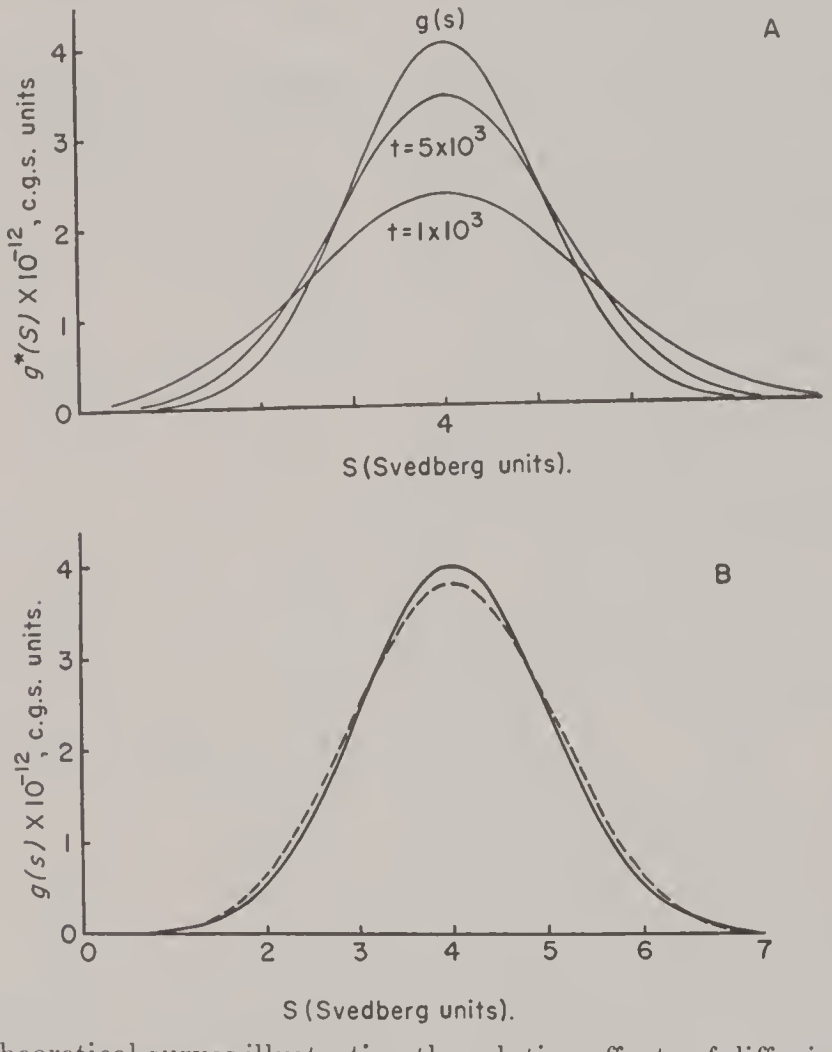

FIG. 35. Theoretical curves illustrating the relative effects of diffusion and heterogeneity in the analysis of boundary shape. A Gaussian distribution of sedimentation coefficients, $g(s)$, was assumed and the calculated curves, $g^*(s)$, at various times are shown in the upper part of the figure. The standard deviation in the assumed distribution was 1.0×10^{-13} sec., and the diffusion coefficient was taken as 5×10^{-7} cm.^{2}/sec. The real distribution curve is labeled $g(s)$, and the other two curves, calculated for the times indicated, show the effect of diffusion. In the lower diagram, the real distribution curve (solid line) is compared with the extrapolated values (dashed line) from calculated curves at 2000 and 5000 sec. This shows the difficulty in extrapolating the curves to infinite time in order to eliminate the effect of diffusion (from Baldwin, 1954b).

distribution curve is equal to half the distance in the boundary separating molecules with sedimentation coefficient, $s_{av} + p$, from those with sedimentation coefficient, $s_{av} - p$ (the subscript, $_{av}$, refers to the mean value). This distance can be written as $p\omega^2 x_{av} t + \cdots$, and the second moment due to heterogeneity is, therefore, $p^2\omega^4 x^2_{av} t^2 + \cdots$ As already shown, the diffusion coefficient must be modified because of the effect of the centrifugal field,

and the second moment resulting from diffusion is $2Dt/(1 - \omega^2 s_{av}t)$. Combining these terms, Williams *et al.* (1952) obtained

$$\sigma^2 = (p\omega^2 x_{av}t)^2[1 + \cdots] + 2D_{av}t[1 + \omega^2 s_{av}t + \cdots] \qquad (64)$$

With the knowledge that the second moment of the gradient curve (about the axis of rotation) is equal to $x_m^2 e^{2\omega^2 st}$ (see Eq. 10 and the integral of Eq. 2, $\bar{x} = x_m e^{\omega^2 st}$), Baldwin (1954b) was able to derive Eq. (64) in a much more general and rigorous fashion. To do this, he made use of the definition of the second moment about the mean as equal to the second moment about any position minus the square of the first moment about this same position. The resulting equation contained terms not present in the more simplified treatment, but these terms were shown to be small, and the equation reduced to Eq. (64). A plot of $\sigma^2/2t$ yields the values of D and p from the intercept and slope, respectively. Also an apparent diffusion coefficient can be calculated from σ^2. If the calculated values are independent of time, the material can be considered homogeneous. Alternatively, σ^2 can be plotted against t, and a linear plot indicates that the first term in Eq. (64) is negligible and that the material is homogeneous (Hall and Ogston, 1955). In a study of the homogeneity of bushy stunt virus, Lauffer (1942) considered the boundary spreading in terms of the diffusion coefficient which was measured independently. He observed that the boundary spreading in the ultracentrifuge was in accord with that expected from diffusion alone. Moreover, he showed that a distribution of sedimentation coefficients with a standard deviation greater than 2% in conjunction with the spreading due to diffusion would lead to boundaries which were clearly more diffuse than those measured experimentally. This treatment, though not expressed explicitly in general terms, is similar to that used by Williams *et al.* (1952). As in the other treatments considered in this section, Eq. (64) does not include factors for systems which exhibit a concentration dependence for the sedimentation coefficient. This, however, has been included in a recent extension of this treatment by Baldwin (1957a).

c. Self-Sharpening of Boundaries Due to the Concentration Dependence of Sedimentation Coefficients. Because of both the dependence of sedimentation coefficients on concentration and the change in concentration across boundaries, the sedimentation coefficient, itself, varies continuously throughout the boundary. This is equally true for single components and for each of the different molecular species in a mixture. Except for very unusual systems (Section IV,9), the molecules on the solvent (or trailing) side of the boundary migrate more rapidly than those on the solution (or leading) side. As a result, there is a continuing tendency for the boundary to sharpen itself in opposition to the blurring caused by diffusion. This

self-sharpening has been discussed by different workers (e.g., Pirie, 1940; Pickels, 1942a; and Gralén, 1944). Nonetheless, others have neglected this factor, and, as a result, unjustified claims have been made regarding the homogeneity of various substances. For some macromolecules like the specific polysaccharides of Types I, II, and III pneumococcus (Record and Stacey, 1948) and deoxyribonucleic acid (Peacocke and Schachman, 1954), the self-sharpening is so pronounced that even in relatively dilute solutions the boundaries appear as thin vertical lines with no evidence of spreading due to diffusion. With tobacco mosaic virus (Schachman, 1951a), the boundary which was first allowed to become diffuse by prolonged sedimentation and diffusion in a low centrifugal field subsequently became very sharp (in the same experiment) merely as a result of an increase in the centrifugal field which caused the boundary to migrate to the bottom of the cell in a short time. Although this demonstration of self-sharpening required a change in the angular velocity of the rotor during the run, it is clear that this tendency exists in all experiments. Parrish and Mommaerts (1954) and Goring and Chepeswick (1956) have repeated this experiment with myosin and deoxyribonucleic acid, respectively, and they also found that broad boundaries can be sharpened by increasing the sedimentation velocity through the use of higher centrifugal fields.

As a result of this self-sharpening effect, the analysis of boundary spreading, either as a measure of diffusion coefficients or as a test of homogeneity, is not meaningful unless (*1*) it is demonstrated that the sharpening is negligible or (*2*) suitable corrections for this effect are made. Pickels (1942a) in a discussion of the measurement of diffusion coefficients in the ultracentrifuge suggested that the rotor be decelerated to low speeds after the boundary had first migrated from the meniscus at a higher speed. Then the spreading could be measured with negligible self-sharpening since the migration of the boundary would be very small. Schachman (1951a) in considerations of the shape of boundaries of tobacco mosaic virus suggested that the boundary spreading experiments be conducted at varying concentrations or varying centrifugal fields so that the results could be extrapolated to either infinite dilution or zero centrifugal field. Extrapolation of the data (apparent diffusion coefficient) to zero centrifugal field provides a measure of the diffusion coefficient but, of course, the patterns would not be sensitive to inhomogeneity. Also the experiments would be difficult to perform in a conventional ultracentrifuge cell since the boundary would migrate very slowly at low speeds, and there would be a long period of restricted diffusion at the meniscus. With synthetic boundary cells such difficulties are circumvented, and the apparent diffusion coefficient can be evaluated at low speeds. On the other hand, extrapolation of the boundary spreading data to infinite dilution eliminates the self-sharpening

without sacrificing the resolving power of the sedimentation velocity method. Thus evidence regarding homogeneity can be provided although there is, of course, a loss in experimental precision as the solutions become more dilute. It is of interest to turn now to the second alternative posed above, i.e., the correction of the experimental patterns for the self-sharpening effect.

Until 1956, no progress had been reported in the development of a quantitative theory for correcting the observed patterns for the distortion caused by the dependence of s upon c. At that time, in a very important paper, Fujita (1956a) presented an approximate solution of the continuity equation for systems exhibiting a linear dependence of s upon c. In this treatment, Fujita assumed that D was independent of c. His additional assumptions were the same as those made by Faxén (1929). To allow for variations in D and to use Eq. (32) rather than Eq. (33) as an expression for the dependence of s upon c, though providing a more general theory, would have made the already formidable mathematical problem almost insuperable. The assumptions made by Fujita do not introduce serious limitations, because the variation in D across a boundary is likely to be less than that found for s, and as Fujita pointed out the effect of a change in the former on the shape of a boundary is certainly less than the effect of a change in s. Furthermore, the linear dependence of s upon c (Eq. 33) is a good approximation of the more general function (Eq. 32) if $kc \ll 1$. With certain approximations and transformations, Fujita obtained equations describing the concentration or concentration gradient as a function of c_0, x, t, ω, s_0, D, and k. These general equations were shown to reduce to the equation of Faxén (Eq. 56) for the boundary spreading in systems with constant sedimentation coefficients, i.e., $k = 0$. Also Fujita showed that the step function described by his equation if $D = 0$, i.e., for infinitely sharp boundaries, depends upon s_0, t, and k in exactly the same way as was found earlier (Eq. 39) by Trautman *et al.* (1954). With the detailed equations, Fujita made some computations for the concentration gradient as a function of a modified coordinate expressing distance from the axis of rotation. These calculations showed that the boundary curves were markedly sharpened and the position of the maximum gradient was noticeably shifted toward the axis of rotation as the value of k increased. Of additional interest was the result that the symmetry of the curves was essentially maintained except at the edges of the boundary. Moreover, the calculated curves showed a marked sharpening effect even for a value of 0.05 for kc. This corresponds to a solution of bovine serum albumin at a concentration of 1.0 g./100 ml. Since calculations with the detailed equations are very laborious, Fujita presented the results of his theoretical treatment in the form of the ratio of the maximum height to the area (H/A) as a function

of k, c_0, D, ω, s_0, and t. In this way, the diffusion coefficient can be evaluated from the ultracentrifuge patterns even for systems showing a dependence of s upon c. Alternatively, Fujita's equations can be employed as a test for homogeneity by comparing the diffusion coefficient calculated from the ultracentrifuge patterns with the values from measurements in the absence of a centrifugal field. Figure 36 shows the variation

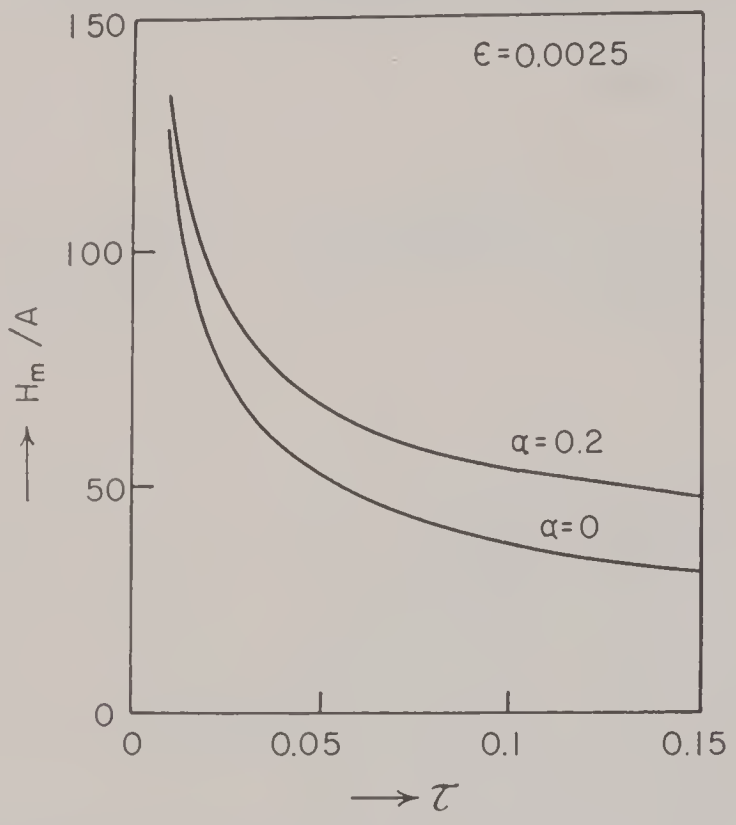

FIG. 36. Theoretical curves illustrating the effect of artificial boundary sharpening on the apparent diffusion coefficient evaluated from the ultracentrifuge diagrams. The ordinate is H_m/A where H_m is the maximum ordinate and A the area of the gradient curve. This ratio is a measure of the diffusion coefficient. The abscissa is τ $(2\omega^2 st)$. The two curves correspond to systems for which s is either independent of c ($\alpha = 0$) or s is markedly dependent on c ($\alpha = 0.2$ where $\alpha = kc_0$). The symbol, ϵ, corresponds to $2D/\omega^2 s_0 x_m^2$ (from Fujita, 1956a).

with time of the height-area ratio for systems in which s is either independent of concentration or decreases by 20% across the boundary. As seen in Fig. 36, the apparent diffusion coefficient, which is proportional to $(A/H)^2$, in the latter case is less than one-half the value for the ideal system. Even for materials having a smaller concentration dependence than that assumed in the calculations for Fig. 36, the correction for sharpening is so important that computations with Fujita's equations are mandatory. To calculate D, use is made of

$$\left[\frac{AF(\xi_m)}{H}\right]^2 = \frac{2D}{\omega^2 s_0}(e^\tau - 1)[1 + (1 - \lambda)^{1/2}]^2. \tag{65}$$

In Eq. (65)

$$\xi_m = \left[\frac{\omega^2 s_0 x_m{}^2 k c_0}{2D}\right]^{1/2} \left[\frac{\lambda^{1/2}}{1 + (1 - \lambda)^{1/2}}\right] \tag{66}$$

and

$$F(\xi_m) = \frac{\phi'(\xi_m)}{1 + \phi(\xi_m)} + 2\xi_m . \tag{67}$$

λ is defined by Eq. (68)

$$\lambda = kc_0(1 - e^{-\tau}) \tag{68}$$

and τ is equal to $2\omega^2 s_0 t$, sometimes referred to as the equivalent time of eentrifugation (Yphantis and Waugh, 1956a). The function ϕ is the equation of the Gaussian curve

$$\phi(\xi_m) = \frac{2}{\sqrt{\pi}} \int_0^{\xi_m} e^{-y^2}\, dy \tag{69}$$

and ϕ' is the well known derivative of that equation. The diffusion eoefficient, D, ean be evaluated from the slope of the plot of $[AF(\xi_m)/H]^2$ versus $(e^{\tau} - 1)[1 + (1 - \lambda)^{1/2}]^2$. In order to evaluate $F(\xi_m)$ from the tables of probability functions, the value of ξ_m, and henee of D must be known. Thus the determination of D requires first the assumption of a value for D and then the ealculation of ξ_m, $F(\xi_m)$ and the plot of the appropriate quantities to see if a straight line results. If the value of D calculated from this line does not agree with the assumed value, the process must be repeated until a self-consistent value of D is found. Figure 37 shows an application of Eq. (65) to boundary spreading experiments with bovine serum albumin (Baldwin, 1957b). Both the eorrected and uncorrected results of (A/H) are presented, and it is elear that the deviation from linearity for the uncorrected data is much greater at the higher concentration. This is a manifestation of the greater change in s across the boundaries in the latter experiment (Eq. 25). Diffusion eoefficients calculated from the slopes of the upper eurves (for each concentration) have the values 7.0×10^{-7} cm.^{2}/sec. and 6.8×10^{-7} em.^{2}/sec. As Baldwin pointed out, these values are in good agreement with the values 6.85×10^{-7} cm.^{2}/sec. and 6.94×10^{-7} cm.^{2}/see. calculated from Gosting's precise diffusion data (quoted by Baldwin *et al.*, 1955). When the ultracentrifuge patterns were used direetly (without eorrection for the self-sharpening) to calculate apparent diffusion coefficients, Baldwin found that the values decreased with time during the experiment as had been observed with tobacco mosaic virus (Schachman, 1951a). Though the value of k is much larger for the virus particles than for serum albumin, the study with tobacco mosaic virus was at a lower

concentration so that the relative change in s across the boundary was about the same, and the apparent diffusion coefficients decreased about 50% during both sets of experiments.

When the sedimenting material is heterogeneous, the plots according to Eq. (65) show upward curvature, or alternatively the calculated apparent diffusion coefficients increase during the experiment. This in itself is a good indication of heterogeneity, but Fujita's theoretical treatment is not

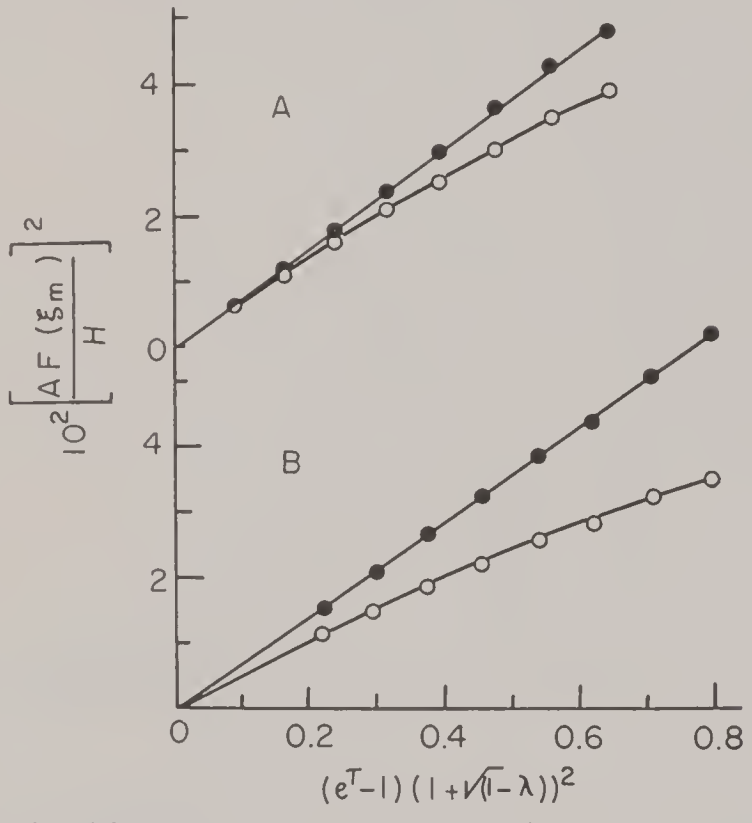

FIG. 37. Analysis of boundary spreading for bovine serum albumin in terms of Fujita's theory. *A* and *B* represent experiments at 0.67 g./ 100 ml. and 1.35 g./100 ml., respectively. The lines drawn through ● are for the values calculated according to Eq. (65). The curved lines through ○ correspond to calculations without correction for the self-sharpening effect (from Baldwin, 1957b).

amenable to a quantitative description of the heterogeneity.[6] It should be stressed that Fujita's solution of the continuity equation applies only to a single component, and discussions of polydisperse systems of components with concentration-dependent sedimentation coefficients must be directed along other lines.

[6] Fujita's theory has been applied recently by Connell (1958) in an analysis of the sedimentation velocity patterns obtained with a preparation of cod myosin. This work provides another demonstration of the importance of including in the calculations a term which corrects for the artificial sharpening of the boundary. Although the boundaries were sharp, giving the qualitative impression that the material was homogeneous, the detailed analyses of the patterns revealed that the material was, in fact, heterogeneous.

In the previous section we discussed the extrapolation of dB/dx to infinite dilution (Gralén, 1944) and the procedure employed by Jullander (1945) to determine the parameters of the distribution curve for systems exhibiting a large dependence of s upon c. Essentially similar procedures have been used by Williams *et al.* (1954) and Williams and Saunders (1954) to obtain true distribution curves ($g(s_0)$ versus s_0) by extrapolation of the

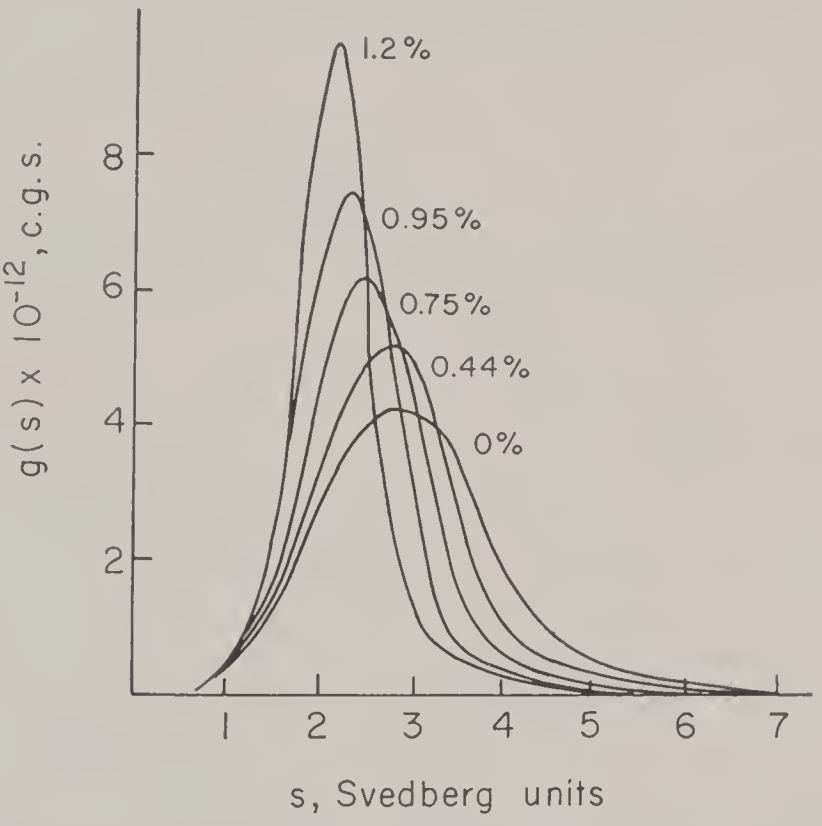

FIG. 38. The effect of concentration on the distribution curves for the sedimentation coefficients of dextran. The curve labeled 0% was obtained by extrapolation of the $g(s)$ values for selected values of s. The marked sharpening of the curves and the shift toward lower values is evident, thereby demonstrating the necessity for extrapolating the data to infinite dilution if the correct distribution curve is to be obtained (from Williams and Saunders, 1954).

curves measured at different concentrations. This is a laborious procedure since each $g(s)$ versus s curve is first determined by extrapolation to infinite time and then the values of $g(s)$ for fixed values of s are plotted against c so as to permit the extrapolation of the $g(s)$ values to infinite dilution. Marked changes were observed at the different concentrations due principally to the effect of concentration on the sedimentation coefficients. Williams and his colleagues derived valuable information about the true distribution by this double extrapolation procedure. Representative results with dextran are shown in Fig. 38. The importance of extrapolating the data to infinite dilution is evident from examination of the curves at

different concentrations. Though the procedure is laborious and suffers from a loss of precision in the more dilute solutions because of the inadequate optical registration, this method appears the most satisfactory of those currently in use. Baldwin (1954a; also see de Lalla and Gofman, 1954) has devised a method of correcting the distribution curves for the dependence of s upon c without resort to the detailed distribution curves at a series of concentrations. This method requires the distribution curve at one concentration (preferably a dilute solution) and data expressing the dependence of s upon c for the preparation as a whole. Following the lead of Jullander (1945), who converted the dc/ds curves to dc/dM curves by multiplication of each ordinate by ds/dM, Baldwin corrected the values of $g(s)$ to infinite dilution values of s by multiplication with ds/ds_0. Similarly, the transformation of the s scale to values of s_0 was achieved directly by integration of the boundary gradient curves to give c at any level and then applying the necessary correction to transform the x value to s and finally to s_0. This method, which gave results in good agreement with the extrapolated curves of Williams and Saunders, (1954) requires the assumption that the k value for the system as a whole applies at each level within the boundary. It is clear from the discussion in Section IV, 4 that this is not strictly valid, but the errors inherent in this assumption are apparently small if the s versus c dependence is not great or if the concentration employed in the experiment is sufficiently small that $s/s_0 > 0.9$. Baldwin (1954a) has also considered the extrapolation procedure of Williams *et al.* (1954) and compared it with another method in which the s values selected at fixed ratios of $g(s)/g(s)_{max}$ are plotted against c. The extrapolated values of s_0 are then used to construct a distribution curve with the ratios of $g(s)/g(s)_{max}$. At present there is no rigorous theoretical basis for either extrapolation procedure.

Although the corrections for the effect of concentration on the boundary shape are still somewhat empirical for polydisperse systems with considerable heterogeneity, a satisfactory theory is now available for systems exhibiting only moderate heterogeneity. This can be used to complement the theory of Fujita (1956a) for homogeneous materials in studies aimed at demonstrating the homogeneity or characterizing in a quantitative manner the degree of heterogeneity of a given sample. Starting with a general formulation of the moments of a composite curve in terms of the sum of individual concentration gradient curves and with the continuity equation containing s and D, both of which are written as functions of the total concentration, Baldwin (1957a) obtained a detailed expression relating the time dependence of the second moment of the gradient curve about the mean. Baldwin's equation reduces to that presented earlier (Eq. 64) if the constants expressing the concentration dependence of s and D are set

equal to zero. The results of this more detailed treatment can be written

$$p = [B'/\omega^4 x_m^2 F(t)]^{1/2} \tag{70}$$

where

$$B' = \sigma^2 - \sigma_0^2 - 2\omega^2 \bar{s} \int_{t_0}^{t} \sigma^2 \, dt - 2(\bar{D}_0 - Kc_0/2)(t - t_0) + 2\omega^2 \int_{t_0}^{t} x' (2k_1 Q_1 + 3k_2 Q_2) \, dt \tag{70a}$$

and

$$F(t) = (t^2 - t_0^2) + (\tfrac{4}{3})\omega^2 \bar{s} (t^3 - t_0^3) \tag{70b}$$

In these equations, $\bar{s}$ is the weight-average sedimentation coefficient at the concentration of the solution placed in the cell, $\bar{D}_0$ is the weight-average diffusion coefficient at infinite dilution, x' is the first moment of the gradient curve, k_1 and k_2 are the constants expressing the relationship of $\bar{s}$ to c ($\bar{s} = \bar{s}_0 - k_1 c - k_2 c^2$), and K is the constant relating $\bar{D}$ to c ($\bar{D} = \bar{D}_0 - Kc$). The quantities, Q_1 and Q_2, are defined by the following

$$Q_1 = \int_{x_m}^{x_p} \frac{(x - x')c(\partial c/\partial x)}{c^p} \, dx \tag{70c}$$

and

$$Q_2 = \int_{x_m}^{x_p} \frac{(x - x')c^2(\partial c/\partial x)}{c^p} \, dx \tag{70d}$$

where c^p is the total concentration in the plateau region at the time, t. Calculations according to Eq. (70) are very laborious, and Baldwin presented in detail the methods for evaluating the various factors which are required (the original paper deals with refractive index units rather than concentrations). After the terms are computed, B' is plotted against $F(t)$, and the slope of the resulting straight line, $p^2\omega^4 x_m^2$, is used in the calculation of p, the standard deviation of the distribution of sedimentation coefficients. This is defined by

$$p^2 = \sum_i \alpha_i (s_{i,0} - \bar{s}_0)^2$$

where α_i is the weight fraction of the i^{th} species, $\bar{s}_0$ is the weight average sedimentation coefficient, and $s_{i,0}$ is the sedimentation coefficient of the i^{th} species, both sedimentation coefficients corresponding to infinite dilution of all of the solute molecules.

This treatment by Baldwin (1957a) is much more rigorous than any of the

previous discussions of this problem, and the various terms are more specifically defined. Eriksson (1953) dealt with the problem of analyzing polydispersity of systems for which diffusion was not negligible. He combined the treatment used by Baldwin and Williams (1950) with the formulation of Gralén (1944); however, no explicit formulation of the concentration effect was attempted. In a more recent paper, Eriksson (1956) deals with the influence of pressure on the analysis of boundaries of polymethyl methacrylate dissolved in ethyl acetate. For organic solvents, such considerations as the effect of pressure on the density and viscosity of the medium are important, but they are likely to be negligible for biological systems except those in which the density difference between the sedimenting particles and the medium is small. Dieu and Oth (1954) also used the same general approach of Baldwin and Williams (1950), but no corrections were introduced for the dependence of s upon c.

When Baldwin applied this theory (Eq. 70) to experimental results with β-lactoglobulin, he found that B' was essentially equal to zero; therefore, the protein was homogeneous with respect to sedimentation rate. With several samples of bovine serum albumin, however, the heterogeneity was clearly evident, and p had values about one-fifth the weight-average sedimentation coefficient. By means of this extremely thorough work, Baldwin showed that the contributions of the terms resulting from the dependence of s upon c were relatively large. Even for dilute solutions (0.67 g./100 ml.) of a protein like bovine serum albumin, which is generally considered as having a small dependence of s on c, (as compared with myosin and fibrinogen, for example) the concentration dependent factor amounted to 26% of the value of B'. This is a substantial factor, neglect of which has led to the conclusion that the sedimenting material is less heterogeneous than is indeed the case.

It should be noted that the determination of the standard deviation of the distribution of sedimentation coefficients requires a value for the diffusion coefficient. If this is not available, the equations of Baldwin can be used in another manner. For this situation, Baldwin defines

$$\sigma^2_{cor} = \sigma^2 - 2\omega^2\bar{s}\int_{t_0}^{t}\sigma^2\,dt + 2\omega^2\int_{t_0}^{t}x'\,(2k_1Q_1 + 3k_2Q_2)\,dt \qquad (70e)$$

which is then plotted against $(t - t_0)$. As can be seen by inspection of Eq. (70a), this plot is linear if the material is homogeneous, i.e., p and B' are equal to zero, and the slope is equal to $2(D_0 - Kc_0/2)$. This method must be used for materials which exhibit a dependence of s upon c, and it supplants the treatment based on Eq. (64). As in that case, here too upward curvature of the plot of σ^2_{cor} versus $(t - t_0)$ indicates heterogeneity. With β-lactoglobulin, Baldwin obtained a straight line the slope of which gave

a value for D in excellent agreement with data in the literature. This theoretical approach, in a more approximate form, was used by Baldwin (1953a) in an examination of the neurotoxin of *Shigella shigae*. Also Field and O'Brien (1955) employed this general treatment in studies of human hemoglobin.

d. Distortion of the Boundary Due to the Johnston-Ogston Effect. At present, the correction for the effect of one component on the sedimentation rate of a slower component migrating in its presence (and the consequent concentration anomaly) consists of the repeated application throughout the boundary of the theory developed for two components. It is assumed that the boundary is composed of a series of n components, the concentrations of which can be obtained ordinarily by measurement of $(dc/dx)\Delta x$ (diffusion is here considered negligible). However, as a result of the changes in s with c, the movement from one surface $(i - 1)$ to the next (i) in the boundary results not only in an increase in concentration because of the appearance of the i^{th} component, but also all components with sedimentation rates less than s_i suffer a decrease in concentration across that surface. If the sedimentation rates of the components could be determined in the various mixtures comprising the boundary, the theory developed in Section IV, 7 could be applied. The resulting corrections would then be satisfactory, but it should be stressed that the treatments presented there did not deal with overlapping boundaries for which diffusion is not negligible. In the absence of detailed knowledge of the k values for each component acting on itself and on other components with lower sedimentation coefficient, only an approximate calculation can be made. De Lalla and Gofman (1954) as well as Baldwin (1954a) have assumed the same k value for all the components of the mixture (this is the only value accessible to experimental determination unless fractionation is achieved) and that this value applies to each of the molecular species acting on itself and on the other components. As shown in Section IV, 6, this is certainly not valid in general, although it appears to be the most reasonable approximation that can be used at this time.

Baldwin (1954a) has used this process of step-by-step correction of c_i (starting from the solvent side of the boundary) for the polydisperse sample of dextran studied by Williams and Saunders (1954) and found that the correction of the boundary shape for the Johnston-Ogston effect is significant. However, the correction is not nearly so large as that caused by the self-sharpening effect. Ogston and Woods (1954) came to the same conclusion during the analysis of their sedimentation data on dextran samples. It should be pointed out that this correction for the Johnston-Ogston effect, as made by these workers, is likely to be an underestimation since the effect of the concentration of a given component on the s of slower

material is usually greater than the effect of the same component on its own sedimentation rate. Although this effect is not treated explicitly by Williams and his colleagues (Williams and Saunders, 1954; Williams *et al.*, 1954), their extrapolation of $g(s)$ versus s curves to infinite dilution includes implicitly a correction for this effect as well as the self-sharpening effect.

c. General Considerations Regarding the Demonstration of Homogeneity. As seen from the above discussion, conclusions regarding homogeneity are apt to be erroneous if they are based on a cursory examination of the ultracentrifuge patterns which reveal a single, sharp symmetrical boundary. It is regrettable that so many claims in the literature are based on little more than such superficial observations. Other conclusions, however, are the result of much more detailed and thorough analyses based on the method suggested by Svedberg and Pedersen (1940). Even these (Lauffer, 1942; Putnam, 1951, 1954; and Davisson *et al.*, 1953) may require revision now based on a reinterpretation according to Fujita's (1956a) theory. A given material may appear to be homogeneous when, in fact, it is heterogeneous, and the self-sharpening compensates for the additional spreading that should be observed due to polydispersity.

The demonstration of homogeneity by means of sedimentation velocity analysis is a laborious task, but the techniques and theoretical background are now available for such an undertaking. Improvement in the sensitivity of optical methods which would permit analysis of more dilute solutions would make the experimental aspects simpler and reduce the demands on the theory. Already, however, the accuracy of the measurement of boundary shape has been enhanced tremendously because of the application of the phase plate as a schlieren diaphragm. For some systems, absorption optical methods represent the obvious approach, but the accuracy with present techniques is much less than with schlieren optical techniques.

Several factors must be included in any rigorous test for homogeneity. Not only must there be a single, symmetrical boundary throughout the experiment (Fujita's theory provides the basis for the conclusion that lack of symmetry, except at the edges of the boundary, is in itself evidence for inhomogeneity), but also the area under the boundary must account quantitatively for all of the material in the solution. For this to be a sensitive test, the experiment should be conducted, if possible, for times sufficient to permit the boundary to traverse the entire cell. This test requires the determination of the optical parameters of the ultracentrifuge and the concentration and refractive index increment of the solute. Alternatively, a synthetic boundary cell can be used at low speeds as a differential refractometer (Klainer and Kegeles, 1955) for the evaluation of the concentration in optical units (area on the photographic plate). If the square rule corrected area in the experiment at the higher centrifugal field does not

remain constant, the sample is not homogeneous. Next, the sample should be examined at a series of concentrations to ascertain whether the dependence of s on c is sufficient to cause much self-sharpening, thereby necessitating the application of Fujita's theory. Most systems will have sufficient change in s across the boundary that calculations according to Eq. (65) are mandatory. The experiments at the different concentrations provide the values of s_0 and k necessary for the implementation of that equation. If the change in s across the boundary is indeed negligible, the spreading can be analyzed directly in terms of σ^2 or an apparent diffusion coefficient. The former should be linear with time and the latter independent of time to satisfy the criteria of homogeneity. Moreover, the diffusion coefficient should agree within about 5% with the value from classic diffusion measurements. This test, it should be noted, is sensitive only for those materials which migrate appreciably during the sedimentation velocity experiment. For small molecules, the diffusion rates are so high and the sedimentation coefficient so small that the resolving power of the ultracentrifuge is too limited to provide a sensitive test for homogeneity. In such cases the boundary spreading, usually measured in a synthetic boundary cell, gives a diffusion coefficient (Schachman and Harrington, 1954). When this cell is employed with larger materials and the speed of the rotor is maintained at low values so that the boundary moves very little, diffusion coefficients can be measured without disturbances due to polydispersity (Schumaker and Schachman, 1957). Of course, these values do not compare in accuracy with those obtained by classic diffusion methods (see review by Gosting, 1956), but they can be obtained with small amounts of material (40 μg. in the case of cytochrome). Such diffusion coefficients can be used in the treatment of Baldwin (1957a) for the determination of the standard deviation of the distribution of sedimentation coefficients if the material does not satisfy the criteria of homogeneity as evidenced by the plot according to Fujita's (1956a) theory. If the dependence of s on c is negligible, the boundary is essentially a Gaussian curve and a plot of $\ln (\partial c/\partial x)$ versus $(x - x_H)^2$ should be linear for values of x on either side of the maximum ordinate, x_H. This test has been applied by Hall and Ogston (1955) and by Baldwin (1957a).

Homogeneity with respect to density can also be examined by analysis of the boundary spreading in experiments in which the buoyancy term is varied by the addition of a third component. With polystyrene latex particles, Cheng and Schachman (1955b) pointed out that a variation of particle density of 0.01% leads to differences of only 0.2% in s if the experiments are conducted in water. However, the addition of D_2O to increase the density of the medium reduced the average net density difference between the particles and the medium to only 0.001 g./ml. Now the same heterogeneity in density among the particles would lead to a varia-

tion of 10% in sedimentation rate. Such a variation in s was not observed, indicating that the particles were very homogeneous with respect to density. Thus homogeneity with respect to density can be assessed through analysis of sedimentation velocity patterns. For material like lipoproteins this approach should prove valuable. Oncley *et al.* (1957) have obtained curves of $g(s)$ versus s for the macromolecules in dilute salt solutions. How these distribution curves vary as the density of the medium approaches that of the macromolecules will indicate whether the heterogeneity is due principally to variations in molecular size or in chemical composition (fraction of lipid). Only the latter would have a marked effect on the partial specific volume. Therefore an increase in the apparent heterogeneity as the buoyancy term decreases indicates a polydispersity in density. This same principle (reducing the buoyancy term by the addition of a third component) has been applied in a different form by Meselson *et al.* (1957) in studies of the heterogeneity of deoxyribonucleic acid with respect to density. In these experiments, large amounts of a dense material, cesium chloride, were added to the solution thereby making the buoyancy term for the macromolecules very small. Upon redistribution of the cesium chloride in the centrifugal field, a density gradient was created; the macromolecules at the bottom of the cell migrated in a centripetal direction while those at the top of the cell sedimented centrifugally. Ultimately an equilibrium distribution was attained with the macromolecules packed as a thin band at a position where the net buoyancy term was equal to zero. Owing to diffusion, the bands are not infinitely thin. Macromolecules of different densities attain different equilibrium positions. Thus deoxyribonucleic acid molecules containing N^{15} were readily differentiated (and separated) from others containing N^{14} (Meselson and Stahl, 1958). In these experiments there was a variation in density of 0.014 g./cm.^{3} between the two types of macromolecules. If a band is not symmetrical there must be heterogeneity with respect to density. When only a single, symmetrical band is observed, the data cannot be interpreted unambiguously in terms of heterogeneity or homogeneity with respect to density. If the band is wide the solution contains either relatively large macromolecules of varying density (with, for example, a Gaussian distribution of densities) or much smaller molecules which are uniform in density. Combinations of these extremes also could produce a symmetrical, single band. However, a choice among these alternatives can be made after further experimentation. This technique is already finding wide application in biological problems.

9. Analysis of Systems of Reversibly Interacting Components

The ultracentrifuge patterns for a system of components which interact with one another in a reversible manner are dependent on the rates of the reactions in the forward and backward direction as compared to the

rate of centrifugal separation of the components. Longsworth and MacInnes (1942), in a fundamental paper dealing with interacting systems in electrophoresis, discussed the various possibilities. Similar considerations apply to the ultracentrifuge. If the association reaction is fast and the dissociation slow, the system will behave as a mixture of the complex and whichever of the two components is present in excess (if neither is in excess, then only the complex will be observed). Conversely, the system would appear essentially as a mixture of two independent components if the dissociating reaction is rapid and the association is slow. When both reactions are slow, but comparable in velocity, the pattern at equilibrium will indicate the presence of both individual components as well as the complex. Such a mixture, in a sense, could be considered as a trivial example of interacting systems since the ultracentrifuge patterns could be interpreted in terms of the independent species, each possessing a different sedimentation coefficient. If, however, the rate of adjustment of the equilibrium is comparable to the rate of separation of the molecular species, the patterns would be complicated and convective disturbances may very well be the result. Analysis of such experiments is a formidable problem, and thus far only an approximate treatment for a special case has been presented (Cann *et al.*, 1957). These workers considered the problem of the isomerization of a single component ($A \leftrightharpoons B$) for which the half-times of the reactions are of the order of the duration of the transport experiment. Finally, there is the system, which is apparently common in biochemistry, in which both the forward and backward reactions are very rapid and the reaction velocities are comparable in magnitude. Equilibrium is maintained despite the tendency toward separation of the species according to their sedimentation coefficients. The consequent readjustment of the concentrations of the various molecular species complicates the ultracentrifuge patterns, and both the shape and movement of the boundaries must be interpreted with caution. In the following discussion, we shall deal principally with this last type of interaction involving, first, only a single component which tends to aggregate reversibly and, second, systems of two components one of which may be a protein or other large molecule, the other component being a small molecule or ion.

a. Association-Dissociation Equilibria Involving a Single Component. Associating-dissociating systems involving rapidly attained equilibria have been recognized readily by their unusual sedimentation behavior. Only a single, almost symmetrical, boundary is usually observed, and s increases with concentration in dilute solutions. At some concentration, depending on the system, the sedimentation coefficient either becomes constant or actually decreases slowly as the concentration is increased still further. The increase in s with c in dilute solutions is presumed to be the result of

a shift in the equilibrium toward the higher aggregates as c increases. As Tiselius (1930) pointed out for electrophoresis, the boundary in such systems moves with a weight-average mobility; therefore, the shift in equilibrium with concentration is manifested by a change in sedimentation rate. Above a certain concentration the equilibrium predominantly favors the more rapidly sedimenting species, and the dependence of s on c then becomes governed by the hydrodynamic effects discussed in Section IV, 4. Behavior of this type was discussed qualitatively by Pedersen (Svedberg and Pedersen, 1940) for horse hemoglobin and by Svedberg and Hedenius (1934) for other hemoglobins. A thorough investigation of the dissociation of hemocyanin was conducted by Brohult (1940). Apparently, the various reactions for this latter material were not so rapid that readjustment of the equilibria could occur during the ultracentrifuge experiments; as a consequence, separate, discrete boundaries were observed in many experiments. Schwert (1949) appears to have been among the first to investigate a rapidly associating-dissociating system in some detail, in his studies of the molecular size and shape of chymotrypsinogen and α- and γ-chymotrypsin. Figure 39 shows his results for the concentration dependence of the sedimentation coefficient of α-chymotrypsin. The straight line portions of the curves at the higher concentrations were extrapolated to infinite dilution to give a value of s_0 corresponding to the larger aggregates, here presumed to be dimers. Extrapolation of the data at the lower concentrations, though hazardous, was employed to give s_0 for the monomer. These values were then used in calculations of the molecular weights of the monomer and dimer. Schwert observed also that in those experiments with solutions presumably containing appreciable quantities of both monomers and dimers the boundary spreading was greater than that observed for either monomers or dimers alone. This was attributed to the fact that the boundary was the site of continually readjusting equilibria. At the trailing edge of the boundary, the concentration is low; hence dimers dissociate into monomers, which, of course, sediment less rapidly than the average material in the plateau region. These molecules thus tend to lag behind the boundary, causing it to be broader than would be observed for a single component. Similar behavior was reported by Oncley and Ellenbogen (Oncley *et al.*, 1952) in their experiments with insulin at low pH. In an attempt to explain the observed dependence of s on c, these workers formulated a qualitative theory in terms of an equilibrium between insulin monomers and trimers. Although the theory is incomplete and the data do not have the precision obtainable today, these studies did much to eliminate the discrepancies then existing between the molecular weights determined by ultracentrifugation and those derived from osmotic pressure or light scattering measurements. Other studies on insulin have

confirmed the finding that at low pH, the curve of s versus c has a positive slope and s_0 is about 1.7 S (Fredericq and Neurath, 1950; Tietze and Neurath, 1953; Schachman and Harrington, 1954). These results in conjunction with other data indicate a molecular weight of 12,000 for insulin under these conditions. Other values for s are obtained at different pH

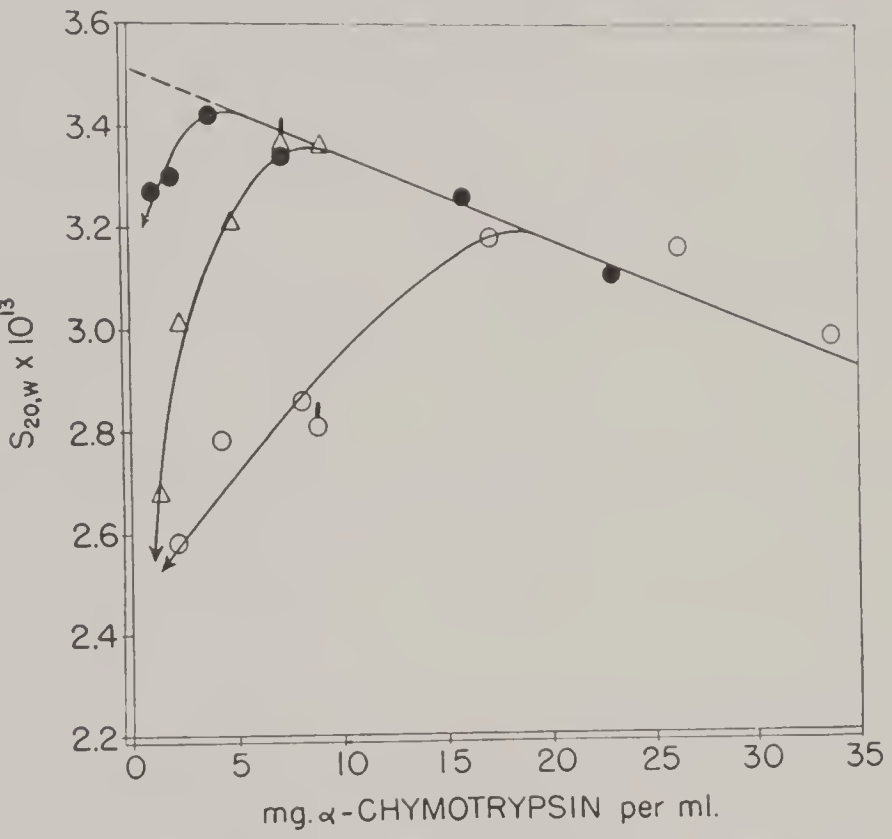

FIG. 39. The dependence of sedimentation coefficient on concentration for a system exhibiting association-dissociation equilibria. Data are for α-chymotrypsin at 25°C. ● refer to experiments at pH 3.86 and ionic strength of 0.2; △ correspond to pH 4.99 and ionic strength of 0.2; △ represents another sample; ○ refer to pH 6.20 and ionic strength of 0.2; and ◔ represents an experiment at 10°C (from Schwert, 1949).

values and in other solvents, e.g., Fredericq (1953) reports a value of 1.2 S at pH 10.

There have now been a great many studies on different proteolytic enzymes. Chymotrypsinogen shows less tendency to aggregate than do the various chymotrypsins (Schwert, 1951; Dreyer *et al.*, 1955), but the reversible association of the former has been found by Massey *et al.* (1955). Trypsin also shows reversible association-dissociation equilibria (Cunningham *et al.*, 1953) and, moreover, the aggregation was prevented by reaction of the protein with diisopropylfluorophosphate. Similarly, Massey *et al.* (1955) found that the diisopropylphosphoryl derivative of chymotrypsin does not aggregate under conditions in which the active enzyme forms

aggregates much larger than dimers. There have been investigations of the dissociation and association of other proteins like papain (Smith *et. al.*, 1954), arachin, and conarachin (Johnson and Shooter, 1950; Johnson and Joubert, 1951; Johnson and Naismith, 1953, 1956; Evans, 1957), soybean protein (Naismith, 1955; Briggs and Wolf, 1957), and casein (von Hippel and Waugh, 1955; Waugh and von Hippel, 1956). Some of these proteins dissociate and associate rapidly so that the equilibria are continually adjusting throughout the boundary; others seem to involve much slower reactions, and the ultracentrifuge patterns show discrete boundaries which are apparently a faithful index of the equilibrium distribution of the molecular species in the solution initially.

A major obstacle to a complete understanding of these associating-dissociating systems can be attributed to the lack of a quantitative theory for the sedimentation of such mixtures. Although weight-average sedimentation coefficients can be measured through the use of the second moment of the entire gradient curve, more information about the type of complexes and their rates of interconversion is potentially available through analysis of the shape of the boundary. Field and Ogston (1955) have considered the boundary spreading for the system, $A \rightleftharpoons nB$, in which the reaction rates both in the forward and backward direction are so rapid that equilibrium is continually maintained at every level in the boundary. They considered the flux of material across an arbitrary moving surface in the boundary and found that the flux was the sum of two terms, the first being proportional to concentration and the second proportional to the concentration gradient. The latter therefore decreases with time due to the spreading of the boundary. Though their resulting differential equation for the transport of material across a given surface could not be directly integrated, they did perform a numerical integration which enabled them to express the spreading of the boundary in terms of σ^2_{cor} versus t. This treatment was applied to the equilibria of hemoglobin in mildly acidic solution. Under these conditions, one molecule apparently dissociates reversibly into two equivalent subunits. When the rate of interconversion of the two forms of hemoglobin (Field and O'Brien, 1955) was assumed to be zero, the plot showed the characteristic curvature of a mixture of two independent substances (this was calculated from Eq. 64). However, the curve calculated for rapidly interacting components (reaction velocity constants equal to infinity) showed no curvature—a characteristic of homogeneous material. The calculated curve was relatively close to the experimental curve, which did not reveal heterogeneity either. Only about 60% of the observed boundary spreading could be attributed to diffusion, and the remainder results from the existence of two molecular species and the shifting in the equilibrium as the concentration changes throughout the boundary. This

treatment showed also that heterogeneity would be revealed in such interacting systems, and there would be increased boundary spreading if the reaction velocities were small. For a system involving only an isomerization of the solute (so that there is no change in the number of molecules as a consequence of the interaction) Cann *et al.* (1957) showed that infinitely fast reactions, with an equilibrium constant of 1, will lead to a boundary that is Gaussian in shape (as for homogeneous materials) and possesses a mobility equal to the arithmetic mean of the values for the two independent species. The theory shows that bimodal curves will result if the reaction rates are much slower.

Another approach to this problem has been introduced by Gilbert (1955) in consideration of the interaction, $A \rightleftharpoons nB$, where n can have values much higher than 2. His theory is based on analogies to chromatography and does not consider the effect of diffusion. Nonetheless, it accounts in detail for some of the puzzling observations of Massey *et al.* (1955) on the sedimentation of α-chymotrypsin at pH 7.9 and low ionic strength. For example, the theory predicts that there will be a single, unsymmetrical boundary if $n = 2$, but that two boundaries will be observed if $n > 2$. Moreover, with suitable data, the theory provides an equilibrium constant. The calculations of the fraction of the total α-chymotrypsin present as hexamer are in excellent agreement with the experimental observations of Massey *et al.* (1955). Also the values of s as a function of c are predicted accurately for both components. Prior to this treatment, it was generally accepted that only a single boundary would be observed in association-dissociation equilibria as long as the reactions were very rapid. Thus for the first time, it has been predicted that two boundaries will result if the equilibria involve aggregates larger than dimers. Under other experimental conditions, the sedimentation coefficients indicate dimers (Schwert, 1949) rather than hexamers, and Gilbert's calculations for this case, too, account for the various experimental results. Though the theory is in a sense unreal because of the lack of consideration of diffusion, it must be viewed as an exciting development which may, with suitable expansion, reveal information hitherto not obtainable. Indeed this approach has been extended very recently by Rao and Kegeles (1958) in a study of the polymerization of α-chymotrypsin. Although this work is concerned mostly with the application of the Archibald method (see Section IV, 1) to chemically reacting systems, Rao and Kegeles following the treatment of Gilbert (1955) showed that monomers, dimers, and trimers were present as an equilibrium mixture. This was revealed by their extension of Gilbert's theory which predicts that a mixture of monomers and trimers will give a double boundary whereas the mixture of all three molecular species gives only a single boundary. The latter was observed experimentally.

It should be recognized that a weight average sedimentation coefficient for the material as a whole can be evaluated even though there are several boundaries of the type described by Gilbert (1955). This calculation requires integration of the ultracentrifuge pattern from the meniscus to a surface in the plateau region ahead of the more rapidly moving boundary. Steiner (1954) has discussed the relationship of the weight average sedimentation coefficient to concentration in terms of the various equilibria.

b. Interactions among Different Molecular Species. In view of the direct relationship between the sedimentation coefficient of a substance and its molecular weight, it might be expected that the ultracentrifuge would find wide application in the study of the interactions of proteins with other molecules and ions, both larger and smaller. Despite several attractive features of the ultracentrifugal approach to the analysis of interacting systems, the number of such studies is indeed limited, and most of those have been concerned with only a single component as discussed in the previous section. An interesting and rewarding series of investigations of interacting components, both of which are proteins and comparable in size, has been conducted by Singer and co-workers on the physical properties of soluble antigen-antibody complexes (Singer and Campbell, 1952, 1953, 1955a, 1955b, 1955c; Singer *et al.*, 1955; Baker *et al.*, 1956). The interaction of trypsin and soybean trypsin inhibitor was examined ultracentrifugally, and the formation of the 1:1 complex at pH 6 was readily distinguished from the results at pH 2.8, where apparently no reaction occurred (Sheppard *et al.*, 1950; Sheppard and McLaren, 1953). Except for some few special examples, which can hardly be classified as typical, the ultracentrifuge scarcely has been employed for the interaction of large and small molecules. It was easy, for example, to demonstrate the binding of methyl green to deoxyribonucleic acid (Kurnick, 1954) as evidenced by the migration of the colored dye with the macromolecular component whose sedimentation coefficient was measured with the schlieren optical system. Similarly, the degree of binding of the coenzyme diphosphopyridine nucleotide (DPN) to various dehydrogenases was measured quantitatively by Velick and his colleagues in a series of investigations using the high speed centrifuge (Velick *et al.*, 1953; Velick and Hayes, 1953; Velick, 1953; Hayes and Velick, 1954; and Velick, 1954). In these experiments, various mixtures of the coenzyme and enzyme, along with a control containing only DPN, were placed in the tubes of a preparative centrifuge rotor which was subjected to sustained operation at high speed for times sufficient to allow most of the enzyme to sediment to the bottom of the tubes. The supernatant fluids were carefully removed from all of the tubes and analyzed for the concentration of DPN. The amount of the separated coenzyme in each of the tubes which originally contained both components was then

compared with the supernatant liquid from the tube which contained only the coenzyme. From the differences in DPN concentration between the latter and each of the other tubes, they calculated the amount of free DPN in each tube, and from the known initial concentration of DPN and enzyme in each tube, they determined the amount of DPN bound per mole of the enzyme for the various mixtures. With these data at different concentrations, they were able to determine the maximum number of binding sites on the enzyme and the association constant.

It should be noted that there is no assurance that the supernatant liquid contains the true equilibrium concentration of the free coenzyme. The process of removing the enzyme and the complex by sedimentation may itself lead to a disturbance of the equilibrium, and the consequent readjustment would probably lead to a value for the DPN concentration which is less than the true equilibrium concentration. To what extent this occurred depends on many factors to be discussed presently, and these general remarks should not be construed to mean that the studies outlined above are invalid.

Before discussing these systems further, it is profitable to examine the experiments of Singer and co-workers. In these studies of mixtures of antigen, antibody, and various soluble complexes of antigen and antibody, a series of boundaries were observed both in the ultracentrifuge and in electrophoresis. As they pointed out on the basis of the discussion of Tiselius (1930), the presence of several discrete boundaries precludes the existence of very rapidly attained equilibria among the various molecular species in the solution. Such rapid, reversible reactions would, according to Tiselius, prevent the resolution of the sedimenting materials into separate boundaries. There are data available, however, which suggest that the reactions between antigen and antibody to form various complexes are reversible, and as Singer and Campbell (1952) demonstrated, the attainment of equilibrium was rapid at least from one direction. To show this, they prepared two separate mixtures containing known, different ratios of antigen to antibody. These preparations were stored for 24 hours, and the ultracentrifuge patterns showed different distributions of the molecular species. To one of these mixtures was added sufficient antigen to convert that solution into a mixture corresponding in composition with the other solution which had been stored for 24 hours. Upon examination of the newly modified solution in the ultracentrifuge within 1 hour after the addition of the prescribed amount of antigen, a pattern similar to that of the older preparation was revealed. Thus readjustment to the new equilibrium concentrations occurred rapidly when the preexisting equilibria were disturbed by a change in the concentration of the antigen. Despite this demonstration of the rapidity of the reaction in at least the one direction,

no apparent disturbance of the equilibrium ensued during the separation of the complexes in the ultracentrifuge experiments. Singer and Campbell concluded, therefore, that the free antigen concentration, determined from the area of the most slowly sedimenting boundary, was a measure of the true equilibrium concentration of that component. They proposed, on the basis of a qualitative discussion of the separation process, that the absence of any additional refractive index gradients between the free antigen boundary and the boundary sedimenting just ahead of it was a satisfactory criterion of the absence of changes during the run. Further, they suggested as another criterion the constancy of the area of the antigen boundary during the experiment. After satisfying themselves that readjustment of the equilibria did not occur during the experiments, they proceeded with a detailed investigation of the nature of the antigen-antibody interaction.

Let us now return to systems in which the various equilibria are continuously maintained throughout the boundary despite the tendency of the different molecular species to become separated under the influence of the centrifugal field. If the complex, C, has a sedimentation rate which is appreciably different from the faster, B, of the two individual components ($A + B \rightleftharpoons C$), the readjustment may cause either depletion or enhancement of the concentration of A in the supernatant region of the ultracentrifuge cell. This occurs because there would be present behind a hypothetical boundary of the most rapidly migrating species (assume it is the complex, C) only components A and B. These two components would react immediately to form C, thereby re-establishing the equilibrium. The newly formed complex would then migrate with its characteristic sedimentation rate, and the equilibrium would again be disturbed only to be re-established by a repetition of the above process. Of course, this does not occur in discrete stages as outlined here; instead, there is a tendency toward separation along with a continuous readjustment. The net effect of the above is a continual depletion of A in the supernatant region as it associates with B to maintain the equilibrium concentration of C. Had the complex possessed a lower sedimentation rate than B, the differential migration of the different species would create a region containing A and C, and C would dissociate to form B and additional A. In this case, the supernatant concentration of A would be greater than the true equilibrium concentration of free A component. This reasoning leads to the conclusion that separate B and C boundaries would not be observed but only a compound boundary with a sedimentation rate intermediate between those of the two species. This type of problem confronted Longsworth and MacInnes (1942) in their electrophoretic investigation of the interaction between ovalbumin and ribonucleic acid. Also Smith and Briggs (1950) and Alberty and Marvin (1950) employed similar reasoning in their electrophoretic investi-

gation of the interaction between methyl orange and bovine serum albumin. The discussion which follows later in this section is directly analogous to the methods used by these workers except that the problem is discussed here in relation to the ultracentrifuge. This treatment specifically avoids consideration of the shapes of the boundaries and deals instead with constituent sedimentation coefficients. Gilbert and Jenkins (1956) are the only workers to consider this problem in terms of the shape of the boundaries. In a preliminary note, they have derived partial differential equations for each of the molecular species in an interacting system. These equations are the direct result of expressions for the conservation of mass, and they include terms in the continuity equation for the chemical production (and disappearance) of each of the species. Thus far the problem has been treated only for systems in which diffusion is ignored. Despite this limitation, this preliminary theoretical development shows promise in providing a means for interpreting these complicated interacting systems. The solutions of the partial differential equations illustrate four important points in the ultracentrifugal analysis of mixtures of rapidly interacting components. (*1*) The amount of slow component observed in a hypothetical ultracentrifuge pattern was only one-fourth of the true equilibrium concentration of that species. (*2*) Although two-thirds of component B was in the uncombined state, no boundary corresponding to that component was detectible. (*3*) Similarly, there was no boundary corresponding to the complex despite the presence in the mixture of appreciable quantities of the complex. (*4*) In place of the two separate faster boundaries, there was a broad boundary with an intermediate sedimentation rate; the breadth of this boundary suggested that two species were represented by the boundary. It should be noted that in the example selected by Gilbert and Jenkins the sedimentation coefficient of the complex was appreciably greater than that of the faster of the two individual components. Therefore, the disturbance of the equilibrium and the reequilibration caused a large depletion of the slower of the two individual components.

It is of interest now to examine the interaction of a protein, P, with a second component, A, which can be an anion, cation, or another molecule. Assume that a series of complexes are formed according to the following equilibria,

$$\begin{aligned} P + A &= PA \\ PA + A &= PA_2 \\ &\cdots\cdots\cdots\cdots \\ PA_{i-1} + A &= PA_i \\ &\cdots\cdots\cdots\cdots \\ PA_{n-1} + A &= PA_n \end{aligned} \tag{71}$$

According to Tiselius (1930), average sedimentation coefficients can be designated for either the protein or the second component despite the fact that both components exist in a variety of different molecular species. During a given period of time, an arbitrary protein molecule exists as free protein part of the time; as the complex, PA, for another fraction of time; as another complex, PA_2, for still another fraction of the total time; and so on, for the remainder of the time period. This given protein molecule would migrate in that time period a distance related to the sum of the products of the sedimentation coefficients of each molecular species times the fraction of the time during which the given molecule exists in that form. Alternatively, all of the molecules can be considered at some instant of time, and the average sedimentation rate of all the protein molecules would be the sum of the products of the sedimentation rates of the individual species times the fraction of the protein occurring in each form.

For the system described above

$$\bar{s}_P = \frac{[P]}{[P_0]} s_P + \frac{[PA]}{[P_0]} s_{PA} + \frac{[PA_2]}{[P_0]} s_{PA_2} + \cdots + \frac{[PA_n]}{[P_0]} s_{PA_n} \qquad (72)$$

where $\bar{s}_P$ is the constituent sedimentation coefficient of the protein, $[P]$, $[PA]$, $[PA_2]$, etc. are the concentrations, in moles per unit volume, of the species indicated, and $[P_0]$ is the total or constituent protein concentration representing all forms of that constituent according to the following expression

$$[P_0] = [P] + [PA] + [PA_2] + \cdots + [PA_n].$$

A similar expression can be written for $\bar{s}_A$, the constituent sedimentation coefficient of the A component, where

$$[A_0] = [A] + [PA] + 2[PA_2] + \cdots + n[PA_n].$$

In keeping with the notation employed earlier for the weight average sedimentation coefficient (see footnote on page 68), we can define the constituent sedimentation coefficient in terms of weight concentrations rather than molar concentrations. If this is done, the individual concentration terms must give the weight of the particular constituent as determined from the weight of the various complexes. Equation (72) would therefore take the form

$$\bar{s}_P = \frac{c_P}{\bar{c}_P} s_P + \frac{(M_P/M_{PA})c_{PA}}{\bar{c}_P} s_{PA} + \frac{(M_P/M_{PA_2})c_{PA_2}}{\bar{c}_P} s_{PA_2} + \cdots + \frac{(M_P/M_{PA_n})c_{PA_n}}{\bar{c}_P} s_{PA_n}. \qquad (72a)$$

This is, of course, identical to Eq. (72). Since the formulation of equilibrium reactions in terms of equilibrium constants customarily involves molar concentrations, we will use Eq. (72) rather than its equivalent, Eq. (72a), despite some slight inconsistency in nomenclature.

Justification for the use of Eqs. (72) and (72a) is provided by consideration of the continuity equations for each of the species involved in the various equilibria. These continuity equations must include terms which allow for the "chemical" production or disappearance of the species under consideration. In this respect, the continuity equations are more complicated than Eq. (5) or the analogous expression for polydisperse systems composed of independent components [for a discussion of a simple system involving interacting components and the effect of the interaction on the continuity equation, the reader should consult Gosting (1956); this problem was also discussed briefly by Williams *et al.* (1958)]. Four terms are required for the equilibria described by Eq. (71), if the net chemical production of a single species, such as PA_{i-1}, is to be included in the equations. These terms include the association of PA_{i-2} and A to give PA_{i-1}, and its reversal, as well as the appearance of PA_{i-1} by the dissociation of PA_i and, finally, the disappearance of PA_{i-1} by reaction with A to give PA_i. Different reaction velocity constants can be assigned to each of these reactions. If weight concentrations are desired, each continuity equation can be multiplied by the molecular weight of the species involved, such as $M_{PA_{i-1}}$ which can be written $[M_P + (i - 1)M_A]$. If the continuity equations for all of the individual molecular species are summed, it can be seen that the terms involving the various reaction velocity constants vanish. This is true even if the different species are not in equilibrium with the components from which they are made. This follows because the total mass of the various reactants and products remains constant. If each reaction is at equilibrium, the various terms cancel in pairs and each continuity equation (before summation) reduces to the form of Eq. (5). In either case the final equation has a form identical to the continuity equation for a single component showing that the mass as a whole behaves in the same manner as a pure component.

It is implicit in this discussion that all of the components are recorded optically in which case the weight average sedimentation coefficient of the entire mixture is determined. This can be related to the individual constituent sedimentation coefficients, $\bar{s}_P$ and $\bar{s}_A$. In certain cases, like that considered here involving the interaction of bovine plasma albumin and methyl orange, the optical systems can give both $\bar{s}_P$ and $\bar{s}_A$.

Equation (72) can be written

$$\bar{s}_P = \frac{1}{[P_0]} \sum_{i=0}^{n} [PA_i] s_{PA_i} \tag{72b}$$

The analogous expression for the A component becomes

$$\bar{s}_A = \frac{1}{[A_0]} \left\{ [A]\, s_A + \sum_{i=0}^{n} i[PA_i]\, s_{PA_i} \right\} \tag{73}$$

For purposes of discussion, we assume that $s_{PA_i} > s_{PA_{i-1}} > \cdots > s_P > s_A$. This will apply in general since the molecular weight of the complexes increases upon addition of the A component. It should be noted, however, that the addition of A to P may cause a configurational change in the protein sufficient to cause the complex, PA, to sediment more slowly than P, despite the increase in molecular weight. Alterations in the partial specific volume may also affect the sedimentation rate of the complex relative to the pure protein. Following Smith and Briggs (1950), we can assume

$$s_{PA_i} = s_P + im \tag{74}$$

where m represents the increment in sedimentation coefficient caused by the binding of a single ion. More terms may be needed in Eq. (74) to describe adequately the change in s caused by binding many units of A. At present, no data are available to furnish the basis for conclusions regarding the relative magnitudes of successive terms. Substitution of Eq. (74) into Eq. (72*b*) and simplification of the resulting equation with

$$\sum_{i=0}^{n} [PA_i] = [P_0]$$

and

$$\sum_{i=0}^{n} i[PA_i] = ([A_0] - [A])$$

leads directly to

$$\bar{s}_P = s_P + rm \tag{75}$$

where r is equal to the number of moles of bound A per mole of protein, $r = ([A_0] - [A])/[P_0]$.

Figure 40 shows the distribution of the various molecular species in the ultracentrifuge at the beginning of an experiment and at a time, t, after the rotor attains the desired speed. It is assumed here for purposes of classifying the various phases, α, β, and γ, that s_A is sufficiently large that a region, the α phase, containing only solvent is produced by the sedimentation of the A component. For small ions, of course, this may not occur, but the experiment could be conducted in a synthetic boundary cell thereby producing a complete boundary of the A component. Application of the moving boundary theory presented earlier along with the knowledge that there are no protein species in the β phase leads to the result

$$s^{\beta\gamma} = \bar{s}_P \tag{76}$$

The theory therefore shows that the observed $\beta\gamma$-boundary moves at a rate corresponding to the sedimentation rate of a hypothetical complex, PA_r, even though there may be in the solution a series of complexes of widely different composition. It should be stressed that we have assumed that the binding of each ion produced the same incremental change in the sedimentation rate of the protein. If no gross configurational change in the protein were to occur, this assumption would be valid and m would then be a measure of the fractional change in the molecular weight of the protein.

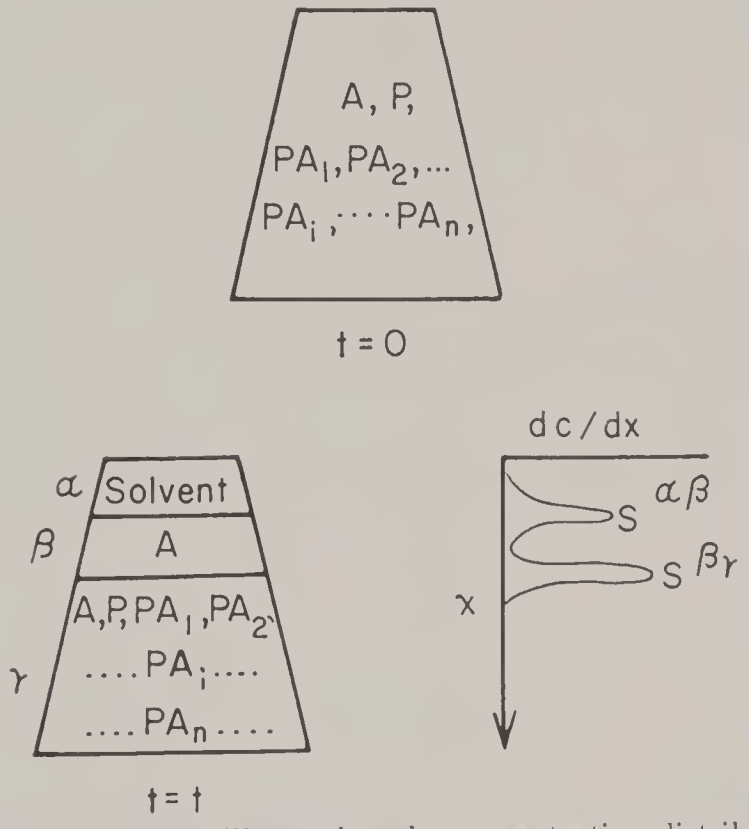

FIG. 40. Schematic diagram illustrating the concentration distribution and the boundaries observed in the ultracentrifugal analysis of a system of interacting components, P and A, which form the complexes, PA_i.

In electrophoresis, the validity of the analog of Eq. (75) has been demonstrated for the binding of methyl orange to bovine serum albumin (Smith and Briggs, 1950). Ultracentrifugal techniques now in common use do not have the precision necessary for a critical test of Eq. (75) and for the evaluation of the constant, m. In general, the term, m, in ultracentrifuge experiments is much smaller than the corresponding term affecting electrophoretic mobilities. However, with the development of a new differential technique (Richards and Schachman, 1957) for the measurement of small differences in sedimentation coefficients, the validity of Eq. (75) can be examined even though $(\bar{s}_P - s_P)$ may be only 0.01 s_P.

Some comment on the use of Eq. (76) is necessary. Often the A con-

stituent is either present in such low concentrations or its association with the protein is so small that it is justifiable to neglect the contribution of A to the refractive index gradient at the $\beta\gamma$-boundary. For such systems, Eq. (76) can be applied directly to the patterns produced by schlieren or interferometric optical methods. This equation can be employed as well to experiments with absorption optics if only the protein constituent absorbs the incident light. Thus Eq. (76) is likely to be useful in studies of the interaction of proteins with small molecules or ions. It is of interest to note that most ultracentrifuge studies of proteins, though not categorized as experiments on interacting systems, are actually of the type considered here since protein molecules interact reversibly (and, presumably, very rapidly) with the ions making up the buffer systems. Generally the small ions are in large excess and the concentration gradient of these ions at the protein boundary is small, so that it is tacitly assumed that the concentration of the electrolyte does not change across the protein boundary; hence the system is rarely considered as one involving association-dissociation equilibria.

If the complexes formed by the association reactions contain large amounts of the A component, the analysis of the ultracentrifuge patterns is more complicated because the refractive index gradient at the $\beta\gamma$-boundary is due, in part, to each constituent. In principle, moving boundary equations, like Eq. (76), can be written for each constituent in terms of the sedimentation rates and concentrations in the β- and γ-phases. These equations are statements of the conservation of mass, and it is implicit in their formulation that the boundary separating the two plateau regions is infinitely sharp. Even if a boundary is blurred due to diffusion, this treatment is valid for a single component since the position of the second moment of the real concentration gradient curve corresponds to the location of the equivalent, hypothetical infinitely sharp boundary. Although the concentrations of both the protein and the A constituents change across the $\beta\gamma$-boundary and separate moving boundary equations can be written for each, there is no evidence that the $\beta\gamma$-boundary written for the A constituent is identical to the $\beta\gamma$-boundary for the protein constituent. On the contrary, Gilbert and Jenkins (1956) have shown that the $\beta\gamma$-boundary is a complex one indicating, in the system they considered, the presence of two complexes. To be sure, their treatment considers the association of large molecules to form a complex which sediments at a rate substantially greater than the faster of the two individual constituents. This analysis is the only one available that is pertinent to the present discussion since it is based on the continuity equations for each of the three molecular species involved in the equilibrium with the added restriction that the relative concentrations are governed by the equilibrium constant for the reaction. For the system

considered here, the difference between $\bar{s}_P$ and s_P is likely to be very small, unlike that treated by Gilbert and Jenkins (1956); nonetheless there are risks involved in the use of both Eq. (76) and the analogous equation for the A constituent. Ideally, use should be made of an optical system which is sensitive to only one of the constituents (see the discussion following on the determination of $\bar{s}_A$ for materials which absorb light in the visible region of the spectrum). This would give $\bar{s}$ for one constituent. The weight average sedimentation coefficient for all of the material in the solution can generally be calculated from the schlieren or interference optical patterns since there is generally little difference among different constituents with regard to their refractive index increment. A combination of these two sedimentation coefficients in conjunction with the two constituent concentrations gives $\bar{s}$ for the second constituent. This is then employed in the equations presented later in this section dealing with the determination of the association constants and number of binding sites. In the discussion which follows it is assumed that means are available for the determination of $\bar{s}_P$. In many situations this information is derived directly from the movement of the $\beta\gamma$-boundary; in others the evaluation of $\bar{s}_P$ may be difficult or not feasible.

Although the determination of $\bar{s}_P$ is direct since the $\beta\gamma$-boundary furnishes a measure of $\bar{s}_P$, there is no corresponding boundary in the experiment illustrated in Fig. 40 which yields a value of $\bar{s}_A$. There are, however, different ways in which $\bar{s}_A$ can be measured precisely, and one or the other of these techniques should encompass all types of systems likely to be examined.

The first method involves the separation cell and requires a precise assay (chemical, physical, or biological) for the small component. The assay must be accurate, and it must be specific for the small component regardless of the form in which the component appears, i.e., free or as complexes with the protein. In order to obtain $\bar{s}_A$ with the separation cell, the sedimentation of the mixture must be confined to periods of time sufficiently short that the protein boundary does not reach the separating plate. Then all of the A component which disappears from the upper compartment migrates in the presence of the faster species, and therefore the measured sedimentation coefficient is $\bar{s}_A$. For accurate results, the experiment should be continued until the $\beta\gamma$-boundary has migrated almost to the barrier. This causes the maximum depletion of A in the upper compartment consistent with the restriction that measurements be made of the net transport of A in the presence of all other molecular species. Such experiments can also be performed in a conventional ultracentrifuge cell with the use of absorption optics if the small component has an absorption spectrum which permits it to be distinguished from the faster component. A wavelength

is selected at which the A component absorbs strongly and the protein is essentially transparent. If the absorption spectrum of the small molecule changes appreciably as a result of binding to the protein, then the wavelength at the isobestic point should be used for illuminating the cell. As before, the amount of A component between the meniscus and an arbitrary surface in the plateau region (containing *all* components) is subtracted from the amount of the A component present originally in the volume element. This gives directly the total amount of A component transported across this arbitrary surface and thus a value of $\bar{s}_A$. Such a calculation can be performed from ultracentrifuge patterns obtained at different times, and in effect this single experiment is equivalent to many experiments in a partition cell with the partition at different positions in each experiment.

A second method for determining $\bar{s}_A$ involves the formation of a boundary between a solution of the protein and a second solution containing the equilibrium mixture of P, A, and the various complexes. Such a boundary, formed by layering techniques, migrates at a rate corresponding to $\bar{s}_A$. Some of the problems inherent in this method are discussed in Section IV, 6. This was the procedure used by Brown *et al.* (1955) to measure the constituent sedimentation coefficient of corticotropin (the A component) in mixtures containing bovine serum albumin.

Finally, $\bar{s}_A$ can be calculated from measurements of the concentrations and sedimentation coefficients from experiments like that illustrated in Fig. 40. This involves the use of the equation for the conservation of mass for species A across the $\beta\gamma$-boundary.

$$s_A{}^{\beta} c_A{}^{\beta} - \bar{s}_A{}^{\gamma} \bar{c}_A{}^{\gamma} = (c_A{}^{\beta} - \bar{c}_A{}^{\gamma}) s^{\beta\gamma} \tag{77}$$

This equation can be rearranged to give

$$\bar{s}_A{}^{\gamma} = s_A{}^{\beta} \frac{c_A{}^{\beta}}{\bar{c}_A{}^{\gamma}} + \left(1 - \frac{c_A{}^{\beta}}{\bar{c}_A{}^{\gamma}}\right) s^{\beta\gamma} \tag{77a}$$

Absorption optical techniques are ideally suited for the implementation of Eq. (77a) since $c_A{}^{\beta}$ and $\bar{c}_A{}^{\gamma}$ can be measured directly along with the necessary sedimentation coefficients. With schlieren optics, the evaluation of $\bar{c}_A{}^{\gamma}$ is not as direct because the area of the $\beta\gamma$-boundary gives the value of $(\bar{c}_A{}^{\gamma} + \bar{c}_P{}^{\gamma} - c_A{}^{\beta})$; data from another experiment may be required for the determination of $\bar{c}_P{}^{\gamma}$. Equation (77a) illustrates clearly the effect of binding of a small ion to a protein on the constituent sedimentation coefficient of the small ion. Since $\bar{s}_P(s^{\beta\gamma})$ is about 10 times s_A, the binding of the small ion to the extent of 50% (i.e., $c_A{}^{\beta}/\bar{c}_A{}^{\gamma} = 0.5$) causes $\bar{s}_A$ to be about 5 times s_A. At the same time, $\bar{s}_P$ is almost equal to s_P. This is in marked contrast to the usual changes in the electrophoretic mobility of

the various components as a result of their interaction, since the mobilities of both the large and the small components may change about the same amount.

We now proceed to examine the equations for interactions of the type described by Eq. (71). For those equilibria, the various association constants can be written as

$$k_i = \frac{[PA_i]}{[PA_{i-1}][A]} \tag{78}$$

where the constant for the i^{th} ion can be written (Klotz, 1946)

$$k_i = \frac{n - (i-1)k}{i} \tag{79}$$

In Eq. (79), k is the intrinsic association constant for the binding of the A component to one of the sites on the protein molecule. Rearranging Eq. (78) so as to give the concentration of each of the complexes and combining these with Eq. (73) along with the substitution of Eq. (79) for the various k_i values gives

$$\bar{s}_A = \frac{1}{[A_0]}\left\{[A]s_A + [P]\sum_{i=1}^{n}\left[([A]k)^i \frac{n(n-1)\cdots(n-i+1)}{(i-1)!}\right]s_{PA_i}\right\} \tag{80}$$

In this form, Eq. (80) is not useful since the sedimentation coefficients of the different complexes are not known. The constituent sedimentation coefficient of the A component can be evaluated in another manner by combining Eqs. (73) and (74) to give

$$\bar{s}_A = \frac{1}{[A_0]}\left\{[A]s_A + s_P\sum_{i=0}^{n} i[PA_i] + m\sum_{i=0}^{n} i^2[PA_i]\right\} \tag{81}$$

For interactions of the type described by Eq. (71), it has been shown (Klotz, 1946; Klotz *et al.*, 1946) that

$$\frac{1}{r} = \frac{1}{nk[A]} + \frac{1}{n} \tag{82}$$

and Smith and Briggs (1950) have evaluated the last term in Eq. (81) as

$$\sum_{i=0}^{n} i^2[PA_i] = ([A_0] - [A])\left(1 + \frac{n-1}{n}r\right) \tag{83}$$

Substitution of Eq. (83) into Eq. (81) gives

$$\bar{s}_A = \frac{1}{[A_0]}\left\{[A]s_A + ([A_0] - [A])\left[s_P + \left(1 + \frac{n-1}{n}r\right)m\right]\right\} \tag{84}$$

or

$$\bar{s}_A = \frac{1}{[A_0]}\left\{[A]s_A + ([A_0] - [A])\left[\bar{s}_P + \frac{n-r}{n}m\right]\right\} \qquad (84a)$$

Equation (84) indicates that the A component can be considered as being transported in part in the form of free A component and in part as a single, hypothetical complex of composition $PA_{(1+r-(r/n))}$. This is despite the fact that the A component is actually in the form of a whole series of complexes of varying composition. The factor, m, which represents the increment of sedimentation coefficient of P caused by the binding of A, can be eliminated from Eq. (84) through the use of Eq. (75). This leads to the final general equation for determining the equilibrium concentration of free A component in the mixture.[7]

$$[A] = \frac{[A_0][\bar{s}_P - \bar{s}_A - \frac{1}{n}(\bar{s}_P - s_P)] + [P_0](\bar{s}_P - s_P)}{\bar{s}_P - s_A - \frac{1}{n}(\bar{s}_P - s_P)} \qquad (85)$$

If the interaction involves many binding sites, the terms containing $1/n$ in Eq. (85) may be negligible, especially since $(\bar{s}_P - s_P) < (\bar{s}_P - \bar{s}_A) < (\bar{s}_P - s_A)$. For this situation, Eq. (85) reduces to

$$[A] = [A_0]\frac{(\bar{s}_P - \bar{s}_A)}{(\bar{s}_P - s_A)} + [P_0]\frac{(\bar{s}_P - s_P)}{(\bar{s}_P - s_A)} \qquad (86)$$

Equation (86) can be simplified still further for those systems for which $\bar{s}_P = s_P$, and Eq. (87) is obtained.

$$[A] = [A_0]\frac{(\bar{s}_P - \bar{s}_A)}{(\bar{s}_P - s_A)} \qquad (87)$$

This, of course, follows directly from Eq. (73) if it is assumed that s_{PA_i} is equal to s_P. It is this equation which forms the basis for the studies of Velick on the interaction of DPN with various dehydrogenases. In order to use Eq. (85) for interacting systems, it is advisable first to calculate $[A]$ from Eqs. (86) or (87) for the different experimental conditions. With the values of $[A_0]$, $[P_0]$, and $[A]$, the corresponding r values are determined and the data plotted in accord with Eq. (82). From the appropriate plot, a value of n can be evaluated which can then be used in Eq. (85) for recal-

[7] Some aspects of the ultracentrifugal analysis of interacting systems of the type considered here have been discussed recently by Williams *et al.* (1958); it can be shown that extension of their theoretical treatment leads to the equation, Eq. (85), presented earlier by Richards and Schachman (1957).

culation of a more exact value of $[A]$ for each experiment. Final evaluation of n and the intrinsic association constant can then be made.

The theoretical discussions presented above take no cognizance of either the sector shape of the ultracentrifuge cell or the inhomogeneity of the centrifugal field. As a result of these factors, there is a dilution of the contents of the cell in the plateau region as sedimentation progresses. This, of course, produces complications because the protein and its complexes are diluted more rapidly with time than the free A component. Some readjustment of the equilibria must ensue. Until theoretical developments provide equations which account for this effect, constituent sedimentation coefficients for both P and A should be evaluated throughout each experiment, and the values obtained should be employed in extrapolation procedures to calculate $\bar{s}_A$ and $\bar{s}_P$ at the beginning of the experiment. These values correspond to known mixtures of the components, and the values of $[A]$ calculated in this manner should provide meaningful quantitative data for characterizing interacting systems. Since experiments can be performed readily at different temperatures, various thermodynamic parameters can be evaluated. It is worth noting that volume changes resulting from the interaction can be measured within certain limits through the examination of the effect of pressure on the various equilibria. If the protein constituents are sufficiently large, the centrifuge experiments can be conducted at different speeds. With the use of a synthetic boundary cell, the original boundaries can be formed at different places (and pressures) in the cell. Thus all the constituent sedimentation coefficients can be measured at different pressures, as desired, and the association constants and thermodynamic quantities determined as a function of pressure.

At present, the method presented here has not been applied to interacting systems which have been examined by other methods such as equilibrium dialysis. Preliminary experiments (Schachman, unpublished) with bovine serum albumin and methyl orange have shown the general applicability of the method, but a rigorous experimental test has not been concluded. Basic to a test of the method is an accurate determination of the term, $(\bar{s}_P - s_P)$, which may be so small that conventional ultracentrifugal methods may not suffice. A direct method for evaluating this quantity is presented in the next section.

10. A Differential Method for the Direct Measurement of Small Differences in Sedimentation Coefficients

Frequently, the sedimentation coefficient of a substance may change so little as a result of a specific treatment that the effect cannot be described quantitatively because of present limitations in experimental precision. Such changes may result from a variation in the buoyancy term caused

by the addition of a third component or from changes in molecular weight or shape caused by limited action of an enzyme or denaturing agent. Also alterations are to be expected in interacting systems of the type described in the previous section. With the recent adaptation of the Rayleigh and Jamin interferometers to the ultracentrifuge, it has become possible to devise a differential method whereby the sedimentation coefficients in two different solutions can be compared directly and the difference measured accurately. This method has been described briefly (Richards and Schachman, 1957), and its application thus far has been very limited. Nonetheless, the sensitivity of the method and its accuracy even at this early stage of development are sufficient to commend it for many experiments involving small changes in macromolecules.

The differential method involves a comparison, at conjugate levels in the cell, of the refractive indices of two solutions contained in separate compartments of a double sector ultracentrifuge cell (Fig. 4). In effect, the interferometer subtracts the optical pattern of the boundary in one-half of the cell from that in the other section of the cell. If both solutions are identical, despite the presence of boundaries, the Rayleigh pattern consists of a series of parallel, straight interference fringes. For the fringes to be straight even in the presence of concentration gradients stemming from the moving boundaries, the two boundaries must migrate and spread at the same rate. Under such circumstances, the refractive index difference at conjugate levels throughout the cell is constant, and the pattern is identical to that observed when water is placed in both halves of the cell. Of course, rotating the light source through 90° to the proper orientation for a schlieren optical system reveals a single boundary, although in fact the optical pattern originates independently from each half of the cell. When one boundary moves more rapidly than the other, the fringe pattern in the region of the boundaries is warped to produce curved fringes whose shape resembles the tracings produced by conventional schlieren optical systems. Depending upon which compartment contains the faster migrating species, the fringe pattern will possess a maximum or a minimum. Representative ultracentrifuge patterns with this technique are shown in Fig. 41 along with conventional schlieren diagrams of the boundaries at nearly corresponding times. Svensson (1949) obtained similar fringe patterns with the Rayleigh interferometer during examination of two identical diffusing boundaries which were slightly displaced from one another. This was done in his experiments in order to produce, by means of the interferometer, curves of concentration gradient versus distance. No use has been reported of the application of the interferometer in the measurement of differences in diffusion coefficients, such as are reported here for sedimentation. With the aid of transport equations, the difference in

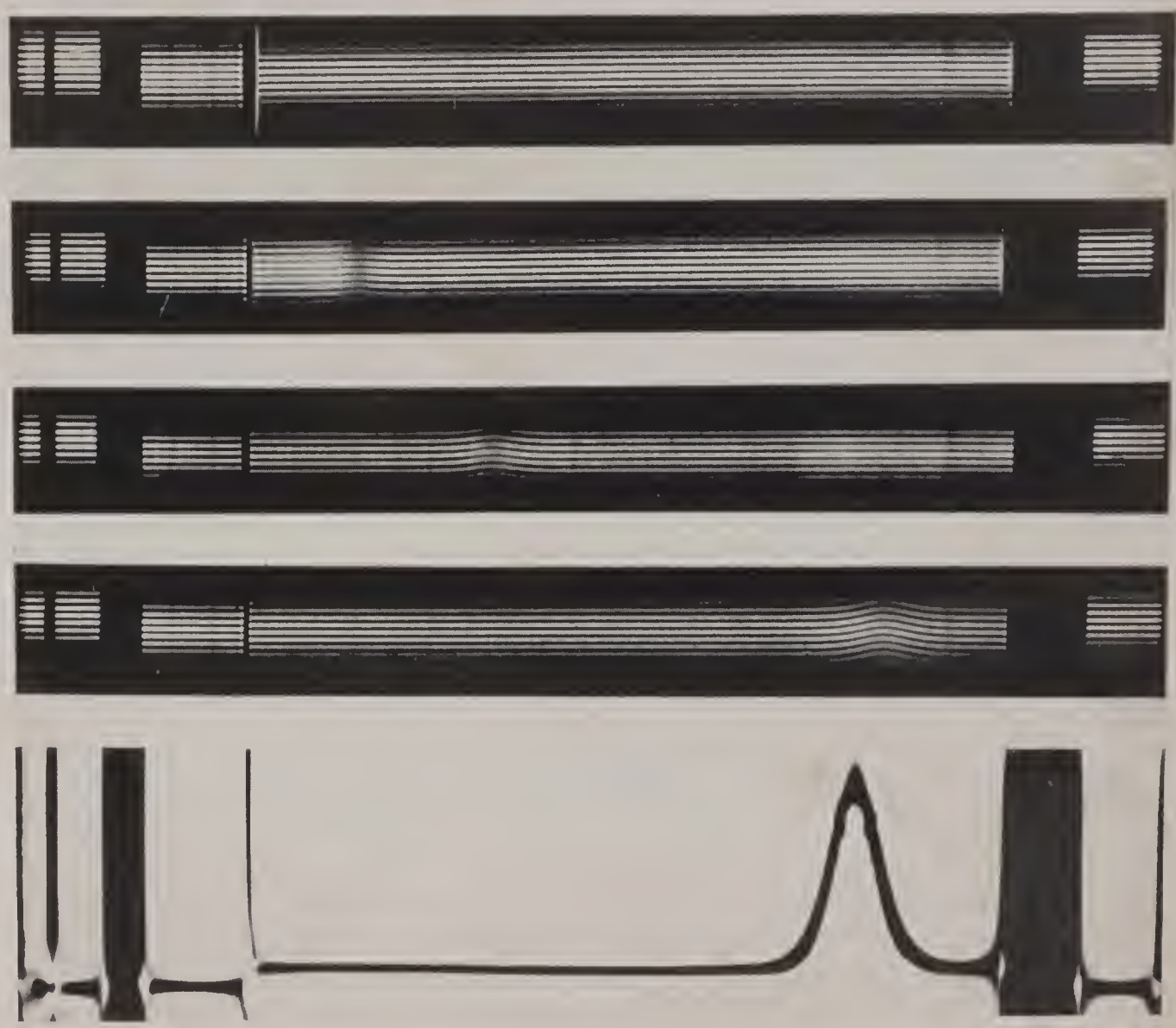

FIG. 41. Ultracentrifuge patterns illustrating a differential method for measuring small differences in sedimentation coefficients (from Richards and Schachman, unpublished). A solution of bushy stunt virus in buffer was placed in one sector of the double sector cell, and the other sector contained a small amount of D_2O in addition to the other constituents. The difference in sedimentation rate of the virus in the two solutions was 1%. Since the sedimentation rates in the two halves of the cell were so similar, the schlieren diagram showed only a single boundary, but the interferometric optical system showed the small difference very clearly. The concentration of bushy stunt virus in each compartment was 0.5 g./100 ml. The patterns from top to bottom correspond to 0 min., 65 min., 88 min., 148 min., and 144 min. The schlieren pattern was obtained with the schlieren diaphragm set at angle of 60°. In order to increase the resolution of the fringe pattern, the rotor was decelerated after the boundary had migrated from the meniscus and the speed was maintained at 5565 r.p.m. for 50 min. Then the rotor was accelerated to the operating speed of 14,290 r.p.m. at which speed it was maintained throughout the experiment. As the boundaries in the two halves of the cell traverse the cell, their separation increases with the result that the area of the Rayleigh pattern increases with time.

sedimentation coefficient can be expressed in terms of parameters directly measurable on the photographic plates. In effect, the area under the curved fringes is determined, and the increase of this area with time provides a direct measure of the difference in sedimentation rate. Actually, it is the rate of change with time of the first moment (about the center of rotation) of the curve defined by the fringes which gives the fractional difference in sedimentation rate, $\Delta s/s_{av}$, where Δs is the difference in sedimentation coefficients between the two migrating substances, and s_{av} is the mean sedimentation coefficient. This is shown as follows (Richards and Schachman, unpublished).

Equation (28) can be written for each of the two solutions which are designated by the subscripts, 1 and 2, the faster and slower moving components, respectively. Subtracting the second equation from the first gives

$$\int_{x_m}^{x_p} \Delta c x dx + \frac{1}{2} c_0(x_{m,1}^2 - x_{m,2}^2) = \frac{1}{2} c_0 x_p^2(e^{-2\omega^2 s_1 t} - e^{-2\omega^2 s_2 t}) \qquad (88)$$

where

$$\int_{x_m}^{x_p} \Delta c x dx$$

is used in place of

$$\int_{x_m}^{x_p} c_1 x dx - \int_{x_m}^{x_p} c_2 x dx$$

and Δc is the difference in concentration at any level, x. It should be noted that Δc is measured directly in the interferometer in terms of the number of fringes. Equation (88) contains terms, $x_{m,1}$ and $x_{m,2}$, corresponding to the menisci in the two compartments of the cell. With suitable precautions in filling the cell or by slight modification of the double sector cell, it is possible to fill the cell so that the menisci are at the same distance from the axis of rotation. If this is accomplished, the second term on the left in Eq. (88) is either equal to zero or small enough to apply the following approximations. With the substitutions,

$$x_{m,1}^2 - x_{m,2}^2 = 2x_{m,av}\Delta x_m \quad \text{and} \quad s_{av} = s_1 - \Delta s/2 = s_2 + \Delta s/2.$$

Eq. (88) can be rearranged to give

$$\int_{x_m}^{x_p} \Delta c x dx + c_0 x_{m,av}\Delta x_m = \frac{c_0 x_p^2}{2} e^{-2\omega^2 s_{av} t}(e^{\omega^2 \Delta s t} - e^{-\omega^2 \Delta s t}) \qquad (89)$$

The exponentials in the parentheses are sufficiently small that the terms can be expanded as a series retaining only the first three terms. Also

$e^{-2\omega^2 s_{av} t}$ can be written as $(x_{m,av}/x_{av})^2$ and $\omega^2 t$ as $(1/s_{av})$ ln $(x_{av}/x_{m,av})$. With these substitutions, Eq. (89) can be written

$$\int_{x_m}^{x_p} \Delta c x dx + c_0 x_{m,av} \Delta x_m = \frac{c_0 x_p^2 x_{m,av}^2}{x_{av}^2} \ln \frac{x_{av}}{x_{m,av}} (\Delta s/s_{av}) \qquad (90)$$

The value of $\Delta s/s_{av}$ is readily evaluated as the slope of the plot of

$$\int_{x_m}^{x_p} \Delta c x dx \text{ versus } \frac{c_0 x_p^2 x_{m,av}^2}{x_{av}^2} \ln \frac{x_{av}}{x_{m,av}}.$$

As a test of the method, small amounts of D_2O were added to different solutions of bushy stunt virus, each of which was compared with a control solution not containing D_2O. The reduction in sedimentation coefficient, $\Delta s/s$, was measured for each solution by the differential method described above, and the values were in excellent agreement with those determined by interpolation of data from conventional ultracentrifuge experiments at higher D_2O concentrations. Thus far, the efforts have been directed largely toward experimental aspects of the problem and attempts at improving the precision of the method by examination of known systems. From these studies, it appears that a change of 1% in sedimentation coefficient can be measured with an accuracy of about 4%. Preliminary experiments with interacting systems have shown that the method will be useful in the direct evaluation of $(\bar{s}_P - s_P)$, but presentation of results at this time would be premature.

11. The Effect of Pressure on Sedimentation

For most systems of interest in biochemistry, the neglect of corrections for pressure effects is justified despite the existence of pressures of about 250 atmospheres in ultracentrifuge cells operated at their maximum angular rotation. There are, however, an increasing number of cases for which consideration of pressure effects is mandatory. Moreover, the large gains in experimental precision in the past few years have reduced the experimental errors so much that corrections for pressure, though amounting to only a few percent in the sedimentation coefficient, are no longer of negligible consequence. Also nonaqueous systems are markedly affected by pressure with corrections amounting to 30% or more. Finally, there are special problems for which the pressure gradient in an ultracentrifuge cell can be exploited to produce information not readily obtained by other methods.

As Svedberg and Pedersen (1940) pointed out, the high pressures can alter the density and viscosity of the solvent as well as the partial specific volume of the solute. The former effects cause the macromolecules to sediment more slowly as the pressure is increased, whereas the latter, which is usually of a smaller magnitude, acts in the opposite sense. Data relating

the viscosity and density of various solvents to pressure are readily available, but similar data for the pressure dependence of the partial specific volumes of proteins, for example, are lacking. There are, however, ultracentrifuge experiments which can furnish valuable information on this point. In principle, the sedimentation velocity can be affected by pressure in still another manner; this is concerned with the change in shape or equivalent hydrodynamic volume (as measured by the frictional factor) resulting from the large pressure. Singer (1947a) considered the configurational changes in flexible macromolecules sedimenting in high centrifugal fields, although this treatment was concerned primarily with the stretching and orienting effect of the centrifugal field.

Mosimann and Signer (1944) were the first to direct attention specifically to the influence of hydrostatic pressure on the sedimentation coefficient with regard to their experiments on nitrocellulose in acetone. They formulated a correction similar to that proposed by Svedberg and Pedersen (1940) for the reduction of sedimentation coefficients to a standard basis (Eq. 26). It is, of course, clear that the correction proposed by Mosimann and Signer (1944) is inherent in Eq. (26). Nonetheless, according to these workers, we can write

$$s_1 = s_P \frac{\eta_P}{\eta_1} \frac{(1 - \bar{V}_1\rho_1)}{(1 - \bar{V}_P\rho_P)} \tag{91}$$

where the subscripts, 1 and P, refer to a pressure of 1 atmosphere and P atmospheres, respectively, and the various symbols refer to the terms defined earlier. A value of 1 atmosphere refers, of course, to the air-liquid interface, although it should be noted that the pressure there is actually slightly greater than one atmosphere. Equation (91) shows that the measured sedimentation coefficient varies during the experiment inasmuch as the boundary from which measurements are made migrates into regions of continually increasing pressure. Moreover, molecules near the bottom of the cell are migrating at rates slower than those in the vicinity of the meniscus because of the pressure gradient through the cell. As shown by Fujita (1956b), this leads to a concentration gradient in the region of the cell ahead of the boundary (i.e., there is no plateau region of uniform concentration), and the boundary then no longer follows the square rule in terms of the dilution of the contents of the cell as a function of distance from the axis of rotation.

From data in the International Critical Tables or Landolt-Bornstein, Mosimann and Signer (1944) evaluated the terms, η_P/η_1 and ρ_P/ρ_1. With the assumption that $\bar{V}_P = \bar{V}_1$, they calculated for the bottom of the cell the values, 1.284 and 1.024, for η_P/η_1 and $(1 - \bar{V}_1\rho_1)/(1 - \bar{V}_P\rho_P)$, respectively, for nitrocellulose in acetone. Thus the correction term changed

by 31.5% throughout the cell for their experimental conditions. They observed that the sedimentation coefficient decreased during the run, but correction of the values according to Eq. (91) raised the values so that the calculated value of s_1 in Eq. (91) actually increased slightly, as would be expected for materials having an appreciable dependence of s upon c. Oth and Desreux (1954) formulated the correction for pressure more explicitly by writing

$$\rho_P = \rho_1(1 + \beta P) \tag{92}$$

$$\eta_P = \eta_1(1 + \alpha P) \tag{93}$$

$$\bar{V}_P = \bar{V}_1(1 - \gamma P) \tag{94}$$

Combining these expressions with Eq. (91) leads to the equation of Oth and Desreux (1954)

$$s_P = s_1(1 - KP) + \cdots \tag{95}$$

where

$$K = \alpha + \frac{\bar{V}_1\rho_1(\beta - \gamma)}{1 - \bar{V}_1\rho_1} \tag{96}$$

Oth and Desreux incorporated this pressure relationship into Eq. (32), and with the use of the square rule (Eq. 13) they derived an equation containing terms for both the concentration and pressure changes during an experiment. Fujita (1956b) has shown, however, that the use of the square rule is unjustified for systems exhibiting a significant dependence of s upon pressure. Since the pressure gradient in a centrifugal field can be described by

$$\frac{dP}{dx} = \rho\omega^2 x \tag{97}$$

the pressure, P, can be written, combining Eqs. (92) and (97)

$$P = \frac{1}{\beta}\left[e^{\rho_1\omega^2(x^2 - x_m^2)/2} - 1\right] \tag{98}$$

In the integration of Eq. (97), it is assumed that the pressure at the meniscus is zero rather than 1 atmosphere. Generally, the compressibility is so small that ρ in Eq. (97) can be considered a constant and the pressure is then expressed as

$$P = \frac{\rho}{2}\omega^2(x^2 - x_m^2) \tag{99}$$

Combining Eqs. (95) and (99) gives

$$s_P = s_1\left[1 - \frac{K\rho\omega^2}{2}(x^2 - x_m{}^2)\right] \tag{100}$$

On the basis of Eq. (100), Oth and Desreux (1954) suggested that the experimental data be corrected for the effect of hydrostatic pressure either by extrapolating the data from one experiment to the meniscus or by extrapolating data at a fixed value of x but at different speeds to values of $\omega^2 = 0$. After the latter extrapolation, the appropriate correction for concentration can be made. According to these workers, the latter procedure is a more precise method for the determination of sedimentation coefficients at atmospheric pressure even though most of the data stems from experiments at much higher pressures. Fujita (1956b) arrived at a similar expression from a more rigorous treatment starting with the continuity equation. Diffusion was assumed to be zero; otherwise the mathematical complexities precluded even an approximate solution. For systems in which s depended only on pressure, Fujita (1956b) was able to obtain an approximate solution of the continuity equation, and it was this solution that led to the conclusions cited earlier that there was no plateau region and the square rule did not hold. This was also pointed out by Eriksson (1956), on the basis of a more mechanistic argument, and considered in terms of analysis of polydisperse systems. Although Fujita (1956b) also treated systems for which the sedimentation coefficient depends on both the pressure and the concentration, the mathematical difficulties were so great that the shape of the curve of concentration versus distance was not computed.

In these considerations, it was assumed that $\bar{V}$ was independent of pressure. Though the compressibility of the solute is likely to be less than that of the solvent, it is clear that some decrease in $\bar{V}$ with pressure must occur. In attempts to demonstrate this and to determine quantitatively the amount of the compressibility, Cheng and Schachman (1955b) investigated the sedimentation of polystyrene latex particles in mixtures of H_2O and D_2O. By appropriate arrangement of the density of the solvent, they observed in a single ultracentrifuge experiment both sedimentation near the meniscus and flotation near the cell bottom. Not only did the term, $(1 - \bar{V}\rho)$, change with pressure, but it actually possessed a different sign at the two pressures. From the known compressibility of water, it is easily shown that the particles themselves were compressed, and equations were presented from which the compressibility could be calculated from the sedimentation data. The compressibility calculated from the ultracentrifuge patterns was in good agreement with that obtained by more conventional methods. This determination involved measurements of sedimenta-

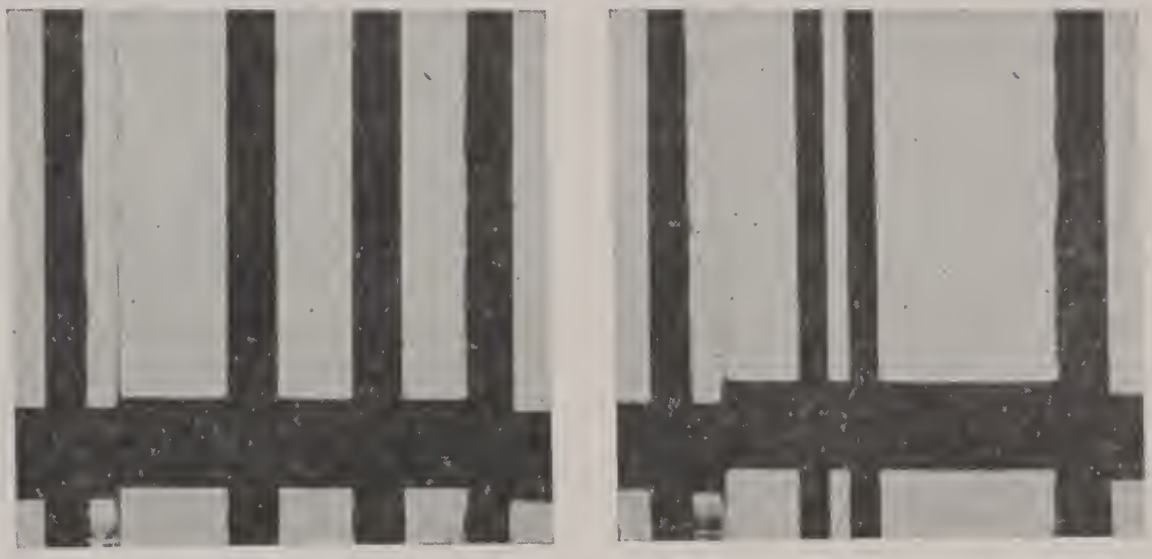

27,690 r.p.m. 44,770 r.p.m.

H_2O and 0.15% Ribonuelease

16,200 r.p.m.

FIG. 42. Ultraeentrifuge patterns illustrating a differential method for the measurement of the small difference in density between a solution of a protein and its solvent (from Stenesh *et al.*, unpublished). A double sector cell was modified so that the two channels communicate through a small groove engraved across the center dividing barrier. Each half of the cell is filled with a compressible fluid such as *o*-fluorotoluene or a silieone fluid, whieh had previously been saturated with the aqueous solutions. A microdrop, about 5λ, of solution is placed in one-half of the eell, and a corresponding drop of the solvent is added to the other. If the compressible fluid is selected carefully, the two drops will settle to the cell bottom while the ultraeentrifuge is at rest. Upon acceleration of the rotor, the continuous phase becomes much more compressed that the aqueous drops, and the latter rise accordingly to levels at whieh their density is equal to that of the surrounding fluid. From

tion coefficients at different pressures and corrections for the effect of pressure on the viscosity and density of the solvent followed by calculations of the change in density (or partial specific volume) of the solute. In principle, it amounts to a determination of all of the quantities in Eq. (91) except $\bar{V}_P$ which is then calculated.

Two other methods for determining the compressibility (or dependence of $\bar{V}$ on pressure) were discussed briefly by Cheng and Schachman (1955b). In consideration of the data of Lauffer *et al.* (1952) on the sedimentation of southern bean mosaic virus in concentrated sucrose solutions, it was stressed that the density of solution corresponding to zero sedimentation rate was apparently less than the density corresponding to zero flotation. Since the former measurements were made near the meniscus where the pressure is only slightly greater than 1 atmosphere, whereas the flotation measurements were made near the cell bottom at pressures of several hundred atmospheres, the difference in density implies that the virus particles themselves were compressed. Data permitting the calculation of the compressibility were not available, and as yet this method has not been pursued in attempts to determine whether meaningful data can be obtained by its application. Another method which was proposed, but not examined further, involves the determination of the equilibrium position of a solid (or solute) in a pressure gradient. This is analogous to the use of the density gradient column (Linderstrøm-Lang and Lanz, 1938) for the precise determination of densities. In practice, the density of the liquid is adjusted so as to be nearly equal to, but slightly less than, that of the solute, and the centrifuge is operated until the material collects as a concentrated zone somewhere in the cell. The position of the band of solute is determined at different speeds (pressures) and from the known compressibility of the solvent, the compressibility of the solute is determined. Had the experiments cited above with polystyrene latex particles been prolonged sufficiently, the particles would have been packed into a thin layer the position of which would be a function of the speed of the rotor. This tech-

knowledge of the compressibility of the various liquids or from previous calibration with drops of known density, the difference in density of the two drops is directly calculated for atmospheric pressure. The drops themselves are distorted in the density gradient, becoming more flattened and therefore appearing thinner in the optical system as the pressure gradient increases at the higher centrifugal field. The black bands in the figure corresponding to the position of the drops result from light being deviated by the drops to such an extent that the optical system does not record the light passing through the cell at the position of the drops. Upon raising the speed of the rotor, the pressure gradient is increased, and the drops reach equilibrium positions which are close together. Greater sensitivity is achieved at the lower fields. The upper figures at 27,690 and 44,770 r.p.m., respectively, were obtained with drops of 0.22% KCl and 0.38% KCl. The lower figure was obtained at 16,200 r.p.m. with drops of H_2O and 0.15% ribonuclease.

nique has now been exploited in a different manner (Stenesh *et al.*, unpublished). Rather than the method being used as a differential compressibility technique, its potential is being assessed as a differential density technique. Two different drops of liquid (a buffer and a dilute protein solution) are placed in separate compartments of a double sector ultracentrifuge cell which is filled with an immiscible liquid such as a silicone oil. The fluid is selected so that its density is slightly less than the two aqueous drops. As a consequence, the two drops rest on the bottom of the centrifuge cell while it is rotating at low speed. Upon acceleration of the rotor, a pressure is developed which causes both the drops and the silicone fluid to become compressed. Since the nonaqueous phase is more compressible, the drops rise in the cell to attain equilibrium positions at which their density is equal to that of the surrounding fluid. The drops are readily detected in the schlieren optical system, and patterns from such experiments are presented in Fig. 42. The difference in density between the two drops is readily evaluated from their position and knowledge of the speed and compressibility of the silicone fluid. With appropriate equations, this density difference is corrected for the pressures extant at the location of the microdrops, and the difference in density corresponding to atmospheric pressure is calculated. In this technique, it must be assumed that the compressibility of the protein solution and its buffer are the same; an assumption which appears admissible since the protein concentration is so low. Preliminary measurements with known drops showed that this technique is capable of accuracy to 1 part in 10^5; theoretical calculations suggest that the method has a potential far greater than that which has so far been achieved. With ribonuclease, measurements of $\bar{V}$ have yielded a value of 0.70 ml./g. in good agreement with values in the literature.

It is clear from the foregoing discussion that the effect of pressure, when manifested at all, is generally due to its impact on the viscosity of the solvent. However, with the growth in the number of investigations of systems in which the term, $(1 - \bar{V}\rho)$, approaches zero, the effect of pressure on both ρ and $\bar{V}$ becomes increasingly more important. With some lipoproteins the buoyancy term at atmospheric pressure is about -0.02, and variations in the sedimentation coefficient during an experiment may amount to 30% due to the compression of the solvent. Depending on the relative compressibilities of solute and solvent, the higher pressures will likely cause the sedimentation velocity to decrease during an experiment but cause the flotation velocity to increase.

V. The Transient States during the Approach to Sedimentation Equilibrium

In view of the long times required to attain sedimentation equilibrium throughout an ultracentrifuge cell filled with a solution of macromolecules of the size of many proteins, it is not surprising that considerable efforts have been directed toward theoretical analyses of the intermediate stages while the solute is being redistributed.

Some of this effort has been involved in estimates of the length of time required before an equilibrium state is achieved. The basis for this is the theoretical treatment of Mason and Weaver (1924) and Weaver (1926) dealing with sedimentation in a gravitational field rather than a centrifugal field. As a result of this work, which showed that the upper limit for the time required to attain equilibrium is equal to twice the time necessary for a solute molecule to sediment from the meniscus to the cell bottom, several expedients have been adopted. First of these is the use of incompletely filled cells containing shallow columns of solution. Svedberg and Pedersen (1940) showed, on the assumption that Weaver's solution applies as well to an inhomogeneous centrifugal field as it does for the homogeneous gravitational field, that the time required to attain equilibrium is proportional to the square of the column height of solution in the centrifuge cell.[8] Thus, reduction of the volume of solution placed in the cell effects a considerable saving in time despite, to be sure, some loss in resolving power. A second approach has involved the initial formation of a concentration gradient in the cell by means of a layering technique (Pasternak *et al.*, 1957). These workers have presented calculations indicating that time can be saved by an appropriate arrangement of both the concentrations and volumes of the two solutions employed in creating the original step distribution. Prior to this, Beams *et al.* (1955) have shown that sedimentation equilibrium was attained in their experiments much sooner than expected on the basis of Weaver's calculations. This was attributed both to the fact that the rotor speed was actually decreasing very slowly in their experiments and to the conclusions based on calculations of Archibald (unpublished) that an equilibrium condition once attained at some speed is not disturbed if the rate of decrease in speed is sufficiently small.

[8] The mathematical solution by Weaver (1926) has been subjected recently to further consideration by Van Holde and Baldwin (1958). Some of the conclusions from this latter study are presented in Section V,2.

A second, and perhaps the major, direction of research activity concerned with transient states resides in the evaluation of concentration functions in terms of both the position in the cell and the time after the initiation of the experiment. This has involved, for the most part, approximate solutions of the continuity equation (Eq. 5) and attempts at the derivation of equations from which numerical computations can be made readily.

Finally, consideration of transient states has led to the important suggestion of Archibald (1947b) that molecular weights can be determined from a knowledge of the concentration distribution (at any time) in the regions near the meniscus and bottom of the cell. So great has been the success and breadth of this method, termed the Archibald method, that a vast amount of data already has been accumulated by its application. It is rapidly becoming one of the most popular methods now available for the determination of molecular weights of both large and small molecules.

1. Molecular Weight Determinations by the Archibald Method

In all of Archibald's theoretical treatments (1938a, 1938b, 1942, 1947a) aimed at producing exact or approximate solutions of the continuity equation, he employed as a boundary condition the requirement that there be no net flow of solute through the surfaces at the meniscus or bottom of the cell. This applies at all times during an experiment. It was not until 1947, however, that Archibald himself (1947b) considered this boundary condition in more detail and recognized that its use permitted the direct determination of molecular weights in experiments of short duration. This latter paper by Archibald forms the basis for the now almost routine application of the ultracentrifuge in the determination of molecular weights. Not only is the method rapid and accurate, but it requires only small amounts of material, all of which can be recovered, and most important, it also provides valuable information about homogeneity.

This method is based on the use of Eq. (4), which expresses the net transport of solute per unit time across a surface at a distance, x, from the axis of rotation. As Archibald pointed out, the cell is closed; therefore the transport *across* the meniscus, x_m, and the bottom, x_b, of the cell must be zero, and Eq. (4) can be written for x_m and x_b

$$c_m s\omega^2 x_m = D(\partial c/\partial x)_m ; \qquad c_b s\omega^2 x_b = D(\partial c/\partial x)_b \tag{101}$$

or

$$(\partial c/\partial x)_m/x_m c_m = (\partial c/\partial x)_b/x_b c_b = \frac{\omega^2 s}{D} \tag{101a}$$

It should be noted that there can be depletion and accumulation at the meniscus and cell bottom, respectively. Equation (4) deals only with

the transport across a surface, and Eq. (101) shows, in fact, that the concentration at the two bounding surfaces changes continuously as $(\partial c/\partial x)$ changes. They both must vary, however, in such a manner that $(1/cx)(\partial c/\partial x)$ remains constant. This assumes that ω is maintained at a constant value. If the speed is changed, both c and $(\partial c/\partial x)$ will change; however $(1/\omega^2 xc)(\partial c/\partial x)$ will still remain constant. Often it is advantageous to alter the speed during an experiment. When the expressions for the meniscus and cell bottom are equated as in Eq. (101a), it is implied that the material is homogeneous; otherwise separate equations must be considered. In the latter instance this method gives $(\omega^2 s/D)_m$ and $(\omega^2 s/D)_b$, and the molecular weights calculated from these values would reveal the heterogeneity.

Different methods of applying Eq. (101) have been employed already, and it is likely that further modifications will be suggested as more workers exploit the Archibald method in the examination of different materials. Thus far the bulk of the work has utilized the schlieren optical system for the production of patterns of $(\partial c/\partial x)$ versus x; integration of the patterns has been necessary for the evaluation of the concentrations at the meniscus and cell bottom. With the adaptation of the Rayleigh and Jamin interferometers, it is likely that the concentration values will be determined by these techniques. It is a matter of conjecture, however, whether the interference patterns will be employed for the evaluation of the concentration gradient. Interference methods appear more precise than schlieren methods. But it has yet to be demonstrated, despite the recent work of Mommaerts and Aldrich (1957, 1958), that the interference patterns can be differentiated to give $\partial c/\partial x$ with an accuracy greater than that given directly by schlieren methods. In general, if a derivative curve is required, it is preferable to employ experimental methods which give it directly than to apply numerical differentiation to integral curves. No critical evidence was given by Mommaerts and Aldrich (1958) to demonstrate the validity of the differentiation procedure which they employed for the evaluation of $\partial c/\partial x$. Moreover, this work, which represents the first application of the Rayleigh interferometer for this type of problem, was not performed with a well characterized substance. In the author's laboratory (Richards and Schachman, unpublished), the Rayleigh interferometer is employed for the determination of the concentration terms in Eq. (101); and it is clear that high accuracy can be achieved by its use. Moreover, there is a large reduction in the time consumed for the computations. The concentration gradient terms are still evaluated from the schlieren patterns.

Representative ultracentrifuge patterns from an experiment utilizing the Archibald method for the determination of the molecular weight of ribonuclease are shown in Fig. 43. As discussed in Section II, the experi-

mental conditions were selected so that the concentration ratio, c_b/c_m, had equilibrium been attained, would have values from 2:1 to 5:1. There are, of course, no rigorous operational rules, and this "rule-of-thumb," though having much to recommend it in general, under special circumstances is inappropriate. Such exceptions include the study of very dilute

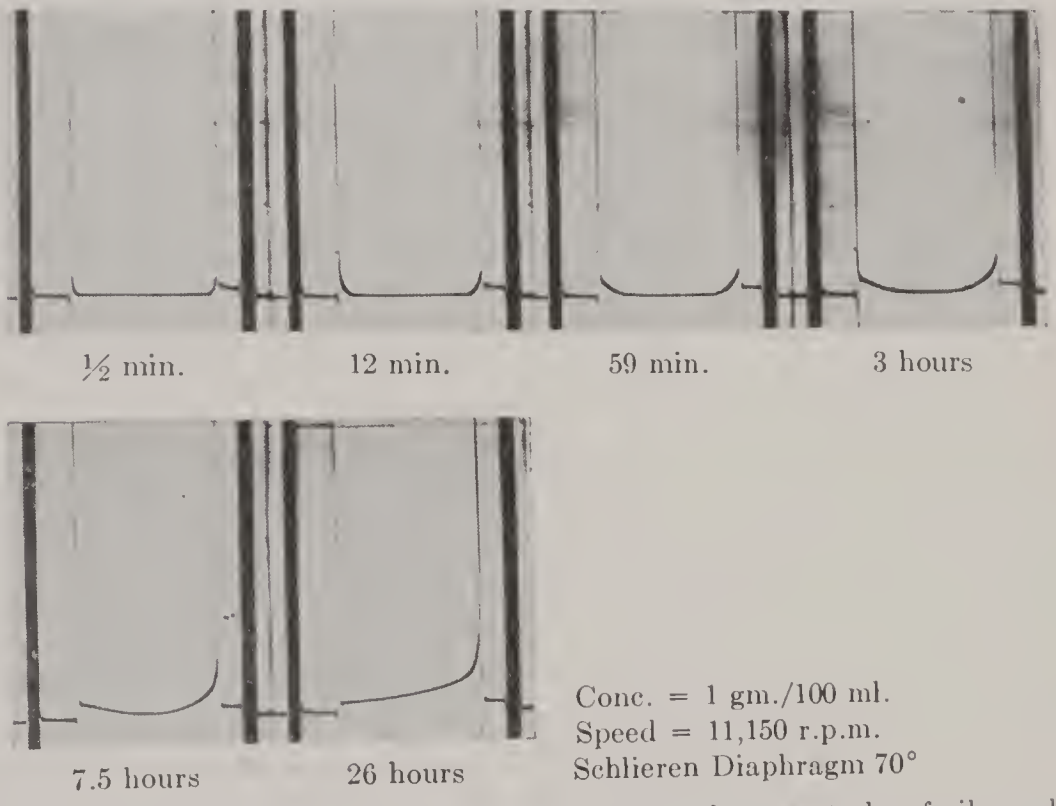

FIG. 43. Representative ultracentrifuge patterns from a study of ribonuclease during the approach to sedimentation equilibrium (from Ginsburg *et al.*, 1956). The centrifugal direction is toward the right. These are photographic prints of the original ultracentrifuge patterns. About 0.1 ml. of carbon tetrachloride was first placed in the cell to create a transparent bottom. Upon acceleration of the rotor, the interface between the aqueous and organic phases assumes the shape of an arc from the axis of rotation. Some interaction between the ribonuclease and carbon tetrachloride occurred after a long period, as is evident from the abrupt curvature near the bottom of the solution column in the pattern at 26 hours. Silicone fluids which are much more inert are presently used in the bottom of the cell.

solutions for which the concentration gradients are so small as to be immeasurable. By increasing the centrifugal field, Klainer and Kegeles (1956) were able to make accurate measurements of $(\partial c/\partial x)_b$ for solutions of ribonuclease at concentrations of only 0.025 g./100 ml. Also in studies of solutions containing aggregates of large molecular weight or impurities with larger molecular weight than the principal component, the higher centrifugal fields cause the preferential depletion of the faster migrating species from the region at the meniscus. Thus, reliable molecular weight

still can be determined despite the presence of aggregates in the original solution (von Hippel *et al.*, 1958). This constitutes a special virtue of the Archibald method which is all the more conspicuous when compared with determinations by light scattering.

The value of $(\partial c/\partial x)$ at the meniscus and bottom of the cell is determined readily from the patterns presented in Fig. 43. Actually the vertical displacement of the gradient curve above the base line is proportional to the concentration gradient, to the optical constants of the ultracentrifuge (cell thickness, optical lever arm, orientation of the schlieren diaphragm, and magnification of the cylindrical lens), and to the specific refractive increment of the solute. Also the concentration gradient is directly related to the concentration of the sedimenting material. Though these parameters are determinable from independent measurements, Klainer and Kegeles (1955) introduced the practice, now widely adopted, of the use of a synthetic boundary cell as a refractometer. With this cell, the solvent (dialysate) is layered onto an aliquot of the solution under investigation, and the area of the resulting boundary is, at once, a direct measure of all of the necessary optical parameters and the initial concentration. Thus $(\partial c/\partial x)$ is recorded in centimeters on the plate. Measurements of the concentration gradient at the bottom of the cell have frequently not been attempted. Brown *et al.* (1954) noted that some of the deviated light near the bottom of the cell was intercepted by the lower disc holder of the ultracentrifuge cell; therefore, a small region of the gradient curve corresponding to the cell bottom was not recorded. Klainer and Kegeles (1955) observed, in addition, a foreshortening of the cell because the optical system, as customarily aligned at that time to allow for maximum gradients, did not direct the light perpendicular to the cell windows. Even when the position of the light source is carefully located now to coincide with the optic axis, some of the light may be interrupted because of difficulties in placing the source at the focal plane of the lower collimating lens and the consequent lack of parallelism of the light traversing the cell. Both of these groups of workers employed a laborious extrapolation procedure to obtain the gradient curve at the bottom of the cell. Not only is the cell bottom difficult to locate, but it also has a shape which leads to other serious difficulties (Ginsburg *et al.*, 1956). The bottoms of the ultracentrifuge cells now in use either have a curvature based upon an arc drawn from the center of the cell or are completely flat. Newer ultracentrifuge cells are apparently free of this difficulty having a bottom representing an arc from the center of the rotor. If the cell bottom does not have the shape of a true sector from the axis of rotation, the molecules sedimenting along radii from the center of rotation strike the cell bottom at the sides of the cell sooner (or later) than others strike the bottom at some distance from the

radial walls of the centerpiece. This would produce, across the cell (at a constant distance from the axis of rotation), a concentration gradient which would, of course, be gravitationally unstable. Convective stirring must occur, and the observed curve of concentration gradient versus distance is thereby distorted from the ideal curve. To circumvent these difficulties a small amount (0.1 ml.) of a dense, water-insoluble, transparent liquid is first introduced into the cell, after which the sample is added. Under the influence of the centrifugal field, the denser liquid settles to the bottom, and the interface between the two liquids assumes the shape of an arc drawn from the center of rotation. This addition of an immiscible liquid (Ginsburg *et al.*, 1956) has the effect of creating in existing cells a bottom of the required shape and with a transparency which facilitates the detection of aggregated material in the solution. When such material is present in the sample, the sharp interface between the aqueous and nonaqueous liquids thickens with time due to the accumulation of sedimented material (Cohen and Schachman, 1957). Dow-Corning No. 555 silicone fluid seems to fulfill the requirements of density, nonmiscibility with water, and inertness toward proteins and is currently being employed widely. An alternative inert liquid of higher density, Kel-F Polymer Oil No. 1, has also been employed (Van Holde and Baldwin, 1958).

The evaluation of c_m and c_b from patterns like those shown in Fig. 43 requires extensive computations, and different procedures have been recommended. If a plateau region exists in the cell, Eq. (31) can be used in conjunction with Eqs. (30) and (8*a*) to give

$$c_m = c_0 - \frac{1}{x_m^2} \int_{x_m}^{x_p} x^2 \frac{\partial c}{\partial x}\, dx \tag{102}$$

An equation similar to Eq. (31) can be derived by considering the mass contained between x_p and x_b. In an analogous manner, this can be rearranged by combination with Eq. (31) and the knowledge that

$$c_b = c_p + \int_{x_p}^{x_b} (\partial c/\partial x)\, dx$$

to give

$$c_b = c_0 + \frac{1}{x_b^2} \int_{x_p}^{x_b} x^2 \frac{\partial c}{\partial x}\, dx \tag{103}$$

These equations were first formulated by Klainer and Kegeles (1955) in their use of the Archibald method for experiments in which the plateau region persists throughout the experiment. After a certain period of operation of the ultracentrifuge, the plateau region is lost, and Eqs. (102)

and (103) are no longer applicable. Evaluation of c_m is then more laborious involving

$$c_m = c_0 + \frac{1}{(x_b^2 - x_m^2)}\left[\int_{x_m}^{x_b} x^2 \frac{\partial c}{\partial x}\, dx - x_b^2 \int_{x_m}^{x_b} \frac{\partial c}{\partial x}\, dx\right] \qquad (104)$$

Equation (104) is the direct result (with a few minor rearrangements) of the statement that the total contents of the cell are independent of time, which can be written

$$\frac{1}{2} qc_0(x_b^2 - x_m^2) = \int_{x_m}^{x_b} qcx\, dx \qquad (105)$$

Certain basic differences in the derivation of Eq. (104) (Ginsburg *et al.*, 1956; Smith *et al.*, 1956) as compared with Eqs. (102) and (103) are noteworthy. In the former, the statement of the conservation of mass includes the entire cell, and therefore transport of material across an arbitrary surface (with its accompanying sedimentation coefficient) is not included. Nor can it be included because, with the disappearance of the plateau region, it is necessary to include in the transport equations a diffusion term as well as the sedimentation term. Equations (102) and (103), however, involve only a part of the cell, and the expression for the conservation of mass must therefore include terms for the sedimentation of material from or into the specified regions. They have their counterpart in the transport Eqs. (28) and (31). Actually Eq. (102) was obtained by Baldwin (1953b) in his treatment of the transport equations for the measurement of sedimentation coefficients of small molecules. Kegeles *et al.* (1957) have derived Eqs. (102) and (103) in another way. Starting with the continuity equation and the transport equation, they obtained the same result without invoking any expressions which are based on the assumption that the sedimentation coefficient is independent of concentration. More recently these same equations were shown (Kegeles and Rao, 1958) to apply to chemically reacting systems in which associating and dissociating reactions occur. This latter point is particularly interesting because it is essential to the application of the Archibald method to interacting systems. For such systems the composition (with regard to the relative amount of monomer and polymer) changes at the two ends of the cell because of the change in the total concentration and the consequent readjustment of the equilibria. Despite this, Eqs. (102) and (103) give the total concentration of solute at the corresponding surfaces.

Equations (102), (103), and (104) furnish the basis for the determination of c_m and c_b, which are then employed in Eq. (101). If a layering technique is used in a separate experiment, the c_0 term (in optical units) is evaluated directly. Alternatively, this can be determined, with much more labor,

from the specific refractive increment, the concentration, and the various optical constants of the ultracentrifuge. The various integrals represented by the above equation are evaluated by numerical integration. If the experiments are conducted at speeds appropriate for sedimentation equilibrium studies, c_m and c_b early in the experiments will be very close to c_0, and the errors in the determination of s/D are attributable principally to $(\partial c/\partial x)_m$ and $(\partial c/\partial x)_b$. According to this procedure, there are no restrictions imposed on the experiment with the synthetic boundary cell except that the measurements of the area be made early and at low speed so that sectorial dilution is avoided. Ehrenberg (1957) has employed a slightly different procedure in order to reduce the labor of the summations required in the above equations. This has necessitated a duplicate experiment in the synthetic boundary cell so that the plateau region in the so-called "area run" suffers the same dilution as in the equilibrium experiment. Mechanical integration of Eqs. (102) and (103) was employed by Smith *et al.* (1956) in preference to arithmetic integration. Charlwood (1957) discussed still another method for evaluating c_m through the correction of c_0 according to Eq. (8*a*). This requires a knowledge of the sedimentation coefficient. Other aspects of this computation are considered by Charlwood (1957). It is clear that the summations in many experiments are small compared to c_0 (if the experiments are at low speed and the length of the experiment is short), in which case c_m can be calculated from Eq. (30) with the assumption that $c_p = c_0$. As indicated earlier, c_m and c_b can be determined readily by application of the Rayleigh interference optical system. No integration is necessary. Dilution in the plateau region is followed readily by observing the lateral movement of the fringes with time across the pattern (this is done in the region of the pattern where the fringes are straight). This gives c_p in relation to c_0. The latter is determined (as in the schlieren method) by an independent experiment with a synthetic boundary cell. Here, too, the interferometric method has the advantage because the fringes are counted; no integration is required. After c_p is determined, c_m and c_b are evaluated from a count of the number of fringes crossed in moving from the plateau region to the corresponding surfaces.

The Archibald method has already been employed with small molecules such as raffinose (Klainer and Kegeles, 1955) and glycyl-L-leucine (Wade *et al.*, 1956) and with proteins like ribonuclease (Klainer and Kegeles, 1956; Ginsburg *et al.*, 1956), lysozyme (Smith *et al.*, 1956), cytochrome, and apomyoglobin (Ehrenberg, 1957), lactoglobulin (Ginsburg *et al.*, 1956), bovine serum albumin (Klainer and Kegeles, 1955; Ehrenberg, 1957), alcohol dehydrogenase, and the old yellow enzyme (Ehrenberg, 1957). Also the method has been applied to apurinic acid (Smith *et al.*, 1956) and ribonucleic acid (Cohen and Schachman, 1957). Even earlier, it found appli-

cation with hormones (Li *et al.*, 1951) with bacitracin (Porath, 1952) and digitonin (Brown *et al.*, 1954). As seen in Table VII, which includes results from two different laboratories, the internal precision is very high; moreover, the results are in excellent agreement with the known molecular weight of ribonuclease, 13,683. For these calculations, the Svedberg equation, $M = RTs/D(1 - \bar{V}\rho)$, was employed (see Section VII for a dis-

TABLE VII

Molecular Weight of Ribonuclease

Concentration (g./100 ml.)	Speed (r.p.m. $\times 10^{-3}$)	Time of picture (min.)	M_m[c]	M_b[c]
0.94[a]	11.15	16	13,300	13,200
		24	13,500	13,400
		48	13,400	13,600
		64	13,400	13,700
0.532[b]	20.20	16	13,400	13,300
		32	13,100	13,300
		48	13,600	13,600
		64	13,200	13,600
0.5[a]	19.93	12		13,100
		24		13,300
0.28[b]	35.60	16	13,600	13,500
		32	13,200	13,100
		48	13,400	13,200
		64		13,300

[a] Values from Ginsburg *et al.* (1956).

[b] Values from Klainer and Kegeles (1956).

[c] These values are revised from those presented in the papers cited. The earlier calculations were based on the value, 0.709 ml./g. (Rothen, 1940), for the partial specific volume. The revision involves the value, 0.695 ml./g. (Harrington and Schellman, 1956).

cussion of this equation); with the use of this relationship, Eq. (101) can be written

$$M_m = \frac{RT}{(1 - \bar{V}\rho)\omega^2} \frac{(\partial c/\partial x)_m}{x_m c_m} \tag{106}$$

and

$$M_b = \frac{RT}{(1 - \bar{V}\rho)\omega^2} \frac{(\partial c/\partial x)_b}{x_b c_b} \tag{106a}$$

If the substance under investigation is homogeneous, $M_m = M_b$ and these

equations can be combined (Schumaker, V., private communication cited and used by Ginsburg *et al.*, 1956) to give

$$M = \frac{RT}{(1 - \bar{V}\rho)\omega^2} \frac{\frac{1}{x_b}\left(\frac{\partial c}{\partial x}\right)_b - \frac{1}{x_m}\left(\frac{\partial c}{\partial x}\right)_m}{\int_{x_m}^{x_b} \frac{\partial c}{\partial x}\, dx} \tag{107}$$

This equation gives accurate results when employed for ultracentrifuge patterns observed after relatively long periods of sedimentation; at such times $(\partial c/\partial x)_b \gg (\partial c/\partial x)_m$. Actually, $(\partial c/\partial x)_m$ has its maximum value as soon as the rotor attains the preselected speed, and the value of the concentration gradient decreases progressively, approaching the value which is obtained when the entire contents of the cell are at equilibrium. The value, $(\partial c/\partial x)_b$, behaves in just the opposite fashion, having its minimum value at zero time and increasing steadily until the equilibrium state is attained. As a consequence, Eq. (107) is not useful for data early in the experiment. For times of 1290, 2690, and 3830 minutes after the desired speed was attained, Ginsburg *et al.* (1956) calculated (with Eq. 107) the values 13,200, 13,300, and 13,200 for the molecular weight of ribonuclease, in good agreement with the results presented in Table VII. It should be noted that this method of handling the data avoids specifically the requirement for a value of c_0 ; moreover, the calculations are reduced to a minimum.

Limitations in experimental precision in the determination of molecular weights reside principally in the measurement of $(\partial c/\partial x)$ at the meniscus and cell bottom. Bizarre interference patterns exist at the juncture of the gradient curve due to the solution and the infinite gradient at the air-solution and lower liquid interfaces; as a result, early in the experiments some uncertainty exists in the precise measurement of the concentration gradients at the interfaces. Resort is usually made to an extrapolation procedure involving data in the region of the two surfaces, but no adequate theory is available as a guide to this extrapolation. The exact location of the meniscus at low speeds introduces some doubts in the extrapolation (Cheng, 1957). Most of this difficulty can be attributed to inadequate location of the light source,[9] but leaning of the meniscus at very low speeds

[9] The location of the meniscus on the photographic plate has been the subject of a recent, detailed analysis (Trautman, 1958). As a result of this thorough treatment, substantial improvements have been made in the procedure employed for the alignment of the optical system. Consequently the image corresponding to the meniscus is now better defined and some of the difficulties in the extrapolation procedure are eliminated. Despite this, there is still a problem of evaluating $\partial c/\partial x$ near the meniscus. Some subjectivity is involved in reading the plates, and different workers may obtain slightly different results from the same ultracentrifuge patterns.

must also be considered. As the run progresses, the gradient curves become less steep at the top and bottom of the cell, and there is a consequent increase in accuracy. Ehrenberg (1957) recommended operation at comparatively high centrifugal fields so that a complete boundary is almost formed. In such a case, measurement of $(\partial c/\partial x)_m$ is facilitated because the refractive index gradient curves become almost horizontal at the meniscus. This procedure imposes more rigorous demands on the precision with which both c_0 and the integral in Eq. (102) are determined since the integral approaches the value of c_0, thereby causing the denominator in Eq. (106)

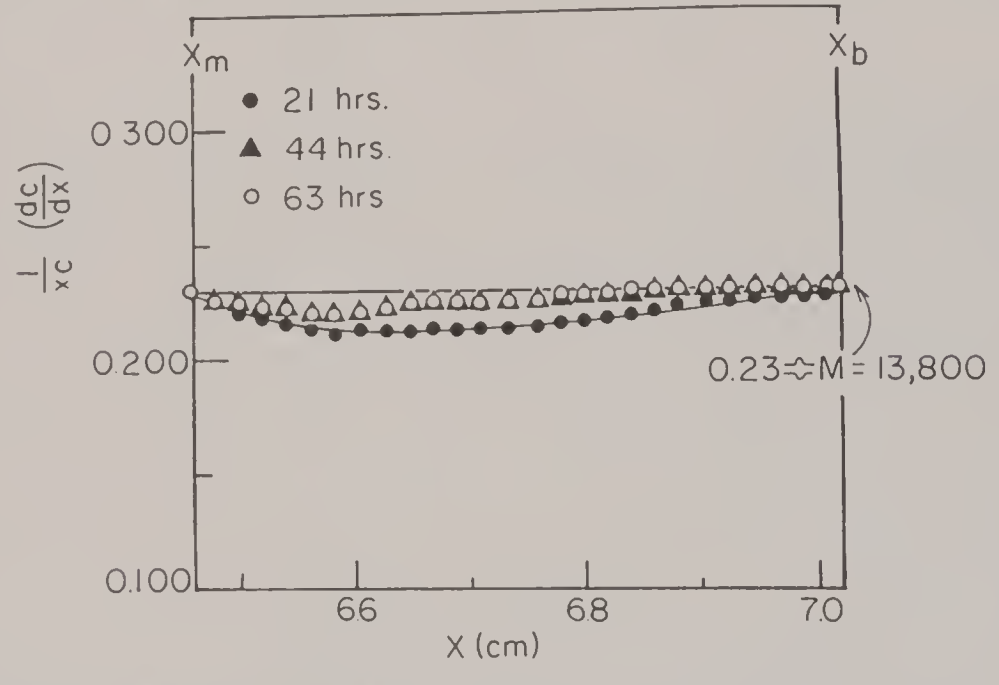

FIG. 44. Archibald plot for data obtained from an ultracentrifugal study of ribonuclease (from Ginsburg *et al.*, 1956). Equilibrium had almost been obtained throughout the cell as indicated by the fact that $(1/cx)(dc/dx)$ versus x was essentially a horizontal straight line.

to approach zero. Also this procedure precludes the use of data from the bottom of the cell, since the refractive index gradients become so great that the optical system cannot record them; the deviated light is intercepted either by the disc holder in the cell or by one or another of the lens mounts in the optical system. This deviated light, as a result, does not even strike the photographic plate. At lower speeds the gradients are not so great and this difficulty is not experienced. In the author's opinion, considerable accuracy is obtained by using all of the data from experiments at relatively low speed and calculating the results in the manner suggested by Archibald (1947b), i.e., a plot of $(1/xc)(\partial c/\partial x)$ versus x. Figure 44 shows such plots for an experiment with ribonuclease, and it is clear that the intercepts, at x_m and x_b, are determined with high precision. This involves, to be sure, long experiments and tedious calculations, but the latter

will no doubt be reduced substantially with the use of interferometric optics.

In the analysis of polydisperse systems also, the Archibald method exhibits great appeal not only through its providing average molecular weights but also because of the insight it provides about the homogeneity or heterogeneity of the system. Equations (106) and (106*a*) can be written for each of the species in the solution, and the equations rearranged to give $M_i c_i$. Summing the independent equations and dividing by $\sum_i c_i$ (which is equal to c^{obs}) gives the weight-average molecular weight

$$M_w = \frac{RT}{(1 - \bar{V}\rho)\omega^2} \frac{(\partial c/\partial x)_m^{\text{obs}}}{x_m c_m^{\text{obs}}} \tag{108}$$

An analogous equation exists for the bottom of the cell. As Archibald (1947b) pointed out, M_w at both the meniscus and bottom of the cell is a function of time, representing the weight-average molecular weight at the specific instant. Since the larger molecules preferentially concentrate toward the cell bottom during an experiment, M_w tends to increase there as the composition changes. Similarly, the depletion of the larger molecular species at the meniscus leads to a decrease there in M_w with time. To obtain the weight-average molecular weight of the initial solution (before redistribution occurs), the data are used to calculate M_w at the meniscus and cell bottom, and these are extrapolated to provide a value corresponding to zero time. This procedure was employed by Ginsburg *et al.* (1956) with known mixtures of lactoglobulin and ribonuclease. The weight-average values determined by the Archibald method were in excellent agreement with those calculated from the known composition and values for the individual proteins. It is noteworthy that a trend is not apparent during the early part of the experiments, although the values at the cell bottom were generally higher than those at the meniscus. An average can be evaluated. With mixtures of sucrose and ribonuclease, Ginsburg *et al.* also obtained a weight-average value which was in excellent agreement with that calculated. Here the trend was easily discernible. Furthermore, with the use of Eq. (107) as well as Eqs. (106) and (106a), it is possible to determine not only accurate weight-average molecular weights but also approximate values for each of the two components and their relative composition in the mixture. By suitable variations in the speed of the rotor at different stages in the experiment, this may provide valuable information in the examination of unknown mixtures. For such polydisperse systems, Trautman (1956) recommended a plot which is, in effect, the concentration gradient (at the meniscus and/or the bottom of the cell) as a function of the integrals in Eqs. (102) and (103). Knowledge of the initial concentration, as he showed, provides an additional point facilitating the construc-

tion of the best fitting curve through the data. Homogeneous materials give a straight line (actually two lines if both regions of the cell are included), the slope of which gives s/D or the molecular weight, and heterogeneous materials exhibit a curvature from which the weight-average molecular weight can be evaluated, and estimates of the composition also can be made. This method has the advantage that data from different speeds can also be incorporated directly into the plots. It should be noted, of course, that the Archibald method gives a weight average value of (s/D) and, therefore, of $[M(1 - \bar{V}\rho)]$, so that variation in $\bar{V}$ among the different components, as well as the heterogeneity in molecular weight, is reflected in the measurement.

Interacting systems also can be examined by the Archibald method. The theoretical aspects of this problem have been considered by Kegeles and Rao (1958). These workers also studied the association-dissociation equilibria of chymotrypsin (Rao and Kegeles, 1958). From a plot of the weight average molecular weight versus concentration they obtained 2.3×10^4 for the value at infinite dilution. This corresponds to the monomer value and is in good agreement with the results given by other techniques. At high concentrations the observed molecular weights were substantially greater than 4.6×10^4, indicating the presence in the solution of trimers or even higher aggregates. In many of the experiments the time and speed of centrifugation were sufficiently low so that c_m and c_b did not differ much from the original concentration. After prolonged sedimentation, however, the concentrations at the top and bottom of the cell are substantially altered. Readjustment in the equilibria should occur, therefore. Rao and Kegeles (1958) found that the molecular weights at the meniscus and cell bottom did vary with time, more or less in the manner expected. There was some evidence, however, that the rates of the association and dissociation reactions were not sufficiently large that equilibrium was maintained throughout the cell. At the meniscus the molecular weight fell as the concentration was lowered due to sedimentation. But the calculated molecular weights seemed to be less than those expected for an equilibrium mixture at the appropriate concentration. It was as if the polymers migrated from the meniscus at a faster rate than other polymers could be formed by the association of the remaining monomers. In a similar manner, the higher polymers accumulated at the cell bottom more rapidly than they could dissociate to maintain the equilibrium mixture. Under the appropriate experimental conditions there was no difficulty in obtaining reliable data which Rao and Kegeles interpreted in terms of equilibria involving monomers, dimers, and trimers.

Archibald, in his very important paper (1947b), also considered other methods of handling the data from experiments during the approach to

sedimentation equilibrium. These methods involve the determination of $\partial c/\partial t$ which can be evaluated numerically. From these values, the integral,

$$\int_{x_1}^{x_2} x \frac{\partial c}{\partial t}\, dx,$$

for a given time is calculated. As a check on the computations, the boundary conditions at x_m and x_b are inserted, for which the integral must then be zero. This follows because the total contents of the cell remain constant; the decrease in concentration in the upper part of the cell is compensated for in the lower part of the cell by an increase in concentration. Besides the boundary surfaces, there are other paired values of x_1 and x_2 for which the integral is zero, and any of these can be employed to give s/D if the values of c and $\partial c/\partial x$ are determined at the corresponding surfaces. Though this appears to be a very laborious procedure and as yet has not been applied often, it has the advantage of not being dependent on accurate knowledge of the concentration and concentration gradient at the ends of the cell. With the interferometric optical systems, employment of this procedure should be greatly facilitated. By a slight modification of the method, Archibald showed how the data can be used for the determination of sedimentation coefficients after s/D is evaluated by one of the other techniques. This has been used by Brown *et al.* (1954) in their experiments on digitonin.

2. Distributions throughout the Entire Cell

Most expressions for the concentration distribution during the transient states before equilibrium is attained have their origin in the theoretical treatments of Archibald. As a result of a very extensive mathematical analysis of Eq. (5) (Archibald, 1942)—actually, Eq. (6) was employed since it was assumed that s and D were constant—equations were developed from which values of c/c_0 were calculated as a function of both distance and time. Archibald's exact solution, which cannot be expressed in a closed form, is written

$$\frac{c(z,t)}{c_0} = \frac{z_b - z_m}{e^{z_b} - e^{z_m}}\, e^z + \sum_{n=1}^{\infty} \frac{\int_{z_m}^{z_b} e^{-z} M(\alpha_n, 1, z)\, dz}{\int_{z_m}^{z_b} e^{-z}[M(\alpha_n, 1, z)]^2\, dz} M(\alpha_n, 1, z) e^{(\alpha_n - 1)\tau} \tag{109}$$

where

$$z = \frac{\omega^2 s}{2D} x^2,$$

$\tau = 2\omega^2 st$ and $M(\alpha_n, 1, z)$ is a solution of the differential equation

$$\frac{d^2M}{dz^2} + \left(\frac{1}{z} - 1\right)\frac{dM}{dz} - \frac{\alpha}{z}M = 0 \tag{109a}$$

and the α_n values are those for which at $z = z_m$ and $z = z_b$

$$\frac{d}{dz}M(\alpha_n, 1, z) = M(\alpha_n, 1, z) \tag{109b}$$

The first term in e^z gives c/c_0 for the equilibrium state, and the other terms in the equation represent the departure from the equilibrium distribution at times short of $t = \infty$. Depending upon the length of the experiment and parameters such as the molecular weight, magnitude of the centrifugal field, and the column height of solution, more or fewer terms are required in the summation. The labor of the computations being excessive prompted Archibald and others to examine various approximate solutions of Eq. (5). According to Archibald (1947a), his approximate solution involves functions from which the concentration distribution can be computed in a matter of 6 to 8 hours. This is to be contrasted with his exact solution (Eq. 109) implementation of which requires, according to Archibald's own estimate, a matter of weeks.

The exact solution given by Archibald (1942) was implemented by Waugh and Yphantis (1953) in their use of the differential analyzer for the evaluation of some of the functions found by Archibald. With the aid of the results from the differential analyzer, Waugh and Yphantis compiled extensive tables of the solute distribution as a function of both distance and time. These tables apply to certain experimental parameters (centrifugal field and position of the meniscus and cell bottom) and to given models of known molecular weight and hydrodynamic properties. Since Waugh and Yphantis were at that time developing their moving-partition separation cell (Fig. 8*b*), they were interested in the average concentration of solute in a region above a specified surface. Consequently, they employed the data from their tables to calculate average concentrations for regions on both the centripetal and centrifugal sides of the separating plate. Figure 45 shows how the ratio, R_s, (average concentration of the centrifugal region relative to that in centripetal section) varies with time and molecular weight. By suitable separation of the contents of the cell after a given time, they were able to calculate, from tables expressing the solution of the differential equation and with the requisite experimental data, the molecular weight of a given substance.

Waugh and Yphantis also employed Archibald's (1947a) approximate solution which applies to situations in which $z_b - z_m$ is of the order of unity. Frequently, the experimental conditions are such that this quan-

tity is greater than 10. It was of interest therefore to examine this approximate solution so as to ascertain the limits of its applicability. As expected, R_s values calculated from the approximate theory were in better agreement with the results of the exact treatment when the molecular weights were low; moreover, the discrepancies even for $(z_b - z_m)$ values of about 10 were small, and the Archibald approximation is useful. Other

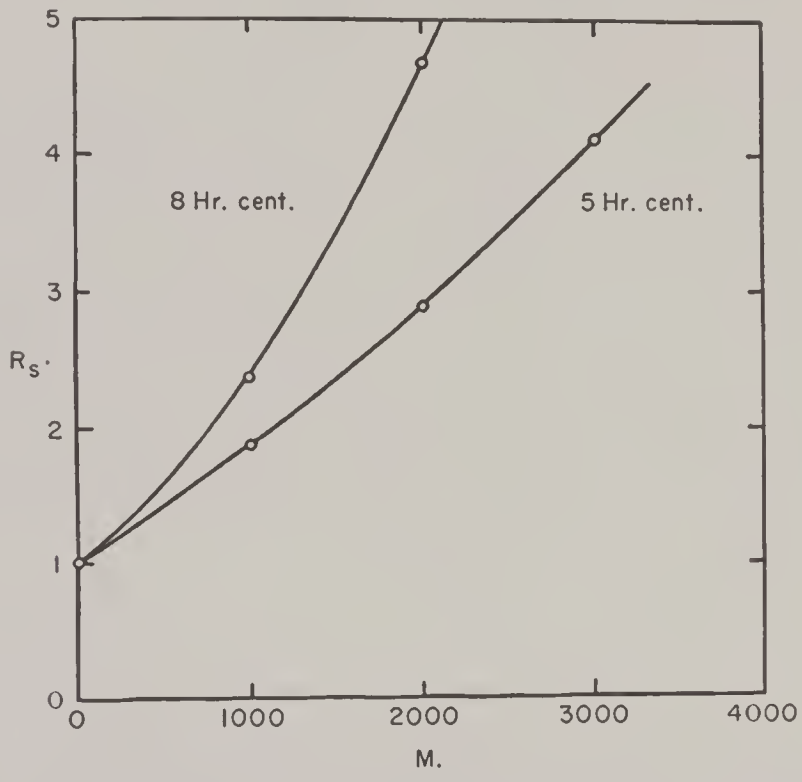

FIG. 45. The concentration ration, R_s, plotted against the molecular weight. The ratio, R_s, is the average concentration of the solution centrifugal to the surface of the partition at $x_p = 6.6$ cm. relative to the average concentration on the centripetal side of the separating plate. The curves are theoretical curves based on the differential analyzer solutions of the differential equations involved in Archibald's solution of the continuity equation. For the calculations, a speed of 59,780 r.p.m. and times of centrifugation of 5 and 8 hours were selected (from Waugh and Yphantis, 1953).

approximations were considered by Yphantis and Waugh (1956a) in a further investigation. In this study, the results were generally expressed as the average fractional supernatant concentration as a function of τ, the effective centrifugation time. This was done in order to present the theoretical calculations in a form convenient for use with the experimental data from the separation cell. For molecules with low diffusion coefficients, the transport equations (e.g., Eq. 28*b*) can be used to determine sedimentation coefficients. A slightly different form is employed by Yphantis and Waugh (1956a). If the diffusion coefficient is large, the plateau region disappears early in the run and the average concentration of the

solution is a function of both s and D. Figure 46 shows, in a convenient form, the change in the average supernatant concentration as a function of equivalent centrifugation time for materials of different molecular weights. It is easily seen that the curves diverge even at relatively low values of τ, therefore a single experimental value of c_u can be attributed to an infinite number of combinations of s and D. Yphantis and Waugh describe a method whereby two experimental determinations of c_u can lead to values of both s and D. In principle, each value of c_u is the basis

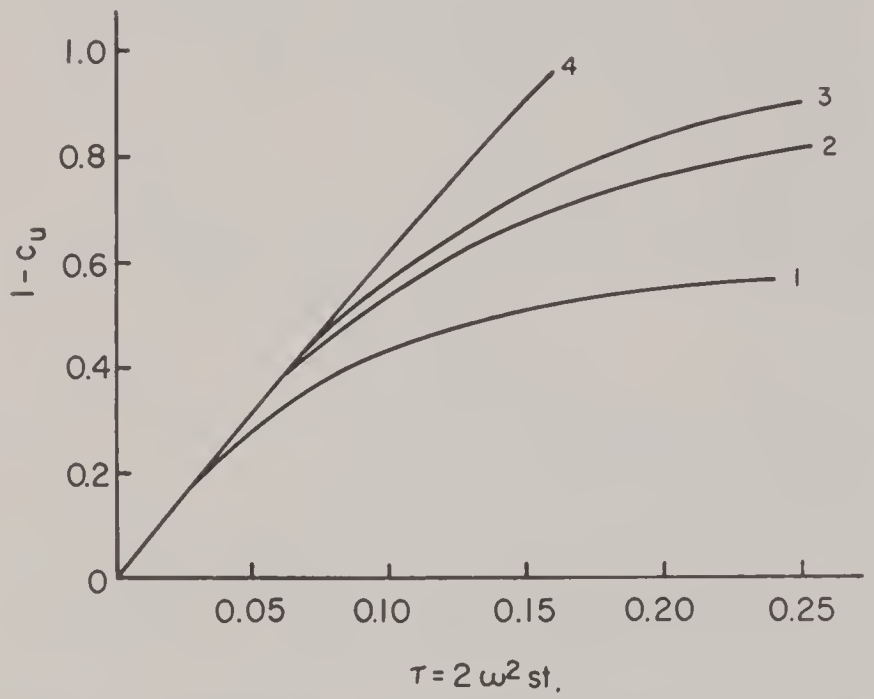

FIG. 46. The change in average supernatant concentration, $1 - c_u$, as a function of average centrifugation time, $\tau = 2\omega^2 st$, for four values of $\delta = \omega^2 s/D$. For curve 1, $\delta = 0.467$, for curve 2, $\delta = 0.933$, for curve 3, $\delta = 1.399$, and for curve 4, $\delta = \infty$ ($D = 0$). These are theoretical curves based on an exact solution of the continuity equation (from Yphantis and Waugh, 1956a).

for a curve of s versus D, since any pair of these values can give the specified value of c_u. When two curves of s versus D are constructed, the point of intersection of the curves defines the values of s and D uniquely. The potential accuracy in the evaluation of both s and D are discussed for materials of different molecular weight and in reference to experimental errors which may be anticipated in the determination of c_u. This method was employed by these workers in the determination of the molecular weight of vitamin B_{12}, and the results were in satisfactory agreement with the known formula weight. In this same study, Yphantis and Waugh considered approximate solutions of the continuity equation and presented detailed comparisons with the calculations from the exact solution. One of these approximations is the so-called rectangular approx-

imation using the solution given by Mason and Weaver (1924). As Yphantis and Waugh showed, this is a good approximation to the exact solution and, moreover, the computations according to it are less laborious than those with the Archibald approximation. Figure 47 illustrates the validity of the rectangular approximation by comparing the curves of the solute distribution as a function of distance as calculated from the exact solution and that assuming a rectangular cell and a uniform field.

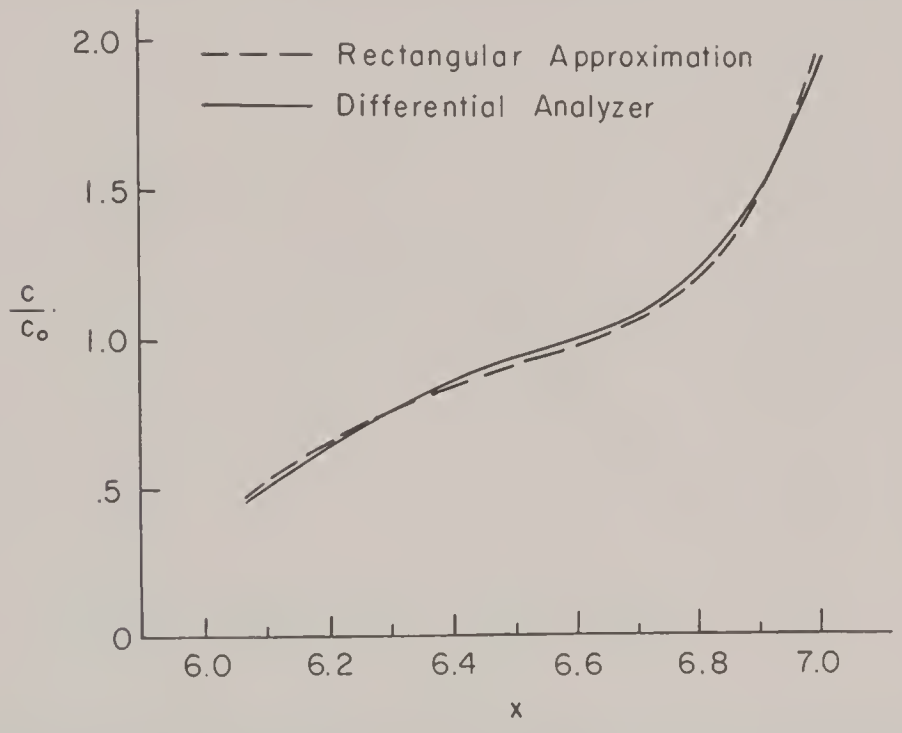

FIG. 47. Theoretical curves showing the solute distribution calculated from an exact solution of the continuity equation as compared to an approximate solution involving the assumption of a rectangular cell and a homogeneous field. For these calculations, the solute was assumed to possess the following properties: $s = 0.356$ S and $D = 2.989 \times 10^{-6}$ cm.^{2}/sec. The curves correspond to 4 hours of centrifugation at 59,780 r.p.m. (from Yphantis and Waugh, 1956a).

Van Holde and Baldwin (1958) also employed the rectangular cell approximation in their consideration of the approach to equilibrium. Employing the solution of Mason and Weaver (1924), they showed that the estimate discussed previously for the time required to attain equilibrium is not applicable for most sedimentation equilibrium experiments. From a re-examination of the Mason and Weaver equation, they were able to derive a relation which expressed the departure from equilibrium as a function of time. As a measure of the deviation from the equilibrium state, they employed the concentration difference across the cell as a criterion. At equilibrium, for a given set of experimental conditions, this concentration difference is a maximum, and therefore $c_b - c_m$ at any

time provided an index of the progress of the experiment. In general, the time required to attain a condition very close to equilibrium in most ultracentrifuge experiments is substantially less than that predicted on the basis of Weaver's (1926) analysis. In other respects, their conclusions were similar to those presented earlier. The solution column should be as short as possible and the centrifugal field as large as possible consistent with the ability of the optical system to record the large refractive index gradients resulting from the high centrifugal fields. With these results as a guide, Van Holde and Baldwin (1958) in experiments with sucrose and ribonuclease showed that sedimentation equilibrium was attained in about 5 hours and overnight, respectively. An experimental test of their equation with a solution of sucrose confirmed the theory in that they were able to predict accurately, throughout the experiment, the concentration difference from the top to the bottom of the cell. The theory involves the diffusion coefficient, and Van Holde and Baldwin showed that a satisfactory diffusion coefficient for ribonuclease can be obtained by analysis of the transient states.

Archibald (1947b) commented on the fact that the plots of c versus x, after the plateau region is lost, rotate about a single point corresponding to a concentration, c_0. In a detailed consideration of this matter, he showed that the value of x corresponding to c_0 is indeed independent of time, and the location of that point can provide a measure of the molecular weight. The solutions of Waugh and Yphantis (1953) with the differential analyzer confirm this conclusion. An experimental test of this during the sedimentation of sucrose showed, indeed, that the so-called hinge point was invariant with time, and the molecular weight calculated from the position of this point was in approximate agreement with the known value (Cheng and Schachman, see Ginsburg *et al.*, 1956).

VI. Sedimentation Equilibrium

1. General Considerations

Although the bulk of their ultracentrifugal investigations have involved the sedimentation velocity method, Svedberg and his collaborators (Svedberg and Pedersen, 1940) from the inception of their pioneering work have used their instruments on occasion to analyze the concentration distribution after equilibrium had been attained. Such equilibrium studies have ranged from the examination of small molecules like inorganic salts (Pedersen, 1934, 1935) and the sodium salt of the dye, eosin (Nichols, 1931), to proteins like carbon monoxide hemoglobin (Svedberg and Fåhraeus, 1926) and *Helix pomatia* hemocyanin (Svedberg and Chirnoaga, 1928). It is of considerable historic interest that the first reported sedimentation equilibrium experiments were concerned with the molecular weight of a protein. After an initial period of excitement with this method, interest in it waned, and the application of the sedimentation equilibrium technique became less frequent. By 1940, reports of sedimentation equilibrium experiments were rare. The last few years, however, have witnessed a renewed interest in the method, along with vigorous activity both on theoretical and experimental lines. As a result of these recent developments, it is safe to predict that the sedimentation equilibrium method will become a very popular one, and its application to areas of chemistry in addition to biochemistry will become widespread.

The expressions describing the concentration distribution in an ultracentrifuge cell, in which equilibrium is attained, can be derived either from thermodynamics or from consideration of the transport of material by sedimentation and diffusion. That such distribution functions can be deduced from thermodynamics constitutes, perhaps, the major appeal of the sedimentation equilibrium method. Many of the theoretical uncertainties implicit in the sedimentation velocity method are absent in the thermodynamic description of sedimentation equilibrium. *By inference*, the thermodynamic approach provides some justification of the kinetic and hydrodynamic treatment since both produce identical results—the former with rigor and scarcely any assumptions, and the latter with approximations and some equivocation in definition of terms. The elementary expressions, derived from both approaches, were given by Svedberg (1925, 1926). These apply only to ideal solutions, but they illustrate

the approaches employed in more thorough treatments which are given later.

When the material migrating across a given surface in a centrifugal direction (Eq. 1) is exactly balanced by the transport centripetally due to diffusion (Eq. 3), equilibrium is attained, and the expression given by Eq. (101) applies at all levels in the cell. Application of the Svedberg equation, $M = RTs/D(1 - \bar{V}\rho)$, gives

$$M = \frac{2RT}{(1 - \bar{V}\rho)\omega^2} \frac{d \ln c}{d(x^2)} \tag{110}$$

Alternatively, equilibrium can be defined as the state in which the escaping tendency of each component at any point in the cell is equal to that for every other point, i.e., the total potential is uniform throughout the system. The total potential is made up of the chemical potential, which is a function of concentration and pressure, and the gravitational (or centrifugal) potential, which is a function of the centrifugal field and, therefore, of position in the cell. With the appropriate expressions for the effect of concentration, RT/c, pressure, $M\bar{V}$, and distance, $-M\omega^2 x$, from the axis of rotation and the derivative of the total potential set equal to zero, an equation results which is identical to Eq. (110). This assumes ideal solutions and neglects variations in density due to concentration and pressure changes in the cell. Young *et al.* (1954) treated this problem rigorously with the aid of the chemical potential, μ, as defined by Gibbs and alternatively, with the partial molal free energy employed by Lewis. Their treatment deals with the activity of the solute and allows for the effect of concentration on density, although no explicit relationship was presented.

Goldberg (1953) contributed a thorough, rigorous description of a system at sedimentation equilibrium in terms of a continuous sequence of phases of fixed volume and infinitesimal depth in the direction of the centrifugal field. Applying the restriction that the total potential is uniform for this heterogeneous equilibrium, he obtained

$$M_i(1 - \bar{V}_i^{(x)}\rho^{(x)})\omega^2 x dx = \sum_{k=1}^{r} (\partial\mu_i/\partial c_k)^{(x)}_{T,P,c_j} dc_k^{(x)} \tag{111}[10]$$

$$i = 0, 1, \cdots r$$

[10] Because of the pressure gradient in the centrifuge cell and the compressibility of the solute and solution, many of the terms in Eq. (111) are dependent on x. Thus the equation is written with (x) to denote that these terms correspond to the surface at a distance x from the axis of rotation. Fixman (1958) has recently considered the basic equation for sedimentation equilibrium; his treatment includes a term for the compressibility.

It is important to note that the calculated molecular weight of any component depends on all components in the system as expressed by the terms, $(\partial\mu_i/\partial c_k)$. Also the density, ρ, introduced through the dependence on pressure, is clearly the density of the solution which is a function of position in the cell. Most applications of the sedimentation equilibrium method assume that $\bar{V}$ and ρ are independent of position in the cell, although it is clear that slight variations, which are in part compensatory, do exist. The density changes both because of the variation in the concentration through the cell and because of the increase in pressure with distance; whereas, the dependence of $\bar{V}$ on concentration is often negligible (especially for proteins), and only a pressure effect need be considered. For most experiments with proteins, the effect of pressure can be ignored since experiments are generally conducted at low centrifugal fields. In order to treat nonideal systems, the chemical potential is expressed in terms of both the concentration and activity coefficient, γ, of the solute to give

$$M_i(1 - \bar{V}_i^{(x)}\rho^{(x)})\omega^2 x dx = RTd \ln c_i^{(x)} + RT \sum_{k=1}^{r} \left(\frac{\partial \ln \gamma_i}{\partial c_k}\right)_{T,P,c_j}^{(x)} dc_k^{(x)} \quad (112)$$

This equation, presented here in the form given by Goldberg (1953), is basic to all sedimentation equilibrium studies, and it or some approximate form of it are employed in the evaluation of all experimental data. Some systems which have been examined involve homogeneous solutes which may or may not exhibit a concentration dependence. Others are concerned with ideal solutions of polydisperse materials. More complicated than either of these two extremes are those systems which exhibit not only a dependence of activity coefficient on concentration but also possess solutes which are polydisperse.

2. Two Component Systems

If the system contains only two components, a homogeneous solute and a solvent, Eq. (112) reduces to a much simpler form which can be written

$$M(1 - \bar{V}^{(x)}\rho^{(x)})\omega^2 x = \frac{RT}{c}\frac{dc}{dx}\left(1 + c\frac{\partial \ln \gamma}{\partial c}\right) \quad (113)$$

This is written for the solute and usually the dependence of $\bar{V}$ and ρ on position are neglected. Many protein solutions seem to exhibit ideal behavior, and for such systems, the term in parentheses in Eq. (113) is equal to unity. It is the integrated form of that simplified equation (see Eq. 110) which was used for the determinations of the molecular weights which were cited above (cf., Pedersen, 1936a, b). For this application ln c is plotted against x^2, and the slope of the resulting straight line is a measure of the molecular weight. Plots which are concave upward indicate polydispersity,

and those which are concave downward are an index of the nonideality of the solution. Since schlieren optical systems yield directly only the concentration gradient, the evaluation of the concentration distribution is laborious, involving numerical integration and the determination of the integration constant. For homogeneous solutes, the data can be plotted as $\ln (1/x)(dc/dx)$ versus x^2, as pointed out by Lamm (1929b). This method has been applied to experiments with ribonuclease (Ginsburg *et al.*, 1956). Although this procedure requires very little effort with regard to calculations, it appears to be an insensitive way of handling the data, and it is difficult to judge precisely when equilibrium is attained. It is of interest, therefore, to examine other treatments of the same data. A more critical examination of all of the data is provided by a plot of $(1/xc)(dc/dx)$ versus x, in the manner suggested by Archibald (1947b). This also has been used by Ginsburg *et al.* (1956) for ribonuclease in experiments of sufficient duration that equilibrium was essentially attained throughout the cell. Not only does this plot provide a precise index of the attainment of equilibrium, but it also involves the use of all of the data and therefore gives a reliable index of the molecular weight, polydispersity and nonideality. If there is polydispersity or nonideality, the plot will have a positive or negative slope, respectively, rather than being a horizontal straight line. Van Holde and Baldwin (1958), in addition to using this procedure, also considered other methods of handling the data. Combination of Eq. (113) with a statement of the conservation of mass (Eq. 105) followed by integration gives

$$\frac{M(1 - \bar{V}\rho)\omega^2}{RT\left(1 + c\dfrac{\partial \ln \gamma}{\partial c}\right)} = \frac{2(c_b - c_m)}{c_0(x_b^2 - x_m^2)} \qquad (114)$$

If the activity coefficient is independent of concentration, measurement of the initial concentration and the concentration difference across the cell at equilibrium gives the molecular weight. For most precise work, the terms on the left of Eq. (114) should be evaluated at a concentration, $(c_b + c_m)/2$, and the molecular weight resulting from such computations corresponds to that concentration. This method is readily used with either schlieren or interferometric optics. Although the latter as yet has not been employed in this manner, it may be preferable both on the basis of simplicity and accuracy.

A second method employed by Van Holde and Baldwin (1958) involves a plot of $(1/x)(dc/dx)$ versus c. For ideal solutions, this gives a straight line the slope of which is used for the calculation of the molecular weight. The actual values of c are not required for this method, since only the slope is necessary; the increase in c throughout the cell is readily determined by

numerical integration of the schlieren patterns. This procedure is similar to the use of Eq. (107), as employed by Ginsburg *et al.* (1956) for the Archibald method. Even for systems showing a dependence of γ on c, the plots are essentially straight lines, and Van Holde and Baldwin (1958) demonstrated that the quantities which are concentration dependent correspond to $(c_b + c_m)$. An additional method employing both (dc/dx) and c at the hinge point has also been suggested and examined by Van Holde and Baldwin (1958). To locate the hinge point, without the labor of evaluating c from the schlieren diagrams, they utilized an approximate method based on an equation of Rinde (1928) for the concentration as a function of distance after a equilibrium is attained. With the adaptation of interferometric optics, especially with the compensating cell of Beams *et al.* (1955) and white light, the location of the hinge point should be both accurate and simple.

Considerations of polydisperse systems were initiated by Lansing and Kraemer (1935) in their treatment of dilute (ideal) solutions. These workers showed that the weight-average molecular weight, M_w, and the so-called z-average molecular weight, M_z, can be evaluated readily from sedimentation equilibrium experiments. With somewhat more difficulty, the number average molecular weight, M_n, can be determined also. These terms are defined by the following equations where n_i is the number of molecules of molecular weight, M_i

$$M_n = \frac{\sum n_i M_i}{\sum n_i} = \frac{\sum c_i}{\sum c_i/M_i} \tag{115}$$

$$M_w = \frac{\sum n_i M_i^2}{\sum n_i M_i} = \frac{\sum c_i M_i}{\sum c_i} \tag{116}$$

$$M_z = \frac{\sum n_i M_i^3}{\sum n_i M_i^2} = \frac{\sum c_i M_i^2}{\sum c_i M_i} \tag{117}$$

By rewriting the expression for the concentration as a function of distance (Eq. 110) and recognizing that each molecular species sets up its own equilibrium distribution, it is easy to sum the equations for all of the components leading to the result that Eq. (110), when applied to polydisperse systems, gives M_w. Similar manipulation with the expression of Lamm (1929b) containing the concentration gradient leads to the conclusion that computations with his equation yield M_z. Analogous treatment of Eq. (114) shows that this method of handling the data gives M_w, and the equilibrium equation analogous to Eq. (107) gives M_z (Van Holde and Baldwin, 1958). If the concentration gradient and concentration are employed as in Eq. (113), assuming ideal solutions, the weight-average

molecular weight results (Archibald, 1947b; Goldberg, 1953). This equation was used by Kegeles (1947) in the determination of the molecular weight of ovalbumin. In this study, Kegeles employed his prismatic cell which permitted the simultaneous recording of both dc/dx and c as functions of x. All of these average values correspond, of course, to only a single position in the cell. To obtain values for all of the material in the cell, i.e., for the initial solution before redistribution has occurred, the various equations must be integrated over the entire cell (Lansing and Kraemer, 1935). The weight-average molecular weight of the initial solution can be calculated from

$$M_w = \frac{\int_{x_m}^{x_b} M_{wx} x c_x \, dx}{\int_{x_m}^{x_b} x c_x \, dx} \tag{118}$$

This can be combined with Eq. (113), for example, to give an expression for M_w for a polydisperse ideal solution in terms of the concentration gradient as a function of distance from the axis of rotation.

$$M_w = \frac{RT}{(1 - \bar{V}\rho)\omega^2} \frac{\int_{x_1}^{x_2} (dc/dx) dx}{\int_{x_1}^{x_2} x \, c_x \, dx} . \tag{119}$$

In Eq. (119), x_1 and x_2 represent surfaces at specific distances from the axis of rotation, and M_w is the weight average molecular weight of the material in the volume element defined by the cell walls and the two surfaces. If the molecular weight for the material as a whole is desired, the boundary conditions for the integration would be the meniscus and the cell bottom. For this situation the integral in the numerator is $(c_b - c_m)$ and that in the denominator becomes $(c_0/2)(x_b^2 - x_m^2)$. This was shown by Svedberg and Pedersen (1940, Eq. 239). Mandelkern *et al.* (1957) also have derived this equation and used it for the analysis of fractions of polyisobutylene. It should be noted that Eq. (114), after modification so as to deal with polydisperse, ideal systems, represents a special case of Eq. (119).

Polydisperse systems which also exhibit nonideality were treated in detail by Schulz (1944) and by Wales and co-workers in a series of papers dealing with the sedimentation equilibrium analysis of these complicated systems (Wales *et al.*, 1946; Wales, 1948; Wales *et al.*, 1948; Thompson, 1950; Wales *et al.*, 1951; Wales and Swanson, 1951; Wales, 1951a; Wales, 1951b). These systems have been considered further by Goldberg (1953) and Mandelkern *et al.* (1957). The latter workers, in particular, accentu-

ated the difficulties in deriving meaningful data from sedimentation equilibrium experiments on nonideal, polydisperse systems. With the present limitations in optical systems as commonly employed, the experiments are restricted to relatively concentrated solutions. Therefore, the nonideality terms (virial coefficients) are important, and it is not certain how many terms in the expression are required. Moreover, the redistribution achieved at equilibrium leads not only to a variation in molecular weight throughout the cell, but also the magnitude and number of the virial coefficients change through the cell. These conclusions apply to synthetic polymers of large molecular weight. With smaller molecules or those exhibiting less deviation from ideal behavior, approximate equations suffice (Wales, 1948; Van Holde and Williams, 1953; Mandelkern *et al.*, 1957). The ambiguity caused by the variation in both the molecular weight and the virial coefficient can be obviated, in part, by the development of accurate techniques which permit measurements at much lower concentrations. Adaptation of interferometric optics in conjunction with cells of long optical path no doubt will facilitate experimentation at concentrations for which the nonideality factors play a less important role than is now the case. Then, perhaps, the older practice of using an average virial coefficient for the whole cell would not introduce serious error. Another approach for the analysis of nonideal, polydisperse systems has been suggested and examined recently by Kegeles *et al.* (1957). On the grounds that there is a balance of forces at each end of the liquid column and, therefore, the gradient of the total potential there is zero, they reformulated the equations usually employed with the Archibald method (1947b) in terms of the gradient of the chemical potential. As indicated above, the chemical potential is expressed in terms of the concentration and activity coefficient of the solute. This leads to Eq. (113). For convenience the experimental data are employed in the calculation of an apparent molecular weight, M_{app}, defined by the following

$$M_{app} = \frac{RT(dc/dx)}{(1 - \bar{V}\rho)\omega^2 xc} = \frac{M}{1 + c(d \ln \gamma/dc)} \qquad (113a)$$

In accord with the practice frequently employed with light scattering or osmotic pressure data, $1/M_{app}$ is plotted against c to give the true molecular weight as $c \to 0$. This treatment was then expanded so as to deal with polydisperse systems, and an analogous equation was described for $1/M_{app}$ in terms of $1/M_w$ and the variation of the activity coefficient with concentration. The virtue of this method as discussed by Kegeles *et al.* (1957) lies in the fact that measurements are made early in the experiment before redistribution has occurred to a significant extent. Thus the sedimentation experiments become similar to the light scattering or osmotic pressure studies for which an average virial coefficient is operative. This method

was applied by Kegeles *et al.* in experiments with polyvinylchloride in tetrahydrofuran, and the results, showing a marked dependence of $1/M_{app}$ on c, are encouraging. From these studies with the Archibald method, it appears that reliable measurements can be obtained at lower concentrations than are generally employed in prolonged sedimentation equilibrium experiments.

Theoretical treatments of nonideal systems have generally involved analogies with the problems of osmotic pressure and light scattering. The former has been utilized by Wales (1948) and others, and it was shown (Wales *et al.*, 1951) that number-average molecular weights can be derived from sedimentation equilibrium data. Others (Tiselius, 1926; Kraemer and Lansing, 1933; and Schulz, 1944) have also discussed the relationship of a sedimentation equilibrium experiment to the measurement of osmotic pressure. Goldberg (1953) has given the relations between sedimentation equilibrium and light scattering. With either of these formulations, the virial coefficients can be expressed conveniently in terms of the quantities capable of direct measurement in the ultracentrifuge. For example, Mandelkern *et al.* (1957) expressed the osmotic pressure dependence on concentration as follows

$$(1 - \bar{V}^{(x)}\rho^{(x)})\omega^2 x c_x/(dc/dx)^{(x)} = (\partial\pi/\partial c)^{(x)} \tag{120}$$

where π is the osmotic pressure. Then the relationship for the osmotic pressure as a function of concentration is introduced to give an expression containing the virial coefficients.

3. Charged Macromolecules

In the previous discussions, it was assumed that the solute molecules were uncharged. Most substances of biological interest are, of course, ionized, and it is pertinent, therefore, to examine the modifications which are required in the preceding equations if they are to be applied to charged solutes. This problem was recognized very early in the development of ultracentrifugation by Svedberg (1925), Tiselius (1926, 1932), and Pedersen (1934), who pointed out that a potential gradient is created in the cell as a result of the differences in the sedimentation velocities of the positive and negative ions. Charge effects are important in sedimentation velocity experiments as well as in sedimentation equilibrium measurements. For a recent theoretical discussion pertinent to the former, see Booth (1954); here we are concerned with sedimentation equilibrium. Since electric neutrality must be preserved throughout the cell, the distribution of charged macromolecules will be markedly different from that of neutral macromolecules of the same molecular weight. By the inclusion of an additional term in each of the sedimentation equilibrium equations for the

different charged species, these workers could account for the effect of the potential gradient in terms of the number of charges on the solute species. Addition of the separate equations for the anions and cations permitted the elimination of the term containing the potential gradient. This resulted, however, in the inclusion of a term, $(1 + n)$, in the right-hand side of Eq. (110). This term represents the number of ions produced when the solute dissociates; n is the charge on the macromolecule. Thus, neglect of this term leads to a value of the apparent molecular weight which is $[1/(1 + n)]$ the true value. At the suggestion of these workers, it has become routine practice to add an excess of neutral, "supporting" electrolyte for the purpose of depressing the potential gradient created by the sedimentation of the macro-ions. The system is then treated as if the solute molecules were un-ionized. While this procedure seems reliable in studies of proteins at a pH not far removed from the isoelectric point, it must be used with caution for materials exhibiting a high ratio of charge to weight. In conjunction with studies of high molecular weight metaphosphates, Lamm (1944) discussed this matter in detail, and more recently, this has been the subject of a critical discussion by Johnson *et al.* (1954b). They were able to show in a direct fashion that, for a two-component, ideal system containing the electrolyte PA_n, a plot of ln c_{PA_n} versus x^2 has a slope which gives $M_{PA_n}/(1 + n)$ rather than M_{PA_n}, as would be the case for the uncharged macromolecule. Actually, these workers employed the molality as the concentration units, and they did not invoke the potential gradient explicitly as did the previous authors. Similarly the effect of "supporting" electrolyte was shown to be the reduction in magnitude (or even elimination) of the term, $n\, d \ln c_A$. If this term does become zero, the data give directly the correct molecular weight of PA_n, as if the electrolyte had been un-ionized. At high values of n, however, even in the presence of "supporting" electrolyte, the term, $n\, d \ln c_A$, is often not negligible, and the theory for un-ionized molecules is not applicable. Under such circumstances, as Lamm (1944) and Johnson *et al.* (1954b) showed, the sedimentation of the polymer and the "supporting" electrolyte must be considered simultaneously. For this situation, separate equations, analogous to Eq. (110), are written for the polymeric electrolyte and for the "supporting" electrolyte. Also an equation expressing electroneutrality is considered. The simultaneous solution of these three equations gives

$$d \ln c_p = \left[\frac{M_{PA_n}(1 - \bar{V}_{PA_n}\rho)\omega^2}{2RT} - \left(\frac{n}{2}\right) \frac{M_{BA}\,(1 - \bar{V}_{BA}\rho)\omega^2}{2RT} \right] d(x^2) \,. \quad (121)$$

This equation, in which M_{BA} and $\bar{V}_{BA}$ are, respectively, the molecular weight and partial specific volume of the "supporting" electrolyte, was derived both by Lamm (1944) and by Johnson *et al.* (1954b) by different

means. It is only approximate, however, the principal restriction being that the polymer is at infinite dilution. Other limitations arise from the fact that the refractive index gradient curve is due to the redistribution in part of the "supporting" electrolyte as well as the macromolecules. Ordinarily, a background experiment with only the "supporting" electrolyte provides a measure of the relative contribution of the latter to the observed pattern of the solution containing the macromolecules, but at high values of n, the redistribution of the macromolecules affects the sedimentation of the "supporting" electrolyte, and additional corrections are required.[11] Finally, the equation used for plotting the data, $\ln (1/x)(dc/dx)$ versus x^2 is not a straight line for three-component systems as it is for the two-component case (Lamm, 1929b, 1944; Johnson *et al.*, 1954b).

Johnson *et al.* (1954b) discussed other methods of treating sedimentation equilibrium data for charged molecules in the presence of a "supporting" electrolyte. By means of a redefinition of the components similar to that suggested by Scatchard (1946) for the interpretation of osmotic pressure data, they were able to assess the various errors and recommend a procedure for systems of unknown charge and molecular weight. This procedure was employed by Johnson *et al.* (1956) in their analysis of the hydrolytic products of hafnium (IV). In earlier experiments, these workers (Johnson *et al.*, 1954a) illustrated the precision with which activity coefficients can be determined by the sedimentation equilibrium method. It is of interest to compare these experiments with those performed much earlier by Pedersen (1934) and Drucker (1937).

4. Multicomponent Systems and Sedimentation in a Density Gradient

Since most macromolecules of biological interest are undoubtedly hydrated in solution, it is imperative that attention be devoted to the effect of solvation in the interpretation of sedimentation equilibrium experiments. This has been the subject of considerable discussion (Kraemer and Lansing, 1935; McBain, 1936; Lansing and Kraemer, 1936). This subject, too, was treated by Goldberg (1953) in his comprehensive analysis of sedimentation equilibrium. According to the latter, there is no need to consider, as previous workers had done, such terms as "apparent molecular weight" and "partial specific volume of the hydrodynamic unit"; for the thermodynamic description of the system permits a choice of components as either the dry substance or the solvated macromolecules (Gibbs, 1948). Thus, fully equivalent and rigorous equations can be written for the dry substance or

[11] With absorption optics this difficulty is eliminated or, at least, reduced. The redistribution of the "supporting" electrolyte will not interfere with the accurate measurement of the concentration distribution of the macromolecules, since the gradient of the former, in general, will not be detected by absorption optics.

for the solvated material. If a fixed amount of solvent is bound to the anhydrous solute to form a complex, the chemical potential of the complex can be written in terms of the chemical potentials of the solute and the solvent in equilibrium with the solute. Differentiation of this equation with respect to pressure gives directly the partial specific volume of the complex in terms of the partial specific volumes of the anhydrous solute and solvent and the number of grams of solvent bound to the solute. As Goldberg pointed out, the sedimentation equilibrium experiments give $M(1 - \bar{V}\rho)$ for either the complex or the anhydrous solute. Since $\bar{V}$ for the complex is rarely measurable, it is preferable to use the terms for the anhydrous solute; thus the molecular weight which is calculated corresponds to the anhydrous material even if the solute molecules are hydrated. It should be noted that $M(1 - \bar{V}\rho)$ for the anhydrous solute is equal to $M(1 - \bar{V}\rho)$ for the complex at infinite dilution.

For systems which contain a third component, such as an electrolyte or sucrose, the situation is somewhat different, and selective association of either of the components of the solvent with the macromolecules may lead to serious errors. This subject is treated in Section VII where multicomponent systems are considered. If the solute does not combine with either of the two components of the solvent or interacts with no preference for either of the components, then the solvent can be considered as a one-component solvent, and the problem is formally identical to that mentioned above. This problem has been considered by Lansing and Kraemer (1936) and by Wales and Williams (1952). A related treatment for sedimentation velocity was given by Schachman and Lauffer (1950). Since studies with proteins are generally made in dilute salt solutions (the electrolyte is added to depress the potential gradients discussed above), it is worth noting that it is tacitly assumed that the salt solution is a one-component solvent. When, however, the concentration of the added third component is large so that the density of the solution is affected markedly, such an approximation is no longer admissible. In such cases, it is mandatory that the possibilities of preferential interaction between the macromolecules and one of the components of the solvent be excluded; otherwise, corrections for such interactions are required.

An interesting and novel type of sedimentation equilibrium experiment has been described recently by Meselson *et al.* (1957). In these experiments, the macromolecules attain an equilibrium distribution in a density gradient which itself represents an equilibrium distribution of much smaller molecules. Initially the solution contains, in addition to the macromolecules at low concentration, a high concentration of a presumably inert substance (cesium chloride has been used in most of the experiments reported thus far), so that the density of the solution is essentially equal to that of the

macromolecules under investigation, e.g., deoxyribonucleic acid (DNA). Under these circumstances, the macromolecules neither sediment nor float initially as the term, $(1 - \bar{V}\rho)$, is almost equal to zero. The density need not correspond exactly with that of the macromolecules, but experimentation is facilitated if they are not too different. After a short period of time, there is considerable redistribution of the smaller molecules with the attainment of an equilibrium distribution after about 24 hours; if the cell is not completely full, this time can be reduced materially. The change in the concentration of the cesium chloride near the meniscus and cell bottom alters the density sufficiently so that the DNA molecules in those regions sediment and float, respectively. Ultimately, a band of DNA is formed at a position where the density of the cesium chloride solution is equal to the effective density of the DNA in that solution. The width of the band is controlled by the resultant of the force of sedimentation which causes the band to be narrow and the force of diffusion which tends to widen the band. To describe the position and the shape of the band, Meselson *et al.* (1957) used Eq. (111) with the modification that ρ itself is a function of x due to the concentration gradient in the cesium chloride solution. Introduction of this function which can be written explicitly in terms of the activity coefficients and the molecular weight of the cesium chloride led to an equation for the concentration distribution of the macromolecules as a function of their molecular weight, partial specific volume, and the density and density gradient of the cesium chloride solution in the region of the band. With several approximations, they obtained an equation for the molecular weight in terms of the standard deviation (width) of the band, the centrifugal field at the mean of the concentration distribution curve, the partial specific volume of the macromolecules, and the density gradient. In this treatment, no consideration was given for possible preferential interaction between the macromolecules and either water or cesium chloride. Thus calculation of molecular weights by this method must be considered with reservations until it is demonstrated that no such preferential association occurs. Whether the errors in the reported measurements are serious or trivial depends upon the extent of any selective binding. Actually the method as used gives the molecular weight not of the anhydrous macromolecules, as implied, but of the complex, since the partial specific volume determined from the position of the band (and the density of the cesium chloride solution in that region) corresponds to the complex. Evaluation of the molecular weight of the anhydrous macromolecules requires knowledge of the composition of the complex which is frequently difficult to determine precisely. In principle, this information regarding the composition of the complex can be inferred from a comparison of the partial specific volumes of the complex and the anhydrous solute, the former being de-

termined from the value of the density of the solution in which the sedimentation rate is zero, and the latter according to standard practice from density and concentration measurements (Lewis and Randall, 1923). Examples of multicomponent systems containing large amounts of a third component are discussed in reference to sedimentation velocity in Section VII, but the comments there are equally pertinent in sedimentation equilibrium. Analogous complications exist in light scattering measurements in multicomponent systems. Meselson *et al.* (1957) showed that a single component leads to a band of Gaussian shape. Departures of the concentration distribution curve from the Gaussian form are, therefore, an indication of polydispersity with respect to either molecular weight or density or both. As yet no demonstration with known materials has been made so as to provide an index of the sensitivity of this method in the detection of inhomogeneity. Since it is somewhat analogous to the problem of diffusion, it is to be expected that this technique will not be particularly sensitive in differentiating between homogeneous and inhomogeneous materials. Only with the highest refinements in experimental precision has the analysis of diffusion boundaries in terms of Gaussian or non-Gaussian form been fruitful in homogeneity studies (see Gosting, 1956, for a critical discussion of this problem). The density gradient method, since it involves the reduction of the buoyancy terms, $(1 - \bar{V}\rho)$, to zero, is very sensitive to any variations in $\bar{V}$ among the macromolecules. In this respect, it is similar to the studies of Cheng and Schachman (1955b) in which heterogeneity with respect to density was examined for polystyrene latex particles by adding D_2O to the medium to reduce the buoyancy term. These studies involved analysis of the relative spreading of the moving boundary in experiments in solutions of different density. From the results already described by Meselson *et al.*, it is clear that this technique of sedimentation equilibrium in density gradients provides valuable information about the densities of the components in the solution. Further, it causes the separation of different molecular species according to their densities and is providing useful and important information for many biological problems. In this regard, it is an example of zone centrifugation in which the bands of solute achieve gravitational stability as a result of the density gradient existing in the medium. This technique differs slightly from the density gradient methods used by many workers (e.g., Hogeboom *et al.*, 1952; Brakke, 1953; Anderson, 1955) in that the latter experiments exploited gradients created independently of the action of the centrifugal field, whereas the work of Meselson *et al.* involved the formation of the density gradient through the sedimentation of the low molecular weight component which was added to increase the density. In the fractionation of lipoproteins by centrifugation in salt solutions, it is clear that density

gradients were formed during the centrifuge experiments, and the stability of the resulting bands is due to these gradients (e.g., Bjorklund and Katz, 1956). It is interesting to note, in summary, that such zone-type centrifuge experiments in which bands are created have been treated in two different ways to give molecular weights. In the one described here, the shape of the band caused by the sedimentation of the cesium chloride gives information relevant to the molecular weight of the macromolecules comprising the band. On the other hand, in the experiments of Cheng and Schachman (1954) (quoted by Ginsburg *et al.*, 1956), the band was used as an indicator of concentration of the redistributing solute, sucrose or serum albumin, and in conjunction with Archibald's equation (1947b) for the hinge point, an approximate molecular weight could be calculated for the material responsible for the formation of the band.

VII. Interpretation of Sedimentation Data

As shown in previous sections, sedimentation velocity experiments provide valuable information regarding the homogeneity of the macromolecules in a given preparation. In those discussions, considerations of homogeneity or distribution functions were restricted to sedimentation coefficients. The translation of these functions into molecular weight distributions requires relationships between sedimentation coefficients and the size and shape of macromolecules. It is in this area of providing parameters describing individual molecules that the sedimentation velocity method finds its widest appeal. In conjunction with other data, the sedimentation velocity method gives not only values of the molecular weight, but also, within certain limits, it reveals information about the shape and hydration of the macromolecules. Moreover, this method, even more than other existing techniques employed in the examination of macromolecules, is applicable over a very wide range, encompassing materials ranging in molecular weight from as low as 300 to 50×10^6 or even higher.

1. The Svedberg Equation

This basic equation, $M = RTs/D(1 - \bar{V}\rho)$, which has been used already in previous sections is derived in different ways, each of which possesses special virtues for illustrating different features. For ideal systems at infinite dilution, each method gives the same result. Perhaps easiest to follow is the so-called microscopic picture which considers individual molecules of well-defined size and shape. At the other extreme are the macroscopic approaches which examine the system as a whole and treat, instead of individual molecules, the total potential of the system.

Svedberg's original derivation (1925) involved a microscopic picture dealing with particles or molecules as kinetic units of a fixed volume and density. This derivation has been used frequently (e.g., Nichols and Bailey, 1949; Edsall, 1953) despite shortcomings owing to ambiguous definitions of some of the terms. Here the derivation is given in the form presented by Schachman and Lauffer (1950) because it is readily modified to encompass the effects of solvation and selective interaction between the macromolecules and one of the other components in a multicomponent system. Consider a particle of mass, m, which causes a volume change, v, when added to a large amount of solution having a density, ρ. Due to the displacement of the medium upon the addition of the particle, its effective mass, $(m - v\rho)$, is less than its true mass. The total centrifugal force on

the particle is equal to the product of the centrifugal field and the effective mass and can be written $\omega^2 x(m - v\rho)$. A complete description of the motion of a particle in a centrifugal field must include terms not only for the force from the external field which causes a directed motion but also for frictional forces exerted by the medium and random forces acting on the particle by the environment. The fluctuating forces (and resulting Brownian movements) change extremely rapidly, and the particles quickly attain a limiting (directed) velocity for which the driving force is counterbalanced by the frictional force. The latter is written as $f(dx/dt)$ where f is the frictional coefficient. To be sure, the velocity of the particles does increase during an experiment, but this increase is slight and its rate very slow. Furthermore, the particles suffer many random movements in an interval of time during which the variation in directed velocity is negligible.

The particles, during their migration, are subjected to an increasing field, but the frictional force, since it is proportional to the velocity, also increases, thereby essentially maintaining a balance of forces. Thus the acceleration of the particles is considered negligible in terms of the force equation, and the motion of a particle can be described by

$$\omega^2 x(m - v\rho) = f(dx/dt) \tag{122}$$

Multiplying both sides by Avogadro's number, N, and substituting the molecular weight, M, for Nm and s for $(dx/dt)/\omega^2 x$ gives

$$M = \frac{Nfs}{(1 - \bar{V}\rho)} \tag{123}$$

In the rearrangement to obtain Eq. (123), the partial specific volume, $\bar{V}$, was substituted for v/m, which is the physical counterpart of the determination of the partial specific volume defined by $\bar{V} = (\partial V/\partial m)_{T,P}$ (the volume change caused by the addition of an infinitesimal amount of solute). The frictional coefficient is related to the volume and shape of the sedimenting unit which here is left unspecified. It is generally accepted for infinitely dilute solutions that the frictional coefficient in sedimentation is the same as that operative in transport by diffusion. From the derivations of Einstein (1905) and Sutherland (1905), the frictional coefficient can be expressed in terms of the kinetic energy and diffusion coefficient by the well-known relation

$$D = \frac{kT}{f} \tag{124}$$

where k is the Boltzmann constant. Combination of Eqs. (123) and (124) gives the Svedberg equation

$$M = \frac{RTs}{D(1 - \bar{V}\rho)} \tag{125}$$

where R, the gas constant, is written for Nk. It should be emphasized that this equation, as written, applies only at infinite dilution, and corrections are required here, as in the equations for sedimentation equilibrium, for nonideal solutions at finite concentrations. Also this equation is restricted to two-component systems containing a solute and solvent. Implicit in this treatment is the assumption that electrostatic effects are absent; otherwise, forces must be included to account for the potential gradient generated by the difference in sedimentation rates of the various ions present in the solution.

Despite the simplicity of this microscopic treatment, other derivations have been sought because of doubts raised about the introduction of both $\bar{V}$ and ρ in Eq. (123). This was the subject of considerable discussion in a conference on the ultracentrifuge organized by the National Academy of Sciences in 1949 (Longsworth, 1950). Unlike the situation in sedimentation equilibrium wherein the thermodynamic treatment shows emphatically that ρ is the density of the solution, only equivocal remarks have been made until recently regarding the density term in sedimentation velocity experiments. At infinite dilution, the difference between the density of the solution and the solvent vanishes, of course, and the distinction becomes meaningless. Nonetheless it is appropriate to examine this question by other means in order to permit the extension of Eq. (125) to systems at finite concentrations.

Alternative approaches have been considered by Lamm (1953), Goldberg (1953), and Williams (1954), who avoided the microscopic picture, in part, by writing the force on a molecule as the negative gradient of the total potential. By this means, both the chemical potential, μ, and the centrifugal potential, $-M\omega^2x^2/2$, were introduced in just the way they are involved in sedimentation equilibrium. To account for the effect of pressure requires the inclusion of a term for the dependence of the chemical potential on pressure, $\partial\mu/\partial P$. This is equal to $M\bar{V}$. In order to evaluate $\partial\mu/\partial x$ (where there are no concentration gradients), the value of $\partial\mu/\partial P$ must be multiplied by dP/dx which is equal to $\rho\omega^2x$ where ρ is the density of the solution. Thus the force, F, on a molecule can be written

$$F = -\frac{1}{N}\frac{\partial}{\partial x}\left(\mu - \frac{M\omega^2x^2}{2}\right) = \frac{M(1 - \bar{V}\rho)\omega^2x}{N} \tag{126}$$

Avogadro's number is included because the potential is expressed per mole. As in the previous treatment, this force is equated to the frictional force to give Eq. (123). Thus Lamm (1953), Goldberg (1953), and Williams (1954) obtained an expression for the sedimentation coefficient in terms of the density of the solution and the partial specific volume of the solute without resort to microscopic concepts for the buoyancy term. A discussion in

many respects similar to that just presented was given by Baldwin and Ogston (1954). They, like Goldberg (1953), also considered in some detail the frame of reference in relation to the driving force. This has also been the subject of discussions by Lamm (1954, 1957). The frictional coefficient can be defined in different ways depending upon the frame of reference chosen, and the latter can be dictated on the basis of convenience. However, the same reference must be used for both sedimentation and diffusion. When the driving force is written as the negative gradient of the chemical potential, as in Eq. (126), it is customary to consider flow equations relative to the local center of mass rather than flow relative to the cell wall, even though measurements are made, of course, with the latter as a frame of reference (Goldberg, 1953). This leads to the introduction of an additional term, $\bar{V}_0\rho$, in both Eqs. (123) and (124) (Baldwin and Ogston, 1954). The extra term, in which $\bar{V}_0$ is the partial specific volume of the solvent, becomes unity as the concentration of solute approaches zero. As Baldwin and Ogston showed, Eq. (125) results regardless of which reference is selected, since the term cancels when the sedimentation and diffusion equations are combined. It is interesting to note here that separate sedimentation equations can be written for the solute and solvent alike, and that these lead to two distinct sedimentation coefficients (Baldwin and Ogston, 1954). In principle, therefore, subscripts should be added to the above sedimentation equations. However, they are omitted here, and the equations, as written, correspond to the migration of the solute. Diffusion measurements, in contrast, yield a single value since the diffusion coefficients for the solute and solvent are equal (see Gosting, 1956, for a proof of this statement).

Another formulation of the Svedberg equation has been given by Oka (1936) and Archibald (1938a), who combined the continuity equation (Eq. 6) with the equation expressing the concentration distribution at sedimentation equilibrium. The thermodynamic equation for ideal, two-component systems can be applied in the form

$$\frac{dc}{dx} = \frac{M(1 - \bar{V}\rho)\omega^2}{RT} xc \tag{113}$$

Introduction of (dc/dx) and the second derivative, (d^2c/dx^2), into Eq. (6) along with the condition for equilibrium, $dc/dt = 0$, followed by rearrangement and cancellation of the appropriate terms gives Eq. (125) directly.

It is important to note still another approach which has yielded the Svedberg equation. In a recent series of papers, the thermodynamics of irreversible processes were applied to rotating systems (Hooyman *et al.*, 1953; Hooyman, 1955, 1956), and it was shown that the general equations

resulting from the basic laws of thermodynamics of irreversible processes led to the correct distribution function for the concentration at sedimentation equilibrium. Moreover, with the same specification of $\bar{V}$ as the partial specific volume of the solute and ρ as the density of the solution, they considered sedimentation velocity experiments. Their phenomenological equations relating the flows and forces led to the Svedberg equation. This approach is important because its generality makes it readily adaptable for treating other sedimentation phenomena in addition to two-component systems (Hooyman, 1956).

2. The Effect of Solvation

Most of the solutes examined in the ultracentrifuge bind considerable amounts of solvent, with the result that the sedimenting unit possesses a weight, volume, and density appreciably different from that of the unsolvated material. With proteins, estimates of hydration amount to about 0.2 g. of water per gram of protein (Edsall, 1953). Thus it is relevant to examine the effect of such hydration both on the sedimentation rate and on the calculations of molecular weights by the Svedberg equation. Previously, this problem was considered in terms of sedimentation equilibrium experiments, and it was shown (Section VI) that correct values of the anhydrous molecular weight obtain despite the fact that the kinetic unit may possess large amounts of solvent. As was true for sedimentation equilibrium, controversial views have been expressed on the effect of hydration in the interpretation of sedimentation-diffusion data. It is now generally accepted, however, that correct values of the anhydrous molecular weight are obtained through the use of Eq. (125) for two-component systems even if the solute molecules are extensively hydrated.

Solvation is difficult to define satisfactorily, partly because the migration of a solid, impermeable sphere (such as a glass bead) causes the movement of relatively large amounts of the surrounding liquid. Such transport of liquid is the consequence of viscous forces operating in the liquid, and considerations of this effect are basic, for example, to the derivation of Stokes' law. Such effects are ignored in the present discussion. Rather we pose the hypothetical problem of comparing (*1*) a macromolecule which contains within it no solvent and acts hydrodynamically as a rigid, impermeable sphere with (*2*) another macromolecule treated in some unspecified (and perhaps unknown) fashion which does not alter the molecular weight and shape but causes the macromolecules to swell to many times the former volume. The latter, now containing a large amount of solvent, is still considered to be impenetrable and rigid. Whether such a hypothetical pair of molecules can be obtained in the laboratory is immaterial to our present

discussion. How will these two materials differ in sedimentation rate, and how will the molecular weight calculations be affected by this transformation of the first macromolecule?

The role of hydration or solvation can be separated into two parts, the first dealing with the effective mass, $M(1 - \bar{V}\rho)$, and the second concerning the frictional coefficient. According to the microscopic picture presented above, and restricted to infinite dilution, the sedimenting unit may be represented by a particle of mass, $(m + h\rho)$, where h is the volume of liquid with density, ρ, which is associated with the particle. If this "hydrated particle" could be handled as such in a "bench-top" experiment, the volume change caused by its addition to a large amount of liquid would be $(v + h)$, and the effective mass can be written $[m + h\rho - (v + h)\rho]$. Note that this reduces to the same value as that inferred previously for the anhydrous particle, i.e., $(m - v\rho)$. Thus the increase in mass of the sedimenting unit as a result of solvation is offset by the extra displacement (or additional buoyancy) of the medium. In this regard, at least, the sedimentation coefficient is not affected by solvation. This is stressed here because the same treatment proves very useful when applied to multicomponent systems. Solvation can also be treated by the macroscopic theories according to the method first used by Goldberg (1953). If α moles of solvent (component 1) combine with 1 mole of solute (component 2) to form the solvated material (component 21), the chemical potential of the sedimenting unit can be written.

$$\mu_{21} = \mu_2 + \alpha\mu_1 \tag{127}$$

Differentiation of this equation with respect to pressure gives the partial molar volumes $(M\bar{V})$

$$M_{21}\bar{V}_{21} = M_2\bar{V}_2 + \alpha M_1\bar{V}_1 \tag{128}$$

Combining this with the expression for the molecular weight of the complex

$$M_{21} = M_2 + \alpha M_1 \tag{129}$$

gives

$$M_{21}(1 - \bar{V}_{21}\rho) = M_2(1 - \bar{V}_2\rho) + \alpha M_1(1 - \bar{V}_1\rho) \tag{130}$$

Slightly different treatments were employed by Lansing and Kraemer (1936) and Baldwin and Ogston (1954) leading to the same result. At infinite dilution, the term $(1 - \bar{V}_1\rho)$, becomes zero, and the macroscopic theory gives the same result as the microscopic picture, i.e., solvation in a two-component system does not affect the term, $M(1 - V\rho)$. Baldwin and Ogston showed further that the last term in Eq. (130) is eliminated,

even at finite concentrations, if the proper activity coefficients are employed in the diffusion equation (see Section VII, 3). This is exactly the point emphasized by Goldberg (1953) in his discussion of this problem for sedimentation equilibrium.

Though solvation does not affect the sedimentation rate as far as the effective mass of the particle is concerned, it does influence the rate of migration by virtue of altering the frictional coefficient. As will be shown later, the frictional coefficient is directly related to both the volume and shape of the kinetic unit. Hence any alteration of these parameters, such as swelling due to hydration, is revealed by a change in the frictional coefficient and, ultimately, in the sedimentation coefficient. However, the diffusion coefficient is affected as well, and Eq. (124) can be written (for an infinitely dilute solution)

$$D = \frac{kT}{f_{21}} \tag{124}$$

The analogous equation for the sedimentation coefficient of the hypothetical hydrated particle is written

$$s = \frac{M_{21}(1 - \bar{V}_{21}\rho)}{Nf_{21}} \tag{123}$$

If these two equations are combined with Eq. (130) along with the restriction that the solutions are infinitely dilute, we obtain

$$\frac{RTs}{D} = M_{21}(1 - \bar{V}_{21}\rho) = M_2(1 - \bar{V}_2\rho) \tag{125}$$

Thus the molecular weight determined from the experimental quantities, s, D, and $\bar{V}$ gives the correct anhydrous molecular weight despite the existence of any solvation. This important conclusion can be stated in an alternative manner. If sedimentation and diffusion measurements were to be performed on both the hypothetical macromolecules described earlier, the molecular weights calculated from both sets of data (with a partial specific volume corresponding to the anhydrous material) would be identical, despite the differences in both s and D which would be observed for the two models.

Of course, knowledge of the partial specific volume of the solvated solute permits the calculation of the molecular weight of the complex. Rarely does the hydrated protein, for example, have a well-defined composition, and operationally it is not feasible to determine the partial specific volume of such a hydrated solute. Therefore, molecular weights from sedimentation and diffusion measurements almost always correspond to the anhydrous material.

3. Nonideal Solutions

The derivations presented above for the Svedberg equation were restricted to solutions at infinite dilution where nonideality terms vanish. As already shown in Section IV,4, the sedimentation coefficient shows a marked dependence on concentration. The diffusion coefficient, as well, exhibits a concentration dependence although experimental investigations of this effect are not nearly so extensive as in the former area. In addition to the hydrodynamic effects which are manifested as the dependence of the frictional coefficient on concentration, diffusion coefficients are influenced by concentration in still another way. The driving force in diffusion, just as in sedimentation, is expressed as the negative gradient of the total potential (in the absence of an external field this becomes $-\partial\mu/\partial x$). Fick's first law (1855) which is basic to all diffusion measurements involves the concentration gradient. Therefore, in the formulation of the flow equation, the force, $-\partial\mu/\partial x$, is written as $-(\partial\mu/\partial c)(\partial c/\partial x)$. Actually the dependence of the chemical potential on concentration, $(\partial\mu/\partial c)$, can be written as $(d\mu/dc)$ since this treatment is restricted to solutions of only two components at constant temperature and pressure. Introducing the well-known relationship between chemical potential and concentration ($\mu = \mu_0 + RT \ln \gamma c$) leads to the general expression for the diffusion coefficient (Onsager and Fuoss, 1932)

$$D = \frac{kT}{f}\left[1 + \frac{d \ln \gamma}{d \ln c}\right] \tag{131}$$

The term in brackets is frequently called the thermodynamic term. Since it generally increases with concentration for macromolecules, as does f, the diffusion coefficient is thought to exhibit less concentration dependence than is observed for sedimentation coefficients. Some workers (Beckmann and Rosenberg, 1945; Singer, 1947b; Flory, 1953) have expressed the thermodynamic term in another way by relating it to the nonideality terms for the dependence of osmotic pressure on concentration.

It is tacitly assumed that f in diffusion is the same as in sedimentation though no rigorous demonstration of this assumption has been made. Kegeles *et al.* (1957) have, in fact, suggested that the frictional coefficients in sedimentation and diffusion are not equal. This is attributed to the role of backward flow in sedimentation, which does not have an exact counterpart in diffusion. Precise experimental data on a well-defined, two-component system are needed in order to resolve this question. Such doubts about the frictional coefficient are restricted to solutions of finite concentration and do not affect the previous conclusions regarding the equality of the frictional coefficients at infinite dilution. On occasion (Sharp *et al.*, 1946a), references have been made to the possibilities of preferential orien-

tation of anisometric particles during sedimentation. Since the frictional coefficient for elongated particles depends on the direction of migration relative to the orientation of the long axis, the existence of a preferred orientation during sedimentation along with randomness during diffusion would, of course, lead to an inequality in the frictional coefficients in the two phenomena. For most substances examined by ultracentrifugation, the orienting influence of the centrifugal field and any tendency toward a preferred orientation to give a minimum frictional resistance are likely to be small compared with the force causing rotational Brownian motion, and randomness of the particles is probably achieved. With several bacteriophages (Putnam, 1950, 1954) and tobacco mosaic virus (Schachman, 1951a), which may be considered as extremes with regard to lack of symmetry in density (in the first instance) and shape (in the latter), it was found that the sedimentation coefficient was independent of centrifugal field despite variations of the latter over 100-fold. This is consistent with the view that even these particles are not oriented preferentially during sedimentation. However, it does not preclude the existence of orientation even at the lowest centrifugal fields employed, as long as the average degree of orientation does not vary over the range of centrifugal fields used in the study. More recent investigations (Taylor *et al.*, 1955; Bendet *et al.*, 1957) of the physical chemical behavior of T2 bacteriophage as a function of pH have led to further consideration of this problem. From measurements of the diffusion and sedimentation coefficients, Bendet *et al.* (1957) concluded that the frictional coefficient for sedimentation was altered more by a change in pH than was the frictional coefficient operating in diffusion. Since they inferred that changes in molecular weight, hydration, and partial specific volume could not be responsible for their observations, the suggestion was made that the particles were oriented during sedimentation analysis and not during diffusion. Thus the frictional coefficients in sedimentation and diffusion may not be considered as equal. In view of the importance of this problem, it is to be hoped that more precise data, especially with regard to diffusion, as well as more knowledge of the structural features of the bacteriophage particles responsible for this unusual behavior will soon be forthcoming. Then the implications of this work with regard to the validity of the Svedberg equation can be better assessed.

Combination of Eqs. (131) and (123) gives the basic equation for the calculation of molecular weights in two-component systems.

$$M = \frac{RTs}{D(1 - \bar{V}\rho)}\left[1 + \frac{d \ln \gamma}{d \ln c}\right] \tag{132}$$

At infinite dilution, the term on brackets becomes unity, and Eq. (132) reduces to the familiar Svedberg equation. Thus sedimentation and diffu-

sion data at different concentrations give not only the molecular weight by extrapolation to infinite dilution, but also in common with light scattering, osmotic pressure, and sedimentation equilibrium, they provide thermodynamic data for the solution.

A rigorous test of Eqs. (132) and (125) has not as yet been made because most accurate sedimentation velocity measurements pertain to charged molecules, like proteins, in multicomponent systems. Some complications are introduced owing to the addition of the extra component which is necessary to depress charge effects. Nonetheless, some of these results are presented here for the purpose of demonstrating the validity of the Svedberg equation. It is hoped that precise data will become available soon for uncharged solutes of known structure. In the meantime, we are forced to employ data from systems which do not, in principle, satisfy the

TABLE VIII[a]

Molecular Weight of α-Chymotrypsinogen

Method	Molecular weight
Amino acid analysis	25,081 ± 336
Light scattering	26,100 ± 1000
Sedimentation-diffusion	
pH 3.0	24,400
pH 7.5	24,000
X-ray diffraction	25,000 ± 800
Osmotic pressure	24,000 ± 500

[a] From Wilcox *et al.* (1957).

theoretical restrictions imposed in the derivation of Eq. (132). Rationalization for the consideration of these data here is provided in the next section. From careful measurements on α-chymotrypsinogen, the molecular weight has been determined by a variety of different methods. The agreement, presented in Table VIII (Wilcox *et al.*, 1957), is striking. Similar agreement is obtained with β-lactoglobulin (Bull and Currie, 1946; Senti and Warner, 1948; Cecil and Ogston, 1949; Halwer *et al.*, 1951). Another test of the Svedberg equation is provided by the results of Baker *et al.* (1955a, 1955b) on several heteropoly acids. From sedimentation and diffusion studies and measurements of the partial specific volume, the molecular weights of silicotungstic acid, phosphotungstic acid, and phosphomolybdic acid were found to be 2.91×10^3, 2.86×10^3, and 1.69×10^3, in excellent agreement with the known values for the three complexes, 2.875×10^3, 2.909×10^3, and 1.706×10^3, respectively. At the other extreme, the particle weight of bushy stunt virus determined by sedimentation and diffusion (Cheng and Schachman, unpublished) was 8.9×10^6, in excellent

agreement with the value from light scattering, 9.0×10^6 (Oster, 1946), and from direct particle counting in the electron microscope, 9.3×10^6 (Williams and Backus, 1949).

Polydisperse solutions give average molecular weights which do not represent any of the well-known averages, M_n, M_w, or M_z, discussed previously. When the sedimentation and diffusion coefficients are the weight-average values, the molecular weight calculated from these data are usually written, $M_{w,w}$ (Jullander, 1945). To relate this value to any of the other averages requires knowledge of the distribution function itself.

4. Effect of Charge on Sedimentation

Owing to the differential sedimentation of an ionized macromolecule and its counter-ions, a potential gradient is established during the sedimentation of charged molecules. This potential gradient is fully equivalent to an externally applied electric field, and allowances must be made for it in the force equation for both sedimentation and diffusion. In effect, the counter-ions are subjected to an additional driving force so that their sedimentation rate is greatly enhanced, whereas, the macro-ions are under the influence of a force in opposition to the centrifugal force. The sedimentation rate of the latter, as a result, is diminished considerably relative to un-ionized macromolecules of the same molecular size, shape, and partial specific volume. In diffusion, the opposite situation exists because the counter-ions, having the larger diffusion rate, cause the acceleration of the macro-ions, while the latter retard the small counter-ions. Since electroneutrality is preserved, the positive and negative ions must migrate at the same rate, and Eq. (125) does not give the molecular weight of the macromolecules. Instead, the equation can be modified, as Svedberg and Pedersen (1940) showed, to give

$$\frac{M}{n+1} = \frac{RTs}{D(1 - \bar{V}\rho)} \tag{133}$$

where n is the number of counter-ions per macromolecule. In deriving this equation, they wrote independent sedimentation and diffusion equations for the cations and anions with a term in each to account for the potential gradient. Applying the restriction that the rates of migration of the positive and negative ions were equal permitted the elimination of the term containing the potential gradient. With several approximations, they obtained Eq. (133) directly. It is implicit in the derivation of Eq. (133) that only the macro-ions and the counter-ions are present in the solution. If other electrolytes are added to the solution, this equation does not apply.

Instead of employing Eq. (133), which requires knowledge of the charge on the macromolecular ion, most workers have followed the practice ini-

tiated by Svedberg and his colleagues whereby the potential gradient is depressed by the addition of an excess of a low molecular weight, neutral electrolyte. Pedersen (unpublished experiments cited by Svedberg and Pedersen, 1940) differentiated between the so-called primary and secondary charge effects, each of which results from the creation of a potential gradient in the ultracentrifuge cell. The former, which is the larger and always causes a reduction in the sedimentation rate of the macromolecule, is attributed to the differential sedimentation of the ionized macromolecule and its counter-ions. In contrast, the secondary charge effect can either enhance or diminish the sedimentation rate of the macro-ions. This effect arises from differences in the sedimentation rates of the positive and negative ions in the "supporting" electrolyte. It is important, therefore, that the "supporting" electrolyte be selected with discretion. A thorough discussion of this problem is given by Svedberg and Pedersen (1940) in terms of a theory developed by Tiselius (1932) along the lines originally suggested by Tolman (1911). From this treatment (see Booth, 1954, for additional theoretical considerations), three independently controlled factors were shown to be involved, and the practical measures now routinely used to depress the primary charge effect have their origin in this theory. The depression of the sedimentation rate of the macromolecules due to the primary charge effect was directly proportional to the concentration of the sedimentating material; thus, reduction of the concentration of the solute minimizes the errors. Similarly, the effect was found to be related directly to the charge and mobility (electrophoretic) of the macro-ions both of which can be diminished if experiments are performed at or near the isoelectric point. Finally, the primary charge effect was inversely proportional to the conductivity of the solution, which can be increased markedly by the addition of electrolyte. Similar theoretical reasoning led to an expression for the secondary charge effect which showed that its magnitude was proportional to the differences in the sedimentation rates of the positive and negative ions in the "supporting" electrolyte. Unlike the primary charge effect, the secondary charge effect does not vanish as the concentration of the sedimenting material approaches zero, nor does it disappear at high salt concentrations. Pedersen's experiments with ovalbumin (Svedberg and Pedersen, 1940) remain as the definitive experimental investigation of this problem, and the importance of the two effects is illustrated by his data.

Recently Pedersen (1958) presented the results of extensive studies of the effect of charge on the sedimentation behavior of bovine serum albumin. In this new work, he examined the influence of different salts (large cations-small anions and the reverse) on the sedimentation of the protein in both acid and alkaline solutions. As expected from theoretical consideration

of the primary charge effect, the sedimentation rate of the protein in salt-free solutions decreased upon the addition of acid. This is a consequence of the increase in the net charge of the macromolecule. Upon the first addition of acid, however, there was a slight increase in the sedimentation coefficient. As Pedersen pointed out, the serum albumin molecules in the electrodialyzed solution (at pH 5.1) were negatively charged; therefore the acid added initially caused a decrease in the net charge. Subsequent addition of acid caused the protein to become positively charged, and the sedimentation coefficient decreased progressively until the hydrogen ion concentration became so high (10^{-2} M) that the charge effect was partially damped by the acid itself. This decrease in sedimentation rate (from 4 S to 1.5 S) is greater than predicted by the theory for the primary charge effect. According to the theory, the sedimentation rate of ionized macromolecules in solutions containing no additional electrolyte should be one-half the rate of the same macromolecules which are either uncharged or in solutions containing swamping electrolyte. Since the observed sedimentation coefficient was lower than that inferred from the theory, Pedersen suggested that the protein itself had been modified at the low pH by a change in shape or by swelling. The presence of neutral electrolyte at a concentration of 0.2 M virtually eliminated the primary charge effect. Moreover, the theory was tested in another way. If there are ions present in the solution in addition to the macro-ion and its counter-ions the charge effect should vanish as the concentration of the macro-ions is reduced to infinite dilution. Although the experimental results of Pedersen were in qualitative accord with this aspect of the theoretical treatment the infinite dilution values (obtained by extrapolation) did not coincide. There was, in fact, a marked difference in the results depending on the type and amount of added electrolyte. In acid solutions containing 0.2 M alkali bromides the protein had a sedimentation rate (at infinite dilution) of about 4.6 S when the cation was lithium and about 4.1 S with cesium as the cation. This was a manifestation of the secondary charge effect. Experiments under different conditions showed that the observed effect is much greater than that calculated from the theory. Furthermore, the secondary charge effect was found to be dependent on the concentration of the added electrolyte, although there is no adequate, general theoretical explanation for this result. Presumably these observations are attributable to specific interactions between serum albumin and the various anions.

In order to apply the theory for the secondary charge effect Pedersen evaluated the sedimentation coefficients of many different anions and cations. He also calculated the sedimentation coefficient of various salts and compiled the results into a useful table. Moreover the experimental determination of the sedimentation coefficient of cesium iodide gave a re-

sult in good agreement with the calculated value. These tabulated results are likely to find wide application in the selection of buffer constituents for experiments with ionizable macromolecules.

Charge effects were shown to be important in studies of the sedimentation of polyvinylpyridinium bromide (Rosen *et al.*, 1951) and sodium polymethacrylate and polymethacrylic acid (Howard and Jordan, 1954). For these systems, interpretation of the experimental data was complicated by the large configurational changes in the polyelectrolytes because of their flexibility and the electrostatic repulsion. Kraut (1954) has discussed some of the experimental results in terms of the primary charge effect.

The addition of an electrolyte to a solution of a macromolecule renders the system no longer amenable to interpretation according to Eq. (125). In a strict sense, that equation is restricted to two-component systems. However, the errors in its use for multicomponent systems containing, for example, 0.1 *M* potassium chloride are much smaller than would be the case had the macromolecules been examined in the absence of "supporting" electrolyte. It is tacitly assumed that the solution of electrolyte can be considered as a one-component solvent with no preferential interaction between the macromolecules and either of the components in the binary solvent. Whether this assumption is valid for the many systems for which it has been applied remains a problem for further investigation. In dilute solutions of "supporting" electrolyte, the errors are likely to be small in any case.

5. Multicomponent Systems

Unlike the situation presented earlier for two-component systems, the terms describing the interaction in multicomponent systems between the macromolecules and any other single component do not cancel from the force equation. The errors resulting from neglect of such preferential interactions may be very large, especially at high concentrations of a third component, and lead to erroneous impressions about the properties of the macromolecules. Though data are rarely available for a complete description of multicomponent systems, some important aspects of the problem are well understood, and a discussion of them at this time is necessary. As in the treatment of solutions containing only two components, the analysis of interaction between the macromolecules and the solvent can be separated into two parts, the first being concerned with the effective mass of the sedimenting unit, and the second directed toward the frictional term. Both macroscopic and microscopic treatments have been employed in the treatment of the first factor with equivalent results. The second factor has been discussed only briefly thus far (Baldwin, 1958), although extensive

work has begun recently on analyzing diffusion in multicomponent systems (see Gosting, 1956, for a review).

If the hypothetical particle considered earlier (with mass, m) combines with a volume, h, of solvent having a density, d, the mass of the sedimenting unit can be written, $(m + hd)$. Since this solvated particle has an effective volume, $v + h$, the mass of the displaced liquid is $(v + h)\rho$ where ρ is the density of the bulk solution. In this notation, d is the density of that portion of the medium which is attached to the particle and migrates with it as a kinetic unit. It could be the same as ρ, or it could have a value either less than or greater than ρ; for example, if the solution contained inorganic salts or sucrose and the solvating medium was only water, d would be less than ρ. Alternatively, some attraction may exist between the macromolecules and the third component, which is more dense than water; for this situation, $d > \rho$. The force on the solvated particle is written, as before, in the form $\omega^2 x[m + hd - (v + h)\rho]$. When this is equated to the frictional force and the equation rearranged, we obtain

$$s = \frac{M\left[1 - \bar{V}\rho + \frac{h}{m}(d - \rho)\right]}{Nf} \tag{134}$$

This formulation (Schachman and Lauffer, 1950) shows clearly that the product, Nsf, is affected by the presence of a third component unless (*1*) $h = 0$ (no interaction), or (*2*) $d = \rho$ (the interaction is not preferential). For either of these situations, Eq. (134) reduces to Eq. (123) as did the two-component system which exhibited interaction between the solute and solvent. It is important to note that another term could be added for the combination of the macromolecule with solution having a density, ρ. This term would, of course, appear in the mass of the sedimenting unit and, as well, in the term representing the mass of the displaced liquid. As a consequence, such interactions would cancel from the equation and be reflected only in the frictional term. Thus the term expressing the effective mass is influenced solely by preferential interactions between the macromolecule and one of the components in a binary solvent. That this result is obtained also by macroscopic theories was shown by Wales and Williams (1952), Ogston (1954), and Katz and Schachman (1955). The latter workers employed a treatment analogous to that of Goldberg (1953) by wiriting for the chemical potential, μ, of the sedimenting unit

$$\mu = \mu_2 + (kn_1 + \alpha)\mu_1 + kn_3\mu_3 \tag{135}$$

where (2) refers to the anhydrous macromolecule, (1) refers to the solvent component present in excess, usually water, and (3) corresponds to the

additional component, say sucrose, urea or D_2O. In writing the equation in this form, it was assumed that $(kn_1 + \alpha)$ molecules of water and kn_3 molecules of the third component were associated with the macromolecule, where k is a proportionality constant, n_1 and n_3 are the total number of molecules of components 1 and 3 in the ultracentrifuge cell, and α is designated as the preferential adsorption coefficient for water. By varying k and α, all possibilities are encompassed. In particular, if $\alpha = 0$ and $k = 0$, the sedimenting unit contains no components of the solvent; if $\alpha = 0$ and $k > 0$, the associated solvent has the same composition as the bulk binary solvent, and finally if $k > 0$ and $\alpha \neq 0$, there will be preferential binding of either water ($\alpha > 0$) or the third component ($\alpha < 0$). Differentiation of Eq. (135) with respect to pressure, assuming that the coefficients are independent of pressure, gives an expression for the molar volumes $(M\bar{V})$. This can be combined with Eq. (123), written for the sedimenting unit at infinite dilution, to give

$$s = \frac{M_2(1 - \bar{V}_2\rho) + \alpha M_1(1 - \bar{V}_1\rho) + kn_1 M_1(1 - \bar{V}_1\rho) + kn_3 M_3(1 - \bar{V}_3\rho)}{Nf} \quad (136)$$

It is readily shown that the last two terms are equal to zero if the solution is infinitely dilute with regard to component 2. Thus Eq. (136) reduces to

$$s = \frac{M_2(1 - \bar{V}_2\rho) + \alpha M_1(1 - \bar{V}_1\rho)}{Nf} \quad (137)$$

which is, of course, directly analogous to Eq. (134). The values of kn_1 and kn_3, no matter how large, have no effect on the product, Nsf, for infinitely dilute solutions of the macromolecule.

Both of these approaches show clearly that preferential interaction requires the inclusion, in the force equation, of a term allowing for this effect. If the third component is present in small amount, the density of the solution, ρ, will be nearly equal to $(1/\bar{V}_1)$, and the second term in Eq. (137) is small. Thus the neglect of this term in all experiments with proteins in dilute solutions of electrolyte does not lead to serious errors. Ogston (1954) has illustrated this with numerical calculations for salt solutions of different concentrations. When, however, large concentrations of sucrose, urea, or electrolytes, for example, are added to the solution, a large increase in ρ occurs, and the second term in Eqs. (134) or (137) may no longer be considered negligible (unless it is demonstrated that $\alpha = 0$). This effect is also present in light scattering measurements as shown experimentally by Ewart *et al.* (1946) in studies on polystyrene in pure and mixed solvents. When the solvents differed in refractive index, the molecular weight calculated from the simple theory for two-component systems was greatly in

error. If the refractive indices of the two components in the solvent mixture were alike, no error resulted. By a simplified treatment Ewart *et al.* (1946) were able to show the relationship between the turbidity (or molecular weight) and a selective adsorption coefficient. Since then, the theory for light scattering in multicomponent systems has been generalized by Kirkwood and Goldberg (1950) and Stockmayer (1950). These workers found that the thermodynamic interaction between the macromolecules and one of the components of the solvent may induce fluctuations in concentration of the latter which are comparable to the fluctuations in composition with respect to the macromolecules themselves. Thus the turbidity, and hence the molecular weight, may be markedly affected by such selective interactions. These theories showed that the selective adsorption coefficient, α, can be written (Wales and Williams, 1952; Katz, 1956)

$$\alpha = (\partial m_3/\partial m_2)_{T,P,\mu_3} = -(\partial \mu_3/\partial m_2)_{T,P}/(\partial \mu_3/\partial m_3)_{T,P} \qquad (138)$$

where m refers to the molality.[12] Katz (1956) has emphasized that α can also be determined from equilibrium dialysis measurements.

For some time now, research workers have attempted to measure the hydration of viruses by comparing the so-called "dry density" (assumed to be the reciprocal of the partial specific volume) with the "hydrated density." Any difference between the two values was attributed to hydration. Since the sedimentation rate is so intimately involved with both the partial specific volume of the solute and the density of the solution, it is not surprising to note the extensive literature devoted to this problem. "Hydrated densities" have been evaluated by determining the density of solution, ρ^0, in which the virus particles neither sediment nor float ($s = 0$). Various agents including glycerol, sucrose, and urea have been added to aqueous solutions of vaccinia virus (MacCallum and Oppenheimer, 1922; Smadel *et al.*, 1938) and herpes virus (Bechhold and Schlesinger, 1931) in order to increase the density and, thereby, to decrease the sedimentation rate. By extrapolating the plot of ηs versus ρ, the density corresponding to zero sedimentation rate was readily evaluated. Often these plots are straight lines, but occasionally they are curved, and procedures for the latter were based largely on the suggestions of Smadel *et al.*, 1938. For a detailed discussion of this aspect of the problem, the reader is referred to

[12] This equation is presented here in the form written by Wales and Williams (1952) and by Katz (1956). In this form α provides a measure of the selective adsorption of component (3) to the macromolecules. Prior to this, e.g. Eq. (137), the selective hydration of the macromolecules was being considered, and α was being employed as a measure of the preferential "binding" of water to the macromolecules. Both Eqs. (137) and (138) can be written for the selective interaction between the macromolecules and either of the two components of the solvent.

Lauffer and Bendet (1954). In at least one study (Lauffer *et al.*, 1952), the densities achieved were so high that the virus particles were caused to float, thereby permitting the determination of ρ^0 with high precision by interpolation of the data. As the number of these investigations increased, several different viruses like influenza virus, tobacco mosaic virus, and southern bean mosaic virus were examined in solutions containing various solutes like D_2O, sucrose, and serum albumin (Lauffer and Stanley, 1944; Sharp *et al.*, 1944, 1946b; Schachman and Lauffer, 1949; Miller and Price, 1946; Lauffer *et al.*, 1952; Lauffer and Taylor, 1953a). Materials other than viruses have also been examined in this way; these include botulinum A toxin (Lauffer and Taylor, 1953b), deoxyribonucleic acid (Katz and Schachman, 1955), and the hyaluronic acid complex (Blumberg and Ogston, 1956). As a result of these studies, it is now apparent that the value of ρ^0 for a given macromolecule depends on the nature of the third component. For tobacco mosaic virus in sucrose solutions, $\rho^0 = 1.27$ g./ml., whereas $\rho^0 = 1.13$ g./ml. for the virus sedimenting in serum albumin solutions (Schachman and Lauffer, 1949). Extensive data with essentially the same results are also available for southern bean mosaic virus (Lauffer *et al.*, 1952). These experiments have been summarized and discussed by Lauffer and Bendet (1954) in a review dealing with the problem of the determination of the hydration of viruses.

In order to relate ρ^0 to a property of the sedimenting unit, the term, $M[1 - \bar{V}\rho + h/m(d - \rho)]$ is rearranged to give $M_c(1 - \bar{V}_c\rho)$ where $M_c = N(m + hd)$ and $\bar{V}_c = (v + h)/(m + hd)$. When $s = 0$, the term, $(1 - \bar{V}_c\rho^0)$ must equal zero and, therefore, $\rho^0 = 1/\bar{V}_c$ (the subscript, c, refers to the complex described earlier). Most experimental data resulting from such studies have, in fact, been reported in this form to give a partial specific volume of the hypothetical particle. It seems more meaningful, however, to calculate another parameter instead (Katz and Schachman, 1955; Ogston, 1954). According to Eq. (137), the value of ρ^0 can be related to α by the following

$$\alpha = -\frac{M_2(1 - \bar{V}_2\rho^0)}{M_1(1 - \bar{V}_1\rho^0)} \tag{139}$$

Thus, measurement of ρ^0 and knowledge of the molecular weights and partial specific volumes of the different components gives α, the coefficient describing the preferential interaction. It should be noted that ρ^0 in conjunction with $\bar{V}_2$ cannot be used to calculate the hydration if by the latter is meant all of the medium associated with the macromolecule as a kinetic unit. For example, the binding of 1 ml. of sucrose solution (with the same composition as the bulk solvent) to 1 g. of protein would not be detected by this method, although, to many workers, this is a logical description

of solvation. But the absence of sucrose molecules, for any reason, in 0.2 ml. of the total solvating medium would be detected with ease, and the conclusion may be drawn, perhaps erroneously depending on a particular point of view, that only 0.2 ml. of solvent were associated with each gram of dry protein. Selective solvation alone is measured by this technique, and resort to other methods is required if knowledge of the total amount of liquid associated kinetically with the protein is desired. Though these other methods, too, are not free of theoretical and experimental limitations, they are beyond the scope of the present discussion, and the reader is referred to the review by Lauffer and Bendet (1954).

No indications of the forces responsible for the selective solvation have been given in the above treatment. They may be attractive in nature; however, another factor has been implicated, apparently successfully, to explain the results with tobacco mosaic virus (Kauzmann, cited by Schachman and Lauffer, 1949). If the sucrose or albumin molecules are considered to be rigid, uncharged spheres of radius, a, it is clear that the center of any of these molecules will not be able to come closer than a distance, a, to the "surface" of the sedimenting particle. This results in a region of thickness, $2a$, surrounding the macromolecules in which the density varies from that of water to that of the solution. According to Kauzmann, this region of varying density can be approximated by assigning a water layer of thickness, a, to the macromolecules and assuming that the liquid more distant than a from the surface of the macromolecule has the density of the bulk liquid. Here only a steric argument is considered, but other factors such as electrostatic attraction or repulsion can be imposed. Thus the mixed solvent cannot be considered as a one-component solvent, and the selective adsorption, as measured by α, may be nothing more than a reflection of steric exclusion of the larger molecules in the binary solvent. This interpretation proposed by Kauzmann has provided apparently satisfactory explanations for the results with the rodlike and spherical virus particles, (Schachman, and Lauffer, 1949; Lauffer *et al.*, 1952), deoxyribonucleic acid (Katz and Schachman, 1955), and the hyaluronic acid complex (Blumberg and Ogston, 1956). These papers should be consulted for detailed information because the use of α in conjunction with the hypothesis of Kauzmann does provide interesting information about the selective permeability of the macromolecules (see Katz and Schachman, 1955). This concept of steric exclusion has been the subject of a more detailed investigation by Katz (1956) in terms of free volume theory, and his conclusions provide a basis for tentative estimates of the potential errors in studies of proteins in 6 M urea, for example.

When D_2O is employed in these studies to increase the density of the solutions, it has been found that the value of ρ^0 (obtained, to be sure, by

a hazardous extrapolation) corresponds to $1/\bar{V}_2$. Thus Sharp and Beard (1950) and Cheng and Schachman (1955a) obtained the partial specific volume of polystyrene latex particles this way. Much earlier, Svedberg and Eriksson-Quensel (1936) found that ρ^0 for hemocyanin corresponded closely to the reciprocal of the partial specific volume. Also Sharp *et al.* (1950) and Sharp and Beard (1954) have used this method for the determination of $\bar{V}$ for several animal viruses. For smaller or more slowly sedimenting materials as well, this method has given results in accord with the classic method of determining $\bar{V}$ (Katz and Schachman, 1955; Martin *et al.*, 1956). In using this method, it is tacitly assumed that $\alpha = 0$, which seems plausible. A more detailed analysis of this is given by Katz (1956). It should be noted that ρ^0 in D_2O solutions gives $\bar{V}$ for the deuterated solute; in this regard, H_2O^{18} would be a preferable reagent.

Often proteins are examined for special reasons in aqueous solutions containing large amounts of urea or other reagents (e.g., Gutter *et al.*, 1956), and for comparative purposes the observed sedimentation coefficients are corrected to the standard state (a medium with the viscosity and density of water at 20°C.) by means of Eq. (26). Such a procedure may lead to serious errors if there is selective solvation, as was demonstrated with data for tobacco mosaic virus in 40% sucrose solutions (Schachman and Lauffer, 1950). If $\bar{V}_2$ was employed in Eq. (26), a value of 128 S for $s_{20,w}$ resulted, whereas the use of $\bar{V}_c$ (evaluated from ρ^0) gave 174 S for $s_{20,w}$. The latter value was in excellent agreement with that obtained directly in buffered solutions containing no sucrose. In the absence of sufficient data for the measurement of ρ^0 and for systems of materials which are presumably inert (like sucrose but probably not urea), an estimate of $\bar{V}_c$ can be made through the implementation of Kauzmann's suggestion about the exclusion of the third component from the immediate vicinity of the macromolecule. It should be recognized, however, that this is only an approximation. Multicomponent systems have been involved in other types of investigations as well. Sihtola and Svedberg (1948) have studied the solvation of cellulose nitrate. For these experiments they used a binary solvent composed of a good solvent and a nonsolvent, and they assumed that there was interaction between the macromolecule and only the good solvent. Their determination consisted, in effect, of the measurement of the enrichment of the nonsolvent in the supernatant behind the sedimenting polymer boundary.

Thus far in the discussion of multicomponent systems, only the effective mass has been treated, and consideration of the frictional term has been postponed. This is not wholly accidental. Little is known about this factor as compared with the former. To be sure, neglect of consideration of the frictional term in multicomponent systems is likely to produce only small errors, but assuredly there will be errors and developments in this

area are eagerly awaited. Ogston (1954) discussed this problem briefly and pointed out that it is tacitly assumed that the migration of the macromolecules does not alter the relative motion that the electrolyte and water would experience in the absence of the macromolecule. This is tantamount to consideration of the binary solvent as a one-component solvent, and its validity in a strict sense is doubtful. Recently, this problem has been receiving careful scrutiny in diffusion studies of multicomponent systems (see Gosting, 1956). With strong electrolytes, it is known that the flows of the individual components are not independent, and the flow of one solute can induce the flow of a second even in the absence of a concentration gradient of the latter. Thus the application of Fick's law separately to each individual component is not valid. Because of the interacting flows which have been demonstrated experimentally, the individual flow equations require revision so as to contain terms for the concentration gradient of each solute. Thus four diffusion coefficients are necessary to describe the flow of two solutes in a three-component system (Gosting, 1956; Dunlop, 1957). Whether the cross-term diffusion coefficients, D_{21} and D_{12}, are negligible for protein solutions containing added electrolyte is not yet known. It has been demonstrated, however, in the system containing raffinose and potassium chloride in water, that the cross-term diffusion coefficients were by no means negligible compared with the main diffusion coefficients, D_{22} and D_{11} (Dunlop, 1957). With the present limited precision in measurement of sedimentation coefficients, which in general is less than in the determination of diffusion coefficients, these factors are likely to be unimportant. However, it is clear that this problem requires much theoretical and experimental investigation, and with improvements in the accuracy of sedimentation experiments, neglect of these factors will no longer be admissable. In this regard, Baldwin (1958) has recently derived an expression for the sedimentation coefficient in terms of the molecular weight and diffusion coefficients in multicomponent systems. This equation resulted from application of the flow equations of Hooyman (1956) for a solute in a centrifugal field. It is presented here, despite the fact that no application of it has been reported to date, because it is the only treatment proposed thus far which considers both factors (the effective mass and the frictional term) in rigorous fashion.[13] For infinite dilution

[13] This treatment has now been presented in greater detail and extended to include charge effects (Williams *et al.*, 1958). It should be noted that the approach using thermodynamics of irreversible processes includes a term for the electrostatic potential gradient, but the theory specifically avoids considerations of the influence of charge as either primary or secondary charge effects. From an operational point of view the latter description possesses merit since it is useful in the design of experiments. It should be emphasized, however, that specific interactions which may alter the sedimentation properties of a protein are not predictable in the same way as are

of the macromolecule (2), the sedimentation coefficient can be written

$$s_2 = \frac{M_2(1 - \bar{V}_2\rho)D_{22}}{RT} \cdot \left\{1 + c_3\left[\frac{M_3(1 - \bar{V}_3\rho)}{M_2(1 - \bar{V}_2\rho)}\right]\left[\frac{\frac{1}{D_{22}}\left(\frac{\partial D_{23}}{\partial c_2}\right)_{c_3,T,P} - \left(\frac{\partial \ln \gamma_2}{\partial c_3}\right)_{c_2,T,P}}{1 + c_3\left(\frac{\partial \ln \gamma_3}{\partial c_3}\right)_{c_2,T,P}}\right]\right\} \quad (140)$$

The diffusion coefficient, D_{22}, is the main diffusion coefficient for the macromolecules and D_{23} is the cross-diffusion coefficient (in this equation the subscript 3 refers to the electrolyte or other solute since 1 has been reserved for water in the previous discussions). Dunlop (1957) has emphasized the errors resulting from the use in the Svedberg equation of diffusion coefficients from three-component systems when suitable corrections are not applied.

6. The Frictional Coefficient

For about 20 years now, sedimentation coefficients, in conjunction with other data such as the diffusion coefficient and partial specific volume, and on occasion the intrinsic viscosity, have been used to calculate the shape and hydration of proteins and other macromolecules of biological interest. So routine has the practice become of inserting the experimental data into the theoretical equations that frequently sight has been lost of the background of the theories and the assumptions implicit in their use. First and foremost is the portrayal of the macromolecule in the form of a particular model having well-defined parameters and properties. Only spherical particles and ellipsoids of revolution were considered at first as models for macromolecules, but with the synthesis of many nonbiological macromolecules, for which rigid spheres and ellipsoids of revolution seemed inappropriate, hydrodynamic theories have been developed for these flexible chain polymers as well. It is generally agreed that the rigid ellipsoids of revolution (a sphere can be considered as a special case with an axial ratio equal to unity) are the most plausible models for simulating native protein molecules. This is not to say, however, that a given protein in solution is a rigid ellipsoid of revolution having a smooth surface. Rather it is thought that the hydrodynamic behavior of many

the primary and secondary charge effects. Another theoretical treatment using the methods of irreversible thermodynamics has just appeared (Peller, 1958). He treated the problem of multicomponent systems in the ultracentrifuge with special reference to those experiments which were presumed to measure the "hydration" of macromolecules. This treatment produced the same result as that given earlier, Eqs. (137) and (139).

proteins can be accounted for most satisfactorily by such a postulated rigid structure. Thus flexibility, deformability, and permeability, though slight or extensive, are overlooked, and the real protein molecule is treated as though it were a rigid ellipsoid of revolution. Such rigid models seem especially inappropriate for denatured proteins, many preparations of ribonucleic acid, polysaccharides of large molecular weight such as dextrans, and hyaluronic acid. Nonetheless, the literature is replete with calculations, even to tenths of angstroms, of the length and thickness of these materials for which rodlike models (prolate ellipsoids) were taken for granted. Deoxyribonucleic acid would appear to represent a special case not belonging clearly to any single category. Though certainly not prolate ellipsoids, these macromolecules also can not be represented adequately by random polymeric chains. Thus models having properties intermediate between the rigid ellipsoids and the flexible chains are required to satisfy the experimental data for this important substance. To some extent, progress is being made in theoretical investigations into the frictional resistance experienced by stiff chainlike particles in their movement through a viscous medium.

Several detailed reviews have become available recently (Scheraga and Mandelkern, 1953; Ogston, 1953; Sadron, 1953; and Edsall, 1953) to supplement the slightly older discussions (Svedberg and Pedersen, 1940; Oncley, 1941; Cohn and Edsall, 1943; and Lauffer, 1944a) on the problems of interpreting the frictional coefficients evaluated from the hydrodynamic data. Differences of opinion and emphases are apparent, to be sure, but the divergence of views is not so wide as may at first sight appear. Some reconciliation is feasible because the differences are attributable not so much to conflicts on theory as to the conceptions held by the various workers as to the nature of a protein molecule in solution. With the present rate of growth of knowledge of proteins, the nature of such molecules in solution should not remain for long an issue of controversy.

Basic to all formulations of the frictional resistance experienced by a particle moving in a viscous medium is the theoretical work of Stokes (1851) which led to the familiar law bearing his name.

$$f = 6\pi\eta r \tag{141}$$

This treatment is restricted to rigid, uncharged, spherical particles of radius, r, migrating in a liquid with viscosity, η, and the particles are considered to be large compared to the molecules in the medium so that the latter can be treated as continuous. It is assumed further that no slippage occurs between the moving particle and the medium. Stokes considered the movement of one particle in a medium and the viscosity corresponds, therefore, to the solvent; data at finite concentrations should

be extrapolated to infinite silution. Modifications of this equation have been made to account for some slippage at the surface of the particles and for wall effects. For small molecules, it is clear that the basic requisites of Stokes' law are not fulfilled, and it is difficult to know exactly how large a particle must be in order for the medium to be considered a continuum. No models of known radius, with a size comparable to proteins, have yet been discovered, and tests of Stokes' law until recently were confined to objects sufficiently large to be seen with ordinary light microscopes. With the use of polystyrene latex particles for calibration purposes in electron microscopy, an opportunity became available to test Stokes' law with models only 5 to 10 times larger than some of the spherical virus particles (Sharp and Beard, 1950; Cheng and Schachman, 1955a). From sedimentation velocity measurements in a series of H_2O-D_2O mixtures, the latter workers obtained the value, 2640 A., for the radius of the particles in excellent agreement with the values, 2600, 2720, and 2730 A. from electron microscopy, light scattering, and low angle X-ray scattering, respectively. Moreover, these particles were shown to be impermeable and not solvated, having a partial specific volume equal to their bulk specific volume. Einstein's viscosity equation was tested as well, and the experimental results were in excellent accord with the Einstein equation. That these results were in accord with the theories lends confidence to the use of these equations, or appropriate modifications of them, with the larger spherical viruses. It should be noted, however, that many protein molecules, if considered for the moment to be rigid spheres of uniform density, would have a radius only one-hundredth that of the latex particles. The demonstration of the validity of Stokes' law for materials of such a size is lacking.

It was recognized very early that many of the macromolecules under investigation were probably not spherical. Workers turned, therefore, to the equations of Perrin (1936) and Herzog *et al.* (1934) for the frictional resistance experienced by ellipsoids of revolution in their movement through viscous media. The frictional coefficients were calculated for ellipsoids with axes oriented in various directions relative to their direction of motion. To give a resultant frictional coefficient characteristic of particles experiencing rotational Brownian motion, the individual coefficients were averaged, and the final equations, one for prolate ellipsoids and the other for oblate ellipsoids, were expressed as the frictional ratio, f/f_0, in terms of the axial ratio. (f_0 is the frictional coefficient of a sphere having a volume equal to that of the ellipsoid). From values of f/f_0 the axial ratio can be calculated either from tables (Svedberg and Pedersen (1940), p. 41 and Cohn and Edsall (1943), p. 406, also see Table IX) or plots of the Perrin equation. If f/f_0 is unity, the particle must be spherical.

The frictional coefficient depends not only on the shape but also on the volume of the sedimenting particles, and this fact must be included in any treatment of sedimentation data. Implicit in most treatments of ultracentrifuge and diffusion data in terms of the shape of the protein mole-

TABLE IX

Dependence of Viscosity Increment, Frictional Ratio, and Combined Parameter, β, on Axial Ratio

Axial ratio	Prolate			Oblate		
	ν[a]	f/f_0[b]	β[c] ($\times 10^{-6}$)	ν	f/f_0	β
1	2.50	1.000	2.12	2.50	1.000	2.12
2	2.91	1.044	2.13	2.85	1.042	2.12
3	3.68	1.112	2.16	3.43	1.105	2.13
4	4.66	1.182	2.20	4.06	1.165	2.13
5	5.81	1.255	2.23	4.71	1.224	2.13
6	7.10	1.314	2.28	5.36	1.277	2.14
8	10.10	1.433	2.35	6.70	1.374	2.14
10	13.63	1.543	2.41	8.04	1.458	2.14
12	17.76	1.645	2.47	9.39	1.534	2.14
15	24.8	1.784	2.54	11.42	1.636	2.14
20	38.6	1.996	2.64	14.8	1.782	2.15
25	55.2	2.183	2.72	18.2	1.908	2.15
30	74.5	2.356	2.78	21.6	2.020	2.15
40	120.8	2.668	2.89	28.3	2.212	2.15
50	176.5	2.946	2.97	35.0	2.375	2.15
60	242.0	3.201	3.04	41.7	2.518	2.15
80	400.0	3.658	3.14	55.1	2.765	2.15
100	593.0	4.067	3.22	68.6	2.974	2.15
200	2051.0		3.48	136.2		2.15
300	4278.0		3.60	204.1		2.15

[a] ν refers to the viscosity increment and corresponds to the intrinsic viscosity when concentration is expressed as volume fraction (from Mehl *et al.*, 1940).

[b] Calculated from Perrin's equation (1936) and tabulated by Svedberg and Pedersen (1940, p. 41).

[c] $\beta = [N/16{,}200\pi^2]^{1/3}(f_0/f)\nu^{1/3}$; calculated and tabulated by Scheraga and Mandelkern (1953).

cules (Oncley, 1941) was the assumption that the volume of the sedimenting unit was either equal to the partial molar volume divided by Avogadro's number (i.e., the volume of a single molecule) or just slightly greater than that value. To encompass the latter situation, the protein was considered to be hydrated, and the volume of the sedimenting particle was thought to be made up of two parts, the anhydrous protein and water of hydration; this can be written as $(M\bar{V}/N)(1 + w/\bar{V}\rho)$ where w is the hydration as

g. H_2O/g. protein. This hypothetical, hydrated particle was then considered as a Stokes sphere, and its frictional coefficient was written in the conventional manner in terms of its radius.

In order to encompass both volume and shape, Oncley (1941) suggested a procedure which has been adopted widely. The frictional coefficient, f, is written

$$f = (f/f_0)f_0 \tag{142}$$

and (f/f_0) is separated into two parts which can be formulated as $(f/f_0)_s \cdot (f/f_0)_h$ where s and h signify the frictional ratios for the shape and hydration factors, respectively. When these are combined, the over-all frictional coefficient can be written

$$f = \left(\frac{f}{f_0}\right)_s \left(1 + \frac{w}{\bar{V}\rho}\right)^{1/3} 6\pi\eta \left(\frac{3M\bar{V}}{4\pi N}\right)^{1/3} \tag{143}$$

Oncley (1941) presented a contour diagram for $(f/f_0)_s(f/f_0)_h$ in terms of the axial ratio and hydration. It is clear from this treatment that the value of f determined experimentally is compatible with many combinations of axial ratio and hydration. If the hydration is assumed to be zero, then a maximum axial ratio can be calculated; alternatively, if it is assumed that the particles are spherical, a maximum value of the hydration can be inferred directly. Neither factor can be evaluated without knowledge of the other. Analogous considerations of the volume and shape of macromolecules in terms of the intrinsic viscosity led to a similar formulation. Here, too, the volume of the dissolved phase is important as shown by Einstein (1906) for spherical particles, and the shape problem can be treated by consideration of ellipsoids of revolution (Simha, 1940). A contour diagram was presented for this combined relationship by Mehl *et al.* (1940). The experimental values of (f/f_0) and $[\eta]$, the intrinsic viscosity, were inserted into these convenient contour diagrams, and a combination of shape and hydration parameters was thus obtained which satisfied the experimental data. By inspection of these combined parameters obtained from the two types of experimental data, by making reasonable approximations of the experimental errors, and by using other auxiliary data, Oncley (1941) estimated both the shape and hydration of many protein molecules. Soon an imposing list of proteins were examined by such procedures, and before long a given value of the hydration was taken for granted, and only the shape factor was considered as unknown. This was clearly an unwarranted extension of the procedure employed by Oncley (1941), who considered both the shape and hydration as unknowns which could be evaluated only by combination of two independent parameters, each of which was a function of the two desired quantities. This pitfall was avoided by Scheraga and Mandelkern (1953), who combined

the Perrin and Simha equations into a single function treating both the volume and shape of the ellipsoids as unknown. Thus the combination of both (f/f_0) and $[\eta]$ led to a unique solution for the axial ratio and thence for the volume of the ellipsoid. Closely similar views have been presented by Sadron (1953) and, since then, by Ogston (1953).

In their discussion of this problem, Scheraga and Mandelkern raised important questions about identifying the hydrodynamically effective volume with that calculated from the partial specific volume as modified to some extent by water of hydration. Instead, they proposed that the experimental quantities be used to calculate the volume and shape of an effective hydrodynamic ellipsoid. Whether this effective particle is equivalent to the protein molecule in solution depends on the nature of the macromolecule. If it is completely rigid and impermeable to solvent, the parameters for the actual configuration and the effective particle would coincide. On the other hand, the dimensions calculated for the equivalent rigid ellipsoid would have little in common with those of the real molecule, if the latter is a voluminous and slightly deformable particle through which some solvent permeates during its movement through the medium. Denatured proteins in 6 M urea would almost certainly constitute an example of this class, and calculations of its hydration (in terms of a slight perturbation of the molar volume divided by Avogadro's number) would scarcely be meaningful. This is especially true if hydration is considered in stoichiometric terms as the result of strong interactions between the water dipoles and specific groups on the protein molecule. A lack of correspondence between the dimensions of the effective ellipsoid and the real particle is also introduced if the latter does not obey faithfully Stokes' law (or the modification of it according to Perrin). In view of these ambiguities, it seems advisable to consider the volume and axial ratios as unknowns and to treat the experimental data in the manner suggested by Scheraga and Mandelkern (1953). Then the effect of potential errors on the calculated parameters can be assessed, and their impact discussed in relation to the structure of the macromolecules.

The volume of the effective hydrodynamic ellipsoid is written as V_e and its axial ratio as p. Since the specific viscosity, η_{sp}, of a dilute solution is proportional to the volume fraction and a factor, ν, related to the shape of the macromolecules, the following relationship follows:

$$\eta_{sp} = \left(\frac{cN}{100M}\right) V_e \nu \tag{144}$$

or

$$[\eta] = \left(\frac{N\nu}{100}\right)\left(\frac{V_e}{M}\right) \tag{144a}$$

where c is the concentration in g./100 ml., and ν is the viscosity increment evaluated by Simha (1940) for ellipsoids of varying axial ratio. Similarly, the frictional coefficient, f, can be written in terms of the volume of the effective particle, where f_0 corresponds to a sphere having the same volume

$$f = 6\pi\eta \left(\frac{3V_e}{4\pi}\right)^{1/3} \left(\frac{f}{f_0}\right) \tag{145}$$

These expressions are then combined with Eq. (123), and the term for the volume is eliminated to give (Scheraga and Mandelkern, 1953)

$$\beta = \frac{Ns[\eta]^{1/3}\eta}{M^{2/3}(1 - \bar{V}\rho)} = (N/16{,}200\pi^2)^{1/3}\nu^{1/3}/(f/f_0) \tag{146}$$

The right-hand side of Eq. (146) provides a definition of β as a function only of the axial ratio of the ellipsoid of revolution. Values of β were calculated from the Perrin and Simha equations, yielding the results shown in Table IX.

It is striking that β is almost totally independent of axial ratio for oblate ellipsoids and varies only slowly for prolate ellipsoids. This constitutes both a disadvantage and an advantage depending on the object of the investigation. If precise shapes of the macromolecules are of interest, the outlook is not encouraging since an error of only 1 or 2% in β leads to widely different values of the axial ratio. On the other hand, this insensitivity of β to axial ratio can be exploited for molecular weight calculations from sedimentation and viscosity data. Inspection of the results tabulated by Scheraga and Mandelkern (1953) and Ogston (1953) for a variety of macromolecules reveals that the β values for proteins are quite similar. Only tentative conclusions can be drawn from such an appraisal, however, since it is doubtful if many of the experimental values reported therein will survive unscathed after re-examination by the more precise techniques now extant. With this reservation, a value of 2.16×10^6 for an average β can be selected and Eq. (146) rearranged, with the grouping of all of the constants, to yield

$$M = \frac{4690(s_{20,w})^{3/2}[\eta]^{1/2}}{(1 - \bar{V}\rho)^{3/2}} \tag{147}$$

where s is reported in svedbergs and $[\eta]$ in $(\text{g./100 ml.})^{-1}$. Proteins with higher β values do exist and, for them, this equation gives misleading results. However, this equation is likely to give values accurate to about 5 to 10% for many proteins.

Values of β equal to 2.04×10^6 have been reported for serum albumin (Tanford and Buzzell, 1954, 1956; Harrington *et al.*, 1956; Loeb and Scheraga, 1956). This is certainly less than the minimum value possible

for rigid ellipsoids of revolution of any shape, but this apparent discrepancy may be attributed to present limitations in experimental precision. Careful studies on the same preparation under identical conditions are eagerly awaited before this question can be resolved. Until the results of such experiments become available, speculations and debates on the significance of values less than 2.12×10^6 are likely to be unprofitable.

After β is determined, the corresponding values of ν or (f/f_0) are read from Table IX and the effective volume, V_e, is calculated from either Eq. (144*a*) or Eq. (145). With these results for the axial ratio and the volume, the dimensions of the ellipsoid having hydrodynamic properties identical to the sedimenting unit are readily calculated. Of the two parameters, (b/a) and V_e, the latter may in the long run prove more interesting, though for years the shape of macromolecules has been the focal point of interest to protein chemists. If the value of V_e is not much larger than that derived from the partial specific volume, it can be concluded that the hydrodynamic unit is very compact, imbibing only a little water. On the other hand, V_e may be much larger, say 5 to 10 times larger, than that calculated from the partial specific volume. This would indicate a voluminous particle, and a report of the hydration of such an entity seems a distortion of the concept of hydration. For such materials, it seems preferable to present the results as the effective volume per gram, a value which can be compared readily with the partial specific volume. The difference between these values may provide the basis for speculations on the structure of the macromolecules. There is no theoretical basis for relating these values (for expressions of differing opinions see Tanford, 1957 and Scheraga and Mandelkern, 1958). Empirically, however, such a comparison may be revealing. If secondary and tertiary structures of protein molecules maintain a high degree of perfection in linking remote regions of the polypeptide chains into a compact macromolecule, then the effective specific volume is likely to be very similar to the partial specific volume. When such intramolecular organization is disrupted without a decrease in molecular weight, the effective volume will increase considerably, whereas, the partial specific volume is hardly altered. As more precise data become available, the experimental relations between V_e and the volume of the molecular domain, as determined for example from low angle X-ray scattering, may prove useful. Then correlations including, as well, the partial specific volume and the often neglected bulk specific volume may provide the background for profitable speculations.

Materials for which V_e proved to be the more interesting factor include polymers of sarcosine (Fessler and Ogston, 1951), the hyaluronic acid complex (Ogston and Stanier, 1951, 1952), and dextran (Ogston and

Woods, 1953). These concepts were also invoked by Scheraga and Mandelkern (1953) to account for the data of Neurath and Saum (1939) on the effect of urea on serum albumin. Another example includes the effect of acid on serum albumin (Yang and Foster, 1954; Harrington *et al.*, 1956; Tanford and Buzzell, 1956; Loeb and Scheraga, 1956). For an interesting discussion of the ambiguities encountered in the analysis of (f/f_0) in terms of shape and effective volume, the reader is urged to examine the data for fibrinogen (Shulman, 1953b; Scheraga *et al.*, 1954).

At the other extreme is the work of Lauffer (1944a, and earlier references) on tobacco mosaic virus. This may be considered a triumph of physical chemical methods, because the prediction of the size and shape of these now familiar rodlike particles on the basis of sedimentation and viscosity data was, at a later date, confirmed by direct visualization of the particles in the electron microscope. In this instance, evidence was available that the particles contained very little water and were rigid. Thus, the axial ratio and then the actual dimensions were calculated from the experimental data. To be sure, the value of β evaluated from all of the existing data leads to a smaller axial ratio than is currently accepted on the basis of electron microscopy. However, it should be noted that β gives the axial ratio corresponding to the hydrodynamic unit and not the dry particle, and much of the data employed in the estimation of β requires revision. If, as suspected, the hydrodynamic unit is just a slightly swollen rodlike particle where the swelling is isotropic, the axial ratio calculated from the hydrodynamic data can be shown to correspond to the anhydrous particle. Thus the hydrodynamic and electron microscopic evidence agree. As Lauffer (1944a) pointed out, the sedimentation coefficient of long rodlike particles is relatively insensitive to length. This concept was expressed quantitatively by Peacocke and Schachman (1954) in considerations of the configuration of deoxyribonucleic acid. By combining Perrin's equation with Eq. (123), they were able to derive an expression for very long anhydrous particles,

$$s = 0.222 \frac{1 - \bar{V}\rho}{\bar{V}\eta} a^2 \ln (2b/a) \tag{148}$$

where b is the long semiaxis and a is the short semiaxis of the ellipsoid of revolution. An equation of this form was given much earlier by Signer (see Svedberg and Pedersen, 1940, p. 435). With this equation and the measured sedimentation coefficient and partial specific volume, a value of 25 A. was estimated for the thickness of deoxyribonucleic acid (Peacocke and Schachman, 1954). Even if the particles are not completely straight, as long as they are very anisometric and the radius of curvature is sufficiently large so that nonbonded segments of the same molecule are not

very close to one another, it is probable that the frictional coefficient increases directly with the molecular weight. As a consequence, the sedimentation coefficient measures the mass per unit length and hence the thickness (or diameter). This thickness for deoxyribonucleic acid is similar to that inferred from other structural information for that material. Since its application to sedimentation data for deoxyribonucleic acid, Eq. (148) has also been employed for the interpretation of the sedimentation behavior for collagen (Boedtker and Doty, 1956; Nishihara and Doty, 1958) and for tobacco mosaic virus (Boedtker and Simmons, 1958).

Flexible chainlike polymers have also been the subject of considerable scrutiny by physical chemical methods, and theories have dealt with the frictional coefficient of such materials. Though these theoretical treatments have found little application in biochemical studies, it is pertinent to present here some brief comments about the models that have been proposed. First of these is the so-called free-draining coil. In this model, the chemical groups, considered as solid, small beads, are held together by rigid links which are connected at a fixed angle with freedom to rotate relative to one another. This leads to a random, flexible chain structure with a configuration described by "random flight" statistics analogous to that employed in the description of the path of a freely diffusing molecule. The size of such macromolecules is expressed either as the radius of gyration or the end-to-end distance (see Flory, 1953, for a detailed treatment). Since the beads in this pearl-string model are small, the frictional effect of each bead is likewise small, and the medium within the molecular domain is considered to be disturbed only slightly by the movement of the macromolecule. It is as if the macromolecule had not been present, and the solvent streams through it undisturbed except for very slight frictional resistance in the immediate vicinity of each bead. For such a hypothetical structure, the frictional coefficient is simply the product of the frictional coefficient per bead times the number of beads in the chain (the degree of polymerization or essentially the molecular weight). Insertion of this conclusion into Eq. (123) leads directly to the important result that the sedimentation coefficient is independent of the molecular weight. This is, of course, directly analogous to the conclusions presented above for elongated rodlike or slightly curved particles. The intrinsic viscosity of randomly coiled macromolecules having no interactions among the beads (free-draining) has been calculated by Debye (1946). If his result is combined with Eq. (123), the sedimentation coefficient can be employed to calculate the mean square end-to-end distance of the random coil.

$$\overline{r^2} = \frac{3600\eta s[\eta]}{(1 - \bar{V}\rho)} \tag{149}$$

The treatment of Flory (1953) gives a similar equation containing a different constant and the mean square distance of a bead from the center of gravity, $\overline{s^2}$. With the upsurge of research activity devoted to synthetic polymers, it soon became clear that few materials, if any, behaved as free-draining coils, and that there was, instead, considerable retardation of the flow of solvent through the macromolecules (flow is considered relative to the macromolecules). In the treatment of the free-draining coil, it was assumed that each bead suffers the same resistance to movement that it would experience in the absence of the neighboring beads which themselves are perturbing the flow of liquid in the immediate vicinity. As the number of segments in the chain increases, the disturbance of flow by the peripheral beads becomes so large that the beads in the interior do not interact with the exterior solvent. In effect, there is hydrodynamic shielding of the interior elements, such that their contribution to the resistance suffered by the macromolecule in moving through the liquid is negligibly small. This problem has been investigated by Kirkwood and Riseman (1948) and Debye and Bueche (1948), the former using the random coil model and the latter a spherical model containing a uniform distribution of beads (also see Peterlin, 1950). Both theories lead to equivalent results despite the different models employed, and they account for the observed relationship between the intrinsic viscosity and molecular weights,

$$[\eta] = KM^{\alpha} \tag{150}$$

where K is a constant for a homologous series of polymers of a given molecular structure, and α varies from 0.5 to 1.0, depending on the molecular weight. Since the solvent on the interior of the macromolecule moves almost in unison with the polymer, Flory introduced the concept of an equivalent hydrodynamic sphere (see Flory, 1953, for review of this work) which is impenetrable to solvent and which experiences the same frictional resistance and causes the same viscosity increment as the actual molecule (note that this is the suggestion employed by Scheraga and Mandelkern in consideration of rigid ellipsoids of revolution). The behavior of this equivalent sphere is then described by Stokes' law and the Einstein viscosity relation. For the equivalent sphere, Flory used the statistical treatments employed for random chain polymers and an intramolecular expansion factor, α, which he had introduced earlier in considerations of the viscosity of polymeric solutions. By this method, Mandelkern and Flory (1952) were able to express the frictional coefficient by the relation

$$f = P'\eta(\overline{s^2})^{1/2} = P\eta(\overline{r^2})^{1/2} \tag{151}$$

where P' and P are constants independent of the size and nature of the

polymer. A similar procedure had been employed by Flory and co-workers for treating the viscosity leading to a simple expression containing another constant, Φ. The relationship of these equations to the Debye-Bueche and Kirkwood-Riseman treatments is given in detail by Flory (1953). When the expressions for the frictional coefficient and the intrinsic viscosity are combined with Eq. (123), a relation containing the sedimentation coefficient, intrinsic viscosity, and molecular weight is derived (Mandelkern and Flory, 1952; Mandelkern *et al.*, 1952).

$$\frac{s[\eta]^{1/3}}{M^{2/3}} = \Phi^{1/3}P^{-1}\frac{(1 - \bar{V}\rho)}{\eta N} \tag{152}$$

The term, $\Phi^{1/3}P^{-1}$, is a constant with the value 2.5×10^6. Experimental data illustrating the validity of this treatment for a variety of systems is given by Mandelkern *et al.*, (1952) (also see Oth and Desreux, 1957). The constants, $\Phi^{1/3}$ and P^{-1}, were originally evaluated for polymers which were homogeneous with regard to molecular weight. More recently, consideration has been given to the effect of heterogeneity on the value of these constants (Gouinlock *et al.*, 1955; Hunt *et al.*, 1956).

Thus far, the theory of Flory has been applied in biochemical problems to experimental data on deoxyribonucleic acid only (Peacocke and Schachman, 1954; and, more recently, Rice and Doty, 1957). Considerations of the configuration of dextran and gelatin have been the subject of investigations by Williams and Saunders (1954) and Williams *et al.* (1954). In these studies, the molecular weights and sedimentation coefficients were evaluated along with the corresponding distribution curves. The results of the two distribution curves then provided the relationship between sedimentation coefficient and molecular weight, thereby yielding valuable information about the configuration of these molecules in solution.

References

Adler, F. T., and Blanchard, C. H. (1949). *J. Phys. & Colloid Chem.* **53**, 803.
Alberty, R. A. (1954). *J. Am. Chem. Soc.* **76**, 3733.
Alberty, R. A., and Marvin, H. H. (1950). *J. Phys. & Colloid Chem.* **54**, 47.
Anderson, N. G. (1955). *Exptl. Cell Research* **9**, 446.
Anfinsen, C. B., and Redfield, R. R. (1956). *Advances in Protein Chem.* **11**, 1.
Archibald, W. J. Unpublished.
Archibald, W. J. (1938a). *Phys. Rev.* **53**, 746.
Archibald, W. J. (1938b). *Phys. Rev.* **54**, 371.
Archibald, W. J. (1942). *Ann. N. Y. Acad. Sci.* **43**, 211.
Archibald, W. J. (1947a). *J. Appl. Phys.* **18**, 362.
Archibald, W. J. (1947b). *J. Phys. & Colloid Chem.* **51**, 1204.
Baker, M. C., Lyons, P. A., and Singer, S. J. (1955a). *J. Am. Chem. Soc.* **77**, 2011.
Baker, M. C., Lyons, P. A., and Singer, S. J. (1955b). *J. Phys. Chem.* **59**, 1074.
Baker, M. C., Campbell, D. H., Epstein, S. I., and Singer, S. J. (1956). *J. Am. Chem. Soc.* **78**, 312.
Baldwin, R. L. (1953a). *Brit. J. Exptl. Pathol.* **34**, 217.
Baldwin, R. L. (1953b). *Biochem. J.* **55**, 644.
Baldwin, R. L. (1954a). *J. Am. Chem. Soc.* **76**, 402.
Baldwin, R. L. (1954b). *J. Phys. Chem.* **58**, 1081.
Baldwin, R. L. (1957a). *Biochem. J.* **65**, 490.
Baldwin, R. L. (1957b). *Biochem. J.* **65**, 503.
Baldwin, R. L. (1958). *J. Am. Chem. Soc.* **80**, 496.
Baldwin, R. L., and Ogston, A. G. (1954). *Trans. Faraday Soc.* **50**, 749.
Baldwin, R. L., and Williams, J. W. (1950). *J. Am. Chem. Soc.* **72**, 4325.
Baldwin, R. L., Gosting, L. J., Williams, J. W., and Alberty, R. A. (1955). *Discussions Faraday Soc.* **No. 20**, 13.
Bauer, J. H., and Pickels, E. G. (1937). *J. Exptl. Med.* **65**, 565.
Beams, J. W. (1930). *Rev. Sci. Instr.* **1**, 667.
Beams, J. W. (1954). *Science* **120**, 619.
Beams, J. W., and Dixon, H. M., III (1953). *Rev. Sci. Instr.* **24**, 228.
Beams, J. W., and Pickels, E. G., (1935). *Rev. Sci. Instr.* **6**, 299.
Beams, J. W., Ross, J. D., and Dillon, J. F. (1951). *Rev. Sci. Instr.* **22**, 77.
Beams, J. W., Snidow, N., Robeson, A., and Dixon, H. M., III (1954). *Rev. Sci. Instr.* **25**, 295.
Beams, J. W., Dixon, H. M., III, Robeson, A., and Snidow, N. (1955). *J. Phys. Chem.* **59**, 915.
Bechhold, H., and Schlesinger, M. (1931). *Biochem. Z.* **236**, 386.
Beckmann, C. O., and Rosenberg, J. L. (1945). *Ann. N. Y. Acad. Sci.* **46**, 329.
Bendet, I. J., Swaby, L. G., and Lauffer, M. A. (1957). *Biochem. et Biophys. Acta* **25**, 252.
Bensusan, H. B., White, J. I., Himmelfarb, S., Blankenhorn, B. E., and Amberson, W. R. (1957). *Am. J. Physiol.* **188**, 219.
Biancheria, A., and Kegeles, G. (1954). *J. Am. Chem. Soc.* **76**, 3737.
Bjorklund, R., and Katz. S. (1956). *J. Am. Chem. Soc.* **78**, 2122.
Blumberg, B. S., and Ogston, A. G. (1956). *Biochem. J.* **63**, 715.
Boedtker, H., and Doty, P. (1956). *J. Am. Chem. Soc.* **78**, 4267.
Boedtker, H., and Simmons, N. S. (1958). *J. Am. Chem. Soc.* **80**, 2550.

Booth, F. (1954). *J. Chem. Phys.* **22**, 1956.
Brakke, M. K. (1953). *Arch. Biochem. Biophys.* **45**, 275.
Bridgman, W. B. (1942). *J. Am. Chem. Soc.* **64**, 2349.
Bridgman, W. B., and Williams, J. W. (1942). *Ann. N. Y. Acad. Sci.* **43**, 195.
Briggs, D. R., and Wolf, W. J. (1957). *Arch. Biochem. & Biophys.* **72**, 127.
Brohult, S. (1940). *Nova Acta Regiae Soc. Sci. Upsaliensis* [4] **12**, No. 4.
Brown, R. A., Kritchevsky, D., and Davies, M. (1954). *J. Am. Chem. Soc.* **76**, 3342.
Brown, R. A., Moyer, A. W., Davies, M. C., and Cox, H. R. (1955). *Arch. Biochem. Biophys.* **58**, 68.
Bull, H. B., and Currie, B. T. (1946). *J. Am. Chem. Soc.* **68**, 742.
Burgers, J. M. (1941). *Proc. Acad. Sci. Amsterdam* **44**, 1045, 1177.
Burgers, J. M. (1942). *Proc. Acad. Sci. Amsterdam* **45**, 9, 126.
Cann, J. R. (1953). *J. Am. Chem. Soc.* **75**, 4213.
Cann, J. R., Kirkwood, J. G., and Brown, R. A. (1957). *Arch. Biochem. Biophys.* **72**, 37.
Cecil, R., and Ogston, A. G. (1948). *Biochem. J.* **43**, 592.
Cecil, R., and Ogston, A. G. (1949). *Biochem. J.* **44**, 33.
Cecil, R., Johnston, J. P., and Ogston, A. G. (1949). *Nature* **163**, 919.
Charlwood, P. A. (1957). *Trans. Faraday Soc.* **53**, 871.
Cheng, P. Y. (1957). *J. Phys. Chem.* **61**, 695.
Cheng, P. Y. and Schachman, H. K. Unpublished.
Cheng, P. Y., and Schachman, H. K. (1955a). *J. Polymer Sci.* **16**, 19.
Cheng, P. Y., and Schachman, H. K. (1955b). *J. Am. Chem. Soc.* **77**, 1498.
Claesson, I. M. (1956). *Arkiv. Kemi* **10**, 1.
Claesson, S. (1946a). *Arkiv Kemi, Mineral. Geol.* **23A**, No. 1.
Claesson, S. (1946b). *Arkiv Kemi, Mineral. Geol.* **24A**, No. 7.
Cohen, S. S., and Schachman, H. K. (1957). *Virology* **3**, 575.
Cohn, E. J., and Edsall, J. T. (1943). "Proteins, Amino Acids, and Peptides." Reinhold, New York.
Connell, J. J. (1958). *Biochem. J.* **70**, 81.
Cunningham, L. W., Tietze, F., Green, N. M., and Neurath, H. (1953). *Discussions Faraday Soc.* **No. 13**, 58.
Davisson, E. O., Gibson, D. M., Ray, B. R., and Vestling, C. S. (1953). *J. Phys. Chem.* **57**, 609.
Debye, P. (1946). *J. Chem. Phys.* **14**, 636.
Debye, P., and Bueche, A. M. (1948). *J. Chem. Phys.* **16**, 573.
de Lalla, O. F., and Gofman, J. W. (1954). *In* "Methods of Biochemical Analysis" (D. Glick, ed.), Vol. 1, p. 459. Interscience, New York.
Dieu, H., and Oth, J. (1954). *Bull. soc. chim. Belges* **63**, 424.
Dreyer, W. J., Wade, R. D., and Neurath, H. (1955). *Arch. Biochem. Biophys.* **59**, 145.
Drucker, C. (1937). *Z. physik. Chem.* **A180**, 359.
Dunlop, P. J. (1957). *J. Phys. Chem.* **61**, 994.
Ecker, P. G., Blum, J., and Hiatt, C. W. (1949). *Rev. Sci. Instr.* **20**, 799.
Edsall, J. T. (1953). *In* "The Proteins" (H. Neurath and K. Bailey, eds.), Vol. 1, Part B, Chapter 7. Academic Press, New York.
Ehrenberg, A., (1957). *Acta Chem. Scand.* **11**, 1257.
Einstein, A. (1905). *Ann. Physik* **17**, 549.
Einstein, A. (1906). *Ann. Physik* **19**, 289.
Enoksson, B. (1948). *Nature* **161**, 934.
Epstein, H. T., and Lauffer, M. A. (1952). *Arch. Biochem. Biophys.* **36**, 371.

Eriksson, A. F. V. (1953). *Acta Chem. Scand.* **7**, 623.
Eriksson, A. F. V. (1956). *Acta Chem. Scand.* **10**, 360.
Evans, W. J. (1957). *Arch. Biochem. Biophys.* **72**, 226.
Ewart, R. H., Roe, C. P., Debye, P., and McCartney, J. R. (1946). *J. Chem. Phys.* **14**, 687.
Faxén, H. (1929). *Arkiv Mat., Astron. Fysik* **21B**, No. 3.
Fessler, J. H., and Ogston, A. G. (1951). *Trans. Faraday Soc.* **47**, 667.
Fick, A. (1855). *Ann. Physik u. Chem.* **94**, 59.
Field, E. O., and O'Brien, J. R. P. (1955). *Biochem. J.* **60**, 656.
Field, E. O., and Ogston, A. G. (1955). *Biochem. J.* **60**, 661.
Fixman, M. (1958). *J. Phys. Chem.* **62**, 374.
Flory, P. J. (1953). "Prineiples of Polymer Chemistry." Cornell Univ. Press, Ithaca, New York.
Forsberg, R., and Svensson, H. (1954). *Optica Acta (Paris)* **1**, 90.
Fredericq, E. (1953). *Nature* **171**, 570.
Frederieq, E., and Neurath, H. (1950). *J. Am. Chem. Soc.* **72**, 2684.
Fujita, H. (1956a). *J. Chem. Phys.* **24**, 1084.
Fujita, H. (1956b). *J. Am. Chem. Soc.* **78**, 3598.
Geddes, A. L. (1949). *In* "Physical Methods of Organie Chemistry" (A. Weissberger, ed.), 2nd ed., Vol. I, Part I, Chapter 12. Interscienee, New York.
Gibbs, J. W. (1928). "The Collected Works of J. Willard Gibbs." I. Yale Univ. Press, New Haven, Connecticut.
Gilbert, G. A. (1955). *Discussions Faraday Soc.* **No. 20**, 68.
Gilbert, G. A., and Jenkins, R. C. Ll. (1956). *Nature* **177**, 853.
Ginsburg, A., Appel, P., and Sehaehman, H. K. (1956). *Arch. Biochem. Biophys.* **65**, 545.
Gofman, J. W., Lindgren, F. T., and Elliott, H. (1949). *J. Biol. Chem.* **179**, 973.
Goldberg, R. J. (1953). *J. Phys. Chem.* **57**, 194.
Golder, R. H. (1953). *J. Am. Chem. Soc.* **75**, 1739.
Goring, D. A. I., and Chepeswick, C. (1955). *J. Colloid Sci.* **10**, 440.
Goring, D. A. I., and Chepeswiek, C. (1956). *J. Phys. Chem.* **60**, 506.
Gosting, L. J. (1952). *J. Am. Chem. Soc.* **74**, 1548.
Gosting, L. J. (1956). *Advances in Protein Chem.* **11**, 429.
Gouinloek, E. V., Jr., Flory, P. J., and Seheraga, H. A. (1955). *J. Polymer Sci.* **16**, 383.
Gralén, N. (1944). Dissertation. Univ. Uppsala, Uppsala, Sweden.
Gutfreund, H., and Ogston, A. G. (1949). *Biochem. J.* **44**, 163.
Gutter, F. J., Sober, H. A., and Petersen, E. A. (1956). *Arch. Biochem. Biophys.* **62**, 427.
Hall, J. R., and Ogston, A. G. (1955). *Biochem. J.* **62**, 401.
Halwer, M., Nutting, G. C., and Briee, B. A. (1951). *J. Am. Chem. Soc.* **73**, 2786.
Harrington, W. F., and Sehachman, H. K. (1953). *J. Am. Chem. Soc.* **75**, 3533.
Harrington, W. F., and Schellman, J. A. (1956). *Compt. rend. trav. lab. Carlsberg, Sér. chim.* **30**, 21.
Harrington, W. F., Johnson, P., and Ottewill, R. H. (1956). *Biochem. J.* **62**, 569.
Hayes, J. E., and Velick, S. F. (1954). *J. Biol. Chem.* **207**, 225.
Henriot, E., and Huguenard, E. (1925). *Compt. rend.* **180**, 1389.
Henriot, E., and Huguenard, E. (1927). *J. Phys. Radium* **8**, 433.
Hersh, R. T., and Schachman, H. K. (1955). *J. Am. Chem. Soc.* **77**, 5228.
Hersh, R. T., and Sehachman, H. K. (1958). *J. Phys. Chem.* **62**, 170.
Herzog, R. O., Illig, R., and Kudar, H. (1934). *Z. physik. Chem.* **A167**, 329.

Hiatt. C. W. (1953). *Rev. Sci. Instr.* **24,** 182.
Hogeboom, G. H., Schneider, W. C., and Striebich, M. J. (1952). *J. Biol. Chem.* **196,** 111.
Hooyman, G. J. (1955). Disseration. Leiden University, Netherlands.
Hooyman, G. J. (1956). *Physica* **22,** 751.
Hooyman, G. J., Holtan, H., Jr., Mazur, P., and de Groot, S. R. (1953). *Physica* **19,** 1095.
Howard, G. J., and Jordan, D. O. (1954). *J. Polymer Sci.* **12,** 209.
Hunt, M. L., Newman, S., Scheraga, H. A., and Flory, P. J. (1956). *J. Phys. Chem.* **60,** 1278.
Johnson, J. S., Kraus, K. A., and Young, T. F. (1954a). *J. Am. Chem. Soc.* **76,** 1436.
Johnson, J. S., Kraus, K. A., and Scatchard, G. (1954b). *J. Phys. Chem.* **58,** 1034.
Johnson, J. S., Kraus, K. A., and Holmberg, R. W. (1956). *J. Am. Chem. Soc.* **78,** 26.
Johnson, P., and Joubert, F. J. (1951). *J. Polymer Sci.* **7,** 605.
Johnson, P., and Naismith, W. E. F. (1953). *Discussions Faraday Soc.* **No. 13,** 98.
Johnson, P., and Naismith, W. E. F. (1956). *Trans. Faraday Soc.* **52,** 280.
Johnson, P., and Shooter, E. M. (1950). *Biochim. et Biophys. Acta* **5,** 361.
Johnston, J. P. (1955). *Biochem. J.* **59,** 620.
Johnston, J. P., and Ogston, A. G. (1946). *Trans. Faraday Soc.* **42,** 789.
Jullander, I. (1945). *Arkiv. Kemi, Mineral. Geol.* **21A,** (8) 1.
Jullander, I. (1948). *J. Polymer Sci.* **3,** 631.
Karush, F., and Schachman, H. K. (unpublished).
Katz, S. (1956). *J. Am. Chem. Soc.* **78,** 300.
Katz, S., and Schachman, H. K. (1955). *Biochim. et Biophys. Acta* **18,** 28.
Kegeles, G. (1947). *J. Am. Chem. Soc.* **69,** 1302.
Kegeles, G. (1952). *J. Am. Chem. Soc.* **74,** 5532.
Kegeles, G., and Gutter, F. J. (1951). *J. Am. Chem. Soc.* **73,** 3770.
Kegeles, G., and Rao, M. S. Narasinga. (1958). *J. Am. Chem. Soc.* **80,** 5721.
Kegeles, G., Klainer, S. M., and Salem, W. J. (1957). *J. Phys. Chem.* **61,** 1286.
Kerby, G. P., Gowdy, R. A., Dillon, E. S., Dillon, M. L., Csáky, T. Z., Sharp, D. G., and Beard, J. W. (1949). *J. Immunol.* **63,** 93.
Kermack, W. O., M'Kendrick, A. G., and Ponder, E. (1929). *Proc. Roy. Soc. Edinburgh,* **49,** Part II, No. **15,** 170.
Kinell, Per-Olof (1947a). *Acta Chem. Scand.* **1,** 335.
Kinell, Per-Olof (1947b) *J. chim. phys.* **44,** 53.
Kinell, Per Olof, and Rånby, B. G. (1950). *Advances in Colloid Sci.* **3,** 161.
Kirkwood, J. G., and Goldberg, R. J. (1950). *J. Chem. Phys.* **18,** 54.
Kirkwood, J. G., and Riseman, J. (1948). *J. Chem. Phys.* **16,** 565.
Klainer, S. M., and Kegeles, G. (1955). *J. Phys. Chem.* **59,** 952.
Klainer, S. M., and Kegeles, G. (1956). *Arch. Biochem. Biophys.* **63,** 247.
Klotz, I. M. (1946). *Arch. Biochem.* **9,** 109.
Klotz, I. M., Walker, F. M., and Pivan, R. B. (1946). *J. Am. Chem. Soc.* **68,** 1486.
Koenig, V. L., and Perrings, J. D. (1952a). *Arch. Biochem. Biophys.* **36,** 147.
Koenig, V. L., and Perrings, J. D. (1952b). *Arch. Biochem. Biophys.* **40,** 218.
Kraemer, E. O., and Lansing, W. D. (1933). *J. Am. Chem. Soc.* **55,** 4319.
Kraemer, E. O., and Lansing, W. D. (1935). *J. Phys. Chem.* **39,** 153.
Kraut, J. (1954). *J. Polymer Sci.* **14,** 222.
Krishnamurti, K., and Svedberg, T. (1930). *J. Am. Chem. Soc.* **52,** 2897.
Kurnick, N. B. (1954). *J. Am. Chem. Soc.* **76,** 417.
Lamm, O. (1929a). *Arkiv Mat., Astron. Fysik* **21B,** No. 2.
Lamm, O. (1929b). *Z. physik. Chem.* **A143,** 177.

Lamm, O. (1937). *Nova Acta Regiae Soc. Sci. Upsaliensis* [4], **10**, No. 6.
Lamm, O. (1944). *Arkiv Kemi, Mineral. Geol.* **17A**, No. 25.
Lamm, O. (1953). *Acta Chem. Scand.* **7**, 173.
Lamm, O. (1954). *Acta Chem. Scand.* **8**, 1120.
Lamm, O. (1957). *Acta Chem. Scand.* **11**, 360.
Lansing, W. D., and Kraemer, E. O. (1935). *J. Am. Chem. Soc.* **57**, 1369.
Lansing, W. D., and Kraemer, E. O. (1936). *J. Am. Chem. Soc.* **58**, 1471.
Larner, J., Ray, B. Roger, and Crandall, H. F. (1956). *J. Am. Chem. Soc.* **78**, 5890.
Lauffer, M. A. (1942). *J. Biol. Chem.* **143**, 99.
Lauffer, M. A. (1944a). *J. Am. Chem. Soc.* **66**, 1188.
Lauffer, M. A. (1944b). *J. Am. Chem. Soc.* **66**, 1195.
Lauffer, M. A., and Bendet, I. J. (1954). *Advances in Virus Research* **2**, 241.
Lauffer, M. A., and Stanley, W. M. (1944). *J. Exptl. Med.* **80**, 531.
Lauffer, M. A., and Taylor, N. W. (1952). *Arch. Biochem. Biophys.* **37**, 457.
Lauffer, M. A., and Taylor, N. W. (1953a). *Arch. Biochem. Biophys.* **42**, 102.
Lauffer, M. A., and Taylor, N. W. (1953b). *Arch. Biochem. Biophys.* **43**, 374.
Lauffer, M. A., Taylor, N. W., and Wunder, C. C. (1952). *Arch. Biochem. Biophys.* **40**, 453.
Lewis, G. N. (1910). *J. Am. Chem. Soc.* **32**, 862.
Lewis, G. N., and Randall, M. (1923). "Thermodynamics and the Free Energy of Chemical Substances." McGraw-Hill, New York.
Li, C. H., Tiselius, A., Pedersen, K. O., Hagdahl, L., and Carstensen, H. (1951). *J. Biol. Chem.* **190**, 317.
Linderstrøm-Lang, K., and Lanz, H., Jr. (1938). *Compt. rend. trav. lab. Carlsberg, Sér. chim.* **21**, 315.
Lindgren, F. T., Elliott, H. A., and Gofman, J. W. (1951). *J. Phys. & Colloid Chem.* **55**, 80.
Loeb, G. I., and Scheraga, H. A. (1956). *J. Phys. Chem.* **60**, 1633.
Longsworth, L. G. (1939). *J. Am. Chem. Soc.* **61**, 529.
Longsworth, L. G. (1943). *J. Am. Chem. Soc.* **65**, 1755.
Longsworth, L. G. (1947). *J. Am. Chem. Soc.* **69**, 1288.
Longsworth, L. G. (1950). *Proc. Natl. Acad. Sci. U. S.* **36**, 502.
Longsworth, L. G. (1951). *Anal. Chem.* **23**, 346.
Longsworth, L. G. (1954). *J. Phys. Chem.* **58**, 770.
Longsworth, L. G., and MacInnes, D. A. (1942). *J. Gen. Physiol.* **25**, 507.
McBain, J. W. (1936). *J. Am. Chem. Soc.* **58**, 315.
MacCallum, W. G., and Oppenheimer, E. H. (1922). *J. Am. Med. Assoc.* **78**, 410.
McFarlane, A. S. (1935). *Biochem. J.* **29**, 407, 660.
Mandelkern, L., and Flory, P. J. (1952). *J. Chem. Phys.* **20**, 212.
Mandelkern, L., Krigbaum, W. R., Scheraga, H. A., and Flory, P. J. (1952). *J. Chem. Phys.* **20**, 1392.
Mandelkern, L., Williams, L. C., and Weissberg, S. G. (1957). *J. Phys. Chem.* **61**, 271.
Martin, W. G., Cook, W. H., and Winkler, C. A. (1956). *Can. J. Chem.* **34**, 809.
Mason, M., and Weaver, W. (1924). *Phys. Rev.* **23**, 412.
Massey, V., Harrington, W. F., and Hartley, B. S. (1955). *Discussions Faraday Soc.* No. **20** 24.
Mehl, J. W., Oncley, J. L., and Simha, R. (1940). *Science* **92**, 132.
Meselson, M., and Stahl, F. W. (1958). *Proc. Natl. Acad. Sci. U. S.* **44**, 671.
Meselson, M., Stahl, F. W., and Vinograd, J. (1957). *Proc. Natl. Acad. Sci. U. S.* **43**, 581.

Meyerhoff, G. (1955). *Makromol. Chem.* **15**, 68.
Milch, L. J. (1953). *Lab. Invest.* **2**, 441.
Miller, G. L., and Price. W. C. (1946). *Arch. Biochem.* **10**, 467.
Mommaerts, W. F. H. M., and Aldrich, B. B. (1957). *Science* **126**, 1294.
Mommaerts, W. F. H. M., and Aldrich, B. B. (1958). *Biochim. et Biophys. Acta* **28**, 627.
Moore, D. H. (1943). *Rev. Sci. Instr.* **14**, 295.
Moore, D. H., and White, J. U. (1948). *Rev. Sci. Instr.* **19**, 700.
Mosimann, H., and Signer, R. (1944). *Helv. Chim. Acta* **27**, 1123.
Naismith, W. E. F. (1955). *Biochim. et Biophys. Acta* **16**, 203.
Neurath, H., and Saum, A. M. (1939). *J. Biol. Chem.* **128**, 347.
Newman, S., and Eirich, F. (1950). *J. Colloid Sci.* **5**, 541.
Nichols, J. B. (1931). *Physics* **1**, 254.
Nichols, J. B., and Bailey, E. D. (1949). *In* "Physical Methods of Organic Chemistry" (A. Weissberger, ed.), 2nd ed., Vol. I, Part I, Chapter 13. Interscience, New York.
Nishihara, T., and Doty, P. (1958). *Proc. Natl. Acad. Sci. U. S.* **44**, 411.
Ogston, A. G. (1953). *Trans. Faraday Soc.* **49**, 1481.
Ogston, A. G. (1954). *Trans. Faraday Soc.* **50**, 1363.
Ogston, A. G., and Stanier, J. E. (1951). *Biochem. J.* **49**, 585.
Ogston, A. G., and Stanier, J. E. (1952). *Biochem. J.* **52**, 149.
Ogston, A. G., and Woods, E. F. (1953). *Nature* **171**, 221.
Ogston, A. G., and Woods, E. F. (1954). *Trans. Faraday Soc.* **50**, 635.
Oka, S. (1936). *Proc. Phys. Math. Soc. Japan* [3] **18**, 519.
Oncley, J. L. (1941). *Ann. N. Y. Acad. Sci.* **41**, 121.
Oncley, J. L., Ellenbogen, E., Gitlin, D., and Gurd, F. R. N. (1952). *J. Phys. Chem.* **56**, 85.
Oncley, J. L., Walton, K. W., and Cornwell, D. G. (1957). *J. Am. Chem. Soc.* **79**, 4666.
Onsager, L., and Fuoss, R. M. (1932). *J. Phys. Chem.* **36**, 2689.
Oster, G. (1946). *Science* **103**, 306.
Oth, J., and Desreux, V. (1954). *Bull. soc. chim. Belges* **63**, 133.
Oth, J., and Desreux, V. (1955). International Symposium on Macromolecular Chemistry, Milan, Ric. Sci., Suppl. A, p. 447. *Intern. Union Pure and Appl. Chem.*
Oth, J., and Desreux, V. (1957). *Bull. soc. chim. Belges* **66**, 303.
Parrish, R. G., and Mommaerts, W. F. H. M. (1954). *J. Biol. Chem.* **209**, 901.
Pasternak, R. A., Nazarian, G. M., and Vinograd, J. R. (1957). *Nature* **179**, 92.
Peacocke, A. R., and Schachman, H. K. (1954). *Biochim. et Biophys. Acta* **15**, 198.
Pedersen, K. O. (1934). *Z. physik. Chem.* **A170**, 41.
Pedersen, K. O. (1935). *Nature* **135**, 304.
Pedersen, K. O. (1936a). *Nature* **138**, 363.
Pedersen, K. O. (1936b). *Biochem. J.* **30**, 948.
Pedersen, K. O. (1936c). *Biochem. J.* **30**, 961.
Pedersen, K. O. (1938). *Compt. rend. trav. lab. Carlsberg, Sér. chim.* **22**, 427.
Pedersen, K. O. (1945). Dissertation. Univ. of Uppsala, Uppsala, Sweden.
Pedersen, K. O. (1958). *J. Phys. Chem.* **62**, 1282.
Peller, L. (1958). *J. Chem. Phys.* **29**, 415.
Perrin, F. (1936). *J. Phys. Radium* **7**, 1.
Peterlin, A. (1950). *J. Polymer Sci.* **5**, 473.
Philpot, J. St. L. (1938). *Nature* **141**, 283.

Philpot, J. St. L. (1939). *Biochem. J.* **33**, 1707.
Philpot, J. St. L., and Cook. G. H. (1948). *Researeh* **1**, 234.
Pickels, E. G. (1942a). *Chem. Rev.* **30**, 341.
Pickels, E. G. (1942b). *Rev. Sci. Instr.* **13**, 426.
Pickels, E. G. (1950). *Machine Design* **22**, 102.
Pickels, E. G. (1952). *Methods in Med. Research* **5**, 107.
Pickels, E. G. (1953). Private communication.
Pickels, E. G., Harrington, W. F., and Schachman, H. K. (1952). *Proe. Natl. Acad. Sci. U. S.* **38**, 943.
Pirie, N. W. (1940). *Biol. Revs.* **15**, 377.
Porath, J. (1952). *Aeta Chem. Scand.* **6**, 1237.
Powell, R. E., and Eyring. H. (1942). *Advances in Colloid Sci.* **1**, 183.
Putnam, F. W. (1950). *Science* **111**, 481.
Putnam, F. W. (1951). *J. Biol. Chem.* **190**, 61.
Putnam, F. W. (1954). *J. Polymer Sci.* **12**, 391.
Rao, M. S. Narasinga, and Kegeles, G. (1958). *J. Am. Chem. Soe.* **80**, 5724.
Record, B. R. (1948). *J. Chem. Soc.* p. 1567.
Record, B. R., and Stacey, M. (1948). *J. Chem. Soe.* p. 1561.
Rice, S. A., and Doty, P. (1957). *J. Am. Chem. Soc.* **79**, 3937.
Richards, E. G., and Schachman, H. K. Unpublished.
Richards, E. G., and Schachman, H. K. (1957). *J. Am. Chem. Soc.* **79**, 5324.
Rinde, H. (1928). Dissertation. Univ. of Uppsala, Uppsala, Sweden.
Robkin, E., Meselson, M., and Vinograd, J. (1959). *J. Am. Chem. Soe.*, in press.
Rosen, B., Kamath, P., and Eirich, F. (1951). *Discussions Faraday Soe.* **11**, 135.
Rothen, A. (1940). *J. Gen. Physiol.* **24**, 203.
Sadron, C. (1953). *Progr. in Biophys. and Biophys. Chem.* **3**, 237.
Scatchard, G. (1946). *J. Am. Chem. Soe.* **68**, 2315.
Schachman, H. K. Unpublished.
Schachman, H. K. (1950). In "Viruses" (M. Delbrück, ed.), p. 64. California Institute of Technology, Pasadena, California.
Schachman, H. K. (1951a). *J. Am. Chem. Soe.* **73**, 4453.
Schachman, H. K. (1951b). *J. Am. Chem. Soc.* **73**, 4808.
Schachman, H. K., and Harrington, W. F. Unpublished.
Schachman, H. K., and Harrington, W. F. (1952). *J. Am. Chem. Soc.* **74**, 3965.
Schachman, H. K., and Harrington, W. F. (1954). *J. Polymer Sci.* **12**, 379.
Schachman, H. K., and Kauzmann, W. J. (1949). *J. Phys. & Colloid Chem.* **53**, 150.
Schachman, H. K., and Lauffer, M. A. (1949). *J. Am. Chem. Soe.* **71**, 536.
Schachman, H. K., and Lauffer, M. A. (1950). *J. Am. Chem. Soe.* **72**, 4266.
Scheraga, H. A., and Mandelkern, L. (1953). *J. Am. Chem. Soc.* **75**, 179.
Scheraga, H. A., and Mandelkern, L. (1958). *J. Phys. Chem.* **62**, 370.
Scheraga, H. A., Carroll, W. R., Nims, L. F., Sutton, E., Backus, J. K., and Saunders, J. M. (1954). *J. Polymer Sci.* **14**, 427.
Schulz, G. V. (1944). *Z. physik. Chem.* **A193**, 168.
Schumaker, V. N., and Schachman, H. K. (1957). *Biochim. et Biophys. Aeta* **23**, 628.
Schwert, G. W. (1949). *J. Biol. Chem.* **179**, 655.
Schwert, G. W. (1951). *J. Biol. Chem.* **190**, 799.
Schwert, G. W. (1954). *Arch. Biochem. Biophys.* **48**, 310.
Senti, F. R., and Warner, R. C. (1948). *J. Am. Chem. Soc.* **70**, 3318.
Sharp, D. G. (1949). *Proe. Soe. Exptl. Biol. Med.* **70**, 54.

Sharp, D. G., and Beard, J. W. (1950). *J. Biol. Chem.* **185**, 247.
Sharp, D. G., and Beard, J. W. (1954). *Biochim. et Biophys. Acta* **14**, 12.
Sharp, D. G., Taylor, A. R., McLean, I. W., Jr., Beard, D., and Beard, J. W. (1944). *Seience* **100**, 151.
Sharp, D. G., Hook, A. E., Taylor, A. R., Beard, D., and Beard, J. W. (1946a). *J. Biol. Chem.* **165**, 259.
Sharp, D. G., Taylor, A. R., and Beard, J. W. (1946b). *J. Biol. Chem.* **163**, 289.
Sharp, D. G., Beard, D., and Beard, J. W. (1950). *J. Biol. Chem.* **182**, 279.
Sheppard, E., and McLaren, A. D. (1953). *J. Am. Chem. Soe.* **75**, 2587.
Sheppard, E., McLaren, A. D., and Johnson, P. (1950). *J. Polymer Sei.* **5**, 375.
Shooter, K. V., and Butler, J. A. V. (1956). *Trans. Faraday Soe.* **52**, 734.
Shulman, S. (1953a). *Arch. Biochem. Biophys.* **44**, 230.
Shulman, S. (1953b). *J. Am. Chem. Soe.* **75**, 5846.
Signer, R., and Egli, H. (1950). *Ree. trav. ehim.* **69**, 45.
Signer, R., and Gross, H. (1934). *Helv. Chim. Acta* **17**, 726.
Sihtola, H., and Svedberg, T. (1948). *Acta Chem. Seand.* **2**, 474.
Simha, R. (1940). *J. Phys. Chem.* **44**, 25.
Singer, S. J. (1947a). *J. Polymer Sci.* **2**, 290.
Singer, S. J. (1947b). *J. Chem. Phys.* **15**, 341.
Singer, S. J., and Campbell, D. H. (1952). *J. Am. Chem. Soc.* **74**, 1794.
Singer, S. J., and Campbell, D. H. (1953). *J. Am. Chem. Soc.* **75**, 5577.
Singer, S. J., and Campbell, D. H. (1955a). *J. Am. Chem. Soe.* **77**, 3499.
Singer, S. J., and Campbell, D. H. (1955b). *J. Am. Chem. Soe.* **77**, 3504.
Singer, S. J., and Campbell, D. H. (1955c). *J. Am. Chem. Soc.* **77**, 4851.
Singer, S. J., and Siegel, A. (1950). *Seienee* **112**, 107.
Singer, S. J., Eggman, L., and Campbell, D. H. (1955). *J. Am. Chem. Soe.* **77**, 4855.
Smadel, J. E., Pickels, E. G., and Shedlovsky, T. (1938). *J. Exptl. Med.* **68**, 607.
Smith, D. B., Wood, G. C., and Charlwood, P. A. (1956). *Can. J. Chem.* **34**, 364.
Smith, E. L., Kimmel, J. R., and Brown, D. M. (1954). *J. Biol. Chem.* **207**, 533.
Smith, R. F., and Briggs, D. R. (1950). *J. Phys. & Colloid Chem.* **54**, 33.
Spinco Division, Beckman Instruments, Inc. (1954). *Tech. Bull. No.* 6004A.
Spinco Division, Beckman Instruments, Inc. (1955). *Tech. Bull. No.* 6016A.
Spinco Division, Beckman Instruments, Inc. (1956). *Tech. Bull. No.* 6021A.
Steiner, R. F. (1954). *Arch. Biochem. Biophys.* **49**, 400.
Stenesh, J., Paigen, K., and Schachman, H. K. Unpublished.
Stockmayer, W. H. (1950). *J. Chem. Phys.* **18**, 58.
Stokes, G. G. (1856). *Trans. Cambridge Phil. Soe.* **9**, Part II, 8.
Sullivan, R. R., and Hertel, K. L. (1942). *Advanees in Colloid Sci.* **1**, 37.
Sutherland, W. (1905). *Phil. Mag.* **9**, 781.
Svedberg, T. (1925). *Kolloid-Z.* **36**, Erg.-Bd. 53.
Svedberg, T. (1926). *Z. physik. Chem.* **121**, 65.
Svedberg, T., and Chirnoaga E. (1928). *J. Am. Chem. Soc.* **50**, 1399.
Svedberg, T., and Eriksson-Quensel, I.-B. (1936). *Nature* **137**, 400.
Svedberg, T., and Fåhraeus, R. (1926). *J. Am. Chem. Soe.* **48**, 430.
Svedberg, T., and Hedenius, A. (1934). *Biol. Bull.* **66**, 191.
Svedberg, T., and Nichols, J. B. (1923). *J. Am. Chem. Soc.* **45**, 2910.
Svedberg, T., and Pedersen, K. O. (1940). "The Ultracentrifuge." Oxford Univ. Press, London and New York. Johnson Reprint Corporation, New York.
Svedberg, T., and Rinde, H. (1923). *J. Am. Chem. Soe.* **45**, 943.
Svedberg, T., and Rinde, H. (1924). *J. Am. Chem. Soc.* **46**, 2677.
Svensson, H. (1939). *Kolloid-Z.* **87**, 181.

Svensson, H. (1940). *Kolloid-Z.* **90**, 141.
Svensson, H. (1946). *Arkiv Kemi, Mineral. Geol.* **22A**, No. 10.
Svensson, H. (1949). *Acta Chem. Scand.* **3**, 1170.
Svensson, H. (1950). *Acta Chem. Scand.* **4**, 399.
Svensson, H. (1951). *Acta Chem. Scand.* **5**, 72.
Svensson, H. (1954). *Optica Acta* **1**, 25.
Tanford. C. (1957). *J. Phys. Chem.* **61**, 1023.
Tanford, C., and Buzzell, J. G. (1954). *J. Am. Chem. Soc.* **76**, 3356.
Tanford, C., and Buzzell, J. G. (1956). *J. Phys. Chem.* **60**, 225.
Taylor, N. W., Epstein, H. T., and Lauffer, M. A. (1955). *J. Am. Chem. Soc.* **77**, 1270.
Thompson, J. O. (1950). *J. Phys. Chem.* **54**, 338.
Thovert, J. (1914). *Ann. Phys.* **2**, 369.
Tietze, F., and Neurath, H. (1953). *J. Am. Chem. Soc.* **75**, 1758.
Tiselius, A. (1926). *Z. physik. Chem.* **124**, 449.
Tiselius, A. (1930). *Nova Acta Regiae Soc. Sci. Upsaliensis* [4], **7**, No. 4.
Tiselius, A. (1932). *Kolloid-Z.* **59**, 306.
Tiselius, A., Pedersen, K. O., and Svedberg, T. (1937). *Nature* **140**, 848.
Tolman, R. C. (1911). *J. Am. Chem. Soc.* **33**, 121.
Trautman, R. (1952). Univ. of Calif. Radiation Lab. Progr. Rept. No. UCRL 1869, Contract No. W-7405-48 (July 8, 1952).
Trautman, R. (1956). *J. Phys. Chem.* **60**, 1211.
Trautman, R. (1958). *Biochim. et Biophys. Acta* **28**, 417.
Trautman, R., and Burns, V. W. (1954). *Biochim. et Biophys. Acta* **14**, 26.
Trautman, R., and Schumaker, V. N. (1954). *J. Chem. Phys.* **22**, 551.
Trautman, R., Schumaker, V., N. Harrington, W. F., and Schachman, H. K. (1954). *J. Chem. Phys.* **22**, 555.
Van Holde, K. E., and Baldwin, R. L. (1958). *J. Phys. Chem.* **62**, 734.
Van Holde, K. E., and Williams, J. W. (1953). *J. Polymer Sci.* **11**, 243.
Velick, S. F. (1953). *J. Biol. Chem.* **203**, 563.
Velick, S. F. (1954). *In* "The Mechanism of Enzyme Action" (W. D. McElroy and B. Glass, eds.), p. 491. Johns Hopkins Press, Baltimore, Maryland.
Velick, S. F., and Hayes, J. E. (1953). *J. Biol. Chem.* **203**, 545.
Velick, S. F., Hayes, J. E., and Harting, J. (1953). *J. Biol. Chem.* **203**, 527.
von Hippel, P. H., and Waugh, D. F. (1955). *J. Am. Chem. Soc.* **77**, 4311.
von Hippel, P. H., Schachman, H. K., Appel, P., and Morales, M. F. (1958). *Biochim. et Biophys. Acta.* **28**, 504.
Wade, R., Winitz, M., and Greenstein, J. P. (1956). *J. Am. Chem. Soc.* **78**, 373.
Wales, M. (1948). *J. Phys. & Colloid Chem.* **52**, 235.
Wales, M. (1951a). *J. Phys. & Colloid Chem.* **55**, 282.
Wales, M. (1951b). *J. Appl. Phys.* **22**, 735.
Wales, M., and Swanson, D. L. (1951). *J. Phys. & Colloid Chem.* **55**, 203.
Wales, M., and Van Holde, K. E. (1954). *J. Polymer Sci.* **14**, 81.
Wales, M., and Williams, J. W. (1952). *J. Polymer Sci.* **8**, 449.
Wales, M., Bender, M., Williams, J. W., and Ewart, R. H. (1946). *J. Chem. Phys.* **14**, 353.
Wales, M., Adler, F. T., and Van Holde, K. E. (1951). *J. Phys. & Colloid Chem.* **55**, 145.
Wales, M., Williams, J. W., Thompson, J. O., and Ewart, R. H. (1948). *J. Phys. & Colloid Chem.* **52**, 983.
Waugh, D. F. (1954). *Advances in Protein Chem.* **9**, 325.

Waugh, D. F., and von Hippel, P. H. (1956). *J. Am. Chem. Soc.* **78**, 4576.
Waugh, D. F., and Yphantis, D. A. (1952). *Rev. Sci. Instr.* **23**, 609.
Waugh, D. F., and Yphantis, D. A. (1953). *J. Phys. Chem.* **57**, 312.
Weaver, W. (1926). *Phys. Rev.* **27**, 499.
Webber, R. V. (1956). *J. Am. Chem. Soc.* **78**, 536.
Wilcox, P. E., Kraut, J., Wade, R. D., and Neurath, H. (1957). *Biochim. et Biophys. Acta* **24**, 72.
Williams, J. W. (1954). *J. Polymer Sci.* **12**, 351.
Williams, J. W., and Saunders, W. M. (1954). *J. Phys. Chem.* **58**, 854.
Williams, J. W., Baldwin, R. L., Saunders, W. M., and Squire, P. G. (1952). *J. Am. Chem. Soc.* **74**, 1542.
Williams, J. W., Saunders, W. M., and Cicirelli, J. S. (1954). *J. Phys. Chem.* **58**, 774.
Williams, J. W., Van Holde, K. E., Baldwin, R. L., and Fujita, H. (1958). *Chem. Revs.* **58**, 715.
Williams, R. C., and Backus, R. C. (1949). *J. Am. Chem. Soc.* **71**, 4052.
Williams, R. C., and Steere, R. L. (1951). *J. Am. Chem. Soc.* **73**, 2057.
Williams, R. C., Backus, R. C., and Steere, R. L. (1951). *J. Am. Chem. Soc.* **73**, 2062.
Wolter, H. (1950). *Ann. Physik* **7**, 182.
Yang, J. T., and Foster, J. F. (1954). *J. Am. Chem. Soc.* **76**, 1588.
Young, T. F., Kraus, K. A., and Johnson, J. S. (1954). *J. Chem. Phys.* **22**, 878.
Yphantis, D. A., and Waugh, D. F. (1956a). *J. Phys. Chem.* **60**, 623.
Yphantis, D. A., and Waugh, D. F. (1956b). *J. Phys. Chem.* **60**, 630.

GLOSSARY OF TERMS

a	Short semiaxis of ellipsoid of revolution
a	Thickness of the cell along the optical path
a_1 , a_2	Constants in power series relating sedimentation coefficient to time
A	Area of gradient curve
A'	Surface area of the hydrated particle per unit hydrated volume in Eq. (37)
$[A]$	Molar concentration of anion, A
$[A_0]$	Total concentration of the anion, A, in moles per unit volume
b	Long semiaxis of ellipsoid of revolution
b	Subscript meaning bottom of cell
B	Width of gradient curve
B'	Value expressing polydispersity in terms of standard deviation in distribution of sedimentation coefficients; it is evaluated from gradient curves
c	Concentration
$\bar{c}$	Total concentration of solute molecules; $\bar{c} = \sum_i c_i$
c_i	Concentration of the i^{th} component
c_m	Concentration at the meniscus
c_0	Concentration at zero time (in mixtures, written as c^0)
c^{obs}	Observed concentration of component
c_p	Concentration in plateau region (*written as c^p on page 146*)
$\bar{c}_P$	Constituent concentration of the protein; i.e. the weight concentration of the protein regardless of the form in which it exists
c_t	Concentration at time, t
c_u	Average concentration of solution withdrawn from the upper compartment of a separation cell at time, t
d	Density of solvating medium
D	Diffusion coefficient
$\bar{D}_0$	Weight-average diffusion coefficient at infinite dilution
D_{sed}	Diffusion coefficient evaluated from the shape of an ultracentrifuge boundary
f	Frictional coefficient
(f/f_0)	Frictional ratio, with subscripts, s, for shape and, h, for hydration
F	As subscript indicates fast component
$F(t)$	Function of time in analysis of boundary spreading for concentration dependent systems
$F(\xi_m)$	A function of the parameter ξ_m , Eq. (67)
$g(s)$	Distribution function for the sedimentation coefficients of a sample
$g^*(s)$	Apparent distribution function for the sedimentation coefficients
h	Volume of solvating medium associated with a single particle or macromolecule
H	Maximum height of gradient curve (H_m in Fig. 36)
I	As subscript indicates indicator component
J	Number of fringes across a boundary
k	Constant expressing dependence of sedimentation coefficient on concentration (e.g. Eqs. (32) and (33))
k	Boltzmann constant; also used as a proportionality constant Eqs. (135), (136)
K	Constant describing dependence of D on c
K	Constant in expression relating intrinsic viscosity to molecular weight

K	Constant expressing dependence of sedimentation coefficient on pressure
k_{BF}	That part of the dependence of sedimentation coefficient on concentration which is attributable to backward flow
k_f	That part of the s vs. c dependence that can be accounted for by the dependence of the frictional coefficient on concentration
k_i	Equilibrium constant for the association of $A + PA_{i-1}$ to give PA_i
K_s	Constant expressing maximum weight in a distribution of sedimentation coefficients
k_1 , k_2	Constants in equation relating the sedimentation coefficient to concentration
k_{21}	Parameter relating dependence of sedimentation coefficient on concentration. The subscript refers to the effect of the concentration of component, 2, on the sedimentation rate of component, 1.
L	Fraction of the total cell volume which was originally above an indicator boundary and then migrated across it; a measure of backward flow
m	In interacting systems, represents the increment in the sedimentation coefficient of a macromolecular component caused by the binding of a single interacting ion or molecule
m	Mass of particle
m	Net amount of mass transported across a surface
m'	Mass contained between two surfaces in a centrifuge cell
m_D	Mass transported centripetally by diffusion
m_s	Mass transported across a surface by sedimentation
n	Charge on a macromolecule (valence)
n	Refractive index
N	Avogadro's number
n_i	Number of molecules of molecular weight M_i
n_1	Number of molecules of component 1
p	Axial ratio of effective hydrodynamic ellipsoid
p	Standard deviation of the distribution curve of sedimentation coefficients
P' and P	Constants in hydrodynamic theory for frictional coefficient of flexible chain macromolecules
P	Subscript meaning pressure of P atmospheres
$[P]$	Molar concentration of protein, P
$[P_0]$	Total concentration of the protein, P, in moles per unit volume
q	Cell constant accounting for the sector angle and the thickness of cell along the optical path, $q = \phi a$
Q_t	Total amount of solute remaining above the surface of the separating partition at the time, t (in mixtures, written as Q')
Q_1 and Q_2	Integrals of functions of the concentration and concentration gradient, Eqs. (70e) and (70d)
r	Number of moles of bound anion per mole of protein
r	Radius of sphere
r'	Ratio of observed concentration of slow component (corrected for sectorial dilution) to the true concentration
r^2	Mean square end-to-end distance in a random coil structure
R	Gas constant
R_s	Concentration ratio expressing the average concentration in a region centrifugal to a given surface as compared to concentration in zone centripetal to the selected surface
s	Sedimentation coefficient

$\bar{s}$	Weight-average sedimentation coefficient
$\overline{s^2}$	Mean square distance of a bead from the center of gravity
s_{app}	Apparent sedimentation coefficient
s_{av}	Average sedimentation coefficient
$\bar{s}_A$	Constituent sedimentation coefficient of the anion component, A
s_D	Differential sedimentation rate
s_i	Sedimentation coefficient of the i^{th} component
s_m	Sedimentation coefficient at maximum of distribution curve
$\bar{s}_P$	Constituent sedimentation coefficient of the protein component, P
s_t	Sedimentation coefficient at time, t
$s_{t=0}$	Sedimentation coefficient at time, $t = 0$
s_0	Sedimentation coefficient at infinite dilution
$s_{20,w}$	Sedimentation coefficient corrected to the value it would have in a solvent having the viscosity and density of water at 20° C. For this conversion it is assumed that the properties of the macromolecule are unaltered.
$s^{\alpha\beta}$, $s^{\beta\gamma}$, $s^{\gamma\delta}$	Migration rate of boundary between two zones indicated by superscript
S	As subscript indicates slow component
t	Time
t_{cor}	Time corrected for the change in viscosity with temperature. This is used in calculating sedimentation coefficients from experiments during which there is a substantial change in temperature
u'	Constant
v	Volume change caused by adding one particle (or molecule) to a large volume of solution
V'	Effective hydrodynamic volume per gram of unsolvated mass
$\bar{V}$	Partial specific volume of solute
V_e	Volume of the effective hydrodynamic ellipsoid
w	Measure of hydration in g. H_2O/g. protein
x	Distance from the axis of rotation
$\bar{x}$	Distance of the boundary from the axis of rotation, measured by the square root of the second moment of the gradient curve
x'	First moment of the gradient curve
x_D	Distance between axis of rotation and differential boundary
x_H	Distance from the axis of rotation to the maximum ordinate of the gradient curve
x_m	Position of meniscus in terms of distance from axis of rotation
x_p	Distance from the axis of rotation to a surface in the plateau region
$\bar{x}_t$	Position of the boundary at time, t
y	Integration parameter
z	Parameter depending on molecular weight and position in cell; $z = \frac{\omega^2 s}{2D} x^2$
α	Constant expressing dependence of viscosity on pressure
α	Exponent in expression relating intrinsic viscosity to molecular weight
α	Moles of a component (e.g. solvent) interacting preferentially with one mole of the macromolecule; a preferential adsorption or interaction coefficient
α, β, γ	As superscripts indicate phases or zones in the ultracentrifuge cell
$\alpha\beta$, $\beta\gamma$, $\gamma\delta$	As superscripts refer to boundaries between the zones indicated by the two symbols

β	Constant expressing dependence of density on pressure
β	Parameter which is a function of the axial ratio of an ellipsoid of revolution
γ	Aetivity eoefficient
γ	Constant expressing dependence of partial specific volume on pressure
γ_s	Coefficient expressing non-uniformity of, or heterogeneity with respect to, sedimentation coefficients
δ	$\omega^2 s/D$
Δs	Change in sedimentation eoefficient during an experiment, resulting from radial dilution
Δs	Differenee in sedimentation eoefficient between two migrating substances, used in theory for a differential method for measuring small differences in sedimentation coefficients
ζ	Constant expressing tortuosity of flow of liquid between particles
η	Viscosity of solvent at temperature of experiment
$[\eta]$	Intrinsic viscosity; in $(g./100\ ml.)^{-1}$
η_{sp}	Specifie viseosity
$\eta_{20,w}$	Viscosity of water at 20° C.
λ	Parameter including sedimentation coefficient, its dependence on concentration, the speed of the rotor and the time, $\lambda = ke_0(1 - e^{-\tau})$
λ	Wavelength of light
μ	Chemical potential
ν	Viseosity inerement
ξ_m	A parameter containing the diffusion and sedimentation coefficients and the dependence of the latter on concentration
π	Osmotie pressure
ρ	Density of solution at temperature of experiment
ρ^0	Density of solution at which the sedimentation rate of the macromolecule is equal to zero
σ	Square root of the seeond moment of the gradient curve about the mean
τ	$2\omega^2 st$, the equivalent time of sedimentation
ϕ	Angle of the seetor cell in radians
ϕ	The integral form of the Gaussian equation
ϕ'	The derivative of the Gaussian equation
Φ	Constant in hydrodynamic theory for the intrinsic viscosity of flexible chain maeromolecules
ψ	Constant which describes the ratio of the sedimentation coefficients of the slow and fast components in a mixture
ω	Angular velocity of the cell in radians/sce.

AUTHOR INDEX

Numbers in italic indicate the pages on which the references are listed.

A

Adler, F. T., 34, 206, 208, *249*, *257*
Alberty, R. A., 75, 77, 142, 159, *249*
Aldrich, B. B., 83, 183, *254*
Amberson, W. R., 116, *249*
Anderson, N. G., 213, *249*
Anfinsen, C. B., 4, *249*
Appel, P., 57, 184, 185, 186, 187, 188, 189, 190, 191, 192, 199, 205, 214, *251*, *257*
Archibald, W. J., 8, 181, 182, 191, 192, 193, 194, 195, 199, 204, 206, 207, 214, 218, *249*

B

Backus, J. K., 244, *255*
Backus, R. C., 125, 225, *258*
Bailey, E. D., 1, 34, 52, 133, 215, *254*
Baker, M. C., 157, 224, *249*
Baldwin, R. L., 1, 37, 66, 67, 69, 79, 80, 85, 87, 88, 90, 93, 102, 125, 129, 130, 131, 135, 136, 137, 138, 142, 143, 145, 146, 147, 148, 150, 162, 169, 181, 186, 187, 198, 199, 205, 218, 220, 228, 235, *249*, *257*, *258*
Bauer, J. H., 17, *249*
Beams, J. W., 15, 22, 38, 39, 41, 47, 181, 205, *249*
Beard, D., 59, 222, 232, 234, *256*
Beard, J. W., 59, 222, 232, 234, 238, *252*, *256*
Beehhold, H., 231, *249*
Beckmann, C. O., 222, *249*
Bender, M., 206, *257*
Bendet, I. J., 108, 223, 232, 233, *249*, *253*
Bensusan, H. B., 116, *249*
Bianeheria, A., 18, 19, *249*
Bjorklund, R., 214, *249*
Blanehard, C. H., 34, *249*
Blankenhorn, B. E., 116, *249*
Blum, J., 17, *250*
Blumberg, B. S., 232, *249*
Boedtker, H., 245, *249*
Booth, F., 208, 226, *250*
Brakke, M. K., 213, *250*
Brice, B. A., 224, *251*
Bridgman, W. B., 34, 134, *250*
Briggs, D. R., 155, 159, 163, 164, 168, *250*, *256*
Brohult, S., 153, *250*
Brown, D. M., 155, *256*
Brown, R. A., 116, 152, 156, 167, 185, 189, 194, *250*
Bueehe, A. M., 246, *250*
Bull, H. B., 224, *250*
Burgers, J. M., 91, 92, 95, 101, *250*
Burns, V. W., 38, 60, *257*
Butler, J. A. V., 51, 134, 135, *256*
Buzzell, J. G., 242, 244, *257*

C

Campbell, D. H., 157, 158, *249*, *256*
Cann, J. R., 136, 152, 156, *250*
Carroll, W. R., 244, *255*
Carstensen, H., 189, *253*
Ceeil, R., 18, 73, 74, 76, 90, 92, 102, 224, *250*
Charlwood, P. A., 187, 188, *250*, *256*
Cheng, P. Y., 32, 81, 95, 102, 150, 177, 179, 190, 199, 213, 214, 224, 234, 238, *250*
Chepeswiek, C., 83, 101, 139, *251*
Chirnoaga, E., 201, *256*
Cieirelli, J. S., 144, 145, 149, 247, *258*
Claesson, I. M., 120, *250*
Claesson, S., 120, *250*
Cohen, S. S., 186, 188, *250*
Cohn, E. J., 237, 238, *250*
Connell, J. J., 143, *250*
Cook, G. H., 22, 41, *255*
Cook, W. H., 234, *253*
Cornwell, D. G., 128, 151, *254*
Cox, H. R., 116, 167, *250*
Crandall, H. F., 136, *253*
Csáky, T. Z., 59, *252*
Cunningham, L. W., 154, *250*
Currie, B. T., 224, *250*

D

Davies, M., 185, 189, 194, *250*
Davies, M. C., 116, 167, *250*
Davisson, E. O., 149, *250*

Debye, P., 230, 231, 245, 246, *250*, *251*
de Groot, S. R., 218, *252*
de Lalla, O. F., 22, 125, 145, 148, *250*
Desreux, V., 133, 176, 177, 247, *254*
Dieu, H., 147, *250*
Dillon, E. S., 59, *252*
Dillon, J. F., 15, *249*
Dillon, M. L., 59, *252*
Dixon, H. M., III, 15, 22, 38, 39, 41, 47, 181, 205, *249*
Doty, P., 245, 247, *249*, *254*, *255*
Dreyer, W. J., 154, *250*
Drucker, C., 210, *250*
Dunlop, P. J., 235, 236, *250*

E

Ecker, P. G., 17, *250*
Edsall, J. T., 4, 215, 219, 237, 238, *250*
Eggman, L., 157, *256*
Egli, H., 101, 102, *256*
Ehrenberg, A., 188, 191, *250*
Einstein, A., 216, 240, *250*
Eirich, F., 94, 228, *254*, *255*
Ellenbogen, E., 153, *254*
Elliott, H., 92, 126, 127, 128, *251*
Enoksson, B., 92, *250*
Epstein, H. T., 29, 223, *250*, *257*
Epstein, S. I., 157, *249*
Ericksson-Quensel, I.-B., 234, *256*
Eriksson, A. F. V., 133, 147, 177, *251*
Evans, W. J., 155, *251*
Ewart, R. H., 206, 230, 231, *257*
Eyring, H., 93, *255*

F

Fåhraeus, R., 201, *256*
Faxén, H., 12, 66, 129, 135, 140, *251*
Fessler, J. H., 93, 101, 243, *251*
Fick, A., 11, 222, *251*
Field, E. O., 148, 155, *251*
Fixman, M., 202, *251*
Flory, P. J., 222, 245, 246, 247, *251*, *252*, *253*
Forsberg, R., 35, *251*
Foster, J. F., 244, *258*
Fredericq, E., 154, *251*
Fujita, H., 1, 11, 70, 103, 130, 131, 140, 141, 145, 149, 150, 162, 169, 175, 176, 177, 235, *251*, *258*
Fuoss, R. M., 222, *254*

G

Geddes, A. L., 34, *251*
Gibbs, J. W., 210, *251*
Gibson, D. M., 149, *250*
Gilbert, G. A., 156, 157, 160, 165, 166, *251*
Ginsberg, A., 57, 184, 185, 186, 187, 188, 189, 190, 191, 192, 199, 205, 214, *251*
Gitlin, D., 153, *254*
Gofman, J. W., 22, 92, 125, 126, 127, 128, 145, 148, *250*, *251*
Goldberg, R. J., 64, 76, 202, 203, 206, 208, 210, 217, 218, 220, 221, 229, 231, *251*
Golder, R. H., 81, 103, *251*
Goring, D. A. I., 83, 101, 139, *251*
Gosting, L. J., 130, 142, 150, 162, 213, 218, 229, 235, *249*, *251*
Gouinlock, E. V., Jr., 247, *251*
Gowdy, R. A., 59, *252*
Gralén, N., 131, 132, 133, 139, 144, 147, *251*
Green, N. M., 154, *250*
Greenstein, J. P., 188, *257*
Gross, H., 133, 134, *256*
Gurd, F. R. N., 153, *254*
Gutfreund, H., 87, *251*
Gutter, F. J., 19, 37, 73, 76, 77, 93, 234, *251*, *252*

H

Hagdahl, L., 189, *253*
Hall, J. R., 138, *251*
Halwer, M., 224, *251*
Harrington, W. F., 25, 27, 28, 60, 62, 67, 71, 73, 77, 78, 84, 85, 88, 97, 98, 99, 100, 103, 105, 109, 118, 119, 120, 121, 122, 123, 124, 140, 150, 154, 156, 189, 242, 244, *251*, *253*, *255*, *257*
Harting, J., 157, *257*
Hartley, B. S., 154, 156, *253*
Hayes, J. E., 157, *251*, *257*
Hedenius, A., 153, *256*
Henriot, E., 15, *251*
Hersh, R. T., 57, 97, 98, 103, 106, 107, 110, 111, 112, 113, 114, *251*
Hertel, K. L., 101, *256*
Herzog, R. O., 238, *251*
Hiatt, C. W., 17, 19, *250*, *252*
Himmelfarb, S., 116, *249*

Hogeboom, G. H., 213, *252*
Holmberg, R. W., 210, *252*
Holtan, H., Jr., 218, *252*
Hook, A. E., 59, 222, 232, *256*
Hooyman, G. J., 218, 219, 235, *252*
Howard, G. J., 228, *252*
Huguenard, E., 15, *251*
Hunt, M. L., 247, *252*

I

Illig, R., 238, *251*

J

Jenkins, R. C. Ll. 160, 165, 166, *251*
Johnson, J. S., 202, 209, 210, *258*
Johnson, P., 155, 157, 242, 244, *251*, *252*, *256*
Johnston, J. P., 92, 98, 108, 116, *250*, *252*
Jordan, D. O., 228, *252*
Joubert, F. J., 155, *252*
Jullander, I., 77, 93, 102, 131, 132, 133, 144, 145, 225, *252*

K

Kamath, P., 228, *255*
Karush, F., 59, *252*
Katz, S., 214, 229, 231, 232, 233, 234, *249*, *252*
Kauzmann, W. J., 94, *255*
Kegeles, G., 18, 19, 25, 26, 31, 37, 73, 76, 77, 93, 149, 156, 184, 185, 187, 188, 189, 193, 206, 208, 222, *249*, *252*, *255*
Kerby, G. P., 59, *252*
Kermack, W. O., 91, 93, *252*
Kimmell, J. R., 155, *256*
Kinnell, P.-O., 1, 70, 133, *252*
Kirkwood, J. G., 152, 156, 231, 246, *250*, *252*
Klainer, S. M., 149, 184, 185, 187, 188, 189, 208, 222, *252*
Klotz, I. M., 168, *252*
Koenig, V. L., 82, *252*
Kraemer, E. O., 132, 205, 206, 208, 210, 211, 220, *252*, *253*
Kraus, K. A., 202, 209, 210, *252*, *258*
Kraut, J., 224, 228, *252*, *258*
Krigbaum, W. R., 247, *253*
Krishnamurti, K., 131, *252*
Kritchevsky, D., 185, 189, 194, *250*
Kudar, H., 238, *251*
Kurnick, N. B., 157, *252*

L

Lamm, O., 9, 31, 33, 34, 66, 130, 131, 204, 205, 209, 210, 217, 218, *252*, *253*
Lansing, W. D., 132, 205, 206, 208, 210, 211, 220, *252*, *253*
Lanz, H., Jr., 179, *253*
Larner, J., 136, *253*
Lauffer, M. A., 29, 71, 72, 92, 93, 97, 102, 108, 131, 138, 149, 179, 211, 215, 223, 229, 232, 233, 234, 237, 244, *249*, *250*, *253*, *255*, *257*
Lewis, G. N., 108, 213, *253*
Li, C. H., 189, *253*
Linderstrøm-Lang, K., 179, *253*
Lindgren, F. T., 92, 126, 127, 128, *251*
Loeb, G. I., 242, 244, *253*
Longsworth, L. G., 33, 34, 37, 41, 82, 103, 108, 152, 159, 217, *253*
Lyons, P. A., 224, *249*

M

McBain, J. W., 210, *253*
MacCallum, W. G., 231, *253*
McCartney, J. R., 230, 231, *251*
McFarlane, A. S., 116, 126, *253*
MacInnes, D. A., 152, 159, *253*
M'Kendrick, A. G., 91, 93, *252*
McLaren, A. D., 157, *256*
McLean, I. W., Jr., 232, *256*
Mandelkern, L., 206, 207, 208, 237, 239, 240, 241, 243, 246, 247, *253*, *255*
Martin, W. G., 234, *253*
Marvin, H. H., 159, *249*
Mason, M., 181, 198, *253*
Massey, V., 154, 156, *253*
Mazur, P., 218, *252*
Mehl, J. W., 239, 240, *253*
Meselson, M., 54, 151, 211, 213, *253*, *255*
Meyerhoff, G., 27, *254*
Milch, L. J., 22, *254*
Miller, G. L., 232, *254*
Mommaerts, W. F. H. M., 83, 139, 183, *254*
Moore, D. H., 21, 37, *254*
Morales, M. F., 185, *257*
Mosimann, H., 175, *254*
Moyer, A. W., 116, 167, *250*

N

Naismith, W. E. F., 155, *252*, *254*
Nazarian, G. M., 181, *254*
Neurath, H., 154, 244, *250*, *251*, *254*, *257*
Newman, S., 94, 247, *252*, *254*
Nichols, J. B., 1, 34, 52, 133, 201, 215, *254*, *256*
Nims, L. F., 244, *255*
Nishihara, T., 245, *254*
Nutting, G. C., 224, *251*

O

O'Brien, J. R. P., 148, 155, *251*
Ogston, A. G., 18, 73, 74, 76, 87, 90, 92, 93, 101, 102, 108, 116, 136, 138, 148, 155, 218, 220, 224, 229, 230, 232, 235, 237, 241, 242, 243, *249*, *250*, *251*, *254*
Oka, S., 12, 218, *254*
Oneley, J. L., 75, 128, 151, 153, 237, 239, 240, *253*, *254*
Onsager, L., 222, *254*
Oppenheimer, E. H., 231, *253*
Oster, G., 225, *254*
Oth, J., 133, 147, 176, 177, 247, *250*, *254*
Ottewill, R. H., 242, 244, *251*

P

Paigen, K., 178, 180, *256*
Parrish, R. G., 83, 139, *254*
Pasternak, R. A., 181, *254*
Peacocke, A. R., 47, 95, 102, 125, 139, 244, 247, *254*
Pederson, K. O., 1, 13, 18, 28, 30, 47, 52, 56, 69, 82, 85, 86, 116, 129, 149, 153, 174, 181, 189, 201, 203, 206, 208, 210, 225, 226, 237, 238, 239, 244, *253*, *254*, *256*, *257*
Peller, L., 236, *254*
Perrin, F., 238, 239, *254*
Perrings, J. D., 82, *252*
Peterlin, A., 246, *254*
Petersen, E. A., 234, *251*
Philpot, J. St. L., 22, 33, 34, 41, 53, *254*, *255*
Pickels, E. G., 13, 15, 17, 19, 21, 25, 27, 37, 57, 58, 59, 60, 84, 139, 231, *249*, *255*, *256*
Pirie, N. W., 139, *255*
Pivan, R. B., 168, *252*
Ponder, E., 91, 93, *252*
Porath, J., 189, *255*
Powell, R. E., 93, *255*
Price, W. C., 232, *254*
Putnam, F. W., 149, 223, *255*

R

Råuby, B. G., 1, 133, *252*
Randall, M., 213, *253*
Rao, M. S. N., 156, 187, 193, *252*, *255*
Ray, B. R., 136, 149, *250*, *253*
Record, B. R., 131, 139, *255*
Redfield, R. R., 4, *249*
Rice, S. A., 247, *255*
Richards, E. G., 49, 50, 169, 171, 172, 173, 183, *255*
Rinde, H., 12, 70, 205, *255*, *256*
Riseman, J., 246, *252*
Robeson, A., 15, 38, 39, 41, 47, 181, 205, *249*
Robkin, E., 54, *255*
Roe, C. P., 230, 231, *251*
Rosen, B., 228, *255*
Rosenberg, J. L., 222, *249*
Ross, J. D., 15, *249*
Rothen, A., 189, *255*

S

Sadron, C., 237, 241, *255*
Salem, W. J., 187, 208, 222, *252*
Saum, A. M., 244, *254*
Saunders, J. M., 244, *255*
Saunders, W. M., 131, 135, 136, 138, 144, 145, 148, 149, 247, *258*
Scatchard, G., 209, 210, *252*, *255*
Schachman, H. K., 25, 27, 28, 32, 47, 49, 50, 51, 57, 59, 60, 61, 62, 64, 66, 71, 73, 77, 78, 81, 84, 85, 88, 94, 95, 97, 98, 99, 100, 102, 103, 105, 106, 107, 109, 110, 111, 112, 113, 114, 118, 119, 120, 121, 122, 123, 124, 125, 134, 135, 139, 140, 142, 150, 154, 169, 170, 171, 172, 173, 177, 178, 179, 180, 183, 184, 185, 186, 187, 188, 189, 190, 191, 192, 199, 205, 211, 213, 214, 215, 223, 224, 229, 232, 233, 234, 238, 244, 247, *250*, *251*, *252*, *254*, *255*, *256*, *257*
Schellman, J. A., 189, *251*
Scheraga, H. A., 237, 239, 240, 241, 242, 243, 247, *251*, *252*, *253*, *255*
Schlesinger, M., 231, *249*
Schneider, W. C., 213, *252*

Schulz, G. V., 206, 208, *255*
Schumaker, V. N., 12, 47, 51, 59, 60, 67, 70, 77, 78, 103, 118, 120, 121, 122, 123, 124, 134, 135, 140, 150, 190, *255*, *257*
Schwert, 76, 153, 154, 156, *255*
Senti, F. R., 224, *255*
Sharp, D. G., 32, 59, 222, 232, 234, 238, *252*, *255*, *256*
Shedlovsky, T., 231, *256*
Sheppard, E., 157, *256*
Shooter, E. M., 155, *252*
Shooter, K. V., 51, 134, 135, *256*
Shulman, S., 18, 244, *256*
Siegel, A., 59, *256*
Signer, R., 101, 102, 133, 134, 175, *254*, *256*
Sihtola, H., 234, *256*
Simha, R., 239, 240, 242, *253*, *256*
Simmons, N. S., 245, *249*
Singer, S. J., 59, 157, 158, 175, 222, 224, *249*, *256*
Smadel, J. E., 231, *256*
Smith, D. B., 187, 188, *256*
Smith, E. L., 155, *256*
Smith, R. F., 159, 163, 164, 168, *256*
Snidow, N., 15, 38, 39, 41, 47, 181, 205, *249*
Sober, H. A., 234, *251*
Squire, P. G., 131, 135, 136, 138, *258*
Stacey, M., 139, *255*
Stahl, F. W., 151, 211, 213, *253*
Stanier, J. E., 243, *254*
Stanley, W. M., 102, 232, *253*
Steere, R. L., 125, *258*
Steiner, R. F., 157, *256*
Stenesh, J., 178, 180, *256*
Stockmayer, W. H., 231, *256*
Stokes, G. G., 237, *256*
Striebich, M. J., 213, *252*
Sullivan, R. R., 101, *256*
Sutherland, W., 216, *256*
Sutton, E., 244, *255*
Svedberg T., 1, 12, 13, 18, 28, 30, 47, 52, 56, 69, 70, 82, 85, 86, 129, 130, 131, 149, 153, 174, 181, 201, 206, 208, 215, 225, 226, 234, 237, 238, 239, 244, *252*, *256*, *257*
Svensson, H., 33, 34, 35, 41, 43, 45, 120, 171, *251*, *256*, *257*
Swaby, L. G., 223, *249*
Swanson, D. L., 206, *257*

T

Tanford, C., 242, 243, 244, *257*
Taylor, A. R., 59, 222, 232, *256*
Taylor, N. W., 97, 108, 179, 223, 232, 233, *253*, *257*
Thompson, J. O., 206, *257*
Thovert, J., 34, *257*
Tietze, F., 154, *250*, *257*
Tiselius, A., 28, 30, 85, 86, 153, 158, 161, 189, 208, 226, *253*, *257*
Tolman, R. C., 226, *257*
Trautman, R., 12, 22, 38, 60, 64, 66, 67, 69, 70, 77, 78, 90, 103, 118, 120, 121, 122, 123, 124, 140, 190, 192, *257*

V

Van Holde, K. E., 1, 95, 162, 169, 181, 186, 198, 199, 205, 206, 207, 208, 235, *257*, *258*
Velick, S. F., 157, *251*, *257*
Vestling, C. S., 149, *250*
Vinograd, J., 54, 151, 211, 213, *253*, *255*
Vinograd, J. R., 181, *254*
von Hippel, P. H., 155, 185, *257*, *258*

W

Wade, R., 188, *257*
Wade, R. D., 154, 224, *250*, *258*
Wales, M., 95, 206, 207, 208, 211, 229, 231, *257*
Walker, F. M., 168, *252*
Walton, K. W., 128, 151, *254*
Warner, R. C., 224, *255*
Waugh, D. F., 4, 12, 17, 19, 29, 30, 59, 60, 86, 142, 155, 195, 196, 197, 198, 199, *257*, *258*
Weaver, W., 181, 198, 199, *253*, *258*
Webber, R. V., 85, 88, 90, *258*
Weissberg, S. G., 206, 207, 208, *253*
White, J. I., 116, *249*
White, J. U., 37, *254*
Wilcox, P. E., 224, *258*
Williams, J. W., 1, 34, 131, 135, 136, 138, 142, 144, 145, 147, 148, 149, 162, 169, 206, 207, 211, 217, 229, 231, 235, 247, *249*, *250*, *257*, *258*
Williams, L. C., 206, 207, 208, *253*
Williams, R. C., 125, 225, *258*
Winitz, M., 188, *257*
Winkler, C. A., 234, *253*

Wolf, W. J., 155, *250*
Wolter, H., 37, *258*
Wood, G. C., 187, 188, *256*
Woods, E. F., 136, 148, 244, *254*
Wunder, C. C., 179, 232, 233, *253*

Y

Yang, J. T., 244, *258*
Young, T. F., 202, 210, *252*, *258*
Yphantis, D. A., 12, 17, 19, 29, 30, 59, 60, 86, 142, 195, 196, 197, 198, 199, *258*

SUBJECT INDEX

A

Antigen-antibody reaction, 157–159
Approach to sedimentation equilibrium, 8–9, 181–199
Archibald method, 8–9, 182–194, 207–208
  for polydisperse, nonideal solutions, 207–208
Associating-dissociating systems, 152–157, 187, 193

B

Backward flow, 92, 96–97, 108–116
  considerations of, 92, 96–97
  measurement of, 108–116
Binding of small molecules and ions to proteins, 157–170
Boundary, 5, 63–70, 128–130, 138–148
  boundary movement and velocity of individual molecules, relationship between, 63–70
  definition of, 5
  Gaussian shape, 66, 130
  self-sharpening of, 138–148
  shape of, 128–129
  width of, as a measure of polydispersity, 131–133
Boundary anomaly in analysis of serum, 116, 126–128
Boundary position as a function of time for systems exhibiting concentration dependent sedimentation coefficients, 102–103
Boundary spreading, due to diffusion, 128–131, 150
  diffusion coefficients from ultracentrifuge boundaries, evaluation of, 129–131, 150
Boundary spreading for associating-dissociating systems, 153

C

Cell distortion, 46, 57
Cells, 21–32, *see also* Double sector cell, Separation cells, Synthetic boundry cell
  compressibility cell, 32
  double prismatic cell, 31
  prismatic windows, 22
  sector angle, 21
Charge effect, 208–210, 225–228
  primary charge effect, 226–227
  secondary charge effect, 226–227
  sedimentation equilibrium, 208–210
Compressibility measurements in the ultracentrifuge, 32, 177–180
Concentration boundary, 103
Concentration determinations, 72–74, 185–188
Concentration distribution throughout the cell, 194–199
Constituent sedimentation coefficient 69, 161–170
Continuity equation, 9–12, 68, 140, 160, 165, 177, 182
  polydisperse systems, 68
  single component, 9–12
Convection, 16, 21, 31, 55–62, 186
  concentration gradient as a stabilizing factor, 58–59
  consideration of pressure gradient, 58–59
  in dilute solutions, 16, 59–60
  distortion of cells, 57
  effect of aggregating systems, 60–61
    of cell bottom, 56–57, 186
    of centrifugal field in stabilizing boundaries, 31, 59–60
    of imperfections in cell walls, 21, 56
    of misalignment of cell, 57
    of sector angle, 21, 57
  mechanical disturbances, effect of, 57–58
  in mixtures of sedimenting components, 62
  nature of, 60–62
  role of sector shaped cell, 56–57
  saw-tooth spikes, observation of, 60–61
  temperature gradients, effect of, 58
    production of, 58

D

Density considerations, 82, 92, 127–128
Density gradient sedimentation equilibrium, 151, 210–214
Differential boundary, 103

Differential density measurements in the ultracentrifuge, 178–180
Differential equation of the ultracentrifuge, 9–12
Differential method for measuring small changes in sedimentation rate, 164, 170–174
Differential sedimentation rates, 103–108
Diffusion coefficient, 5, 11, 59, 139, 141–148, 150, 199
  evaluation of, 59, 139, 141–148, 150, 199
Distribution curve of sedimentation coefficients, as a measure of polydispersity, 131, 133–136
Double sector cell, 22–25
  interference optics, for, 24
  schlieren optics, for, 22–25

F

Fick's first law, 11
Frictional coefficient, 216, 221, 222–223, 236–247
  effect of hydration, 239–243
  for ellipsoids of revolution, 238–240, 244–245
  in sedimentation and in diffusion, 222–223
  for spheres, 237–238
  for flexible chain like molecules, 245–247

H

Hinge point, 199, 205, 214
Homogeneity, demonstration of and criteria for, 149–151, *see also* Polydisperse systems
Hydration, 210–211, 231–233, 239–240, 243
Interacting systems, 69, 151–170, 187, 193
  analysis of, 151–170, 187, 193
  constituent sedimentation coefficient, 69, 161–170
  readjustment of equilibria during sedimentation of, 157–160
  relationship to electrophoresis, 152, 159–160

I

Interaction(s) among different molecular species, 157–170
  between bovine serum albumin and methyl orange, 159–160, 164, 170
Interferometric optics, applications, 183, 188, 192, 194, 205, 207
Interpretation of sedimentation data, 215–247

J

Johnston-Ogston effect, 116–128
  detailed theory, 120–122
  simplified theory, 117
  test of theory, 119, 123

L

Light absorption optics, 3, 47, 51–55, 210
  analysis of plates obtained by absorption optics, 53–54
  characteristics of photographic plates, 53
  counterbalance cell, 54
  filters for, 52, 55
  photomultiplier tubes, application of, 54–55

M

Maximum ordinate of gradient curve, 64–67
  and second moment, relationship between, 66–67
Mixtures of several components, 116–128
Molecular weight averages, 205–207, 225
Molecular weight determinations, 181–199, 201–219, 224–225, 241–243
  approach to sedimentation equilibrium, 181–199
  Archibald method, 182–194, 207–208
  sedimentation and diffusion (Svedberg equation), 215–219, 224–225
  sedimentation and viscosity, 241–243
  sedimentation equilibrium, 201–214
Moving boundary theory, 69–70, 108, 113
Multicomponent systems, 210–214, 228–236
  complications due to cross term diffusion coefficients, 234–236
  effect of selective solvation, 229–233
  preferential adsorption coefficient, 230–231
  relation of sedimentation studies to light scattering investigations, 230–231
  steric effects, 233–234

N

Non-ideals olutions, 202–204, 206–208, 222–224
thermodynamic effects, 202–204, 206–208, 222–224

O

Optical methods, 3, 32–55, 210
absorption optics, 3, 47, 51–55, 210
interference methods, 38–50
compensating cell, 40, 46–47
light chopper, 41
white light fringe, 40–41
Jamin or Mach-Zender interferometer, 33, 38–41
Lamm scale method, 33–34
Rayleigh interferometer, 33, 41–47
conditions for interference, 42
design for ultracentrifuge, 43–45
Rayleigh mask, 45
simple design, 41–42
upper aperture, 45–46
refractive index gradient methods, 33–38
schlieren diaphragms, 37–38
bar as, 37
phase plate as, 37–38
slit as, 37
wire as, 37
schlieren methods, 33–36
cylindrical lens method, 33–36
scanning method, 33–36

P

Partial specific volume, 216–217, *see also* Hydration, Solvation
Plateau region, 5, 12, 63–64, 186–187
Polydisperse systems, 128–151
diffusion effect, 129–131
expressions for polydispersity, 131–138
Johnston-Ogston anomaly in distorting boundaries, 148–149
self-sharpening of boundaries, 138–148
Pressure effect, in sedimentation equilibrium, 202
in sedimentation velocity, 70, 174–180
corrections for, 175
effect on plateau region, 70, 175

R

Radial dilution, 70–73
correction for, 71
effect of dilution in sedimentation velocity studies, 71–72
in polydisperse systems, 71
Radial dilution equation, 12, 63–64, 71–73
test of, 73
Random coil, 245–247
Redistribution of buffer ions, 23–25, 28, 51, 60, 70, 209–210
complications of, 23–25, 28, 51, 70, 209–210
effect in stabilizing boundaries against convective disturbances, 60
Rodlike particles, 244
Rotor, 13–21
adiabatic cooling of, 19
analytical, 16–21
stretching of, 13, 17–21
temperature of, 14–19

S

Scheraga-Mandelkern equation, 242
Second moment of the gradient curve, 64–67
and maximum ordinate, relationship between, 66–67
Sedimentation coefficient, 5, 9, 10
definition, 10
dependence on concentration, 71–72, 77–81, 90–103, 138–148, 153–155
in associating-dissociating systems, 102, 153–155
backward flow effect, 92, 96–97
considerations of mixtures, 95–100
density effect, 92
effect during individual experiments, 71–72, 77–81
on shape of boundary, 91, 138–148
extrapolation procedures for evaluation of sedimentation coefficient at infinite dilution, 102
theory for, 90–103
in terms of flow through a porous plug, 101
viscosity effect, 92–94
determination of, 75–90, *see also* Weight average sedimentation coefficients

Sedimentation coefficient—*continued*
application of partition cell, 85–86
of synthetic boundary cell for small molecules, 83–85
correction for radial dilution during experiment, 77–81
for temperature variation during experiment, 75–76
to standard conditions, 81–83
moving boundary method, 75–85
transport method, 85–90
weight average value for polydisperse systems, 87
zero time correction, 79
distribution curve, 131, 133–138
standard deviation of, 131, 136–138
Sedimentation equilibrium, 6–9, 151, 201–214
basic equation for, 202–203
of charged macromolecules, 208–210
in density gradient, 151, 210–214
effect of hydration, 210–211
elementary theory, 202
general considerations, 6–9
multicomponent systems, 210–214
non-ideality effects, 203–208
polydispersity, 205–208
supporting electrolyte, 209–210
for two component systems, 203–208
Sedimentation of slow component in presence of faster species, 108–116, 121
Sedimentation velocity, 5–6, 9, 63–180
general considerations, 5–6, 9
measurement of transport across a surface, 67–68, 85–90
position of boundary from axis of rotation, 65
radial dilution, 63–64, 70–75
weight average sedimentation coefficient, 67–68
Self-sharpening of boundaries, 138–148
Separation cells, 28–31
fixed partition cell, 28–30
movable partition cell, 29–30
Serum, ultracentrifugal analysis of, 126–128
Small molecules, 83–85, 88–89
Solvation, 210–212, 219–221
in two component systems, 210–212, 219–221
Stokes' law, 237
Svedberg equation, 215–219, 224–225
continuity equation and concentration distribution at equilibrium, 218
force on a molecule in a centrifugal field, 216–217
macroscopic considerations, 217–218
microscopic considerations, 215–217
restrictions on its use, 217
test of, 224–225
thermodynamics of irreversible processes, 218–219
Synthetic boundary cell, 25–28, 47, 83–85, 103–116, 121, 139, 149–150, 163, 167, 185
design and construction, 25–28
interacting systems, 167
in measurement of backward flow, 108–116
of dependence of sedimentation coefficient on concentration, 103–108
of differential sedimentation rates, 103–108
of diffusion coefficients, 139, 150
of sedimentation rate of slow component in presence of faster species, 108–116, 121
as a refractometer, 47, 149, 185
for small molecules, 83–85, 163

T

Temperature, measurement and control of, 14–19
Transient states, 9, 181–199
duration of, 181
Transport, by diffusion, 11
by sedimentation, 10–11, 67–69, 85–90, 166–167

U

Ultracentrifuge, types of, 1, 13–16
air driven, 1, 15
electrically driven, 13–15
magnetically suspended, 15–16
oil driven, 1

W

Weight average sedimentation coefficients, 67–69, 87, 157, 161–165

ECKED
2008

VERIFIED
2013
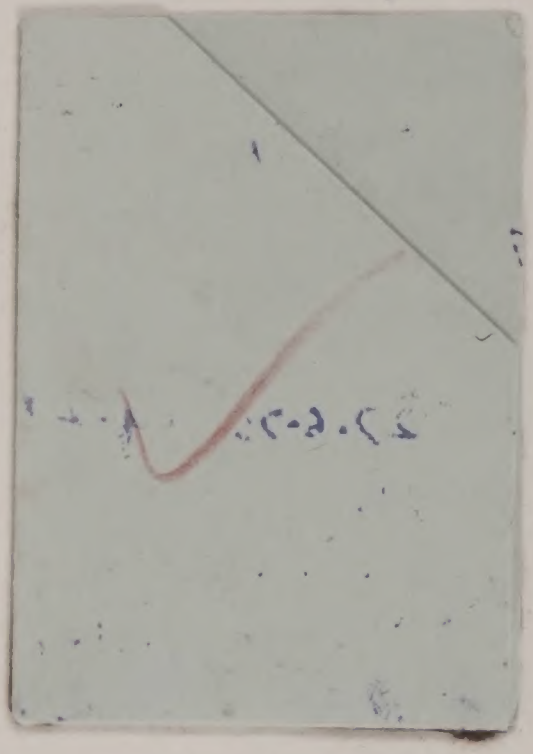
CFTRI-MYSORE
4217
Ultracentrifugat